



Universidad del País Vasco Euskal Herriko
Unibertsitatea

Universidad del País Vasco
Facultad de Medicina y Odontología
Departamento de Fisiología

Post-translational Modifications in Liver Disease

Tesis doctoral para optar al grado de Doctor, presentada por:

Imanol Zubiete Franco

2017

Directoras de Tesis:

Dra. María Luz Martínez Chantar

Dra. Marta Varela Rey

Portada: Mosaico en forma de hígado de imágenes de inmunofluorescencia representativas de las tres partes de esta tesis. A la izquierda, IF de LC3 en hepatocitos. En el centro, IF doble de NEDD8 y α SMA de hígado fibrotico y a la derecha IF de FLAG en células de hepatoma Huh7 expresando FLAG-LKB1. Rodeando al hígado aparecen las modificaciones postraduccionales estudiadas.

Agradecimientos/Acknowledgements

Primero me gustaría agradecerle a Malu la oportunidad de hacer la tesis en su laboratorio. En estos cuatro años he aprendido todo tipo de cosas que me ayudaran a seguir haciendo ciencia, desde planificar un experimento a escribir un paper, con suficientes dosis de independencia para aprender de los errores. Gracias por tener tanta paciencia conmigo y por todas las discusiones (a pesar de algunas ideas tontas que he llegado a tener) que hemos tenido a lo largo de estos cuatro años.

Al profesor José María Mato, Alicia, y Bego por su ayuda en temas administrativos y de beca importantes y por mantener al CIC bioGUNE en lo alto.

A mi co-directora Marta por meterme en el “maravilloso” mundo de la autofagia y los ajos macho. Pero sobretodo me gustaría agradecerle el demostrarme que correr 20 geles de una sentada no es nada del otro mundo y que solo depende de ponerle un poco de ganas y empeño. Suerte con tus futuros proyectos de autofagia, espero estar lo más lejos posible.

A mis compañeros de tesis Pablo y Lucía, por su ayuda en todo lo relacionado con la tesis. Me lo he pasado muy bien en los distintos congresos dando charlas o defendiendo los posters, estando hasta tarde, buscando reactivos o descifrando protocolos. Hacer la tesis ha sido bastante más fácil con vuestra ayuda y gran parte del trabajo que hay aquí es gracias a vosotros.

A Teresa por aguantarme a mí y a los demás en el labo y nunca perder su sonrisa y tono diplomático. Gracias por tu ayuda con todos los papers, sin duda, sin tu ayuda serian algo completamente distintos.

A Juan que fue el primero en enseñarme cómo funcionaba el labo. Me acuerdo del primer experimento que me enseñó en cultivos. Que si hay que silenciar LKB1 y que si luego tenemos que silenciar RasGRP3 para ver si se reduce el efecto de sobre expresar LKB1 y no te olvides de los controles y luego duplica todo etc... todavía me da dolor de cabeza recordarlo. Juan esta siempre dispuesto a echar una mano cuando hace falta y gran cantidad del trabajo de esta tesis se la debo a su ayuda. Siempre tiene una teoría para explicar cualquier resultado inesperado y aparte de ser un gran científico es mejor persona. No conseguí acabar el paper de LKB1 pero ya creo que le queda poco.

A los miembros de la patrulla monger, por hacer que el trabajo en el laboratorio se pase volando. La Amama alfa de la patrulla es mi becario Fer, que siempre sabe cuándo vienes con ropa nueva o cuando sales de fiesta y que puede contarte todos los chismes del centro cuando no se esta quejando de algo. No olvidare los meses en los que empezamos la semana transfectando células el lunes para hacer pulldowns el miércoles (¡Alabado sea el pulldown!) para acabar la semana revelando un film en blanco. Según cuenta la leyenda, Fer sigue modificando la imagen de LKB1 SUMO. David es lo más parecido a una biblioteca del labo. Gracias a él conseguimos comprar reactivos raros, encontrar primers y protocolos. Le agradezco mucho su paciencia conmigo a pesar del coñazo que le daba con todo. A Sergio, el mastodon baby del labo, que no tiene voz interior. Gracias por ilustrarnos con datos sobre Japón, coches, motores y relojes. No olvidare los años de vida que me robaste con tus gritos porcinos. A Taibolas, que estuvo poco, pero nos alegró los días con sus dilemas filosóficos y con sus poses de modelo. A Jorge, el mazado, que llego para empezar la tesis cuando a mí me quedaba poco en el labo pero creo que no tendrá ningún problema en adaptarse, suerte con el serious mass. Sobre todo gracias a todos por no dejarme disfrutar de la tesis.

A Naiara por ayudarme con todo el tema ratón/hígado/ELISA cuando llegue al labo. Sobre todo me ayudó con las PCRs y ELISAs (aunque creo que nunca conseguiré hacer una PCR tan rápido como ella, ni batir el tiempo de viaje entre CIC bioGUNE y Gorniz) y aunque siempre andaba de un lado del edificio al otro como una loca siempre encontraba un hueco para ayudar y resolver algún dilema con el protocolo. Le agradezco también las charlas críticas sobre experimentos y los puntos que se podrían mejorar. A Naiara le ayudaba Sara, chica trabajadora con sentido del humor curioso que también me ayudó mucho al principio sobre todo con los reactivos de la caspasa 3.

A Vir la reina de las inmunes. Gran parte de esta tesis se pudo hacer gracias a su gran manejo de los anticuerpos y a pesar de que siempre esta liada con trabajo siempre encuentra algún momento para encontrar y mandar esa inmuno de hace seis meses. También se agradecen las galletas y golosinas que traía al labo para todo el mundo.

A Marta Txiki por su ayuda con todo lo relacionado con LC3 y autofagia y por todos los fines de semana que teníamos que entrar para seguir haciendo autofagia.

A Ashwin por su ayuda con el ChIP, por su sentido del humor y por su punto de vista sobre la política Vasca. A Encarni y a Marta Palomo por su ayuda y alegrar el labo durante el poco tiempo que estuvieron con nosotros.

A Gotxi por amenizar el día con una selección variada de canciones de distintos géneros musicales.

A Urra, lo más cercano a una madre de laboratorio, que me cuidaba los días que me quedaba hasta las tantas y me daba un poco de chocolate cuando más lo necesitaba. A pesar de estar constantemente pisando lo recién fregado nunca me echó la bronca, solo cuando me quedaba demasiados días seguidos hasta tarde. Gracias a ella los días largos se hacían más llevaderos sobre todo escuchándole cantar ópera.

A Paula por su ayuda con las muestras humanas que fueron de gran ayuda para el paper de NEDD8 y su ayuda con la parte clínica de la introducción.

Al grupo de Juanma incluyendo a Espe, Felix, y Laura que tuvieron que aguantarnos todas las semanas tanto en el labo como en la oficina. Gracias a su donación de reactivos conseguíamos seguir haciendo algún experimento en los momentos malos. También me gustaría agradecer a los miembros de la plataforma de metabolómica Diana, Sebastiaan y Quica por su ayuda con la medición de los metabolitos.

A Felix Elortza y Mikel Azkargorta de la plataforma de proteómica por no rendirse con las muestras de bio-Ub aunque al final esa parte no entra en esta tesis.

A Patricia Aspichueta por su ayuda con todo el tema relacionado con la uni.

A Arkaitz Carracedo por los ratones *Stk11-KO*.

A Rosa Barrio, Jim Sutherland y Manuel Rodríguez por su ayuda con SUMO y donar plasmidos.

Al grupo de Edurne Berra por las muestras de ratón en hipoxia y el uso de la cámara.

A Antton y Santos, por ayudarme a desconectar del trabajo los fines de semana y por lo bien que me lo he pasado en los distintos conciertos.

A mis padres, Begoña y Emilio, por darme la oportunidad de estudiar lo que más me gustaba y siempre apoyarme. También les doy las gracias por no darme una patada en el culo y cuidarme estos dos últimos años de tesis. A mis hermanos Unai y Gorka por lo bueno y lo malo. A mis aities por preguntar qué tal va “eso” y que tal están los “bichitos”. A Sara e Iñigo, espero que esta tesis le inspire a hacerse científico. Aprovecho también para agradecerle al resto de mi familia por su apoyo.

Y finalmente a Justyna, la chica del este, que vino cuando me quedaba poco para acabar la tesis. A ella le doy las gracias por escucharme, animarme y darme fuerzas para seguir trabajando e incluso hizo que no me importara ir a trabajar los fines de semana. Esta etapa se acaba y nos toca empezar una nueva y mejor, sin el estrés de la tesis, desde cero.

Finally, since keeping traditions alive is important: Thank you Bag!



Table Of Contents

Table of Contents

Figures and Tables	viii
Abbreviations	3
1.1 Resumen.....	9
1.2 Summary.....	14
2. Introduction	21
2.1 Chronic Liver Disease	21
2.1.1 Non-alcoholic Fatty Liver Disease	21
2.1.2 Lipid Homeostasis	22
2.1.3 Lipophagy.....	22
2.1.4 Autophagy and NAFLD	23
2.2 Methionine and liver disease	24
2.2.1 S-adenosylmethionine and the methionine cycle	24
2.2.2 Regulation of the methionine cycle	25
2.2.3 Methionine adenosyltransferase and Glycine N-methyltransferase	26
2.2.3 Study of hypermethioninemia	26
2.3 NAFLD treatment.....	28
2.4 NAFLD progression	29
2.5 Liver Fibrosis and Cirrhosis	29
2.5.2 Cell types and pathways involved in fibrosis	30
2.5.3 Fibrosis research.....	36
2.5.4 Treatment of fibrosis.....	37
2.6 Hepatocellular Carcinoma	37
2.6.1 NAFLD and HCC.....	37
2.6.2 HCC treatment	37
2.6.3 Molecular pathways in HCC	38
2.7 Liver Kinase B1	40
2.7.1 LKB1 targets	41
2.7.2 LKB1 in the liver	42
2.7.3 LKB1 post-translational modifications	43
2.8 Post-translational Modifications.....	43
2.8.1 Addition of functional groups	43
2.8.2 Addition of polypeptides	44
2.8.3 NEDDylation.....	45
2.8.4 SUMOylation	46
3. Objectives	51
4. Experimental Procedures.....	55
4.1 Cell Isolation, Culture and Treatments	55
4.1.1 Primary Cells	55
4.1.3 Commercial Cell Lines	56
4.1.4 Cell Treatments.....	56
4.2 DNA and RNA	57

4.2.1 Cell Transfection	57
4.2.2 Plasmid Constructs	57
4.2.3 RNA extraction and processing.....	58
4.3 Protein	59
4.3.1 Protein Extraction and Analysis.....	59
4.3.2 Protein immunoprecipitation assays.....	61
4.4 Immunostaining Assays.....	64
4.4.1 Histology, Immunohistochemistry and Immunohistofluorescence	64
4.5 Cell Viability	66
4.6 Animal Experiments.....	67
4.6.1 Generation of the <i>Stk11/Gnmt-dKO</i> mouse.....	68
4.6.2 Animal treatments	68
4.7 Human Samples	70
4.8 Liver Metabolomics analysis.....	71
4.9 Methionine and SAMe measurements.....	71
4.10 Lysosomal enzymatic activity	71
4.11 Energetic metabolic profile	71
4.12 ATP Detection Assay.....	71
4.13 Statistical Analysis	72
5. Results.....	73
5.1 Methionine and S-Adenosylmethionine levels are critical regulators of PP2A activity modulating lipophagy during steatosis.....	75
5.1.1 Background	75
5.1.2 SAMe and autophagy flux.....	75
5.1.3 <i>Gnmt-KO</i> mice have reduced MTOR activation and autophagic flux.....	75
5.1.4 SAMe, methionine, MTOR and PP2A methylation	78
5.2 Deregulated NEDDylation in liver fibrosis	81
5.2.1 Background	81
5.2.2 Altered NEDDylation in liver fibrosis	81
5.2.3 NEDDylation inhibition ameliorates bile acid- and CCl ₄ -induced cell death.....	85
5.2.4 NEDDylation inhibition decreases liver inflammation.....	85
5.2.5 NEDDylation plays a role in hepatic stellate cell activation.....	89
5.2.6 NEDDylation inhibition decreases fibrosis by inducing hepatic stellate cell apoptosis.....	93
5.3 SUMO2 retains LKB1 in the nucleus and increases hepatoma cell survival	95
5.3.1 Background	95
5.3.2 LKB1 expression is induced in low GNMT tumors from HCC patients	95
5.3.3 LKB1 localizes to the nucleus.....	97
5.3.4 LKB1 is modified by SUMO2 controlling its subcellular localization.....	98
5.3.5 LKB1 is SUMOylated during hypoxia.....	102
5.3.6 Acetylation is a prerequisite for SUMOylation.....	102
5.3.7 LKB1 in hypoxic liver	102
5.3.8 LKB1 SUMOylation increases cell survival.....	105
6. Supplemental	109

7. Discussion.....	113
8. Conclusions	123
8.1 Methionine and S-Adenosylmethionine levels are critical regulators of PP2A activity modulating lipophagy during steatosis	123
8.2 Deregulated NEDDylation in liver fibrosis	123
8.3 SUMO2 retains LKB1 in the nucleus and increases hepatoma cell survival.....	123
9. Bibliography	127
10. Support	153

Figures and Tables

Figures:

Figure 1. Sequential progression from NAFLD to HCC	21
Figure 2. Formation of the autophagosome	23
Figure 3. Hepatic methionine cycle.....	25
Figure 4. Fibrosis destroys the hepatic parenchyma	31
Figure 5. The PDGF and TGF- β pathways are profibrogenic in hepatic stellate cells	34
Figure 6. Liver Kinase B1	40
Figure 7. LKB1 is active in the cytoplasm	41
Figure 8. Post-translational modifications increase proteome complexity	44
Figure 9. Ubiquitin-like proteins share a similar life cycle	45
Figure 10. Generation of the Gnm1/Stk11-dKO mouse.....	67
Figure 11. Experimental procedures using MLN4924 in mice.....	69
Figure 12. SAMe and methionine alter autophagic flux in hepatocytes.....	76
Figure 13. SAMe and methionine reduce MTOR.....	77
Figure 14. Both SAMe and methionine are required for autophagy inhibition.....	77
Figure 15. Methylated PP2A inhibits MTOR.....	79
Figure 16. Methylated PP2A inhibits autophagic flux	80
Figure 17. NEDDylation is altered in human and murine fibrosis.....	82
Figure 18. NEDDylation in mouse liver cells	83
Figure 19. NEDDylation inhibition improves bile acid induced hepatic injury.....	84
Figure 20. NEDDylation inhibition improves liver health in CCl ₄ treated mice	86
Figure 21. NEDDylation inhibition decreases liver inflammation and reduces Kupffer cell activation.....	87
Figure 22. NEDDylation inhibition reduces fibrosis.....	88
Figure 23. NEDDylation plays a role in hepatic stellate cell activation	90
Figure 24. NEDDylation plays a role in Smad signaling	91
Figure 25. NEDDylation inhibition induces hepatic stellate cell apoptosis through c-Jun stability ...	92
Figure 26. LKB1 levels are increased in the absence of GNMT.....	95
Figure 27. Loss of LKB1 in the Gnm1-KO mouse improves liver health	96
Figure 28. LKB1 has a nuclear localization despite normal STRAD α levels.....	97
Figure 29. LKB1 is modified by SUMO2	99
Figure 30. SUMO2 increases LKB1 nuclear localization by disrupting its union with STRAD α	100
Figure 31. LKB1 SUMOylation increases during hypoxia	101
Figure 32. Acetylation is a prerequisite for LKB1 SUMOylation	103
Figure 33. Nuclear LKB1 increases hepatoma cell survival.....	104
Figure 34. NEDD8 influences the TGF- β pathway at different points.....	116
Figure 35. A SUMO/acetyl switch might control LKB1 localization.....	120

Supplemental Figure 1. Fibrosis from different etiologies increases hepatic NEDDylation 109

Supplemental Figure 2. Inflammation and fibrosis is present at the start of MLN4924 treatment... 110

Tables:

Table 1. Treatments and compounds used for in vitro experiments..... 56

Table 2. List of plasmids used in cell transfections..... 58

Table 3. List of siRNAs used in in vitro silencing assays 59

Table 4. List of mouse primers used..... 60

Table 5. List of human primers used..... 61

Table 6. List of commercial antibodies used for Western blot..... 62

Table 7. List of commercial antibodies used in immunohistochemistry 65

Table 8. List of antibodies used in immunofluorescence 65

Table 9. Characterization of liver fibrosis patients..... 69

Table 10. Characterization of HCC patients..... 70

Table 11. Oncomine database search for the STRAD α gene..... 98

Abbreviations



Post-translational Modifications in Liver Disease
Imanol Zubieta Franco

Abbreviations

4E-BP1- Eukaryotic Translation Initiation Factor 4E Binding Protein 1

5,10-MTHF- 5,10-Methylenetetrahydrofolate

5-MTHF- 5-Methyltetrahydrofolate

ACC1- Acetyl-CoA carboxylase 1

AFP- Alpha feto-protein

AKT- Serine/threonine kinase

ALT- Alanine aminotransferase

AMP- Adenosine monophosphate

AMPK- 5' adenosine monophosphate-activated protein kinase

APPBP1- Amyloid- β precursor protein binding protein 1

ARK- AMPK related kinase

AST- Aspartate aminotransferase

ATG- Autophagy gene

ATM- Ataxia telangiectasia mutated

ATP- Adenosine triphosphate

AU- Arbitrary units

BA- Bile acid

BAX- Bcl-2 associated protein X

BCL-2- β -cell lymphoma 2

BDL- Bile duct ligation

bFGF- Fibroblast growth factor

BHMT- Betaine homocysteine methyltransferase

BMP- Bone morphogenetic protein

CAMKK- Calcium/Calmodulin dependent protein kinase kinase

CAND1- Cullin-associated NEDD8-dissociated protein 1

CBS- Cystathionine-6-synthase

c-CBL- Casitas b-lineage lymphoma

CCL- C-C Motif chemokine ligand

CCl₄- Carbon tetrachloride

CCR- C-C Motif chemokine receptor

CDC2- Cell division cycle protein 2 homolog

cDNA- Complementary DNA

CDT1- Chromatin licensing and DNA replication factor 1

ChIP- Chromatin immunoprecipitation

CHLO- Chloroquine

CHREBP- Carbohydrate response element binding protein

COL1A1- Collagen type I alpha 1 chain

COP9- Constitutive photomorphogenesis 9

CRL- Cullin-RING E3 ubiquitin ligase

CXCL- C-X-C motif ligand

DAMP- Damage/danger associated molecular patterns

DAPI- 4',6-Diamidino-2-phenylindole

DCA- Deoxycholic acid

DEAZA- 3-Deazaadenosine

DEB- Drug eluting beads

dKO- Double knockout

DMSO- Dimethyl sulfoxide

DNA- Deoxyribonucleic acid

ECAR- Extracellular acidification rate

ECM- Extracellular matrix

EGF- Epidermal growth factor

EGFR- Epidermal growth factor receptor

ELISA- Enzyme-linked immunosorbent assay

FAT10- Ubiquitin D

FBS- Fetal bovine serum

FBW7- F-box and WD repeat domain containing 7

FSAP- Factor VII-activating protease

FXR- Farnesoid X receptor

G6PD- Glucose-6-phosphate dehydrogenase

GCN5- General control of amino-acid synthesis 5-like 2

GDF- Growth and differentiation factor

GLUT1- Glucose transporter type 1

GNMT- Glycine N-methyltransferase

Post-translational Modifications in Liver Disease

Imanol Zubiete Franco

GSH - Glutathione	LPS - Lipopolysaccharide
HBV - Hepatitis B virus	LTBP - Latent TGF- β binding protein
HCC - Hepatocellular carcinoma	MAPK - Mitogen-activated protein kinase
HCV - Hepatitis C virus	MARK - Microtubule affinity regulating kinase 1
HCY - Homocysteine	MAT - Methionine adenosyltransferase
HDAC - Histone deacetylase	MB-3 - Butyrolactone-3
HECT - Homologous to the E6-AP carboxyl terminus	MCP-1 - Monocyte chemotactic protein-1
HFD - High fat diet	MDD - Methionine deficient diet
HGF - Hepatocyte growth factor	MDM2 - Murine double minute 2
HIF - Hypoxia inducible factor	MLP29 - Mouse liver progenitor cells
HMGR - 3-Hydroxy-3-methylglutaryl-CoA reductase	MMP - Matrix metalloproteinase
HRP - Horse radish peroxidase	mRNA - Messenger RNA
HSC - Hepatic stellate cell	MS - Methionine synthase
HSC70 - Heat shock cognate protein 70	MTA - 5'-Methylthioadenosine
HuR - Human antigen R	MTHFR - Methylene tetrahydrofolate reductase
IF - Immunofluorescence	MTORC1 - Mechanistic target of rapamycin complex 1
IHC - Immunohistochemistry	MTT - 3-(4,5-Dimethylthiazol-2-yl)-2,5-diphenyltetrazolium bromide
IP - Immunoprecipitation	N/L - Ammonium chloride and leupeptin
ISG15 - Interferon-stimulated protein, 15 KDa	NADPH - Nicotinamide adenine dinucleotide phosphate
JAK - Janus kinase	NAE1 - NEDD8 activating enzyme E1 subunit 1
JNK - Jun N-terminal kinase	NAFL - Non-alcoholic fatty liver
K178R - Lysine 178 to arginine mutation (LKB1)	NAFLD - Non-alcoholic fatty liver disease
K48R - Lysine 48 to arginine mutation (LKB1)	NASH - Non-alcoholic steatohepatitis
KAT2A - Lysine acetyltransferase 2A	NCOR - Nuclear receptor corepressor 1
KC - Kupffer cell	NEDD8 - Neural precursor cell expressed, developmentally down-regulated 8
KDa - Kilodalton	NEDP1 - NEDD8-specific protease 1
KO - Knockout	NK - Natural killer cells
LAMP2A - Lysosome-associated membrane protein type 2A	NLS - Nuclear localization sequence
LAP - Latency-associated protein	NO - Nitric oxide
LC3 - Microtubule-associated proteins 1A/1B light chain 3A	NOS - Nitric oxide synthase
LCMT-1 - Leucine carboxyl methyltransferase-1	NSCLC - Non-small cell lung cancer
LDL - Low-density lipoprotein	NUAK - AMPK-related kinase 5
LKB1 - Liver kinase B1	OCR - Oxygen consumption rate

Abbreviations

PAI1 - Plasminogen activator inhibitor-1	RNA - Ribonucleic acid
PBS - Phosphate buffered saline	ROS - Radical oxygen species
PC - Phosphatidylcholine	RT - Room temperature
PCR - Polymerase chain reaction	RT-qPCR - Retrotranscription and real time quantitative PCR
PD - Pulldown	RXR - Retinoid X receptor
PDGF - Platelet-derived growth factor	SAE - SUMO activating enzyme
PDGFR - Platelet-derived growth factor receptor	SAH - S-adenosylhomocysteine
PE - Phosphatidylethanolamine	SAHH - S-adenosylhomocysteine hydrolase
PEMT - Phosphatidylethanolamine N-methyltransferase	SAMe - S-adenosylmethionine
PGD - Phosphogluconate dehydrogenase	SBE - Smad binding element
PI3K - Phosphatidylinositol 3-kinase	SCF - Skp2-cullin-F-box
PI3P - Phosphatidylinositol 3-phosphate	SENP - Sentrin-specific proteases
PIAS - Protein inhibitor of activated STAT	SH2 - Src homology 2
PJS - Peutz-Jeghers syndrome	SHP-2 - Tyrosine-protein phosphatase non-receptor type 11
PKA - Protein kinase A	SIM - SUMO interacting motif
PKC - Protein kinase C	SIRT1 - Sirtuin 1
PP2A - Protein phosphatase 2A	SKP2 - S-phase kinase-associated protein 2
PPAR - Peroxisome proliferator-activated receptor	SLC2A1 - Solute carrier family 2 member 1
PS - Phosphatidylserine	SMURF - Smad specific E3 ubiquitin protein ligase
PSAG - Penicillin, streptomycin, anfotericine B and glutamine	SNON - Ski-like proto-oncogene
PSG - Penicillin, streptomycin, and glutamine	SOCS - Suppressor of cytokine signaling
PTEN - Phosphatase and tensin homolog	SPARC - Secreted protein acidic and rich in cysteine
PTM - Post-translational modification	SQSTM1 - Sequestosome 1
RAF - Rapidly accelerated fibrosarcoma	SREBP1C - Sterol regulatory element-binding protein 1c
RANBP2 - RAN binding protein 2	STAT - Signal transducer and activator of transcription
RANGAP - Ran GTPase activating protein	STK11 - Serine/threonine kinase 11
RAR - Retinoic acid receptor	STRADα - STE-20-related adaptor alpha
RAS - Rat sarcoma	SUMO - Small ubiquitin-like modifier
RasGAP - Ras GTPase activating protein	TACE - Transcatheter arterial chemoembolization
RasGRP3 - Ras guanyl releasing protein 3	TFEB - Transcription factor EB
RASSF - Ras association domain-containing protein	TG - Triglyceride
RBX - RING box protein	TGF-β - Transforming growth factor beta
RING - Really interesting new gene	TGIF - TGF- β induced factor homeobox 1

Post-translational Modifications in Liver Disease

Imanol Zubieta Franco

THF- Tetrahydrofolate

TIMP- Tissue inhibitor of metalloproteinases

TKR- Tyrosine kinase receptor

TKT- Transketolase

TLR- Toll-like receptor

TNFR- TNF receptor

TNF- α - Tumor necrosis factor alpha

TRAIL- TNF-related apoptosis-inducing ligand

TRIP12- Thyroid hormone receptor interactor 12

TSC- Tuberous sclerosis complex

TUNEL- terminal deoxynucleotide transferase dUTP nick end labeling

T β R- TGF- β receptor

UB- Ubiquitin

UBA3- Ubiquitin-activating enzyme 3

UBC9- Ubiquitin carrier protein 9

UBE- Ubiquitin conjugating enzyme

UBL- Ubiquitin-like

UCP-2- Uncoupling protein 2

UFM1- Ubiquitin fold modifier 1

ULK1- UNC51-like kinase 1

UVC- Ultraviolet C

VEGF- Vascular endothelial growth factor

VHL- Von Hippel-Lindau tumor suppressor

VLDL- Very-low-density lipoprotein

WB- Western blot

WIPI- WD repeat domain phosphoinositide-interacting protein

WT- Wild type

α SMA- Alpha smooth muscle actin

Resumen/Summary

Post-translational Modifications in Liver Disease
Imanol Zubieta Franco

1.1 Resumen

La enfermedad hepática crónica es un término que incluye una larga lista de patologías hepáticas y que suele finalizar con la pérdida de integridad del parénquima hepático degenerando en cirrosis y carcinoma hepatocelular (CHC). La enfermedad hepática crónica puede estar causada por distintas etiologías, como la infección por los virus de la hepatitis B y C, toxinas, consumo de alcohol y drogas, enfermedades autoinmunes y hereditarias y la enfermedad del hígado graso no alcohólica (EHGNA). Se han investigado múltiples mecanismos moleculares que dan lugar a la enfermedad hepática crónica, aunque hoy en día la contribución de las modificaciones postraduccionales a esta enfermedad es un área aún por estudiar.

Las modificaciones postraduccionales (PTM) se producen por la conjugación reversible de una proteína o un grupo funcional a determinada proteína diana. Las PTM regulan tanto la activación como la inactivación de sus proteínas dianas, e inducen cambios en la localización celular, degradación/estabilidad, formación de complejos, etc. Dentro de las modificaciones postraduccionales, nuestros estudios se han dirigido a las denominadas “*Ubiquitin like*” (UBL), que incluyen todas las modificaciones ocasionadas por proteínas cuya función sea similar a la ubiquitina. Se estima que hay alrededor de 16 UBL con funciones y actividades distintas. Todas ellas comparten un ciclo de vida parecido con similitudes en su activación y procesamiento. Hoy en día, hay tres UBL que concentran la atención de la mayoría de las investigaciones: la ubiquitina, SUMO y NEDD8. NEDD8 (Neural precursor cell expressed developmentally downregulated-8) es una de las UBL más similares a la ubiquitina (59%) pero tiene dianas y funciones completamente distintas. La principal función de NEDD8 consiste en estabilizar las proteínas a las que modifica alargando su vida media. La proteína diana mejor conocida de esta UBL son las conocidas como “*cullins*” que forman parte de los complejos cullin-RING-ligasas (CRL). Las CRL son complejos E3 que ubiquitinizan a una gran variedad de proteínas involucradas en distintos procesos celulares como el ciclo celular, crecimiento celular, replicación del ADN, y transmisión de señales. Recientemente, se han

identificado nuevas dianas de NEDD8 diferentes a las CRL como son Mdm2, T β R11 y HuR. Por su parte, SUMO (small ubiquitin-related modifier) es una UBL que está compuesta por 3 isoformas: SUMO1, SUMO2, y SUMO3. La unión de SUMO a diferentes proteínas diana esta mediada por una secuencia consenso para este motivo, y las modificaciones que provoca tienen varias funciones en su correspondiente diana. Entre las más relevantes se encuentran cambios en la localización celular y la actividad de la proteína diana, así como su capacidad de interacción con otras proteínas para la formación de diferentes complejos macromoleculares. La conjugación de grupos funcionales a moléculas biológicas también ha sido ampliamente estudiada. Uno de los grupos funcionales más estudiados es la fosforilación, sin embargo, otros grupos funcionales como la metilación y acetilación también están adquiriendo importancia durante los últimos años. La metilación y la acetilación pueden afectar tanto a las proteínas como al ADN de la célula, pero son principalmente conocidos por su contribución al código de las histonas. Este código es el que determina el grado de empaquetamiento del ADN alrededor de las histonas y puede dar lugar a la represión de la transcripción génica.

El principal objetivo de este proyecto es el estudio de la contribución de las modificaciones postraduccionales al desarrollo de la enfermedad hepática crónica derivada del hígado graso no alcohólico en sus diferentes estadios: esteatosis, fibrosis y CHC.

La EHGNA es una de las principales enfermedades hepáticas crónicas en los países desarrollados, y se encuentra asociada a factores de riesgo del síndrome metabólico (obesidad, resistencia a la insulina, dislipidemia e hipertensión), incluyendo alteraciones como la esteatosis hasta la esteatohepatitis no alcohólica (EHNA). Una alta proporción de pacientes con EHGNA sufren alteraciones en el metabolismo de la metionina y la S-adenosilmetionina (SAME). SAME es el principal donante de grupos metilo en el organismo y su síntesis está controlada por las enzimas metionina adenosiltransferasa (MAT) y glicina N-metiltransferasa (GNMT). GNMT metaboliza SAME en la célula evitando su acumulación. En humanos, la pérdida de la expresión o la actividad de GNMT conllevan el desarrollo de EHNA, cirrosis y CHC. Centrándonos en el desarrollo de EHNA, hemos

identificado recientemente que la pérdida de la capacidad autofágica del hígado es uno de los mecanismos por los que se induce la acumulación de vesículas lipídicas en el hígado en ausencia de GNMT. En la autofagia, la célula recicla componentes citoplasmáticos mediante su secuestro en vacuolas y posterior fusión con lisosomas donde son degradados. La autofagia permite a la célula reciclar componentes para regenerar ATP en condiciones de escasez de energía (la autofagia suele estar inhibida en condiciones de energía abundante) y en ciertos casos eliminar componentes celulares dañados o viejos como por ejemplo las mitocondrias. En el modelo de ratón *Gnmt-KO* (que desarrolla de forma totalmente espontánea EGHNA, cirrosis y CHC por la acumulación crónica de SAME) descubrimos que la autofagia estaba inhibida en los hepatocitos debido a una disfunción lisosomal. Este efecto resultó estar mediado por la regulación de la actividad de la fosfatasa PP2A (protein phosphatase 2A) a través de su metilación y no a través de MTOR (mechanistic target of rapamycin) aunque desconocemos el mecanismo por el que actúa esta fosfatasa.

Uno de los principales riesgos en el desarrollo de la enfermedad crónica EGHNA es su progresión a fibrosis, cirrosis y CHC. Durante la fibrosis se genera una matriz extracelular compuesta por colágeno y otras proteínas extracelulares. En condiciones normales la matriz extracelular sirve para ayudar a regenerar el hígado tras un insulto que ha dañado el parénquima hepático, sin embargo, durante enfermedades crónicas como la enfermedad hepática crónica el insulto es persistente y por lo tanto la matriz extracelular se mantiene en con el tiempo incluso aumentando hasta el punto en el que se pierde la función hepática. La célula principal implicada en la repuesta fibrótica es la célula estrellada (HSC). Las HSC se encuentran de un modo inactivo en un hígado sano presentando gotas de vitamina A en su citoplasma. Tras el daño hepático estas células se activan, reduciendo sus niveles de vitamina A, aumentando su motilidad y su producción de colágeno. Las HSC son actualmente una diana para el tratamiento de la fibrosis aunque todavía no se ha descubierto un tratamiento efectivo que pueda evitar o reducir su activación o inducir su muerte vía apoptosis. Nuestros resultados muestran que la PTM NEDD8 se encuentra aumentada en ratones y pacientes humanos con fibrosis. Este aumento ocurre en los principales tipos celulares del

hígado: el hepatocito, la célula estrellada, y las células proinflamatorias de Kupffer. Por tanto, inhibiendo la NEDDilización se previno la aparición de la fibrosis en ratones en diferentes modelos de esta patología. Es importante señalar que la inhibición de esta PTM afecta de forma diferente a los distintos tipos celulares en el contexto fibrótico. En hepatocitos, la inhibición de la NEDDilización protege de la apoptosis, mientras que en las células de Kupffer previene la activación y en las HSC induce la respuesta apoptótica a través de la estabilización de c-Jun. La PTM NEDD8 también ejerce una función en la estabilidad de la proteína señalizadora SMAD2. Esta proteína transmite la señal desde los receptores de TGF- β (la citoquina transforming growth factor beta es una de las citoquinas mas fibrogenicas) y nuestros resultados también demuestran que NEDD8 puede ser importante en su estabilidad, facilitando la activación de los genes profibrogenico. También encontramos indicios de que SMAD2 puede ser directamente una diana de NEDD8 y que es modificada por este PTM. En conjunto, nuestros resultados demuestran la importancia de la PTM NEDD8 en el desarrollo y la regresión de la fibrosis.

Los pacientes cirróticos pueden progresar a CHC, siendo ésta la segunda causa de muerte por cáncer. El CHC aparece por la modulación (activación/inhibición) de diversas rutas de proliferación que se activan en los hepatocitos convirtiéndole en uno de los tumores más difíciles de tratar con éxito ya que al atacar una ruta el tumor compensa con otra vía. El CHC tambien presenta otra dificultad en su tratamiento ya que casi siempre está presente en un hígado cirrótico lo que reduce las posibilidades de tratamiento al estar el órgano ampliamente dañado. La quinasa hepática B1 (LKB1) identificada previamente como un supresor de tumores por su habilidad en activar AMPK e inducir muerte celular se ve aumentada en pacientes con un CHC avanzado. En ausencia de GNMT tanto en pacientes como en el modelo de ratón *Gnmt-KO*, la actividad de LKB1 se encuentra inducida y se requiere su presencia para el desarrollo de fibrosis y CHC como se demuestra en el hígado completamente sano que presentan el modelo de ratón doble *KO Gnmt/Stk11* donde se anula la expresión de LKB1 en un entorno donde GNMT está ausente. La característica que define la actividad protumoral de LKB1 en el hígado es su asociación con la vía de Ras. Hemos podido

identificar que tanto la inducción como el silenciamiento de LKB1 en modelos in vivo de ratón, así como en células de hepatoma, regula los niveles del activador de la vía Ras, RasGRP3. Este hecho se produce tanto a nivel de ARN mensajero como de proteína. En este contexto es importante señalar que en CHC se detecta un aumento de la localización nuclear de LKB1 a pesar de que no se produzcan cambios significativos en su proteína adaptadora STRAD α (STE20-related kinase adaptor alpha). Nuestros resultados demuestran que LKB1 se encuentra SUMOilado por SUMO2 y que esta modificación es la responsable de la pérdida de unión a STRAD α y de su posterior retención en el núcleo. Esta SUMOilación ocurre en la lisina 178 que se localiza dentro de la secuencia consenso para SUMO en LKB1. La SUMOilación de LKB1 aumenta en un entorno hipóxico característico de los tumores y requiere un paso previo de acetilación para que se produzca. La SUMOilación de LKB1 y su localización nuclear confiere ventajas proliferativas y un mayor rendimiento metabólico a los tumores hepáticos. LKB1 nuclear actúa como un factor de transcripción regulando la actividad de genes proliferadores y metabólicos entre ellos RasGRP3.

En conclusión, nuestros resultados muestran que las modificaciones postraduccionales tienen una contribución importante en la aparición de las distintas fases de la enfermedad crónica hepática. En la primera fase, la esteatosis, la metilación contribuye a inhibir la autofagia mediante la activación de la fosfatasa PP2A mientras que la NEDDilización facilita la aparición de fibrosis al facilitar la activación y supervivencia de las células estelares. Finalmente la SUMOilación de la proteína LKB1 facilita la supervivencia y replicación del tumor hepático al retener a la quinasa en el núcleo.

1.2 Summary

Chronic liver disease is a term that includes a long list of hepatic pathologies that end with the loss of hepatic parenchyma and leads to cirrhosis and hepatocellular carcinoma (HCC). Chronic liver disease can be caused by different etiologies such as hepatitis B and C virus infection, toxins, alcohol and drug abuse, autoimmune and hereditary disease, and non-alcoholic fatty liver disease (NAFLD). Research into the multiple mechanisms that give rise to chronic liver disease have been extensively studied but the contribution of post-translational modifications to this disease is still lacking.

Post-translational modifications (PTM) are the reversible addition of a protein or functional group to a target protein. PTMs can regulate the activity/inactivity of target proteins, changes in subcellular localization, degradation/stability, complex formation, etc. Within the PTMs, our studies have been directed towards the “Ubiquitin-like” (UBL) proteins that are similar to ubiquitin. There are an estimated 16 UBLs with different functions in the cell but all of them share similar activation and processing. Currently, the three most studied UBLs are ubiquitin, SUMO, and NEDD8. NEDD8 (Neural precursor cell expressed developmentally downregulated-8) is the UBL that is most similar to ubiquitin (59%) but it has completely different targets and functions. NEDD8 is mainly involved in protein stability and the proteins it modifies have an increased half-life. Its most studied targets are the cullins, which form part of the cullin-RING-ligases (CRL). CRLs are E3 complexes that ubiquitinate a large variety of proteins involved in different cellular processes such as cell cycle, cell growth, DNA replication, and signal transmission. Recently, new NEDD8 non-CRL targets have been identified such as Mdm2, T β RII, and HuR. SUMO (small ubiquitin-related modifier) is an UBL composed of 3 isoforms: SUMO1, SUMO2, and SUMO3. Conjugation of SUMO to its target proteins is controlled by a consensus sequence. The effects that SUMO exerts on its target proteins include changes in cellular localization and protein activity, protein interaction and ability to form macromolecular complexes.

The main objective of this project is to study the contribution of post-translational modifications to the development of chronic liver disease derived from non-alcoholic fatty liver in its different stages: steatosis, fibrosis, and HCC.

NAFLD is one of the main chronic liver diseases in developed countries and is commonly associated with metabolic syndrome risk factors (obesity, insulin resistance, dyslipidemia, and hypertension) and ranges from steatosis to non-alcoholic steatohepatitis (NASH). A large portion of patients with NAFLD suffer alterations in the metabolism of methionine and S-adenosylmethionine (SAME). SAME is the principal methyl group donor in the cell and its synthesis is controlled by the enzymes methionine adenosyltransferase (MAT) and glycine N-methyltransferase (GNMT). GNMT metabolizes SAME to avoid its accumulation in the cell. In humans, loss of GNMT expression or activity leads to the development of NAFLD, cirrhosis, and HCC. Working on the development of NAFLD, we recently identified that the loss of hepatic autophagy is one of the mechanisms that induces the accumulation of lipid droplets in the liver in the absence of GNMT. In autophagy, the cell recycles cytoplasmic components by sequestering them in vacuoles and their posterior fusion with lysosomes that degrade the contents. We discovered in the *Gnmt-KO* mouse model (that spontaneously develops NAFLD, cirrhosis, and HCC due to the chronic accumulation of SAME) that autophagy was inhibited in hepatocytes due to dysfunctional lysosomes. This was due to the regulation of the phosphatase PP2A's activity via its methylation.

One of the main risks of NAFLD is its possible progression to fibrosis, cirrhosis, and HCC. During fibrosis an extracellular matrix composed of collagen and other extracellular proteins is deposited in the liver. The main cell involved in this response is the hepatic stellate cell (HSC). HSC are normally found in an inactive state in healthy livers with vitamin A droplets in their cytoplasm. During hepatic injury, these cells are activated and in the process reduce their vitamin A levels, increase their motility and the production of extracellular matrix. HSC are currently a therapeutic target for the treatment of fibrosis although no effective treatment that can reduce their activation or induce HSC cell death has been discovered. Our results show that the PTM NEDD8 is increased in mice and human patients with fibrosis. This increase occurs in the main types of hepatic cells: hepatocytes, hepatic stellate

cells, and the proinflammatory Kupffer cells. In line with this, when NEDDylation is inhibited we could prevent the development of fibrosis in different fibrotic mouse models. Importantly, inhibiting NEDD8 affects the different cell types in varying ways during fibrosis. In hepatocytes, the inhibition of NEDDylation protects them from apoptosis, while at the same time reducing Kupffer cell activation and inducing the apoptotic response through c-Jun stabilization in HSC. These results demonstrate the importance of the PTM NEDD8 in the development and regression of fibrosis.

Cirrhotic patients can progress to HCC, the second cause of cancer related death. The dysregulation (activation/inhibition) of a diverse set of proliferation pathways that are activated in hepatocytes leads to the development of HCC. The liver kinase B1 (LKB1), previously identified as a tumor suppressor due to its ability to activate AMPK and induce cell death, is increased in patients with advanced HCC. In the absence of GNMT, both in patients and in the *Gnmt-KO* mouse model, the activity of LKB1 is induced and is required for the development of fibrosis and HCC as seen by the double *KO Gnmt/Stk11* mice that lack LKB1 and GNMT and have healthy livers. The protumoral activity of LKB1 is associated with the Ras pathway. We observed that expressing and silencing LKB1 in mice and hepatoma cells controls the levels of RasGRP3, an activator of the Ras pathway, which happens both at the mRNA and protein level. In this context, we detected an increase in the nuclear localization of LKB1 in HCC although no significant changes in the levels of its adaptor protein STRAD α were found. Our results show that LKB1 is SUMOylated by SUMO2 and that this modification inhibits the formation of the LKB1-STRAD α complex retaining LKB1 in the nucleus. SUMOylation occurs on lysine 178 which is also found within a SUMO consensus sequence. SUMOylation of LKB1 increases in a hypoxic environment, a characteristic of solid tumors, and requires a previous acetylation step to occur. LKB1 SUMOylation and nuclear localization gives hepatic tumors a growth advantage and increased metabolic performance. LKB1 can also act as a transcription factor regulating the activity of proliferation and metabolic related genes such as RasGRP3.

In conclusion, our results show that post-translational modifications have an important contribution to the development of the different stages of chronic liver disease. In steatosis, methylation helps inhibit autophagy while NEDDylation facilitates the appearance of fibrosis. Finally, SUMOylation of LKB1 increases the survival and replication of the hepatic tumor.

Post-translational Modifications in Liver Disease
Imanol Zubieta Franco

Introduction



Post-translational Modifications in Liver Disease
Imanol Zubieta Franco

2. Introduction

2.1 Chronic Liver Disease

Chronic liver disease is a term that encompasses a wide range of hepatic pathologies lasting longer than 6 months that progressively destroy the liver parenchyma generally ending in cirrhosis and hepatocellular carcinoma (HCC) (1,2) and is one of the leading causes of death in the U.S. and in Europe (1,2). Chronic liver disease can be caused by a wide range of pathologies including hepatitis B and C virus infections, toxins, alcohol and drug abuse, autoimmune diseases, hereditary diseases and Non-alcoholic Fatty Liver Disease (NAFLD) (1,3).

2.1.1 Non-alcoholic Fatty Liver Disease

NAFLD is emerging as one of the most common causes of chronic liver disease in the western hemisphere (1) with 10 to 25 % of the general population affected with some form of NAFLD (4). NAFLD is a clinical term that includes a set of hepatic diseases starting from simple triglyceride accumulation in hepatocytes (steatosis, non-alcoholic fatty liver; NAFL) to hepatic steatosis with inflammation and fibrosis (non-alcoholic steatohepatitis; NASH) (**Figure.1**) (3,5).

NAFLD is generally considered the hepatic manifestation of the metabolic syndrome, a clustering of several conditions that increase the probability of developing cardiovascular disease and diabetes (1,2). Among the conditions of the metabolic

syndrome that can lead to NAFLD are obesity, type 2 diabetes, insulin resistance, hypertension and dyslipidemia (1,4). NAFLD is more frequent in patients with diabetes (50%) and obesity (76%) and is almost universal in morbidly obese patients (6). NAFLD cases are expected to rise in the near future as patients with metabolic syndrome increase in developed countries (1).

The main theory for the progression of NAFLD is the “two hit” hypothesis (5). According to the two hit hypothesis the liver suffers an initial “hit” in the form of dyslipidemia which leads to NAFL/steatosis. NAFL is generally considered a less progressive form of NAFLD with very few steatotic patients fully progressing to NASH (3) and it is usually treated by eliminating the underlying cause such as suggesting a change in lifestyle (1). Because only around 10% of NAFL patients progress to NASH, researchers believe that a second “hit” is required for the disease to advance (5,7). Possible second hits are increased endorecticular stress and increased radical oxygen species (ROS) production (5,7). Increased ROS due to insulin resistance, overtime, leads to increased mitochondrial dysfunction and more hepatocyte apoptosis which in turn develops into hepatitis, hepatocyte ballooning and fibrosis (5).

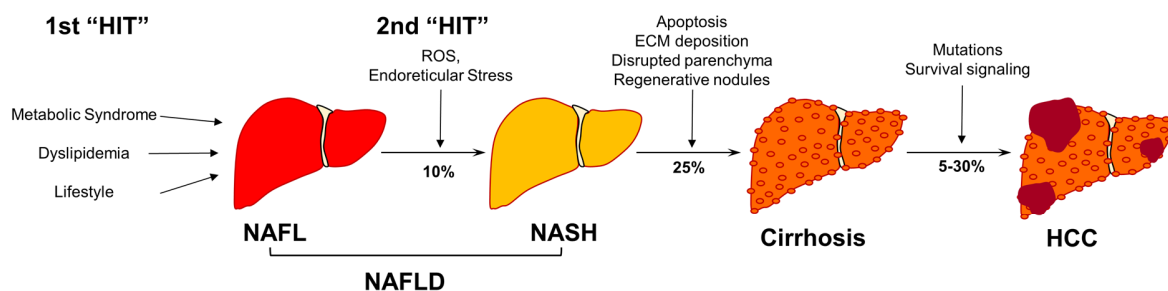


Figure 1. Sequential progression from NAFLD to HCC. Non-alcoholic fatty liver (NAFL) develops after a 1st “hit” increases triglyceride levels. A 2nd “hit”, in the form of reactive oxygen species (ROS) or endorecticular stress, can lead 10% of NAFL patients to develop non-alcoholic steatohepatitis (NASH). Continued damage in 25% of patients can result in the activation of the fibrotic response and the formation of cirrhosis. Finally, approximately 5-30% of cirrhotic patients may develop hepatocellular carcinoma (HCC), the primary tumor of the liver.

2.1.2 Lipid Homeostasis

As mentioned previously, an excess accumulation of fat in the liver is one of the primary manifestations of NAFLD. The liver is one of the main organs responsible for the storage and metabolism of fatty acids, and hepatic steatosis results mainly from an excessive delivery of lipids into the liver, and from a misbalance in *de novo* lipid synthesis and catabolism in hepatocytes. There are several pathways by which the liver can regulate lipid metabolism and that can be altered during NAFLD (7):

De novo lipogenesis/Import: The liver is able to synthesize fatty acids by *de novo* lipogenesis using glucose and proteins via acetyl CoA. Lipids can also be imported from the peripheral adipose tissues which are a large source of fatty acids. Finally, fatty acids from the diet are transported to and processed directly by the liver.

β -oxidation/Lipid disposal: The liver can break down fatty acids via β -oxidation as a means of obtaining energy from them. The liver can also export lipids in VLDL (very-low-density lipoproteins) to other tissues in the body. When synthesis and import of fatty acids is increased with respect to β -oxidation or transport, lipids accumulate in the liver.

Lipid storage and breakdown: Excess fatty acids are stored as triglycerides in highly dynamic organelles called lipid droplets. They can grow in response to increased fatty acid quantities or shrink in size and disperse the accumulated fatty acids when required (8). Until recently, it was thought that only a few lipases were responsible for the release of fatty acids stored in lipid droplets. However, this was unable to explain how hepatocytes (that have low lipase levels) are able to quickly mobilize large amounts of their lipid droplets when needed (9). One recently discovered mechanism by which hepatocytes catabolize their lipid droplets is a type of autophagy called lipophagy (10).

2.1.3 Lipophagy

2.1.3.1 Autophagy

Lipophagy is a type of autophagy dedicated to the digestion of stored lipids in lipid droplets (10,11). Autophagy, which translates as eating oneself, is a conserved cellular recycling pathway that delivers

specific cellular cargo to acidic lysosomes for digestion. This cargo can range from proteins to entire organelles and allows the cell to maintain energy homeostasis in times of stress such as starvation (11–13). There are three main forms of autophagy:

Microautophagy: The least studied form of autophagy. This form involves the direct sequestration of cargo by invaginations of lysosomal and late endosomal membranes followed by its degradation (14).

Chaperone-mediated autophagy (CMA): This form of autophagy targets proteins that contain the KFERQ motif. This motif is recognized by the heat shock cognate protein 70 (Hsc70), forming a substrate protein-chaperone complex. This complex is then delivered to the lysosome surface, where it is recognized by the CMA receptor lysosome-associated membrane protein type 2A (LAMP-2A). Finally, the target protein unfolds and enters the lysosome with the help of LAMP-2A (15).

Macroautophagy: Macroautophagy entails the formation of a new double-membrane vesicle, or autophagosome that isolates specific cargo from the rest of the cytoplasm and delivers it via membrane fusion to lysosomes for degradation. The whole process requires the coordinated activity of approximately 30 proteins and is strictly regulated (16). Since macroautophagy is involved in the digestion of many types of cellular components, different terms have appeared to specify the cargo that is isolated: mitophagy for mitochondria, lipophagy for lipids, peroxiphagy for peroxisomes, ribophagy for ribosomes, myelinophagy for myelin and xenophagy for microorganisms (17,18).

2.1.3.2 Macroautophagy

Macroautophagy (referred to mainly as autophagy) is mainly carried out by the autophagy gene (Atg) proteins that were discovered in yeast genetic screens (19). The formation of an autophagosome requires at least three steps: initiation, nucleation, and elongation/enclosure (**Figure.2**).

Initiation: Autophagy initiation results in the activation of ULK1 (UNC51-like kinase) and its recruitment to the phagophore or pre-autophagosomal structure. This in turn recruits

the Atg14, vps15, vps34, and Beclin-1 complex with active class III PI3K (phosphatidylinositol 3-kinase) activity (20,21).

Nucleation: The PI3K complex produces PI3Ps (phosphatidylinositol 3-phosphate) which further recruit Atgs to the phagophore. These include, WIPI1 and WIPI2 (WD repeat domain phosphoinositide-interacting protein) which allow for the maturation of the autophagosome by recruiting Atg9 and facilitating the lipidation of LC-3 (16,22). Atg9 is currently the only known member that controls membrane delivery to the growing autophagosome (23). The initial membrane originates from either the endoplasmic reticulum, the golgi or the mitochondria, although it is still unclear which organelle is the most important (24).

Elongation/Closure: Elongation and closure of the autophagosome requires the formation of two different Atg complexes: the ATG12-ATG5-ATG16 complex and the ATG7-ATG3-LC3 complex. Both of these complexes are ubiquitin-like conjugation systems that are formed in cascades (16). The ATG7-ATG3 system cleaves the insoluble microtubule-associated protein 1 light chain 3 (LC3/Atg8) into a soluble form or LC3-I. The ATG12-ATG5-ATG16 system then binds a lipid moiety (phosphatidylethanolamine) to LC3-I, in the presence of Atg3 and Atg7, to form LC3-II (25). LC3-II is essential for correct autophagosome function and is a molecular signature of the autophagosome (26,27).

2.1.3.3 Regulation of autophagy

Autophagy is a complex process that is tightly regulated. Some of the main check points for autophagy are mechanistic target of rapamycin (MTOR) and 5' adenosine monophosphate-activated protein kinase (AMPK) (**section 2.7.1.1**) (28). MTOR is the nutrient sensor of the cell and when abundant, MTOR inhibits the initiation of autophagy by phosphorylating and inhibiting Ulk1 (28). This ensures that autophagy is not active when there is an abundance of nutrients for the cell. On the other hand, under prolonged starvation, AMPK activates Ulk1 by phosphorylation at different residues (28). AMPK can also inhibit MTOR (**section 2.7.1.2**). Along with MTOR and AMPK, Atg and lysosomal gene expression can also be regulated. The HLH-leucine zipper

transcription factor EB (TFEB) has been identified as a master regulator of Atg and lysosomal genes, importantly; TFEB is also controlled by MTOR. MTOR phosphorylates TFEB leading to its retention in the cytoplasm and reducing its ability to activate autophagy (29).

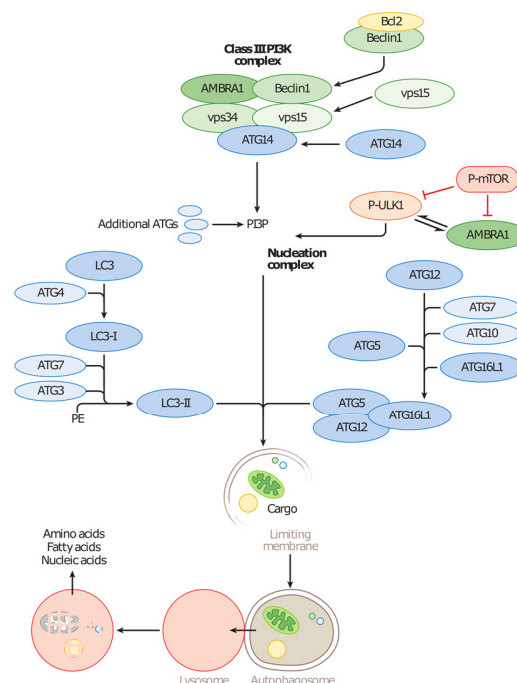


Figure 2. Formation of the autophagosome. Schematic representation showing some of the proteins and steps required for the formation of the autophagosome in macroautophagy and its posterior fusion with the lysosome. Adapted from (11)

2.1.4 Autophagy and NAFLD

Since autophagy is able to remove large quantities of lipids in hepatocytes, autophagy may play a protective role in the pathogenesis of NAFLD. Autophagy can protect the liver from the first "hit" by eliminating the accumulation of lipids in hepatocytes (10). In the initial report, Singh et al. demonstrated that autophagy was able to digest lipid droplets by surrounding small droplets or pinching parts from larger lipid droplets. Inhibiting autophagy or silencing Atg genes in hepatocytes leads to an increase in lipid droplet accumulation suggesting that a defective autophagy may induce lipid accumulation in livers. Autophagy might also

be able to protect the liver from the second “hit” by eliminating damaged mitochondria that increase reactive oxygen species, misfolded proteins that increase ER stress, and toxic lipid species such as sphingolipid derived ceramides (30). At the same time autophagy supplies the hepatocyte with ATP to sustain an antioxidant response as hepatocytes are prone to drug induced oxidative stress and damage (31). On the other hand, hepatocytes or mice overexpressing parts of the autophagy pathway have reduced lipid accumulation and improved liver and insulin resistance (10,32). Importantly, drugs known to induce steatosis such as antiretrovirals act by inhibiting autophagy (33) and drugs like the anticonvulsant carbamazepine have been shown to reduce hepatic steatosis by activating autophagy (34). This experimental evidence suggests that autophagy could be inhibited during NAFLD. Several mechanisms have been proposed that may cause NAFLD:

- Overnutrition leads to a hyperactivation of MTOR which in turn leads to a chronic inhibition of autophagy. This then leads to further lipid accumulation (12).
- In situations of hepatic steatosis, increased lipid accumulation can change the membrane lipid composition of both autophagosomes and lysosomes reducing their fusogenic capacity. Lysosomes from high fat diet (HFD) fed mice have up to 60% less cholesterol in membranes and lumen, and have a reduced fusion with autophagosomes. In addition, HFD lysosomes also show reduced fusion with autophagosomes from healthy mice (35).

Due to the dynamic nature of autophagy, only a few studies examined autophagy in human samples. The study of autophagic flux requires the use of autophagy inhibitors to monitor the differences between groups, making the study of autophagy flux in humans complex. However, biopsies have shown that SQSTM1, a protein that recognizes ubiquitinated cargo, accumulates in steatosis pointing to an inhibited autophagy (36).

2.2 Methionine and liver disease

Lipid metabolism is not the only aspect affected by liver disease. Many patients with liver disease suffer from hypermethioninemia, a condition that was first

discovered by Kinsell in 1947, after demonstrating that liver cirrhosis patients had reduced methionine clearance after an intravenous injection (37). Similarly, patients with alcoholic liver disease have elevated levels of methionine in plasma that correlates with the prognosis of malignancy (38). Earlier, Best demonstrated that rats fed with a diet deficient in methyl groups (methionine, choline, and folates) developed steatohepatitis, fibrosis and HCC (39), underscoring the importance of methionine levels in the liver.

2.2.1 S-adenosylmethionine and the methionine cycle

Methionine is an essential amino acid that is the precursor to S-adenosylmethionine (SAME, SAM or AdoMet), which is the universal biological methyl donor. Despite being synthesized in all cells of the body, the liver amounts for approximately 85% of all reactions using SAME and approximately 50% of methionine metabolism (40,41). SAME is involved in transmethylation reactions that donate its methyl group to DNA, RNA, proteins, sugars, phospholipids, and even atoms such as arsenic (40,42). SAME is not only restricted to transmethylation reactions. It also takes part in the synthesis of polyamines, compounds necessary for cell division and in the liver, intestine and brain it takes part in transsulfuration reactions as a precursor for cysteine and glutathione, a potent cellular antioxidant (43–45).

In the liver, SAME is synthesized from L-methionine and ATP by methionine adenosyltransferase I and III (MATI/III, **section 2.2.3.1, Figure.3**). SAME can then be demethylated by glycine N-methyltransferase (GNMT, **section 2.2.3.2, Figure.3**) or approximately 200 other putative SAME methyltransferases to S-adenosylhomocysteine (SAH) (46). Alternatively, SAME can be decarboxylated by adenosylmethionine decarboxylase and its remaining aminopropyl group enters the polyamine synthesis pathway (**Figure.3**). One aminopropyl group is transferred to putrescine to form spermidine and another to spermidine to form spermine (43,44). SAH levels are controlled by SAH hydrolase (SAHH) which reversibly catalyzes it into homocysteine (HCY) and adenine. HCY can enter the liver specific transsulfuration pathway as a

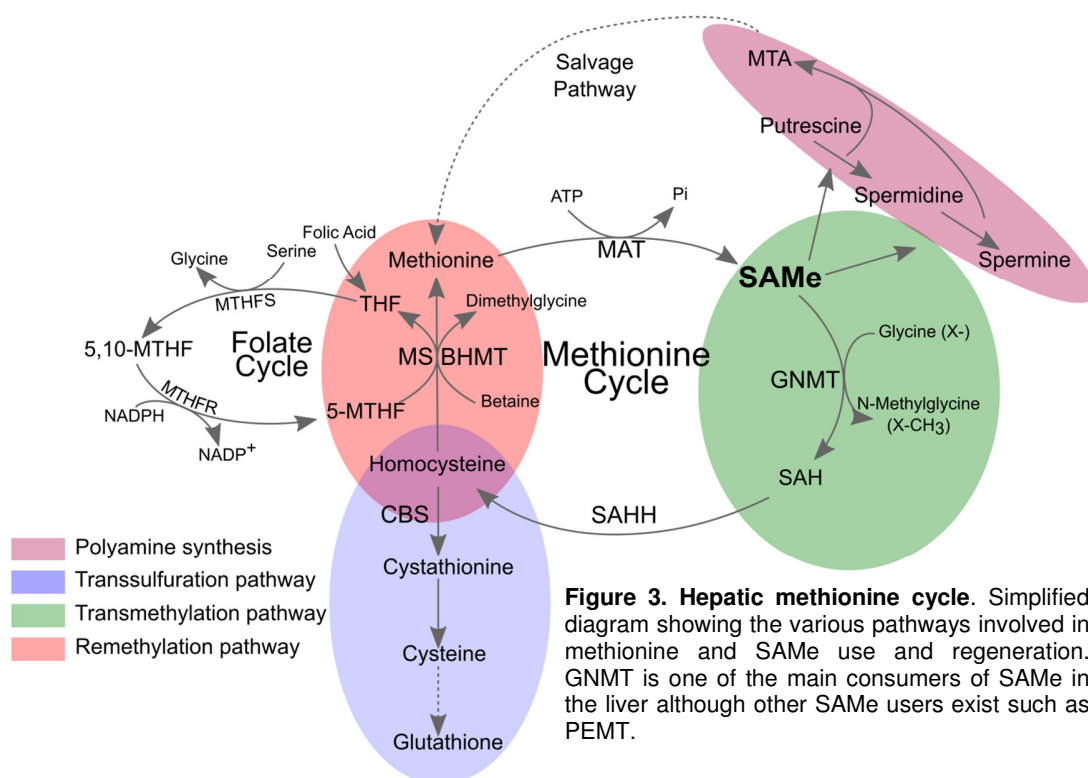


Figure 3. Hepatic methionine cycle. Simplified diagram showing the various pathways involved in methionine and SAMe use and regeneration. GNMT is one of the main consumers of SAMe in the liver although other SAMe users exist such as PEMT.

substrate for cystathionine-6-synthase (CBS) whose products lead to cysteine and glutathione or it can regenerate methionine via remethylation (**Figure.3**) (47).

Methionine can be regenerated from HCY by two different pathways, the remethylation and the methionine salvage pathway. In the remethylation pathway, HCY can be remethylated by two different enzymes: betaine homocysteine methyltransferase (BHMT) or methionine synthase (MS). BHMT uses betaine, a product of the choline cycle, to regenerate methionine. MS requires normal levels of folate and vitamin B₁₂ and is coupled with the folate cycle. MS uses 5-methyltetrahydrofolate (5-MTHF) as a methyl donor for HCY, the products being tetrahydrofolate (THF) and methionine. THF is converted to 5,10-methylenetetrahydrofolate (5,10-MTHF) by 5,10-methylenetetrahydrofolate synthetase (MTHFS) which is then used to regenerate 5-MTHF by methylenetetrahydrofolate reductase (MTHFR) (**Figure.3**). The second pathway involves the polyamine synthesis pathway. When SAMe is used to form polyamines the resulting by product is 5'

methylthioadenosine (MTA). MTA is a potent inhibitor of the polyamine pathway (48), of methylation reactions (49,50), and of SAH hydrolase (51) so it is quickly removed by the methionine salvage pathway, which transforms MTA back into methionine (**Figure.3**) (48).

2.2.2 Regulation of the methionine cycle

The methionine cycle is tightly regulated by the products of its various reactions (**Figure.3**). SAMe can inhibit MTHFR and activate CBS. This ensures that when there is excess SAMe, homocysteine is diverted to form cysteine and glutathione and methionine regeneration is reduced and when SAMe levels are low, homocysteine is channeled into methionine regeneration to increase SAMe production (44,52). SAH is a potent inhibitor of methylation reactions as most methyltransferases are inhibited by concentrations of SAH that are similar to the concentrations of SAMe that activate them (45). For this reason, SAH is taken into account to predict the methylation capacity of the cell and the ratio of SAMe/SAH is used as the indicator of methylation capacity of the cell

(53). The levels of SAME are tightly regulated by its main enzymes: MAT and GNMT.

2.2.3 Methionine adenosyltransferase and Glycine N-methyltransferase

2.2.3.1 Methionine adenosyltransferase isoforms

MAT is the enzyme that activates methionine by using ATP to synthesize SAME (41). Almost all lifeforms have MAT (except some parasites) and it is extremely well conserved from bacteria to humans (59% sequence identity) (54). MAT is also considered one of the essential genes needed to sustain life (55).

In mammals, there are two MAT genes, *MAT1A* and *MAT2A*, located on different chromosomes. Both genes encode for two homologous catalytic subunits, $\alpha 1$ and $\alpha 2$, respectively and have an 85% amino acid identity (56). There is also a third gene, *MAT2B*, that encodes the β regulatory subunit which is only expressed in fetal/proliferating liver and extrahepatic tissues (57). The *MAT1A* gene is expressed mainly in adult and differentiated liver and the $\alpha 1$ subunit that it encodes can form two isoenzymes: MATI or MATIII. MATI is a tetrameric enzyme whereas MATIII is a dimeric enzyme (56). The *MAT2A* and *MAT2B* genes are expressed mainly in fetal/proliferating liver and extrahepatic tissues. *MAT2A* forms a tetrameric isoenzyme called MATII, and in some cases the product of the *MAT2B* gene, the β subunit will bind to MATII but not with MATI/III. (57,58).

Each of the three isoenzymes has different kinetic properties related with their activity. MATII has the lowest K_m for methionine (4-10 μM), MATI has an intermediate K_m (23 μM -1 mM) and MATIII has the highest K_m (215 μM -7 mM) (59). Inhibition by its product follows an opposite trend with MATII strongly inhibited by SAME (IC_{50} =60 μM), and MATI minimally inhibited (IC_{50} =400 μM). MATIII on the other hand, is strongly stimulated by SAME (8x more activity with 500 μM SAME) (60). This data suggests that cells that express *MAT1A* have higher levels of SAME, and that increasing levels of methionine will increase the levels of SAME. On the other hand, cells expressing *MAT2A* will have stable levels of SAME regardless of the fluctuations in methionine concentration because a small increase in SAME will inhibit

MATII. The β regulatory subunit further increases the inhibition of SAME on MATII and in situations where SAME is needed the β regulatory subunit is no longer expressed (57).

2.2.3.2 Glycine N-methyltransferase

GNMT is the enzyme that produces SAH and sarcosine (N-methylglycine) by using SAME and glycine as substrates (**Figure.3**). GNMT is considered the cellular regulator of intracellular SAME levels and it is very well suited to carry out this function. Its main substrate is glycine which is very abundant, non-essential, and easily regenerated when transformed to sarcosine. Sarcosine has no known metabolic function and can be used in the reaction to generate 5, 10-MTHF and glycine allowing the folate cycle to continue (**Figure.3**). Like MATIII, the activity of GNMT is increased with SAME, although, unlike other methyltransferases, its activity is not inhibited by increased levels of SAH (61). The expression of *GNMT* is also similar to that of *MAT1A*: it is reduced in fetal liver and rapidly increases after birth (62). It is one of the most abundant enzymes in the liver (1-3% of cytosolic protein) and is also expressed in pancreas, prostate and in the peripheral nervous system (62,63). The main activity of GNMT in the liver is to regulate the SAME/SAH ratio to ensure that no aberrant methylation reactions occur. The futile reaction that GNMT catalyzes ensures that the methyl group from SAME is not lost but is instead inactivated becoming available again through the folate cycle (**Figure.3**). High levels of 5-MTHF inhibit GNMT ensuring that when the levels of SAME are low, GNMT will not completely deplete them further (61).

2.2.3 Study of hypermethioninemia

Hypermethioninemia is a condition that is found in many NAFLD patients and is generally due to GNMT, *MAT1A* and SAHH deficiency (64). In order to study these conditions, two mouse models have been created that mimic hypermethioninemia but differ in SAME content: the *Mat1a-KO* and *Gnmt-KO* mouse models.

2.2.3.1 *Mat1a-KO* mouse model

Mat1a-KO mice are characterized by the absence of the *MAT1A* gene (but not the *MAT2A* gene) expression (65). The liver is the organ most affected in this knock-out because it is the main organ in which *MAT1A* is

expressed. These mice have significantly increased levels of methionine and extremely reduced levels of S-adenosylmethionine (SAME) and glutathione (GSH) (65). Importantly, these mice are more susceptible to steatosis and liver injury, and they develop non-alcoholic fatty liver disease (NAFLD) and hepatocellular carcinoma (HCC) spontaneously on a normal diet by 8 and 18 months respectively (65). The reduced SAME in the livers of the *Mat1a-KO* mice leads to altered carbohydrate and lipid metabolism seen by increased triglyceride and glucose levels (65). Additionally, these mice produce smaller very-low-density lipoproteins (VLDLs) with reduced triglyceride (TG) content which also leads to increased TG accumulation in hepatocytes (66). Increased triglycerides induce the expression of the cytochrome P450 CYP2E1 and uncoupling protein 2 (UCP-2). CYP2E1 metabolizes xenobiotics such as carbon tetrachloride (CCl₄) and ethanol leading to the production of reactive oxygen species (ROS) and lipid peroxidation. UCP-2 uncouples the respiratory chain from oxidative phosphorylation and is related to mitochondrial ROS production. Both these enzymes are responsible for increased vulnerability of *Mat1a-KO* mice to hepatic insults by increasing ROS levels in the liver (67). Progression to HCC is caused by the increased proliferative gene expression found in this mouse model that is similar to that seen in MAT2A expressing liver (fetal/regenerating liver) (65,67), however, they have reduced liver regeneration after partial hepatectomy because they are unable to increase cyclin D1 levels and to respond to the mitogenic effect of hepatocyte growth factor (HGF), suggesting that chronic hepatic SAME depletion results in loss of responsiveness to mitogenic signals during liver regeneration (68,69).

These results highlight the need for a tight regulation of SAME. This model mimics the hypermethioninemia found in many patients with cirrhosis in which transmethylation reactions and plasma methionine clearance are reduced (37,70), and the downregulation and hypermethylation of the *MAT1A* gene has also been found in patients with severe NAFLD when compared to mild NAFLD patients suggesting that this gene is important in the development of NAFLD (71).

2.2.3.2 *Gnmt-KO* mouse model

Gnmt-KO mice are characterized by the absence of GNMT protein levels (72). The livers of these mice have increased serum transaminases, significantly increased levels

of methionine and SAME and a 100 fold increase in the SAME/SAH ratio (73). This model develops NASH at 3 months, fibrosis at 5 months and HCC as early as 8 months spontaneously (73). A different knock-out model (*Gnmt*^{-/-}) developed by Dr. Chen's group also develops HCC but it takes almost twice the amount of time for it to develop, approximately 17 months. Interestingly, in this model there are differences between the sexes with females developing signs of disease much faster than males. This model also has hypoglycemia, hepatomegaly, increased cholesterol, and glycogen accumulation although the reasons for these differences are unclear (74,75).

Gnmt-KO mice develop fatty liver due to an increased phosphatidylethanolamine N-methyltransferase (PEMT) pathway flux that uses the excess SAME to convert phosphatidylethanolamine (PE) into phosphatidylcholine (PC). PC is used as a precursor for triglycerides and despite the increase in PEMT activity observed in *Gnmt-KO* livers, *Gnmt-KO* mice have low PE levels but only slightly increased PC. The slight increase in PC is because PC is quickly consumed for the production of diglycerides and triglycerides (76). Interestingly, VLDL from *Gnmt-KO* mice have increased ApoE and less PE, and they produce more and larger VLDLs. *Gnmt-KO* mice also have increased VLDL clearance, mainly in the liver and the heart. Additionally these mice have increased expression of *Plin2* (perilipin 2 or adipophilin) a protein involved in the production and maintenance of lipid droplets, making lipid droplets in *Gnmt-KO* mice more dynamic (76,77). One of the most important aspects of this model is due to the global hypermethylation of its DNA especially in the promoter regions, leading to the silencing of some members of the RASSF and SOCS gene families (73) that play a key role in inhibiting the RAS and JAK/STAT pathways (78). This leads to a hyperactivation of RAS and its downstream effectors, providing proliferative and survival advantages and leading to HCC. Like *Mat1a-KO* mice, *Gnmt-KO* mice have an impaired liver regeneration although in the case of *Gnmt-KO* mice, regeneration is impaired due to an inhibition of the AMPK/LKB1/eNOS cascade (79). This model provides further evidence for the need to tightly control SAME.

Like the *Mat1a-KO* model, the *Gnmt-KO* model also mimicks human disease. HCC patients have reduced or no GNMT (80) and approximately 40% of HCC patients have a loss of heterozygosity of GNMT (80,81). Furthermore, patients at risk of developing HCC, alcohol-induced cirrhosis or HCV, have a down regulation of GNMT (82). Along similar lines, three patients with mutations in the *GNMT* gene have been discovered and they have mild to moderate liver disease with elevated serum aminotransferases (83,84).

Excessive amounts of SAME have been experimentally countered in *Gnmt-KO* mice by using a methionine deficient diet (MDD) or with an oral supplementation of nicotinamide. A methionine deficient diet reduces the amount of methyl groups available for the organism normalizing the amount of SAME. *Gnmt-KO* mice fed a methionine deficient diet have normal levels of SAME and methionine and do not develop steatosis (76). Treating *Gnmt-KO* mice with nicotinamide reduces the levels of SAME by activating the enzyme nicotinamide N-methyltransferase that uses SAME to synthesize N-methylnicotinamide. Like with the methionine deficient diet, nicotinamide treated mice have improved liver health and reduced SAME levels (85).

2.2.3.3 *Gnmt-KO* mice and autophagy

Work from our laboratory has demonstrated that livers from *Gnmt-KO* mice are characterized by decreased autophagic flux in both fed and starved conditions contributing to the hepatic steatosis observed in this mouse model. This inhibition is due to the increased levels of SAME and methionine present in this mouse model as hepatocytes cultured with SAME and methionine also have an inhibited autophagic flux. Along similar lines, we observed that *Gnmt-KO* mice fed a methionine deficient diet normalize their SAME and methionine levels and reactivate hepatic autophagic flux ameliorating steatosis (86).

2.3 NAFLD treatment

To date, there is no single specific cure or effective treatment for NAFLD. The current therapies are mainly focused on treating the underlying causes of NAFLD by changing the patient's lifestyle (87,88), although there are some pharmacological treatments with limited effectiveness (87).

Weight loss is recommended for NAFLD patients as it eliminates the amount of adipose tissue in the body and reduces the load of fatty acids that can reach the liver. Obesity is also an underlying cause for insulin resistance, another NAFLD risk factor. However, weight loss has to be gradual as losing too much weight in a short amount of time or "crash dieting" can damage the liver even further (89). A modified diet can help reduce weight. Controlling energy intake and food composition can help reduce weight and fatty acid intake. Finally, an increase in physical activity can reduce weight, intrahepatic fat, fatty acid uptake, and improve insulin sensitivity [a minimum of 140 min/day of fast walking (87,90,91)]. However, most clinics and hepatological centers don't have the resources and time required to control patients and even when under maximum incentive and monitoring, patients are mostly unable to maintain the desired weight loss and life style changes (92) increasing the need for pharmacological treatments.

There are few pharmacological agents that have been tested for NAFLD due to two different reasons. Since treatment of the underlying cause can usually reduce and even cure NAFLD many researchers and doctors have given this disease a low priority for drug development. NAFLD is also a slowly evolving disease making drug trials longer and more costly. Additionally, since histology is the only means by which NAFLD regression can be assessed, biopsies are necessary making trials more complex (93). The principal pharmacological treatments are set in two categories: insulin sensitizers and hepatoprotective agents.

Insulin sensitizers: Glitazones are the compounds that have the most evidence-based data for the treatment of NASH (93). These compounds increase insulin sensitivity in adipocytes increasing their fatty acid uptake and reducing the uptake in other organs leading to improved insulin sensitivity, they upregulate adiponectin, and have anti-inflammatory effects on Kupffer cells (93). Trials have shown that they can improve histological features, reduce aminotransaminase levels and improve insulin resistance (94). Unfortunately, these compounds have side effects like increased weight gain (adipocytes accumulate more fatty

acids) which may be harder to eliminate, cardiovascular complications, increased rate of bone loss in women, and may increase risk of bladder cancer (93), although this has not been confirmed. Additionally, the beneficial effects are quickly lost after treatment discontinuation (95). Metformin is another drug that is being tested. Metformin activates AMPK (**section 2.7.1.1**), reduces glucose production and improves peripheral glucose usage (96). This drug is safe and improves glycemia but it has not shown to be able to improve liver histology and other disease parameters (93). Currently, other insulin sensitizers with antiinflammatory and antifibrotic effects such as farnesoid X receptor (FXR) agonists, like obeticholic acid, and PPAR α and δ agonists are being investigated. Bile acids act through the farnesoid X receptor which has a wide range of metabolic effects. Small trials have shown that obeticholic acid can improve histology, insulin sensitivity, weight-loss, transaminase levels, and even fibrosis (**section 2.5**), although there are some side effects such as pruritus, increased LDL levels and a possible increase in cardiovascular risk (93,97). Other promising compounds are Glucagon-like peptide-1 receptor agonists and and GTF505 that act through PPARs (93).

Hepatoprotective agents: Since oxidative stress is an important factor in the development of NAFLD, antioxidant agents such as vitamin E have been extensively studied. Vitamin E can improve liver outcome in combination with other treatments (98). It improved steatosis, inflammation, hepatocyte ballooning, and reduced serum transaminases in one study (94). However, these results are hard to reproduce and have only been partially repeated in other studies and their use comes with secondary effects and not recommended for diabetic patients, NAFLD patients without histological confirmation or NAFLD patients with cirrhosis (99).

2.4 NAFLD progression

NAFLD is a progressive disease that can progress from simple steatosis to hepatosteatosis with fibrosis. Of the most serious cases of NAFLD, it is estimated that about 25% advance to the next stage of chronic liver disease which is fibrosis/cirrhosis (**Figures.1 and 4**) (100,101).

2.5 Liver Fibrosis and Cirrhosis

Continued and sustained damage of the liver can activate a fibrogenic response leading to fibrosis and eventually to cirrhosis. Fibrosis is the formation and deposition of excess extracellular matrix (ECM) proteins resulting in the disruption of normal parenchymal architecture and activity. It results from the prolonged activation of the wound healing response leading to chronification (**Figure.4**), a characteristic of diseases such as chronic liver disease (**section 2.1**) (102). Unlike other organs, liver fibrosis can evolve over decades (103,104) and may eventually develop into cirrhosis. Cirrhosis, considered an advanced stage or end-stage of liver fibrosis, is characterized by distorted hepatic vasculature and thick fibrotic septa (scar tissue) that surround regenerative nodules (104,105).

Hepatic lobules are characterized by a sinusoid surrounded by hepatocytes on a loose basal membrane called the space of Disse. During cirrhosis, increased fibrogenesis results in sinusoidal remodeling that fills the space of Disse with ECM and replaces the dead hepatocytes with fibrous scars (**Figure.4**). Additionally, the release of proangiogenic factors results in the capillarization of the sinusoid leading to intrahepatic shunts. Collectively, this results in increased resistance to blood flow which gradually builds up into portal hypertension. Portal hypertension is the underlying cause for the majority of the complications related to cirrhosis (105,106). It leads to ascites, splenomegaly and hepatorenal syndrome due to altered bloodflow (a life threatening condition). Portal hypertension can also reduce blood flow to hepatocytes further reducing hepatic activity. Reduced liver function is also responsible for many of the symptoms of cirrhosis and can cause hypoalbuminemia, excessive bleeding due to lack of coagulation factors, and jaundice due to abnormal bilirubin removal (105). Additionally, portal hypertension can lead to intestinal blood being shunted away from the liver, which coupled with reduced hepatocyte function can result in hepatic encephalopathy. Hepatic encephalopathy is caused by excessive toxins (mainly ammonia) in the blood, usually removed by the liver, that reach the brain resulting in confusion and coma and may cause death (107).

Cirrhosis is generally an indolent and asymptomatic disease and many patients can go undiagnosed (108) until liver complications are present. Asymptomatic cirrhosis is referred to as compensated cirrhosis because the liver in these patients is still functional, however, when the cirrhotic liver fails and the more serious symptoms become apparent (hepatic encephalopathy, ascites, jaundice) the disease becomes decompensated which may be life threatening (109). Biopsy is still the gold-standard method for diagnosis of liver fibrosis and cirrhosis (105,110). It can identify the underlying cause of fibrosis and allows for the monitoring of disease progression by the staining of ECM proteins. However, liver biopsies are invasive procedures, cause pain and discomfort, and may cause major complications such as internal bleeding (111). Sampling error can also occur as the whole liver is not equally affected by fibrosis. Analysis can also suffer from intra- and interobserver variation. Importantly, liver biopsies cannot predict disease progression (112). This has led to the search for more simpler, reliable and noninvasive diagnostic methods. These methods include serum tests, ultrasonography and transient elastography. Serum tests are used to detect levels of fibrosis-specific markers, however these tests are unable to determine in which organ the fibrosis is located. Ultrasonography can detect changes in liver parenchyma but it is highly operator dependent and may require histological confirmation (113). Transient elastography [Fibroscan (114,115)] detects liver stiffness (fibrosis makes the liver stiff) by detecting the velocity of an elastic wave in an area that is much larger than that of a biopsy. This test is also useful for detecting liver steatosis but is unable to determine the underlying cause of the disease.

2.5.2 Cell types and pathways involved in fibrosis

2.5.2.1 Cell types involved in fibrosis

Fibrosis is a reaction to a sustained wound that activates different pathways and involves several resident hepatic cells. The three main types of cells involved in fibrogenesis are hepatocytes, Kupffer cells and hepatic stellate cells (**Figure.4**).

Hepatocytes: Hepatocytes are generally the target of damage inducing agents in the liver (toxins, viruses, lipids, bile acids, etc...)

and are usually responsible for initiating the fibrogenic response. Damaged hepatocytes release ROS and cytokines such as TNF- α and TRAIL which attract immune cells to the damaged area (116). Other cytokines, such as TGF- β , can also activate and attract hepatic stellate cells. In severe insults to the liver, hepatocytes can undergo apoptosis and form apoptotic bodies. These bodies are detected by macrophages which engulf them and become activated further releasing cytokines (116,117). Pro-inflammatory cytokines such as TRAIL, FAS-ligand and TGF- β also have a pro-apoptotic effect on hepatocytes.

Kupffer cells: Kupffer cells are the resident macrophages of the liver that are located in the lumen of the sinusoid. In healthy liver, Kupffer cells remove old and damaged erythrocytes and clear pathogens from the blood. During fibrosis, Kupffer cells engulf apoptotic bodies and also release ROS and cytokines such as TGF- β , TNF- α and TRAIL that contribute to activate hepatic stellate cells. Kupffer cells are also macrophages so they can respond to lipopolysaccharide from the gut. Cirrhotic patients have a more permeable intestine which allows more bacterial products to reach the liver (116).

Hepatic stellate cells: Hepatic stellate cells (HSC; previously known as lipocytes, Ito cells, and perisinusoidals cell) are the main cell type involved in the production of ECM and the fibrogenic response in the liver (104,118). In healthy liver, HSCs are located in the space of Disse in a quiescent state. Quiescent HSCs accumulate vitamin A (retinoid) droplets and almost all the vitamin A stored in the liver is found in these cells [80-90% (119)]. The quantity and size of the vitamin A droplets in HSCs varies between species and even within the different areas of the liver (120,121). HSCs are star shaped cells with protrusions surrounding the sinusoid pores and in contact with the hepatocytes (122). During liver injury quiescent HSCs are "activated" or in other words transform from a quiescent vitamin A rich cell into a proliferating, fibrogenic, and contractile myofibroblast-like cell. Hepatic stellate cells have a cycle with three major phases: initiation, perpetuation and resolution.

Initiation: Initiation results in early changes in HSCs that render the cell more responsive to other cytokines and stimuli. In this early stage,

stimulation is composed mainly of paracrine cytokines derived from damaged hepatocytes and Kupffer cells. Endothelial cells from the sinusoid can also contribute to initiation by activating latent TGF- β found in the matrix (**section 2.5.2.2**) and platelets can also release cytokines such as PDGF, TGF- β and EGF (123).

Recent work has shown that HSC are capable of phagocytosis like macrophages. HSC express phosphatidyl serine (PS) receptors that are found mainly in macrophages (124), and that recognize the PS found in membranes of apoptotic bodies. After phagocytosis of apoptotic bodies, HSC induce the transcription of TGF- β and collagen resulting in their activation via PI-3K and MAPK (125). Additionally, HSCs can recognize and engulf DNA from dead cells (known as damage/danger-associated molecular patterns, DAMPs) initiating their activation (126). This ability to phagocytose apoptotic bodies and DAMPs is important because HSC are located right next to the hepatocytes and they are the first cells to come in contact with hepatocyte apoptotic bodies. Kupffer cells require migration into the liver parenchyma to have access to the apoptotic bodies.

Perpetuation: Perpetuation of HSC leads to changes in seven different activities of primed HSCs. The seven behavioral changes, *vitamin*

A metabolism, matrix degradation, proliferation, chemotaxis, cytokine release, fibrogenesis, and contractility, result in the formation of the fibrogenic scar at the site of the damaged liver. In the perpetuating phase, autocrine as well as paracrine signaling is present between HSC and other hepatic cells.

Vitamin A metabolism: One of the earliest characteristics discovered of activating HSCs was the gradual loss of vitamin A droplets in the cytoplasm as activation progressed (127). It is unclear why HSCs metabolize their vitamin A into retinoic acid, but it appears to be a necessary step in their activation as HSCs treated with excess retinoids are unable to activate (128). HSCs express retinoic acid receptors (RAR) and retinoid X receptors (RXR) and their activation with retinoic acid leads to the synthesis of collagen (129,130). Quiescent HSCs also express peroxisome proliferator-activated receptor gamma (PPAR γ) a receptor associated with adipocytes and related to fatty acid metabolism. During activation, the activity of PPAR γ is downregulated (131) and the use of PPAR γ ligands have been used to stop fibrotic activity in cultured HSCs (132) and in animals (133). Recent studies have shown that autophagy (**section 2.1.3.1**), like in hepatocytes, may be the main method of mobilizing the HSC lipid droplets to increase energy availability. Inhibiting autophagy or

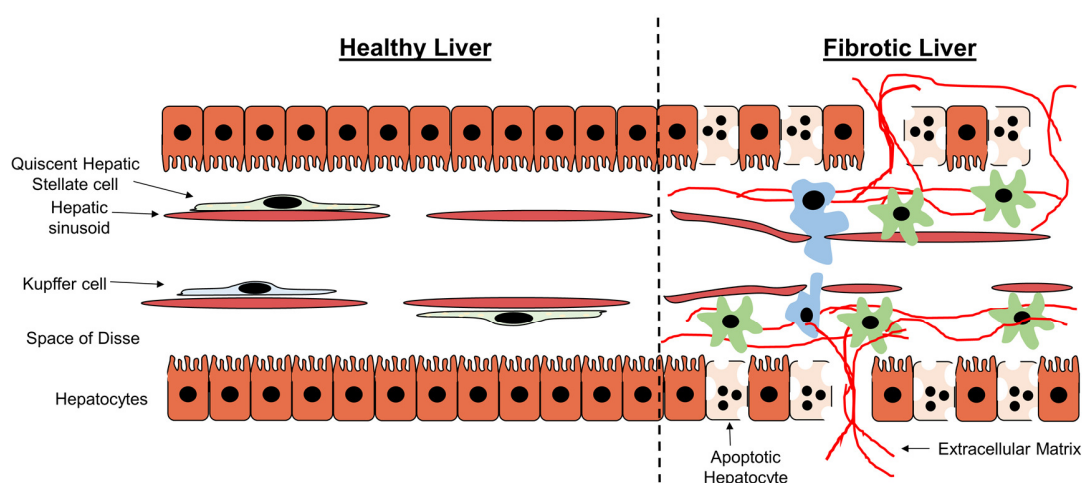


Figure 4. Fibrosis destroys the hepatic parenchyma. Healthy hepatic (left panel) lobules are formed from hepatocytes on a loose basal membrane (space of Disse) surrounding a sinusoid. The space of Disse is also where quiescent hepatic stellate cells are found, while Kupffer cells can be found in the hepatic sinusoid. During a sustained injury to the liver (right panel), hepatocytes enter apoptosis activating both Kupffer and hepatic stellate cells. Activated hepatic stellate cells produce extracellular matrix replacing the dead hepatocytes, distorting the hepatic parenchyma and increasing portal hypertension.

autophagy deficient HSC were unable to activate and fibrosis was reduced despite liver damage (134,135).

Matrix degradation: Fibrogenesis involves degradation and production of ECM. In early stages of the disease, activating HSC degrade the basal lamina and surrounding connective tissue and gradually replace it with fibrotic scar matrix. HSCs release a wide range of matrix-metalloproteinases (MMP) along with their inhibitors, tissue inhibitor of metalloproteinases (TIMP) (136,137). HSCs express MMPs that degrade the basal lamina such as MMP-2 and MMP-9 (138,139), however they also continuously synthesize TIMPs that inhibit the activity of many MMPs. TIMP-1 is considered an HSC survival factor with anti-apoptotic activity and transgenic mice overexpressing TIMP-1 in the liver have delayed regression of liver fibrosis (140,141). In more advanced stages of cirrhosis TIMPs can completely inhibit the degradation of the thick fibrotic septa reducing the possibility of complete regression. Initial matrix remodeling can also release and activate latent TGF- β (**section 2.5.2.2**) that further activates nearby HSCs.

Proliferation: Activation of HSCs also induces cellular proliferation. The most potent mitogen identified to date is platelet derived growth factor (PDGF, **section 2.5.2.2**) (142). During activation, HSCs upregulate PDGF receptors and begin production of PDGF, leading to paracrine and autocrine loops (143). Other mitogens for HSCs are VEGF, EGF, and bFGF (144–146).

Chemotaxis: HSC have the ability to migrate towards cytokine chemoattractants (147) usually found at the point of injury in the liver. Potent chemoattractants for HSC are PDGF (148) and MCP-1 (149). HSC move by spreading of the tip towards the stimulant then the cell body and finally retracting the trailing parts of the cell using myosin (150). At the point of injury, HSC find increased levels of adenosine (adenosine levels can be increased 100 fold in areas of injury) which can inhibit PDGF induced chemotaxis and increase collagen and TGF- β mRNA expression (151). This allows the HSCs to accumulate and deposit ECM at the injured area.

Cytokine release: Activated HSCs release a plethora of cytokines that can regulate other

cells involved in liver injury through autocrine and paracrine signaling. They are capable of modulating immune cells, other HSCs, and hepatocytes. Among the immunokines secreted by HSCs are MCP-1, CCL21, CCL5, TNF- α , CCR5 and additionally they express toll-like receptors (TLRs) that enable them to detect bacterial products such as LPS (131). Other chemokines secreted by HSCs are PDGF, TGF- β , VEGF, bFGF, HGF, and EGF (131). The amount of paracrine and autocrine signaling involved in liver fibrosis can lead to a vicious cycle of constant co-activation between HSCs and immune cells further magnifying the severity of the disease.

Fibrogenesis: The main function of an activated HSC is to produce ECM at the site of liver injury. TGF- β is the most potent cytokine involved in ECM synthesis (152). The primary fibers in ECM are collagen type I and III which replace collagen type IV fibers found in healthy livers (131) and HSCs are more fibrogenic when grown on collagen type I than type IV (153). Fibronectin, a fiber deposited by endothelial cells, can also activate HSCs (154). As fibrosis progresses and ECM density increases, liver stiffness increases. This stiffness due to increased ECM deposition is the concept behind Fibroscan (**section 2.5**) (114,115). Liver stiffness may also be a factor in HSC activation and activity as seen in HSC culture in gel substrates (155), in which the stiffness of the gel appears to be more important than the components of the gel.

Contractility: HSCs express filaments related to contraction such as alpha smooth muscle actin (α -SMA) and myosin (156,157) and exert contractile activity which is a major contribution to hepatic hypertension.

Resolution: Resolution is the process by which the deposited ECM is removed and the liver parenchyma and function is restored. Resolution requires that activated HSCs either revert to a quiescent state or are removed via apoptosis (131). Recent studies have shown that a fraction of myofibroblasts undergo reversion to a state similar to quiescent HSC both *in vitro* and *in vivo*, however, these reverted HSC reactivate faster than quiescent HSCs resulting in faster and more aggressive fibrosis (158,159). Natural killer cells are the immune cells in charge of initiating HSC apoptosis through TRAIL and interferon γ

pathways (160). Mice that have their NK population depleted with the anti-asialo-GM1 antibody or are genetically deficient for NK cells (160,161) have increased fibrosis and when NK cells are activated fibrosis is reduced. Fibrosis is also increased in patients that take immunosuppression drugs, which reduce the cytotoxicity of NK cells (162). NK cell function might also be the reason why some patients develop faster fibrosis than others and why fibrosis accelerates with age as NK cell activity decreases with age (163).

Non-hepatic stellate cells: HSCs are not the only fibrogenic cell type that contributes to fibrosis in the liver. Many studies have shown that this may depend on the type of lesion and the progression of the disease. Other possible sources for myofibroblasts are portal fibroblasts (164), bone marrow (165), and cells undergoing epithelial-mesenchymal transition (166). Portal fibroblasts are thought to be the primary fibrogenic cell in cholestatic liver diseases (164). Bone marrow may contribute cells in more chronic and persistent fibrosis and may also supply cells in small quantities to healthy liver (167).

2.5.2.2 Main pathways involved in fibrosis

Platelet-derived growth factor

Platelet-derived growth factor (PDGF) (**Figure.5**) is a growth factor that promotes cellular proliferation and survival, cell migration and cytoskeletal reorganization, angiogenesis, and embryonic development (168). It has a high sequence identity with the receptor binding domain of vascular endothelial growth factor (VEGF) and they are usually referred to as the PDGF/VEGF family of growth factors. PDGF is considered the most potent mitogen for HSCs although it is not the only one that they can respond to. PDGF is composed of four secreted extracellular ligands (PDGF-A, PDGF-B, PDGF-C, and PDGF-D) which join as disulfide linked dimers with either homo- or heterodimerization, only PDGF-A and PDGF-B are able to heterodimerize (PDGF-AB) (168). It was originally thought that the only source of this growth factor was the α -granules in platelets, however, further research demonstrated that other cells such as endothelial cells can also produce PDGF (169).

PDGF binds to and activates the PDGF receptor (PDGFR). PDGFR is a tyrosine kinase receptor composed of five immunoglobulin-like domains in the extracellular receptor region and a tyrosine kinase in the cytoplasmic region. It has two isoforms called PDGFR- α and - β . Upon binding with PDGF, the receptors dimerize (PDGFR- $\alpha\alpha$, PDGFR- $\beta\beta$, or PDGFR- $\alpha\beta$) and autophosphorylate each other resulting in their activation. PDGFRs activate various pathways related to proliferation and migration such as the Ras-ERK/MAPK, PI3K/Akt, Jak/STAT, and PLC- γ pathways (**Figure.5**) (168). Their autophosphorylation also acts as docking sites for proteins containing SH2 or PTB domains. Although similar, the receptors may carry out different functions depending on their homo- or heterodimerization state, this system allows for increased specific control over PDGF signaling depending on the required situation (168). PDGF-AA binds only PDGFR- $\alpha\alpha$ and PDGF-DD binds only PDGFR- $\beta\beta$, PDGF-CC and PDGF-AB bind both PDGFR- $\alpha\alpha$ and PDGFR- $\alpha\beta$. PDGF-BB is the only homodimer that can bind all three of the receptor combinations. In HSCs, PDGFR- β is the predominant receptor isoform expressed during activation and PDGF-BB and PDGF-DD are the most potent forms of the growth hormone for HSCs (131,168).

Due to its potent activity on HSCs, the PDGF pathway is under tight control by different means. Extracellular PDGF-C and -D contain a CUB (complement C1r/C1s, Uegf, Bmp1) domain that inhibits their union with the receptor and requires cleavage for any activity to be possible. The CUB domain, once cleaved, then acts as a competitive inhibitor of the proteases (170). PDGF-B is cleaved by Factor VII-activating protease (FSAP) at its active site, rendering it biologically inert (171). ECM proteins also exert an important role in control of PDGF. Collagen fibers and the protein secreted protein acidic and rich in cysteine (SPARC) can bind active forms of PDGF and retain them. During liver damage, MMPs degrade the collagen releasing the bound PDGF which further activates nearby HSCs. Additionally, SPARC can only bind PDGF at a pH above 6.6 and since in liver lesions the pH is generally reduced, SPARC releases PDGF in damaged areas creating a chemotactic gradient for HSCs (172). Control is also found at the receptor level. When

activated, the dimerized receptors can be internalized and degraded by lysosomes to eliminate the signal. Also, the activated receptors can attract phosphatases such as PTEN or the SHP-2 tyrosine phosphatase that quickly end signaling. Other proteins such as RasGAP (an inhibitor of RAS), can bind through its SH2 domains and negatively regulate RAS signaling (173). Experimental removal of these mechanisms in mice leads to increased fibrogenesis and fibrotic liver.

Transforming growth factor beta

Transforming growth factor beta (TGF- β) is a cytokine that belongs to the transforming growth factor superfamily of cytokines which include other factors such as BMPs (bone morphogenetic protein), Activins, GDFs (growth and differentiation factor), and

Nodals and all members have a similar sequence and signaling pathways. These factors control diverse processes such as cell proliferation, recognition, differentiation, apoptosis and specification of developmental fate during embryogenesis (152,174). TGF- β includes three isoforms - β 1, - β 2, and - β 3, and all isoforms appear to have different functions in embryogenesis. However, the - β 1 isoform is the most studied form in liver disease and TGF- β will refer to TGF- β 1 from now on.

TGF- β is synthesized as a precursor that is cleaved intracellularly by furin, the cleaved section remains covalently attached to TGF- β outside the cell and is known as the latency-associated peptide (LAP). LAP can bind Latent TGF- β binding protein (LTBP) which anchors the complex in the matrix creating a reservoir of latent TGF- β . Active

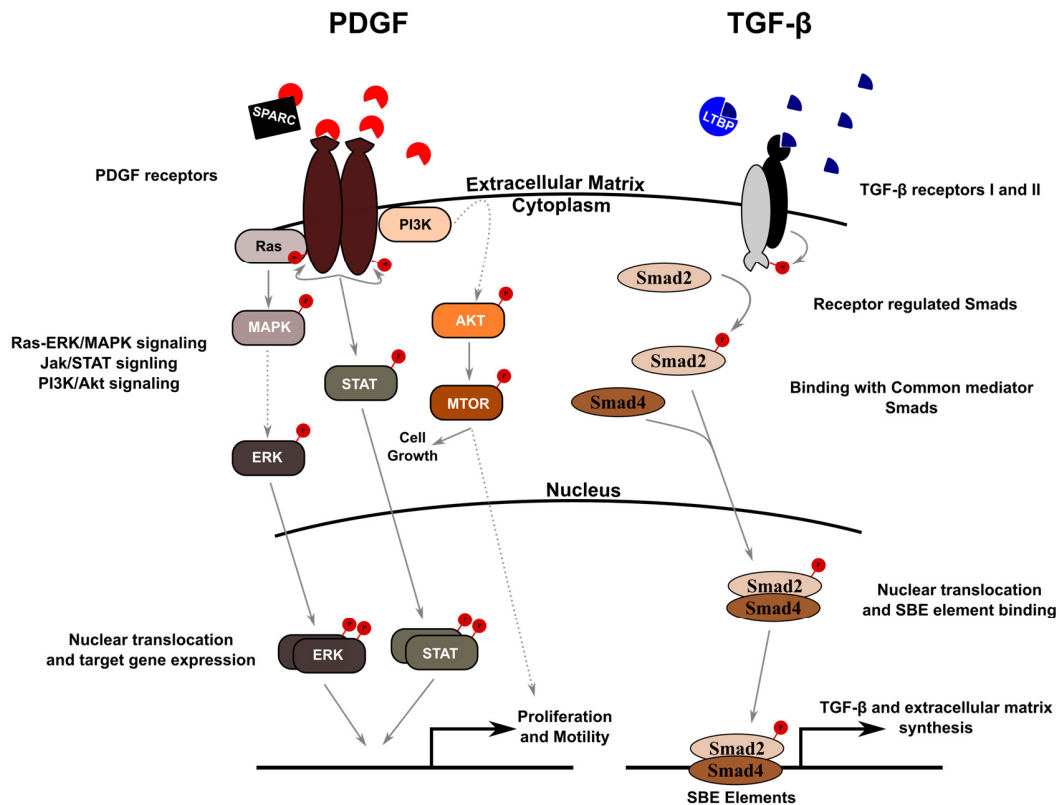


Figure 5. The PDGF and TGF- β pathways are profibrogenic in hepatic stellate cells. Diagram showing the main pathways activated by PDGF (left) and TGF- β (right). When activated by PDGF, PDGF receptors dimerize and autophosphorylate leading to their activation. Activated receptors can then initiate different signaling cascades such as the Ras-ERK/MAPK, Jak/STAT and PI3K/Akt pathways. In HSC, PDGF leads to proliferation and increased motility. When activated by TGF- β , TGF- β receptors dimerize and T β RII phosphorylates and activates T β RI. T β RI can then activate the receptor-regulated Smad, Smad2, which binds the common mediator Smad, Smad4, and translocates to the nucleus to initiate ECM synthesis.

TGF- β is a dimer bound together by a disulfide bridge further strengthened by hydrophobic interactions (174).

TGF- β binds and activates TGF- β receptors (T β R) (**Figure.5**), of which there are three different forms T β RI, T β RII, and T β RIII (152,174). The receptors have serine/threonine kinase activity with an N-terminal extracellular ligand binding domain, a transmembrane region, and with kinase activity in the cytoplasmic C-terminal. T β RIII, also known as betaglycan, is a coactivator that lacks an intracellular domain and aids with receptor activation (175). T β RII binds the ligand and dimerizes with T β RI, this results in the phosphorylation of the T β RI GS domain and its subsequent activation. Activated T β RI in turn initiates the TGF- β signaling cascade by phosphorylating the receptor-regulated Smads or R-Smads.

Smads are the effector proteins of the TGF superfamily ligands, relaying the signal from the membrane to the nucleus where they initiate gene transcription. There are 8 Smad proteins placed in three categories: receptor-regulated Smads (R-Smads) which include Smads 1, 2, 3, 5, and 8, common-mediator Smads (Co-Smads) which include Smad 4, and inhibitory Smads (I-Smads) which include Smads 6 and 7. Smads 1, 5, 6 and 8 are receptor-regulated Smads of the BMP subfamily. When T β RI is activated, Smads are recruited to the receptor and phosphorylated resulting in their activation and increased affinity for Smad 4. The Smad2/3/4 heteromeric complex then translocates to the nucleus. This nuclear complex has an immediate effect in the expression of several hundred genes (176), both positively and negatively. Many Smad target genes contain a Smad binding element (SBE, **Figure.5**) that the Smads proteins bind to, however, this binding has a relatively low specificity and is very weak which is why in the nucleus, the Smad complex recruits different DNA binding proteins such as CREBP, SP1, and E2F and members of the basal transcription machinery such as p300, CBP, ARC105, and Smif (177). Additionally, the Smad complex can elicit a different response in different cells by recruiting cell-specific factors (174). TGF- β signaling is terminated when the activated Smads are either dephosphorylated or degraded. Some R-Smad phosphatases

include PPM1A, MTRM4, and PP2A (under hypoxic conditions) which can remove Smad phosphorylation in the cytoplasm and prevent TGF- β signal transmission (178). Ubiquitin mediated degradation is the main method by which Smad complexes in the nucleus are targeted for destruction. This is done by Smurf-2 (SMAD Specific E3 Ubiquitin Protein Ligase 2), a HECT domain containing ligase that ubiquitinates nuclear Smads and targets them for proteasomal degradation (179).

Like PDGF, the TGF- β pathway is tightly controlled. Control of this pathway can happen at four different levels: Ligand, receptor, Smad signaling and at the transcriptional level. TGF- β availability is controlled by LAP and LTBP and creates reservoirs of the protein that are embedded in the matrix. During tissue remodeling, this latent TGF- β is made bioactive by MMPs that degrade the surrounding matrix. This is also a means of making TGF- β available in the injured areas (the areas that suffer remodeling). Another protein, α 2-macroglobulin, can bind free TGF- β and inhibit its union with its receptor. Coactivators like betaglycan can facilitate binding of ligand with receptor (174,175).

Receptors are also a point of control in the TGF- β pathway. The immunophilin FKBP12 can inhibit T β RI by binding to its unphosphorylated GS region and inhibiting its activation by T β RII (180). Once the receptors are activated, the receptor complex is internalized into the cell in either clathrin coated early endosomes or caveolin-1-positive lipid raft vesicles. If the receptor complex is internalized in clathrin dependent vesicles, then the signal is propagated as the receptor complex is placed near smad-associated proteins and Smads, however, if the receptors are shifted into caveolin-1-positive lipid raft vesicles then the signal is eliminated as these vesicles are placed near Smurf2-Smad7 complexes that ubiquitinate the receptors and target them for degradation (181). One of the possible proteins in charge of deciding the fate of the receptor complex is the E3 ubiquitin ligase c-Cbl that can NEDDylate (**section 2.8.3**) the receptor complex selecting it for clathrin dependent vesicles. Inhibition of c-Cbl NEDDylation leads to the receptors ubiquitination instead and its subsequent degradation by internalization in

caveolin-1-positive lipid raft vesicles (182). Internalization of the receptors also depletes the levels of TGF- β in the extracellular medium (183).

R-Smads are also tightly regulated and controlled. One of the target genes of the TGF- β signaling cascade is Smad 7 which is one of the I-Smads. Smad 7 inhibits the phosphorylation of R-Smads by binding T β RI and blocking the other Smads creating a negative feedback loop. Smad 7 can also bind Smurf 2 and target the receptors for degradation (174).

TGF- β signaling is also negatively controlled at the transcriptional level. c-Ski, SnoN, and TGIF are three proteins that can negatively regulate Smad transcription. These proteins act by recruiting transcriptional repressors, such as NCoR or HDACs, and interfere with Smad binding to transcriptional activators (174). Another transcriptional repressor is c-Jun. c-Jun is also a TGF- β target gene and its expression increases as the signal is transmitted. This repressor binds to the Smad complex and sequesters it in the nucleus reducing its binding to transcriptional coactivators and reducing transcription of TGF- β genes (184,185).

2.5.3 Fibrosis research

The use of animal models has helped to discover much of what is known about liver fibrosis. Unfortunately, there is no single animal model that recapitulates every single aspect of human disease and all models have their own strengths and weaknesses, the most important being that rodents have different immune reactions, gene regulations, etc. Animal models, however, allow for the study of problems that cannot be studied in humans, multiple sampling time points, restriction of experimental variables to a minimum, and the study of the intact liver as part of an organism (186). Some of the most used models are:

Carbon tetrachloride or CCl₄ intraperitoneal administration is a common toxic insult used to induce liver fibrosis. CCl₄ is converted to the CCl₃[•] radical by the cytochrome CYP2E1 in the liver leading to hepatocyte death, necrosis and activation of fibrosis. Repeated administration can cause signs of fibrosis within two weeks of treatment (186). Some advantages of this model are that it is relatively easy to perform

and the results are generally reproducible. Other CYP2E1 related toxic compounds are DMN and DEN. These compounds also lead to HCC even if their treatment is discontinued (187) which makes them more useful for studies in the relationship between fibrosis and HCC.

Bile duct ligation or BDL is a surgical procedure that involves the ligation of the bile duct leading to obstructive cholestasis. Hepatocyte death is a result of bile acid induced toxicity. BDL is considered a model for secondary biliary fibrosis and involves the activation of periportal myofibroblasts. This model induces inflammation with fibrosis and the proliferation of intrahepatic bile ducts (188). Some of the disadvantages of this model include that it is an invasive technique with a high technical difficulty and less constant fibrosis (186).

Methionine choline deficient diet or MCD is a model used to study the progression of NAFLD through to fibrosis. This model works by reducing the levels of methyl donors in the organism and affecting the methionine cycle and glutathione synthesis (189), leading to oxidative stress. Some of the drawbacks of this model are that the animals lose weight and are hyper-sensitive to insulin, aspects that are not normally found in NAFLD patients (186).

Genetic models: Many different genetic murine strains have been created to determine the contribution of specific factors to fibrosis. These models are typically either Knock out or increased expression models that try to determine if the genetic change increases or reduces fibrosis spontaneously or after a specific insult. One common model used is the *Mdr2-KO* mouse model (190). This model lacks the *Mdr2* flippase that prevents the excretion of phospholipids into the bile and results in nonsuppurative inflammatory cholangitis, HCC and metastasis at approximately 12 months of age (191). The *Gnmt-KO* mouse model (**section 2.2.3.2**) has also been used to study the immune system during the development of fibrosis. In *Gnmt-KO* mice, NK cells have increased cytotoxic activity and express more TRAIL, contributing to the proinflammatory background in the liver (192). Additionally, these mice are more sensitive to endotoxin damage but depletion of NK cells and their replacement with TRAIL -/-

NK cells results in hepatoprotection from Lipopolysaccharide induced damage (192), and double knock out mice for TRAIL and GNMT are also protected from BDL induced damage (193).

2.5.4 Treatment of fibrosis

Like with NAFLD there is no effective cure for fibrosis. Current treatment involves removing the underlying insult causing chronic liver disease. Most patients that remove the underlying cause of disease have a reversal of fibrosis, this was seen in patients treated for hepatitis B virus, which had improved inflammation and necrosis after one year and improved fibrosis after 5 years (194). Similar problems as in NAFLD exist for the development of effective drugs in fibrosis. Since biopsy is still the gold standard for fibrosis, all trials are more complex. Additionally, fibrosis progression or reversal can take years to be visible making trials even more costly and difficult. Improved non-invasive markers are required to make cheaper and more reliable clinical trials (195).

2.6 Hepatocellular Carcinoma

Approximately 5-30% of cirrhotic patients develop hepatocellular carcinoma (HCC, **Figure.1**) (196). HCC is the sixth most common cancer, the second most common cause of cancer-related mortality worldwide and the most common form of liver cancer with 70-85% of total liver cancer (197,198). The major risk factors for HCC are Hepatitis B virus infection, Hepatitis C virus infection, aflatoxin B1 intoxication, NAFLD, and alcoholism. HCC generally appears in a background of cirrhotic liver making it a very difficult cancer to treat.

2.6.1 NAFLD and HCC

The anticipated rise in NAFLD cases during the next few years is expected to counter the fall in HBV and HCV derived HCC due to the improved treatment of these infections (199). Many of the risk factors for NAFLD, such as obesity and metabolic syndrome, are also considered risk factors for HCC and other cancers (199,200). Dyslipidemia can also increase by 2-3 fold the incidence of HCC in patients with HCV infection (199). NAFLD patients have a reduced risk of developing HCC when compared to other chronic liver diseases [almost half that of HCV (201)], however, NAFLD patients may be more likely to develop

HCC without cirrhosis as there have been cases reported of NAFL patients with this type of tumor (202). In contrast, alcoholic HCC is almost exclusively found in cirrhotic livers (203). Even though NAFLD appears to have a reduced risk of HCC, the overall five-year survival appears to be similar to that of other etiologies (204).

2.6.2 HCC treatment

HCC is an extremely complex pathology to treat that is worsened by the fact that it generally appears on a cirrhotic liver background. In order to improve patient survival, patients diagnosed with chronic liver disease regardless of etiology are subjected every six months to an abdominal echography in order to screen for HCC. Determining tumor markers such as alfa-fetoprotein (AFP) does not appear to have any benefits as AFP is a predictor of advanced disease and poor prognosis (205,206). The goal is to detect solitary tumors ≤ 20 mm in size that have a low probability of vascular invasion and intrahepatic spread (207), increasing the probability of effective treatment. Therapy for HCC can be divided into three categories: surgical, locoregional, and systemic which are used depending on the tumor extension, cirrhotic state and co-morbidities of the patient.

2.6.2.1 Surgical therapy

Surgical procedures for HCC include resection and transplantation. These techniques are used mainly in localized tumors with no spread (206).

Resection involves the removal of the tumor tissue along with parts of the surrounding non-tumor tissue. Due to its aggressive nature, the ideal patients are those that have no cirrhosis and only one tumor, but this method generally has good 5-year survival rates. Cirrhotic patients may also undergo resection but must be carefully selected to avoid complications such as liver failure (206). Tumor recurrence is a problem in the first 5 years after resection [almost 70% of cases (206)] and is made more probable by factors such as portal hypertension, multifocality, size, poor histological differentiation, satellites, and vascular invasion (208,209).

Liver transplantation is a technique used on patients that fulfill the Milan criteria (single nodule < 5 cm or up to three nodules ≤ 3

cm or less, without vascular invasion or extrahepatic spread). The Milan criteria offers a 4-year survival of 75% with a recurrence of 15% (210). Unfortunately, the shortage of donors means that only the sickest patients are selected and that many patients that fulfill the criteria may have their cancer advance to a point where they are no longer eligible for a transplant.

2.6.2.2 Locoregional therapy

These types of treatment are used in combination with surgery or when surgery is not an option. They are mainly used in intermediate-stage HCC and include ablation and the different types of TACE.

Tumor ablation induces tumor necrosis by injection of chemicals or by temperature. Ablation is usually performed percutaneously and induces tumor necrosis leaving the remains to be absorbed by the liver. Chemical ablation is usually performed by injecting chemicals such as ethanol and acetic acid and can achieve 100% tumor necrosis in tumors less than 2 cm big (206). Temperature ablation uses techniques such as radiofrequency, microwave, laser, and cryoablation. Radiofrequency ablation is more effective than ethanol injection for tumors bigger than 2 cm, however, its effectivity is severely reduced for tumors bigger than 5 cm (206). Ablation is not recommended for tumors near major blood vessels, the biliary tree, the heart or bowels (211). Survival after ablation is similar to that of surgical resection (206).

Transcatheter arterial chemoembolization or TACE is a selective intravascular delivery of drugs, such as cisplatin or doxorubicin, into the arteries supplying the tumor followed by its embolization. This leads to tumor death that begins by chemotherapy and is followed by ischemia. TACE is mainly reserved for patients with preserved liver function, no cancer related symptoms, multinodular HCC, no vascular invasion or extrahepatic spread. The 2-year survival for patients that meet this criteria is around 63% (212). After initial success, the tumor can revascularize opening up new opportunities for treatment; however, the capacity for keeping the tumor under control is lost resulting in reduced survival for patients. The embolization and subsequent hypoxia in the tumor leads to the expression of

pro-angiogenic factors such as VEGF and PDGF which has led to the use of sorafenib (systemic treatment) with TACE, however, no significant increase in survival has been found (213). Other forms of TACE such as DEB-TACE and TARE are also used. DEB-TACE uses drug-eluting beads (DEB) that slowly release anthracycline in the tumors along with standard artery embolization. DEB-TACE is a means of maintaining a high drug concentration in the tumor while reducing the systemic adverse side effects (214). Transcatheter arterial radioembolization or TARE is the use of glass or resin spheres loaded with β -emitting agents such as Yttrium-90 or Holmin-166 (206,215). This method ensures that the radiation is only released in the tumor area, and if done properly, secondary effects are minimal (216). This technique is not indicated for patients with hepatopulmonary shunts as the beads may end up in the lungs and in some cases they may end up in the gastrointestinal tract (217).

2.6.2.3 Systemic Treatment

Systemic treatment is usually given to patients that have advanced HCC or when all other treatments have failed. Currently the only treatment that has a proven survival benefit is sorafenib. Sorafenib is a multikinase inhibitor (receptor tyrosine kinase and threonine/serine kinase inhibitor) that is able to block multiple kinases, among them many kinases active in HCC such as VEGFR, PDGFR, Raf-1, and B-Raf (206). Other treatments such as everolimus and sunitinib are other systemic drugs with heterogeneous potency against specific targets. Everolimus is an inactivator of MTORC1 reducing cell growth and proliferation and sunitinib is another receptor tyrosine kinase inhibitor. Various different combinations of drugs are being tested in clinical trials in an attempt to improve drug efficacy (206).

2.6.3 Molecular pathways in HCC

One of the main difficulties in treating HCC is that many pathways are activated and inhibiting one will generally be compensated by other pathways, which is why multikinase inhibitors like sorafenib were created. These pathways are generally affected either directly or indirectly by gene mutations, amplifications, and promoter methylation which lead to their aberrant activation/inactivation (200,206).

Some of the most important alterations in HCC are:

Telomerase promoter mutations:

Telomeres are the tips of linear chromosomes and telomerases are used to protect them from fusion and destruction by nucleases. Telomerase is the enzyme complex responsible for maintaining the telomeres after every cell division and is usually not expressed in mature cells leading to the gradual loss of telomeres after every division. After a certain amount of telomere loss, the DNA damage pathway is activated and the cell either enters senescence or apoptosis. Mutations in the TERT promoter are the most common mutation in HCC (30-60%) and are also the most common form of TERT activation (218). Additionally TERT mutations may already be found in cirrhotic preneoplastic lesions (200).

TP53 mutations: TP53 is a tumor suppressor protein that promotes cell cycle arrest and apoptosis in response to DNA damage. The importance of this protein is made evident when over 50% of all cancers have some form of inactivating mutation in the TP53 gene (219). TP53 mutations in HCC depend on etiology and can range from 18% to 50% (220). It is considered a driver mutation as it can predispose hepatocytes to other lesions and carcinogens.

Other Mutations: Other genes commonly mutated are *CTNNB1* (Wnt signaling), *ARID1A* (chromatin remodeling), and Axin 1 (Wnt signaling). Additionally, some tumors can contain amplifications of VEGFA and TERT or amplifications of the Myc and Met genes (206).

Activated pathways: HCC tumors generally have a variety of activated pathways that make it an extremely difficult cancer to treat. There are four major pathways altered in HCC, which are: Tyrosine kinase receptor (TKR) signaling, TGF- β signaling, JAK/STAT signaling, and Wnt/ β -catenin signaling.

TKR signaling: Tyrosine kinase receptor signaling involves major growth and migration pathways. TKRs usually activate pathways such as Ras-MAPK, PI3K/Akt, c-MET, c-Myc and VEGF signaling. Ras-MAPK and PI3K/Akt signaling are up-regulated in almost 50% of early HCCs and in almost all advanced HCCs (78). Ras-MAPK is activated by upstream TKRs such as EGFR, IGFR, and MET

signaling and leads to the activation of proliferation genes. PI3K-Akt signaling leads to altered MTOR signaling that also promotes cellular growth and is also activated in around 50% of HCC (221). Ras-MAPK is generally activated by hypermethylation of Ras inhibitor genes such as *NORE1A* and *RASSF1A15*, but not usually by direct mutations of K-Ras (206). Hepatocyte growth factor-MET signaling is associated with poor prognosis (78). VEGF signaling plays a prominent role in HCC tumor angiogenesis, which is one of the reasons behind TACE therapy. HCC neoangiogenesis leads to leaky and malformed capillaries which can form hypoxic areas in the tumor. Hypoxia induces the expression of hypoxia inducible factor 1 and 2 (HIF), and these factors have been shown to increase tumor chemo- and radio resistance also leading to the failure of embolization therapies this being the reason why HIFs are associated with poor prognosis (222).

TGF- β signaling: This signaling pathway is generally a tumor suppressor during early phases of the disease but may favor invasiveness and angiogenesis in more advanced disease (223). TGF- β is also involved in the endothelial to mesenchymal transition which promotes tumor metastasis and HCC expressing late TGF- β genes are considered to have a poor prognosis (224).

JAK/STAT signaling: JAK/STAT signaling activates genes that promote proliferation, migration and differentiation. This pathway is usually affected by inactivation of the pathway inhibitors SOCS1 and SSI-1 (78).

WNT/ β -catenin signaling: This pathway is involved in embryogenesis, differentiation, proliferation and tumorigenesis and is altered in around 50% of HCC (225). The most common mutations in this pathway occur in the *CTNNB1* gene which stabilizes β -catenin and leads to activation. Other less common mutations in this pathway are found in the *AXIN1* and *AXIN2* genes (3%-16%) (226). Tumors that have *CTNNB1* mutations are considered to have a good prognosis (227). Research is still being done to discover new pathways involved in HCC, among them the LKB1-AMPK axis.

2.7 Liver Kinase B1

Liver kinase B1 [LKB1 or serine/threonine kinase 11 (STK11)] is a serine/threonine protein kinase that is ubiquitously expressed. LKB1 was originally discovered and classified as a tumor suppressor as the gene mutated in patients suffering from Peutz-Jeghers syndrome (PJS, **Figure.6**) (228). PJS is a familial cancer syndrome that presents with gastro-intestinal polyps, and a distinctive pigmentation around the lips, oral mucosa, genitalia, or palmar surfaces (229). The gastro-intestinal polyps that develop in PJS patients can grow big enough to cause obstruction, pain, and gastrointestinal bleeding with anemia (230) additionally, these patients have an increased probability of developing cancers, especially of the lung, ovary, breast, colon and pancreas (231). LKB1 is one of the most commonly mutated genes in sporadic lung cancer, in which 20% to 40% of non-small cell lung carcinomas (NSCLC) have this mutation (232) along with 20% of cervical tumors (233). Deletion of both alleles of *Stk11* in mice leads to death during embryogenesis (234) and heterozygous mice develop gastrointestinal polyps (235,236). Specific deletion of LKB1 in different tissues leads to a different phenotype depending on the tissue and can range from altered differentiation, hyperplasia, to aggressive carcinomas (237–239).

There is only one isoform of the *STK11* gene, found on chromosome 19p13.3, which is 23kb long and comprises 10 exons of which nine are coding (240). Human LKB1 is a 433 amino acid protein (mouse has 436 amino acids), with 3 domains: an amino-terminal domain (N-terminal, 1-49), a kinase domain (49-309), and a carboxy-terminal domain (C-terminal, 309-433, **Figure.6**) (240). The N-terminal domain contains a nuclear localization sequence (NLS), but other than that the N- and C-terminal domains have no identifiable functional domains (240).

LKB1 is generally found in both the cytoplasm and the nucleus of the cell, and when overexpressed it tends to accumulate in the nucleus. Under normal conditions LKB1 forms a heterotrimeric complex with STRAD α (STE-20-related adaptor) and MO25 (mouse protein 25 or calcium binding protein 39). STRAD α is a pseudokinase that lacks several key catalytic residues, it binds LKB1 and acts as an allosteric activator of LKB1 while at the same time it shuttles the complex from the nucleus to the cytoplasm by blocking the N-terminal NLS and facilitating the union of the complex to the exportins CRM1 and exportin 7 (**Figures.6** and **7**) (241,242). The only known function of MO25 in the complex is to stabilize the STRAD α -LKB1 union (242). Both STRAD α and MO25 α have two isoforms with high

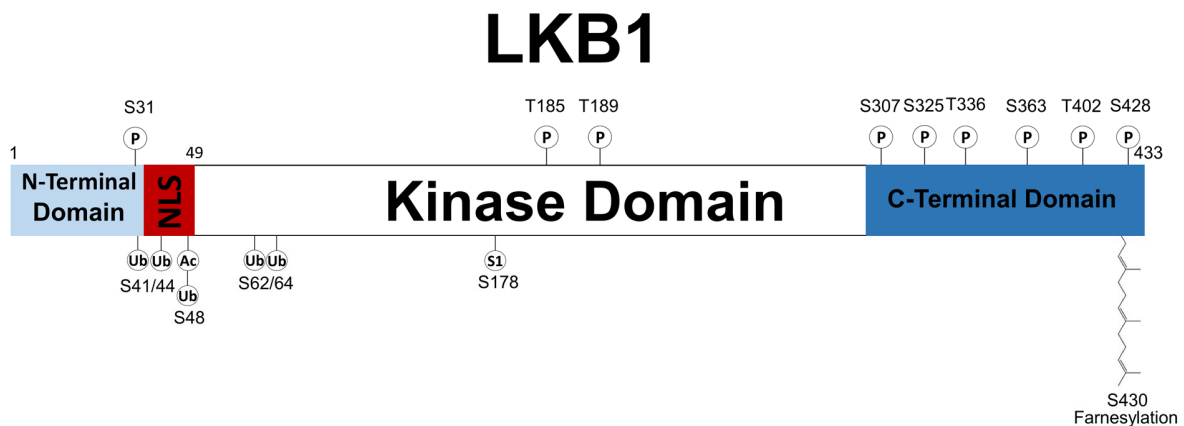


Figure 6. Liver Kinase B1. LKB1 is a 433 amino acid long serine/threonine kinase with a kinase domain, an N-terminal and a C-terminal domain. The N-terminal domain contains a nuclear localization sequence (NLS) that targets the kinase to the nucleus. LKB1 is modified by various post-translational modifications such as phosphorylation, farnesylation, acetylation, SUMOylation, and ubiquitination. Numbers indicate known modified residues P= phosphorylation, Ub= Ubiquitin, Ac= Acetylation, S1= SUMO1, T= Threonine, S= Serine.

sequence homology called STRAD β and MO25 β respectively.

2.7.1 LKB1 targets

When in a complex with STRAD α and MO25, LKB1 is considered to be constitutively active. LKB1 is mostly known for its ability to phosphorylate and activate 5' AMP-activated protein kinase (AMPK).

2.7.1.1 AMPK

AMPK is an ubiquitous cellular energy sensor that is activated when the ratio AMP:ATP increases and once activated it shuts down anabolic pathways that consume ATP and activates catabolic pathways that produce ATP to restore energy homeostasis. AMPK is a heterotrimeric complex composed of the catalytic subunit AMPK α , and the regulatory subunits AMPK β and γ . Each subunit has three different isoforms encoded by different genes which can lead to at least 12 different AMPK combinations (243). AMPK has four binding grooves, one of which is always occupied and another that is always free. The remaining two grooves are bound with ATP, ADP, or AMP and their ratios determine which molecule is bound to the groove, allowing for a more sensitive response to energy stress. When the two remaining grooves are bound with AMP, T172 of the activation loop in the α subunit becomes resistant to dephosphorylation and is more likely to be phosphorylated resulting in the activation of AMPK (240). LKB1 is the major upstream kinase for AMPK at T172 under energy shortage conditions (240), however, CaMKK2 is also known to phosphorylate AMPK at the same residue during changes in calcium concentration (244).

Activated AMPK limits energy consuming pathways and promotes energy producing pathways. AMPK limits energy consumption by inhibiting fatty acid and sterol synthesis by phosphorylating and inactivating ACC1 and HMGCR (245). Additionally, AMPK is also able to inhibit the activity of SREBP1c and ChREBP, two transcription factors involved in the transcription of lipogenic genes (246,247). AMPK is also able to stop gluconeogenesis by inhibiting enzymes such as enolpyruvate carboxykinase and glucose-6-phosphatase (248). AMPK also inhibits autophagy by phosphorylating ULK1 (**section 2.1.3.1**). Finally, AMPK can inhibit protein synthesis by

activating the tuberous sclerosis complex (TSC1 and 2) that inhibits MTORC1 (249).

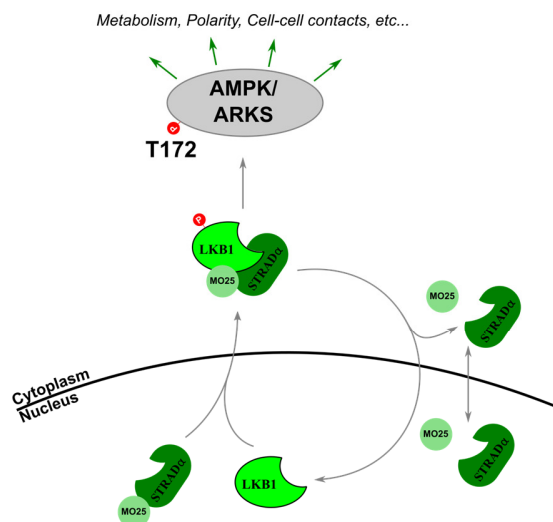


Figure 7. LKB1 is active in the cytoplasm. LKB1 requires the formation of a heterotrimeric complex with STRAD α and MO25 to exit the nucleus and acquire kinase activity. Once in the cytoplasm, LKB1 phosphorylates and activates the AMPK related kinases or ARKS (among them AMPK) which have a diverse set of functions. STRAD α and MO25 are normally found throughout the cell.

2.7.1.2 MTORC1

Mechanistic target of rapamycin complex 1 (MTORC1), composed of MTOR, raptor and mLST8, is the complex in charge of integrating nutrient availability with cellular signals from upstream kinases. The complex is especially activated by the branched chain amino acids [leucine, isoleucine, and valine (250)]. When activated, MTORC1 initiates protein synthesis, activates cell growth proteins, and inhibits autophagy. MTORC1 phosphorylates proteins like 4E-BP1 and S6K1 leading to ribosomal and protein synthesis (251) and can regulate the transcription of Cyclin D1, HIF1 α , and MYC which lead to increased cell growth, cell cycle progression, and angiogenesis (252). MTORC1 is dysregulated in most cancers (253) due to its importance in cell growth and replication. Activation of the LKB1-AMPK pathway leads to the inhibition of MTORC1 signaling by the activation of its TSC inhibitor and direct phosphorylation of raptor by AMPK (249). The inactivation of MTORC1 by LKB1-AMPK is the main route by which LKB1 acts as a tumor suppressor and cells that do not

have a functional LKB1 have increased MTORC1 signaling (254).

2.7.1.3 AMPK related kinases

LKB1 is also able to phosphorylate and activate approximately 12 different AMPK related kinases (ARKs, **Figure.7**) which have a highly conserved sequence around T172, but do not associate with the γ -subunit of AMPK (255). The ARKs have received less attention than AMPK but they are related to a variety of processes such as cell polarity, cell migration and gene transcription (240). Some of the more important ARKs are NUA1 and 2 involved in cell motility and protection from nutrient and oxidative stress (256,257) and MARK1-4 which are ARKs involved in cell polarity. *Drosophila* and *C. elegans* MARK orthologues (Par-1) are required for oocyte polarity and embryo asymmetric division respectively (258,259). When LKB1 is overexpressed in epithelial cells, they polarize, even forming a full brush border without cell-cell contacts (260). The ability to polarize cells is also seen as an LKB1 anti-tumor effect as loss of polarity is common in cancer cells.

2.7.2 LKB1 in the liver

2.7.2.1 Liver Regeneration

The importance of LKB1 in cell metabolism by controlling AMPK is seen in the liver where the LKB1-AMPK axis performs some non-canonical functions. One of the main functions of LKB1-AMPK is seen in liver regeneration. One of the most potent mitogenic cytokines for hepatocytes is HGF which is necessary for DNA synthesis after liver injury. HGF activates c-Met and the Ras/ERK/MAPK pathways which leads to proliferation (261). HGF also activates the LKB1-AMPK axis which leads to increased endothelial nitric oxide synthase (eNOS) activity. eNOS produces nitric oxide (NO) a gaseous second messenger mainly known for its ability to induce vasodilation. Increased NO levels activate inducible nitric oxide synthase (iNOS) which further increase the levels of NO in the cell (262,263). The increase in NO inactivates MAT1/III by S-nitrosylation which reduces the levels of SAmE (264). High levels of SAmE, like in *Gnmt-KO* mice, are known to block HGF induced proliferation (265), because increased SAmE leads to the methylation and activation of protein phosphatases like protein phosphatase 2A (PP2A) which can dephosphorylate LKB1,

AMPK and eNOS turning the pathway off (69). AMPK is also able to induce the transfer of HuR from the nucleus to the cytoplasm. HuR (Human antigen R) is an RNA binding protein that increases the half-life of target mRNAs. During regeneration HuR favors the survival of pro-growth mRNAs such as cyclin A2 and D1 (266). The use of eNOS inhibitors such as NIO or L-NAME blocks the regenerative pathway by not being able to reduce MAT1/III activity and maintaining high levels of SAmE.

2.7.2.2 LKB1 and HCC

LKB1 has been implicated in the proliferation of HCC in tumors derived from NASH. Cells isolated from mouse *Mat1a-KO* tumors (SAmE-D cells) have increased pLKB1 (S428) and pAkt, which is activated independently from the PI3K pathway and is probably due to direct interaction with LKB1. SAmE-D cells also have increased p53 levels but they are retained in the cytoplasm, stabilized by the deubiquitinating enzyme HAUSP. HAUSP is stabilized by the cytoplasmic shuttling and stabilization of HuR by LKB1. These cells are also more resistant to apoptosis, as exposure to UVC results in delayed nuclear accumulation of p53. Knock down of LKB1 reduces pAkt, increases nuclear p53 and HAUSP and induces apoptosis. These results are also found in mouse *Mat1a-KO* tumors and in human tumors derived from ASH and NASH as they all have increased cytoplasmic p53 and pLKB1 (267).

A different tumor cell line derived from *Gnmt-KO* tumors called OKER cells also displays increased pLKB1. In this model, the chronic high levels of SAmE induce the over activation of the Ras/ERK/p90^{RSK} pathway that disconnects LKB1 from AMPK. Like with *Gnmt-KO* mice, OKER cells have increased methylation of Ras inhibitors such as SOCS1 and RASSF1A while the Ras activator RasGRP3 is overexpressed. Demethylating agents and Ras inhibitors lead to a reduced Ras pathway and an activated AMPK resulting in increased apoptosis and cell death. Additionally, xenograft tumors can be blocked by demethylating agents or knock down of LKB1. A similar relationship is also found in human HCC where GNMT levels are inversely related to LKB1 and RasGRP3 levels and the higher the latter the worse the prognosis (268). This data shows that LKB1 can be either a

tumor suppressor or a protumor gene depending on the situation and the organ.

2.7.3 LKB1 post-translational modifications

LKB1 can be modified by various post-translational modifications that can affect its localization and activity (see next section). LKB1 has four auto-phosphorylation sites at threonines 185, 189, 336, and 402 (**Figure.6**), however, mutations of these sites to alanine show no effect on LKB1 catalytic activity or subcellular localization (240).

One of the major phosphorylation sites for LKB1 is serine 428 (mouse 431) which is necessary for LKB1 nuclear export and cell cycle arrest activity (240). This serine can be phosphorylated by p90^{RSK1}, cAMP-dependent protein kinase A (PKA), and protein kinase c (PKC)- ζ in response to the different upstream stimuli that activate them (269,270). PKC- ζ can also phosphorylate serine 307 in endothelial cells and this may be necessary for nuclear export of LKB1 (271). Other phosphorylated residues include serine 363 which is phosphorylated by ataxia telangiectasia mutated (ATM) during ionizing radiation (272) and serine 325 which is phosphorylated by ERK (273). Phosphorylation of serine 325 and serine 428 may be important in melanoma with the mutation BRAF^{V600E}. In this type of melanoma, both S325 and S428 can uncouple LKB1 from AMPK and result in tumor cell proliferation (274). Recent studies such as the BRAF^{V600E} study have shown that S428 may not be necessary for LKB1 activation or that it may be context dependent (274,275). Serine 31 lies in a consensus sequence for phosphorylation by AMPK or ARKs but it has yet to be properly characterized (276).

LKB1 can also be prenylated at serine 430 (mouse 433) with a farnesyl moiety (277) (**Figure.6**). Its proximity to s428 does not appear to affect its phosphorylation and mutation of S428 does not appear to affect LKB1 prenylation (269). In organs such as testis and spleen, a different LKB1 isoform exists that lacks the last 63 residues and thus cannot be prenylated nor phosphorylated (278) and prenylation does not appear to affect cellular localization of LKB1 (269).

LKB1 can also be acetylated. Acetylation can occur at nine different lysine residues spread throughout the protein (K44, 48, 96, 97, 296, 311, 423, and 431, **Figure.6**), however, only lysine 48 appears to have a considerable effect on its localization. Acetylation of K48 inhibits LKB1 translocation to the nucleus by reducing its affinity for STRAD α and LKB1 is deacetylated by the deacetylase SIRT1 (279).

LKB1 can also be ubiquitinated by the Skp2/SCF complex. Polyubiquitination at lysines 41, 44, 48, 62, and 64 increase the stability of the LKB1 complex and favor the binding of LKB1 to MO25 (**Figure.6** and **7**). This mechanism appears to be upregulated in HCC leading to increased LKB1 levels in later stages of the disease (280). Recently, LKB1 was shown to be SUMOylated by SUMO1 (**section 2.8.4**), which increased its interaction with AMPK (AMPK contains a SUMO interaction motif) and results in higher AMPK phosphorylation. LKB1 is SUMOylated more during starvation when AMPK activation is needed (281). Finally, LKB1 can also be NEDDylated (**section 2.8.3**), a modification that increases its stability and is increased during HCC (282).

2.8 Post-translational Modifications

The human genome is estimated to contain around 20,000 to 25,000 genes (genome) (283), however, there are an estimated 1,000,000 proteins (proteome) (284). This vast difference can be explained by post-translational modification of mRNA and proteins. Genomic recombination, initiation of transcription at different promoters, different transcription termination, and alternative transcript splicing are a few ways of increasing protein diversity from the same set of genes (285). The remaining diversity is obtained from post-translational modifications (PTM) that occur during the "life cycle" of the protein (**Figure.8**).

2.8.1 Addition of functional groups

Many different types of functional groups can be used as post-translational modifications. Some of the most widely studied are:

Phosphorylation: Protein phosphorylation is one of the most studied forms of PTM. It mainly involves the addition of a phosphate

group to the side chains of serine, threonine, and tyrosine. Phosphorylation is involved mainly in cell signal transduction affecting many cellular processes such as cell proliferation, growth, and apoptosis. Phosphorylation is a reversible process and allows the target protein to quickly react to a stimulus and perform an action for a limited time. Phosphorylation is carried out by protein kinases which use ATP as the principal donor and the phosphate group is removed by protein phosphatases (286).

Methylation: Methylation is the addition of one-carbon methyl groups (-CH₃) to nitrogen (N-methylation) or oxygen (O-methylation) from an amino acid side chain. Methylation can increase hydrophobicity and mask negative amino acid charges (286). The most common donor of methyl groups is SAMe (section 2.2.1) and the reaction is catalyzed by various methyltransferases. Methylation is mostly known for the histone code, a sequence of methylated and acetylated histone amino acids that can regulate the amount of chromosomal condensation (287).

Acetylation: Acetylation is the addition of an acetyl group (CH₃CO-) most commonly to lysine ε-NH₂. This reaction is catalyzed by various acetyltransferases and the reverse reaction is catalyzed by deacetylases. Acetylation is involved in protein stability, localization, protein synthesis, and is also known for the histone code (287,288). One acetyltransferase that has received a lot of

attention during the past few years is sirtuin1 (SIRT1). This deacetylase has been involved in gene silencing, ageing, cancer, and metabolism (289).

2.8.2 Addition of polypeptides

Another big class of post-translational modifications is the covalent addition of a polypeptide. The biggest groups of polypeptides that are reversibly attached to other proteins are ubiquitin-like proteins (UBL) which can elicit a wide range of effects, ranging from protein stability to DNA repair. UBLs are named after ubiquitin (Ub), the first and most famous of these kinds of proteins to be discovered in 1975 (290). Ubiquitin is mainly associated with the stability of the target protein as polyubiquitinated proteins are signaled for destruction via the proteasome (291). However, recent work has uncovered different roles for ubiquitin sometimes even depending on the type of chains formed on the substrate (292).

UBLs have a similar sequence to Ub and share a similar 3D structure. Additionally, the UBLs share a similar conjugation pathway that involves an E1 activating enzyme, an E2 conjugating enzyme, and an E3 ligase (Figure.9) (293). UBLs are first processed so that the terminal glycine is available for the reaction. The E1 activating enzyme first activates the UBL with ATP and transfers it to the E2 conjugating enzyme, which is then transferred to the E3 ligases which will determine the final substrate the UBL will be

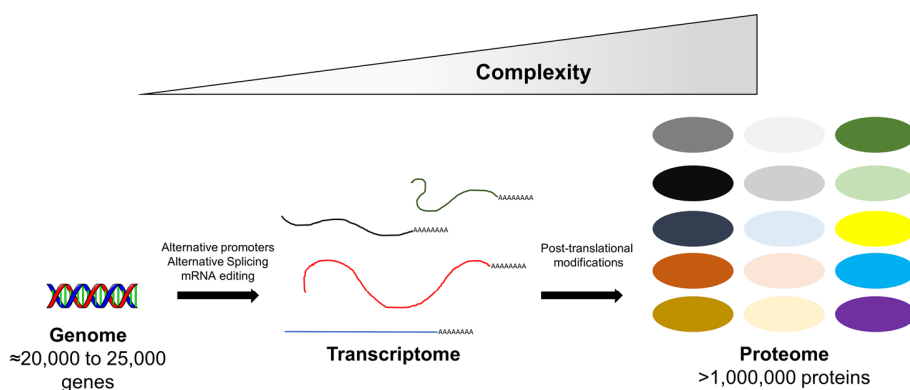


Figure 8. Post-translational modifications increase proteome complexity. Post-translational modifications can increase protein diversity from the 20,000 to 25,000 genes present in the human genome to over 1,000,000 proteins with varying activities, stability and localizations.

covalently attached to (293,294). E1, E2, and E3 enzymes are extremely specific and only load their corresponding UBL despite the extreme similarities between all UBLs (293). All UBLs come with their own set of deconjugating enzymes that efficiently remove the UBL from the substrate and process the precursor. Like the conjugating enzymes, the deconjugating enzymes work mainly with their specified UBL. There are around 16 UBLs (293) and the most studied ones are Ubiquitin, NEDD8 and SUMO while lesser known UBLs are ISG15 (immune system), FAT10 (immune system), Atg8 and 10 (Autophagy), and Ufm1 (erythroid differentiation) (11,293).

2.8.3 NEDDylation

NEDDylation is the covalent addition of Neural precursor cell expressed developmentally downregulated-8 (NEDD8) to a substrate protein. NEDD8 is the UBL that is

most similar to Ub [59% similarity in humans (295)] but despite this similarity both proteins are conjugated to different substrates and carry out different functions in the cell. NEDD8 is mainly localized in the nucleus and is expressed in most adult tissues (296).

The E1 activating enzyme for NEDD8 is the E1 NEDD8 activating enzyme (NAE) which is composed of a regulatory subunit, amyloid- β precursor protein binding protein 1 (APPBP1), and a catalytic subunit known as ubiquitin-activating enzyme 3 (UBA3) (**Figure.9**). This cascade has two E2 enzymes known as ubiquitin-conjugating enzyme E2M (UBE2M or UBC12) and ubiquitin conjugating enzyme E2F (UBE2F). All known NEDD8 E3 ligases belong to the RING subclass and can also function as E3 ubiquitin ligases (297). The most studied E3s are RING-box protein 1 (RBX1) and RBX2 which are components of

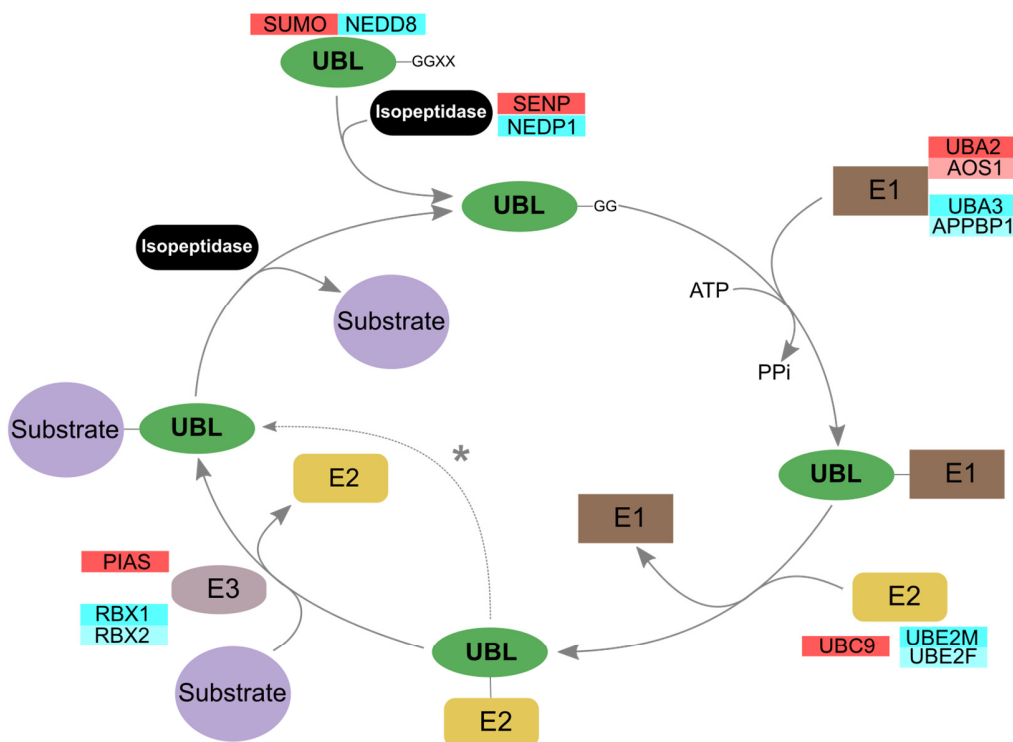


Figure 9. Ubiquitin-like proteins share a similar life cycle. Ubiquitin-like proteins (UBL) share a similar activation and life cycle. A specific isopeptidase produces a mature UBL by exposing the terminal Gly-Gly (-GG) motif which allows the specific E1 to use ATP to activate the UBL. The UBL is then transferred to a specific E2 conjugating enzyme and then to the substrate with the help of a specific E3 ligase. The cycle is closed when the specific isopeptidase cleaves the UBL from the substrate again exposing the terminal Gly-Gly motif. The SUMO specific E2, Ubc9, can attach SUMO directly to the target substrate (*) without the help of an E3 by detecting the SUMO specific consensus sequence. In red are the specific enzymes dedicated to SUMOylation and in blue are the specific enzymes dedicated to NEDDylation.

the cullin-RING ligases (CRL). NEDD8 is deconjugated from its substrates through the deNEDDylating cysteine protease NEDP1 (also known as SENP8 or DEN1) and CSN5, a subunit of the COP9 signalosome that removes NEDD8 from CRL (298). NEDP1 works mainly on non-CRL targets and cleaves the NEDD8 precursor to expose its terminal glycine (299).

2.8.3.1 NEDD8 Targets

NEDD8 is mainly involved in the regulation of the cell cycle and DNA replication, signal transduction, and centrosome and cytoskeletal regulation (300). These effects are mainly mediated through the activity of its most studied and important substrate: cullins. Cullins are scaffold proteins for the Cullin-RING E3 ubiquitin ligases (CRL) which are large ubiquitinating complexes that target many different substrates for destruction. Addition of NEDD8 allows the cullin to dissociate from its inhibitor Cullin-associated NEDD8-dissociated protein 1 (CAND1) and bind the RING domain protein to form the CRL. CRLs can then bind with a substrate receptor that will determine the substrate that gets ubiquitinated. CRLs can bind many different substrate receptors which is the reason why they can target so many different proteins for destruction (301). Interestingly, CRLs require that the NEDD8 moiety be constantly removed otherwise the CRL complex is destabilized and degraded, so CRLs go through cycles of addition and removal of NEDD8 with the help of the COP9 signalosome (301).

Recently, more targets for NEDD8 have been discovered other than the CRLs. These also include a range of different proteins performing different cellular roles. Some of these proteins are HuR (302), EGFR, T β R11, VHL, Smurf1, and a subset of ribosomal proteins (300,303). One of the most important NEDDylated proteins is p53. NEDDylation of p53 by Mdm2 leads to the attenuation of its transcriptional activity (304). Mdm2 can also autoNEDDylate itself increasing its stability.

2.8.3.2 NEDD8 and Cancer

Since NEDD8 targets, especially the CRLs, are involved in many tumor sensitive pathways it is not surprising to find that many cancers have dysregulated components of the NEDD8 pathway (305) and mutations of CRL

adaptors like FBW7 are found in 6% of all cancers and almost 30% of leukemias and gastrointestinal cancers (306). Additionally, cullin upregulation is associated with cancer and tumor progression (307). Some of the cancers in which dysregulated NEDDylation has been studied are lung cancer (308) and liver cancer (282). In HCC tumor prognosis correlated with the upregulation of the NEDDylation pathway. The RNA binding protein HuR (highly expressed in malignant lung and gastric tumors) is also NEDDylated by Mdm2. Mdm2 NEDDylation of HuR retains it in the nucleus and protects it from proteasomal degradation. HuR lysine mutants (K283, 313, 326R) that are incapable of NEDDylation or Mdm2 mutants increase the cytoplasmic localization of HuR and its ubiquitination leading to proteasomal degradation (302).

Recently, MLN4924, a first in class inhibitor of NAE1 (309) and the NEDD8 pathway was developed and its use leads to increased tumor cell death by blocking the cells at the S-phase of the cycle and leading to DNA re-replication. This is because the replication licensing factor CDT1 is stabilized by the absence of CRL activity (310,311). In HCC, the use of MLN4924 on hepatic tumor cell lines leads to increased PEMT flux and altered oxidative phosphorylation and cell apoptosis. Additionally, inhibition with MLN4924 leads to reduced stability of LKB1 and Akt, implicating these kinases as possible NEDD8 substrates (282).

2.8.4 SUMOylation

SUMOylation is the addition of a small ubiquitin-related modifier (SUMO) moiety to the target protein. SUMO is expressed in all eukaryotes and higher eukaryotes express several isoforms (312). SUMO has a 20% amino acid sequence identity with Ub and contains a unique 20 amino acid flexible N-terminal used for the formation of SUMO chains (294). Humans have 4 SUMO isoforms, SUMO 1, 2, 3, and 4. SUMO 1-3 are ubiquitously expressed in all tissues but SUMO 4 appears to be restricted to kidney, lymph node, and spleen (313). SUMO2 and 3 (usually referred as SUMO2/3) are 97% identical but only have a 50% similarity with SUMO1 (294). SUMO1 and SUMO2/3 have different substrates and may have different effects on their targets while SUMO1 tends to

monoSUMOylate its targets; SUMO2/3 forms polySUMO chains on its substrates (314,315).

Like all UBLs, SUMO has its own corresponding E1, E2, and E3 enzymes (**Figure.9**). The E1 activating enzyme is composed of SUMO-activating enzyme 1 (SAE1 or AOS1) and SUMO-activating enzyme 2 (SAE2 or Uba2). This heterodimer uses ATP to activate all types of SUMO. There is only one known E2 enzyme for SUMO called Ubc9 which is unique in that it is able to detect and bind to a specific SUMO conjugating site found on SUMO substrates (**next section**) (316). The final E3 ligases are composed of two different groups: Siz/PIAS and RanBP2. The Siz/PIAS group of E3 ligases contains six members in humans called protein inhibitors of activated STAT (PIAS) composed of PIAS1, isoforms PIAS α and PIAS β , PIAS3, and PIAS γ (317). RanBP2 is an unrelated protein that is found in the nuclear pore and is involved in nucleocytoplasmic shuttling (318). The E3 ligases give the system flexibility and specificity. Similarly, like the other UBLs, SUMO has its own set of deSUMOylases that specifically remove SUMO from its target proteins. Sentrin-specific proteases (SENP) - 1, -2, -3, -5, -6, and -7 all remove SUMO from its substrates and cleave the precursor SUMO to its terminal glycine residue (319). SENP6 and 7 mainly deconjugate SUMO2/3 chains from substrates (320). SENPs normally don't distinguish between SUMO1 and SUMO2/3 but they do have different cellular localization. SENP1 and 6 are found in the cytoplasm and the nucleus (321–323), while SENP2 is found at the nuclear pore (324) and SENP5 is found mainly in the nucleolus (325). SUMO4 is an exception in the SUMO family as it does not appear to be able to be cleaved by SENPs to form a mature form with a terminal glycine (326).

2.8.4.1 The SUMO consensus sequence

The SUMO acceptor lysine is embedded in a small motif that is recognized by the E2 Ubc9. The consensus motif is ψ KXD/E (where ψ is a hydrophobic residue, K is the acceptor lysine, and X is any amino acid) (327). Mutation of the lysine or other amino acids of the motif can lead to reduced SUMOylation of the protein. In some cases the motif can be extended and may require a downstream phosphorylation site to favor SUMOylation (ψ KXD/EXX(pS)P, called

phosphorylation-dependent SUMOylation motif) (328) or the site is flanked by negatively charged amino acids (ψ KXD/EXXEEEE, called negatively charged amino acid dependent SUMOylation motif) (328). Approximately 50% of SUMO substrates have a consensus site (329), the other forms of substrate conjugation are due to SIM-dependent SUMOylation and E3 ligase-dependent SUMOylation. During SIM-dependent (SUMO interacting motifs) SUMOylation, proteins that contain SIMs bind a SUMO moiety that is bound to Ubc9 bringing the acceptor lysine in close proximity for the reaction to occur (330). E3 ligase-dependent modification requires that the target protein recognize the E3 PIAS to bring the acceptor lysine close enough for the reaction to occur (331).

2.8.4.2 SUMO targets

Like most UBLs, SUMO is involved in many different processes. Some of the most important ones are protein localization, activity, and stability. SUMO modified proteins are involved in many diverse cell functions such as nucleocytoplasmic shuttling, DNA repair, mitosis, cell development and differentiation, senescence, and apoptosis (332–334). One of the first targets discovered for SUMO was the nuclear pore transport protein RanGAP which is SUMOylated by the E3 RanBP2 (335,336). Additionally, SUMO has been related to DNA repair mechanisms as loss of PIAS4 and SUMO can lead to loss of ubiquitinated proteins necessary for DNA repair to work efficiently (337,338). The discovery of a SUMO consensus site has led to the discovery of many SUMO target proteins outside the nucleus such as Akt1 (339,340), Argonaute 2 (341,342), MATI1 (343), p85 (344) and STAT5 (345), all involved in different cell processes.

2.8.4.3 SUMO and Cancer

The SUMO pathway is involved in many different cellular pathways that are involved directly or indirectly in growth and division making the pathway a target for cancer. Ovarian (346) and lung adenocarcinoma (347) have increased expression of Ubc9 while SENP1 is overexpressed in prostate cancer (348) and thyroid oncocytic adenoma (349). Ubc9 is also overexpressed in other types of cancer (350,351). Additionally, patients with multiple

Post-translational Modifications in Liver Disease

Imanol Zubiete Franco

myeloma have enhanced SUMOylation in cell lysates and high expression of SUMO isoforms is linked with poor outcome (352). In other studies, researchers found that SUMOylation of Akt1 led to increased Akt activity resulting in more cell proliferation and tumorigenesis. A mutation that is found in many tumors E17K leads to increased SUMOylation of Akt1 resulting in increased activity and a worse outcome (339). In breast cancer, patients with a G73A polymorphism in the Ubc9 gene have a reduced ability for repairing DNA double stranded breaks resulting in increased cancer rates and an association with tumor grade (353,354). For the same reasons that SUMO can promote tumor formation and growth, it can lead to tumor suppression. Over expression of

SENPs can favor the deSUMOylation of Mdm2 and its subsequent degradation leading to increased p53 stability (355).

In HCC, Tomasi *et al.* found that Ubc9 was upregulated by both protein and mRNA levels. In liver, Ubc9 is phosphorylated by Cdc2 which increases Ubc9 stability. Increased SUMO levels were able to reduce phosphorylation of Ubc9 by reducing Cdc2 levels. Both Cdc2 and Ubc9 are increased in HCC along with pUbc9 (356). Other groups have also reported that SUMO1 is increased during HCC when compared to the adjacent healthy tissue and the increase in SUMO1 leads to an increased cell cycle (357) and increased multidrug resistance (358).

Objectives



The image shows two chemical structures. The first is a methyl group, represented as CH₃O, with a single bond extending from the oxygen atom. The second is a peptide chain consisting of two glycine residues (Gly-Gly) followed by a lysine residue (Lys). The lysine residue is shown with a carbonyl group (C=O) and a single bond extending from the oxygen atom.

Post-translational Modifications in Liver Disease
Imanol Zubieta Franco

3. Objectives

The principal aim of this project consists in the study of post-translational modifications in the development of liver disease from non-alcoholic liver disease, through fibrosis, and finally to hepatocellular carcinoma. The three minor objectives for this project are as follows:

Gnmt-KO mice have abnormally high serum levels of SAMe and methionine and quickly develop liver steatosis. In hepatocytes, the major mechanism for lipid catabolism is autophagy which can quickly mobilizes lipid reserves in a process called lipophagy. Defects in this process have been related to steatosis development in the liver. Recent studies in yeast have shown that methionine and SAMe can inhibit autophagy and we have shown that *Gnmt-KO* mice have an inhibited autophagic flux which contributes to steatosis due to the elevated levels of SAMe and methionine. **The first objective** is to determine the mechanisms by which high levels of SAMe and methionine can block autophagy in the liver and the contribution of PP2A and MTOR to the block.

The post-translational modification NEDD8 is involved through its main substrate, the cullin-RING ligases, in many different cell processes. Recent work has uncovered that the NEDDylation pathway is dysregulated in many different types of cancer such as in the lung and liver. Many of the pathways involved in HCC are also affected during liver fibrosis and cirrhosis, the steps before liver cancer. **The second objective** of this project is to determine if the NEDDylation pathway is altered during the formation of liver fibrosis and the role that NEDDylation may play in the evolution of this disease.

Recent work on LKB1 in the liver has uncovered a different role for this kinase in cell growth and proliferation. Contrary to other organs, LKB1 is necessary for liver regeneration after partial hepatectomy and may have a protumoral role. In liver cancer derived from SAMe deficiency or excess, LKB1 is activated and this activation results in a tumor like phenotype. Additionally, HCC patients with upregulated LKB1 levels have a worse prognosis. Work on the mechanisms by which LKB1 can induce tumor growth and proliferation in the liver are being uncovered and among them is the upregulation of the RAS pathway through inhibition of RAS inhibitors and upregulation of RAS activators. Additionally, LKB1 is mainly considered to be active only in the cytoplasm but research has shown that it may have an important role in the nucleus although little work has been done to study the mechanisms that maintain it there. **The third objective** is to study the mechanisms by which LKB1 overexpression can result in liver malignancy and the post-translational mechanisms that determine the localization of LKB1 in the cell as well as the possible effects that nuclear LKB1 can have on cell survival.

Post-translational Modifications in Liver Disease
Imanol Zubieta Franco

Experimental Procedures



Post-translational Modifications in Liver Disease
Imanol Zubieta Franco

4. Experimental Procedures

4.1 Cell Isolation, Culture and Treatments

4.1.1 Primary Cells

4.1.1.1 Mouse Hepatocytes

Primary hepatocytes from 3-month old male wild type (WT) (C57BL/6J strain) and GNMT knockout (*Gnmt-KO*) mice were isolated by perfusion with collagenase type I (Worthington, USA) as described previously (359). In brief, animals were anesthetized with isoflurane (1.5% isoflurane in O₂), the abdomen was opened and a catheter was inserted into the inferior vena cava. The liver was perfused with buffer A [Phosphate Buffered Saline (PBS), 5 mM EGTA, 37°C and oxygenated] and the portal vein was cut. Subsequently, the liver was perfused with buffer B [Phosphate Buffered Saline, 37°C and oxygenated] to remove the EGTA. The liver was then perfused with buffer C [PBS, 1 mM CaCl₂, collagenase type I (Worthington, USA), 37°C and oxygenated]. Once the perfusion was complete, the liver was placed in a petri dish containing Minimum Essential Medium (MEM, Gibco, USA) and the gall bladder was carefully removed after which the liver was gently disaggregated with forceps. The digested liver was then filtered through a sterile gauze; hepatocytes were collected and washed three times in MEM (First wash: 400 rpm, 4 min. Subsequent washes: 500 rpm, 5 min). After the final wash the supernatant was removed (supernatant from the three wash steps was conserved and used to isolate Kupffer cells and hepatic stellate cells, **section 4.1.1.2** and **4.1.1.3**) and the pelleted cells were resuspended in fresh 10% fetal bovine serum (FBS, Gibco) MEM supplemented with 1% penicillin, streptomycin, and glutamine (PSG, Gibco).

Primary hepatocytes were seeded over previously collagen-coated culture dishes at a density of 7600 cells/mm² in 10% fetal bovine serum (FBS; Gibco) MEM supplemented with 1% PSG and placed at 37°C in a humidified atmosphere of 5% CO₂-95% air. After 2-4 hours of attachment, the culture medium was replaced with fresh 10% MEM or 0% FBS MEM depending on the treatments to be performed (**Table.1**).

4.1.1.2 Primary mouse Kupffer Cells

Supernatants from the hepatocyte wash (**section 4.1.1.1**) were joined together and centrifuged 1350 g for 10 min at 4°C. The pellet was resuspended in 10 ml buffer (150 mM NaCl, 6 mM KCl, 10 mM HEPES and 6 mM NaOH) and then loaded onto a 25/50% percoll PLUS (GE Healthcare, UK) gradient and again centrifuged at 1350 g for 30 min at 4°C with minimum acceleration/deceleration. The non-parenchymal cells were collected with a pipette from the interface between the two density cushions of 25% and 50%. Collected cells were centrifuged again at 1350 g for 10 min at 4°C and the resulting pellet was resuspended in RPMI cell medium (Gibco). Kupffer cells were removed from the media by selective adherence, by incubating the resuspended cells on uncoated plastic culture plates for 8 min at 37°C. Afterwards the media was removed and used for primary mouse hepatic stellate cell isolation (**next section**). Primary Kupffer cells were incubated in 0% RPMI medium supplemented with 1% PSG at 37°C in a humidified atmosphere of 5% CO₂-95% air.

4.1.1.3 Primary mouse Hepatic Stellate Cells

The remaining media was centrifuged again and the resulting pellet was resuspended in RPMI. The hepatic stellate cells were then seeded on uncoated plastic culture plates and cultured in RPMI medium 0% FBS and supplemented with 1% PSG at 37°C in a humidified atmosphere of 5% CO₂-95% air.

4.1.1.4 Bcl3 cell line

Barcelona Clinic liver cancer 3 (Bcl3) human cell lines were derived from resected hepatocellular carcinoma patients with Hepatitis C virus infection. Cell cultures were maintained in DMEM/F12 1:1 (Gibco) supplemented with 10% FBS, 1% PSG, 1% Sodium pyruvate (GE Healthcare Life Sciences) and 1% Non-essential amino acids (Gibco) at 37°C in a humidified atmosphere of 5% CO₂-95% air.

4.1.3 Commercial Cell Lines

Huh7

Huh7, human hepatocarcinoma cells, were purchased from the American Type Culture Collection (ATCC) and were cultured in Dulbecco's Modified Eagle Medium (DMEM; Gibco) supplemented with 10% FBS and 1% PSG and 1% Fungizone (Anfotericine B, Gibco) (PSAG).

MLP29

Mouse Liver Progenitor 29 (MLP29) cells were purchased from ATCC and were cultured in DMEM supplemented with 10% FBS and 1% PSAG.

LX-2

LX-2 cells are immortalized human hepatic stellate cells that still retain the ability to respond to transforming growth factor beta (TGF- β) and platelet-derived growth factor (PDGF) (360). LX-2 cells were purchased from Merck-Milipore, Germany, and cultured in DMEM 2% FBS supplemented with 1% PSAG.

All commercial cell lines were cultured at 37°C in a humidified atmosphere of 5% CO₂-95% air.

4.1.4 Cell Treatments

Primary hepatocytes and commercial cell lines were subjected to different treatments in the present work. Reagents, concentrations and FBS percentage in the culture medium are presented in **Table 1**.

4.1.4.1 Hypoxia

For hypoxia experiments, cells were incubated in an Invivo₂ 400 hypoxia Workstation (Baker Ruskinn, USA) at 1% O₂ for 24 hours and lysed/fixed in the hypoxia chamber unless otherwise stated.

Table 1. Treatments and compounds used for *in vitro* experiments.

Compound	Dose	Vehicle	Function/Target	Supplier	%FBS
3-Deazaadenosine	20 μ M	dH ₂ O	Inhibitor of methylation reactions	Sigma Aldrich	10
Ammonium Chloride	20 mM	dH ₂ O	Raises Lysosomal pH (N/L)	Sigma Aldrich	0
Butyrolactone-3	100 μ M	DMSO	Inhibits GCN5	Abcam	10
Chloroquine	60 μ M	dH ₂ O	Inhibitor of lysosome mediated proteolysis	Sigma Aldrich	0
Deoxycholic acid	50 μ M	dH ₂ O	Toxic bile acid	Sigma Aldrich	0
Ex-527	30 μ M	DMSO	Selectively inhibits SIRT1	Sigma Aldrich	10
Insulin	0.5 μ g/ml	Culture Medium	Metabolic hormone	Sigma Aldrich	0
Leupeptin	100 μ M	dH ₂ O	Protease inhibitor (N/L)	Sigma Aldrich	0
Lipopolysaccharide	200 ng/ml	Culture Medium	Endotoxin	Sigma Aldrich	0
L-Methionine	0.125-1 mM	Culture Medium	Multiple functions	Sigma Aldrich	0
MLN4924	3 μ M	DMSO	Inhibits NAE1	Millenium Pharmaceuticals	0
Okadaic Acid	1 nM	-	PP2A inhibitor	Sigma Aldrich	0
SAME	0.5-4 mM	Culture Medium	Multiple functions	Abbott	0
TGF- β	8 ng/ml	dH ₂ O	Multifunction cytokine, involved in fibrosis	Peprtech	0

4.2 DNA and RNA

4.2.1 Cell Transfection

Plasmid cDNA transfection

The protocol for commercial cell line transient transfection using Lipofectamine 2000 (Invitrogen, USA) was as follows:

DNA-Lipofectamine complex formation: Lipofectamine 2000 (2.5 μ l/1 μ g DNA) was diluted in 500 μ l of OPTI-MEM (Gibco) medium for transfections in 60 mm culture plates and in 1 ml for transfections in 100 mm culture plates and incubated for 5 min. After incubation, the mixture was added to 500 μ l of OPTI-MEM (1 ml for 100 mm plates) containing plasmid DNA (1 to 6 μ g depending on the experiment), and incubated for at least 20 min at room temperature (RT) to allow for the formation of the DNA-Lipofectamine complexes.

Cell transfection: DNA-lipofectamine complexes previously formed were added to the culture plates containing the corresponding culture medium with 10% FBS but without antibiotics and with the cells in suspension. For experiments involving FLAG-LKB1 and HIS₆-SUMO, the ratio of 3 μ g plasmid/1,000,000 cells was used and in experiments that required transfection of two or more plasmids a ratio of 2:2:1 μ g was used. DNA-lipofectamine complexes, cells and media were mixed to a concentration of 62,500 cells/ml and then plated in the appropriate culture plate. The mixture with cells was left overnight and the culture media was replaced next morning with fresh culture medium supplemented with antibiotics. Approximately 6 hours after the media change, the cells were either lysed or subjected to the corresponding treatment depending on the experiment. Transfection efficiency was confirmed by Western blotting or RNA expression analysis.

The protocol for transient transfection using jetPRIME (Polyplus transfection, France) in LX-2 cells and primary cells was as follows:

2 μ g of plasmid were diluted in 200 μ l of jetPRIME buffer, briefly vortexed, 4 μ l of jetPRIME reagent were added (for LX-2 cells, due to toxicity, half the quantity of jetPRIME reagent was used), the mixture was briefly vortexed again and then incubated at RT for 10 min. After the incubation, the mixture was added to the cells in suspension with the appropriate culture medium supplemented with FBS and antibiotics and the mixture was left overnight. Primary hepatocytes were maintained with the mixture for 4 to 6 hours after which fresh media was added. For the LX-2 pulldown assays, cells were transfected with 3 μ g of His₆-NEDD8, the next day the transfection mixture was replaced with fresh media and left for 6-8 hours. Finally a new transfection mixture with 3 μ g of CS2-FLAG Smad2 was added to the media and also left overnight. Transfection efficiency was confirmed by Western blot or RNA expression analysis.

The plasmids used in this study are listed in **Table 2**.

4.2.2 Plasmid Constructs

SUMO mutant LKB1 plasmid construction

Putative SUMO sequence binding sites on LKB1 were analyzed using the SUMOplot Analysis Program (<http://www.abgent.com/SUMOplot>, Abgent, USA). The 4 highest ranking sites predicted by SUMOplot were used to create the mutants (lysines 96, 97, 178 and 235; **Table.2**). Lysines were mutated to arginines (R). An additional acetylation mutant (K48R) was also created based on (279). The mutant LKB1 plasmid constructs were created using the QuickChange kit for directed mutagenesis (Stratagene, USA), according to the manufacturer's instructions, with two complementary oligonucleotides and with the pcDNA3-FLAG LKB1 plasmid as a template. The products were sequenced (STABvida, Portugal) to ensure that only the correct lysine had been mutated.

Table 2. List of plasmids used in cell transfections.

Plasmid	Source	Id.
CS2 FLAG-Smad2	Addgene	#14042
pcDNA3-His ₆ -NEDD8	Dr. Rodríguez	-
pcDNA3-His ₆ -ΔGG-NEDD8	Dr. Xirodimas	-
V5-NEDP1	Dr. Xirodimas	-
pcDNA3-FLAG-LKB1	Addgene	#8590
pcDNA3-FLAG-KD LKB1 (K78I)	Addgene	#8591
FLAG-SENP1	Dr. Rodríguez	-
FLAG-SENP2	Addgene	#18047
pcDNA3-RGS SENP3	Addgene	#18048
pcDNA3-RGS SENP5	Addgene	#18053
FLAG-SENP6	Addgene	#18065
p3xFLAG-CMV-10-SENP7	Addgene	#42886
pCMV-FLAG PIAS1	Dr. Rodríguez	-
pCMV-FLAG hPIASα	Addgene	#15209
pCMV-FLAG hPIASβ	Addgene	#15210
pCMV-FLAG hPIASγ	Addgene	#15208
pECE-FLAG SIRT1	Addgene	#1791
pcDNA4-STRADα	Dr. Rodríguez-Nieto	-
pcDNA3-His ₆ -SUMO1	Dr. Rodríguez	-
pcDNA3-His ₆ -SUMO2	Dr. Rodríguez	-
pcDNA3-His ₆ -SUMO3	Dr. Rodríguez	-
pcDNA-V5 Ubc9	Dr. Rodríguez	-
pcDNA3-FLAG-LKB1 K48R	Site-directed mutagenesis	-
pcDNA3-FLAG-LKB1 K96R	Site-directed mutagenesis	-
pcDNA3-FLAG-LKB1 K97R	Site-directed mutagenesis	-
pcDNA3-FLAG-LKB1 K178R	Site-directed mutagenesis	-
pcDNA3-FLAG-LKB1 K235R	Site-directed mutagenesis	-
pcDNA3-LacZ	Invitrogen	-

Gene Silencing

Cells were transfected with specific siRNAs at a final concentration of 84 nM to 100 nM using JetPRIME, Dharmacon (GE lifesciences, USA) or Lipofectamine 2000 reagents. The siRNAs used and their conditions are detailed in **Table 3**. Gene silencing efficiency was confirmed by Western blot or mRNA expression.

4.2.3 RNA extraction and processing

4.2.3.1 RNA isolation

Total liver, cultured hepatocytes, Kupffer cell, hepatic stellate cell or commercial cell line RNA was isolated using TRIzol reagent (Invitrogen) according to manufacturer's instructions. 5 μg of Glycogen (Ambion, USA) were used in the RNA precipitation step to facilitate RNA pellet visibility. RNA concentration was determined spectrophotometrically in the Nanodrop ND-100 spectrophotometer (ThermoFisher Scientific, USA).

Table 3. List of siRNAs used in *in vitro* silencing assays.

siRNA	Concentration	Provider	Id.	Conditions
NAE1	100 nM	Qiagen	SI00901187	jetPRIME, o/n
PP2A catalytic subunit α	84 nM (hepatocytes) 100 nM (MLP29)	Sigma-Aldrich	SASI_Mm01_00038232	DharmaFECT (hepatocytes), Lipofectamine 2000 (MLP29), twice during a 48h period, o/n
PP2A catalytic subunit β	84 nM (hepatocytes) 100 nM (MLP29)	Sigma-Aldrich	SASI_Mm01_00126453	DharmaFECT (hepatocytes), Lipofectamine 2000 (MLP29), twice during a 48h period, o/n
c-Jun	100 nM	Qiagen	SI00300580	jetPRIME o/n
siControl	100 nM	Qiagen	SI1022076	jetPRIME o/n

4.2.3.2 Retrotranscription and Real Time quantitative PCR (RT-qPCR)

1-2 μ g of isolated RNA were treated with DNase I (Invitrogen) and cDNA was synthesized with M-MLV reverse transcriptase in the presence of random primers and RNaseOUT (all from Invitrogen). cDNA for RNA (500 ng) samples isolated from primary hepatic stellate cells was synthesized with SuperScript III reverse transcriptase (Invitrogen) without previous DNase I treatment. Resulting cDNA was diluted 1/10 (1/20 if 2 μ g were used) in RNase free water (Sigma-Aldrich, USA). PCRs were performed using either the BioRad iCycler iQ5 Thermalcycler, with iQ SYBR Green Super Mix (Bio-Rad, USA) or the ViiA 7 Real time PCR System, with SYBR Select Master Mix (Applied Biosystems, USA). For the iCycler, 5 μ l of cDNA were used and including the specific primers the total reaction volume was 20 μ l in a 96-well plate (BioRad). For the ViiA 7, 1.5 μ l of cDNA were used and including the specific primers the total reaction volume was 6.5 μ l in a 384-well plate (Applied Biosystems). All reactions were performed in triplicate. PCR conditions for the primers were optimized, and 40 cycles with a melting temperature of 60 $^{\circ}$ C, and 30 sec for each step, were used.

Primers were designed using the Primer 3 software (361) via the NCBI-Nucleotide webpage (<http://www.ncbi.nlm.nih.gov/nucleotide/>) and synthesized by Sigma Aldrich. Primer sequences are detailed in **Tables 4 and 5**. After checking the specificity of the PCR products with the melting curve, data was normalized to the expression of a housekeeping gene (GAPDH or 18S).

4.3 Protein

4.3.1 Protein Extraction and Analysis

Extraction of total protein was performed as described previously (266). Cells were washed with PBS buffer and resuspended in 200 μ l of lysis buffer [Caspase buffer: (HEPES 10 mM pH 7.4, 0.1% CHAPS, DTT 125 mM, EDTA 2 mM), RIPA: (1.6 mM NaH₂PO₄, 8.4 mM Na₂HPO₄, 0.5% Azide, 0.1 M NaCl, 0.1% SDS, 0.1% Triton X-100, 5 mg/ml sodium deoxycholate) and NP-40: (50 mM Tris-HCl pH 8.5, 150 mM NaCl, 1% NP-40, 5 mM EDTA)]. All lysis buffers except caspase buffer were supplemented with protease and phosphatase inhibitor cocktails (Roche, Switzerland). In the case of frozen liver tissue, approximately 50 μ g of tissue was homogenized by using a Precellys 24 tissue homogenizer (Precellys, France) in 500 μ l of buffer. In all cases, the lysates were centrifuged (13000 rpm, 20 min, 4 $^{\circ}$ C) and the supernatant (protein extract) was quantified for total protein content by the Bradford protein assay (Bio-Rad) or by BCA protein assay (Pierce, USA) depending on the type of lysis buffer used and determined using a Spectramax M3 spectrophotometer (Molecular Devices, USA).

Table 4. List of mouse primers used.

Gene	Forward Primer (5'-3')	Reverse Primer (5'-3')
<i>Bax</i>	CTGGATCCAAGACCAGGGTG	GTGAGGACTCCAGCCACAAA
<i>Bcl-2</i>	CCAGCATGCGACCTCTGTTT	CTTGTGGCCCAGGTATGCAC
<i>Ccl2</i>	GACCCCAAGAAGGAATGGG	ACCTTAGGGCAGATGCAGTT
<i>Ccr1</i>	GAGGGCCCCGAAGTACTT	GGCTACAGGTACGGTGAGTG
<i>Ccr2</i>	ATCCACGGCATACTATCAACAT	CAAGGCTCACCATCATCGTAG
<i>Ccr5</i>	GTCAGAACGGTCAACTTTGGG	GTGTGGAAAATGAGGACTGCAT
<i>Col1a1</i>	CAGTCGCTTCACCTACAGCA	CGGGAGGTCTTGGTGGTTTT
<i>Col1a2</i>	GGCTCTAGAGGTGAACGTGG	CACCAGGGGCACCATTAACT
<i>Cxcl2</i>	GTCCCTCAACGGAAGAACCA	CTCAGACAGCGAGGCACATC
<i>Gapdh</i>	TTGATGGCAACAATCTCCAC	CGTCCCGTAGACAAAATGG
<i>Gnmt</i>	ACCAGTATGCAGATGGGGAG	CCAATTGTCAAAGGATGGCT
<i>Il-1b</i>	GCCACCTTTTGACAGTGATGAG	GACAGCCCAGGTCAAAGGTT
<i>Il-6</i>	GCTGGTGACAACCACGGCCT	AGCCTCCGACTTGTGAAGTGGT
<i>Mmp9</i>	TTGCTTCAGCTCCACAGAGA	TGGTTGTAGAGGGCAAGGAC
<i>Nae1</i>	CAGTATTGGCAAGAACCAGAGC	AACATCTGCTAAACGCAGCA
<i>Nedd8</i>	CAGCAGCGGCTCATCTACAG	CAGGGCAAGGAGGTAACCGG
<i>Nos2</i>	GGCAGCCTGTGAGACCTTTG	GCATTGGAAGTGAAGCGTTTC
<i>Ppp2ca</i>	GGCCTGAGTATGTGCACTGT	GATGGCCCGCAAGGATTCTA
<i>Ppp2cb</i>	GGATCCTGCCACCATCACAA	GTTGATGTGGTACGTGTGCG
<i>Stk11</i>	GTCAGCTGGGGTCACACTTT	TGGTGAAGTCTCCTCTCCCA
<i>Strada</i>	ACTGCGCTCTGACTCCTAGA	GAGGCTGCTCTCCAAACAGT
<i>Tgfb</i>	TTGCTTCAGCTCCACAGAGA	TGGTTGTAGAGGGCAAGGAC
<i>Tnfa</i>	CGTCAGCCGATTTGCTATCT	CGGACTCCGCAAAGTCTAAG

Western blotting

Protein extracts were boiled at 95 °C for 5 min in SDS-PAGE sample buffer (250 mM Tris-HCl pH 6.8, 500 mM β -mercaptoethanol, 50% glycerol, 10% SDS and bromophenol blue). An appropriate amount of protein (between 5 and 30 μ g), depending on protein abundance and antibody sensitivity, were separated by sodium dodecyl sulphate-polyacrylamide gel electrophoresis (SDS-PAGE) in 8% to 15% acrylamide gels (depending on the molecular weight of the protein of interest), using a Mini-PROTEAN Electrophoresis System (Bio-Rad). Gels were transferred onto nitrocellulose membranes by electroblotting using a Mini Trans-Blot cell (Bio-Rad). Membranes were blocked with 5% nonfat milk in TBS pH 8 containing 0.1% Tween-20 (Sigma Aldrich) (TBST-0.1%), for 1 hour at RT, washed three times with TBST-0.1% and incubated overnight at 4 °C with commercial primary antibodies. Primary antibodies and their optimal incubation conditions are detailed in **Table 6**. Membranes were then washed three times with TBST-0.1% and incubated for 1 hour at RT in blocking solution containing secondary antibody conjugated to horseradish-peroxidase (HRP, **Table.6**). Immunoreactive proteins were detected by using Western Lightning Enhanced Chemiluminescence reagent (ECL, PerkinElmer, USA) and exposed to Super Rx-N X-ray films (Fuji, Japan) in a Curix 60 Developer (AGFA, Belgium).

4.3.2 Protein immunoprecipitation assays

Protein-Protein complexes were immunoprecipitated as follows:

Cell lysate preparation: Cells were lysed in NP-40 buffer. Whole-cell lysates were processed and quantified for protein content as described in **section 4.3.1**.

Covalent cross-linking of antibodies to beads: In order to limit the recovery of light and heavy antibody chains during immunoprecipitation, antibodies were covalently cross-linked to Protein A-Sepharose beads (Sigma Aldrich). 100 μ l of beads were washed 5 times with PBS (5000 rpm, 5 min, 4 °C) and incubated overnight with the primary antibody: Strada (Santa Cruz Biotechnology, USA, 5 μ g), mTOR (Cell Signaling Technology, USA, 5 μ g), pSmad2 (Cell Signaling Technology, 5 μ g) and IgG2 (BD Pharmingen, USA) as a negative control. After incubation, beads were washed two times (2500 rpm, 5 min, 4°C) with sodium borate buffer (0.2 M Borate, 3 M NaCl, pH 9), and covalently cross-linked with borate buffer containing dimethyl pimelimidate for 30 min at RT with agitation. Beads were then washed two times with borate buffer and incubated with 0.2 M ethanolamine, pH 8, for 2 hours protected from light at RT with agitation. The covalent cross-linking reaction was stopped by washing beads twice with fresh glycine buffer (200 mM, pH 2.5). Beads were washed twice with PBS with 0.1% azide and kept at 4 °C until incubation with the protein extracts.

Table 5. List of human primers used.

Gene	Forward Primer (5'-3')	Reverse Primer (5'-3')
<i>COL1A1</i>	CAAGAGTGGTGATCGTGGGT	CACGGTGACCCTTTATGCCT
<i>G6PD</i>	GTCCTGCATGAGCCAGATAGG	GGTCGATGCCGTAGATCTGG
<i>GAPDH</i>	AATGAAGGGGTCATTGATGG	AAGGTGAAGGTCGGAGTCAA
<i>NAE1</i>	TTGTGGCCAAAGAGGGTCAA	ATGATTACCCACAGCGGCAG
<i>NEDD8</i>	CTACAGACAAGGTGGAGCGAA	CTCCTCTCAGAGCCAACACC
<i>PAI1</i>	CAATCGCAAGGCACCTCTGA	AAACACCCTCACCCGAAGT
<i>PGD</i>	GGGTCTTCCCTCACTCGTC	TAAGTTCTGGCCATGACGG
<i>RASGRP3</i>	GCAGAATGCCTCTCACCACT	GGGAGGTAGGCTGCGATTTAG
<i>RN18S</i>	CCGATAACGAACGAGACTCTGG	TAGGGTAGGCACACGCTGAGCC
<i>SLC2A1</i>	GGCTTCTCCAAGTGGACCTC	CCGGAAGCGATCTCATCGAA
<i>TKT</i>	CAGGGATGCCATTGCACAAG	CAGGAATGTATAGACCCCGC
<i>ACTA2</i>	CTTGTCAGGAGTCCGCTC	TTTCTTGGGCCTTGATGCGA

Immunoprecipitation assay: Covalently cross-linked beads were incubated with 500 μ g of protein lysate overnight at 4 °C with agitation (IgG controls were a mixture from all the lysates). After incubation beads were washed five times with NP-40 lysis buffer and bound proteins were eluted by heating at 95 °C for 5 min in SDS PAGE buffer without β -mercaptoethanol to avoid light and heavy chain contamination. Immunoprecipitated proteins (IP) and original cell extracts (Input) were analyzed by Western blotting with the appropriate antibodies.

Nickel-Histidine affinity purification using nickel-nitriolotriacetic acid (Ni²⁺-NTA) beads

Huh7 cells were transfected with pcDNA3-His₆ SUMO 1, 2, or 3 and a FLAG-LKB1 plasmid as described before (**section 4.2.1**). For some specific experiments other plasmids were also co-transfected (**Table.2**). 36 hours after transfection cells were collected for the purification protocol. LX-2 cells were transfected with pcDNA3-His₆ NEDD8 or pcDNA3-His₆- Δ GG-NEDD8 and CS-FLAG Smad2 as described before (**section 4.2.1**) and collected 36 hours after transfection.

Table 6. List of commercial antibodies used for Western blot

Antibody	Id.	Supplier	Dilution	Incubation Solution
4-EBP1	9452	Cell Signaling Technology	1/1000	TBST-0.01%-Milk 5%
AMPK	07-350	Milipore	1/1000	TBST-0.01%-Milk 5%
c-Jun	9165	Cell Signaling Technology	1/1000	TBST-0.01%-BSA 3%
Demethylated PP2A	05-577	Upstate	1/100	TBST-0.01%-Milk 5%
FLAG	F1804	Sigma Aldrich	1/500	TBST-0.01%-Milk 5%
GAPDH	ab8245	Abcam	1/10000	TBST-0.01%-Milk 5%
JNK	9252	Cell Signaling Technology	1/1000	TBST-0.01%-Milk 5%
LC3B	2775	Cell Signaling Technology	1/1000	TBST-0.01%-Milk 5%
LKB1	3050	Cell Signaling Technology	1/1000	TBST-0.01%-Milk 5%
MTOR	2983	Cell Signaling Technology	1/1000	TBST-0.01%-Milk 5%
NAE1	API3067C	Abgent	1/1000	TBST-0.01%-Milk 5%
NEDD8	ab81264	Abcam	1/1000	TBST-0.01%-Milk 5%
p4E-BP1 S65	9451	Cell Signaling Technology	1/1000	TBST-0.01%-Milk 5%
p53	sc-126	Santa Cruz Biotechnology	1/1000	TBST-0.01%-Milk 5%
pAMPK T172	2531	Cell Signaling Technology	1/1000	TBST-0.01%-Milk 5%
pJNK T183/Y185	446826	Life Technologies	1/1000	TBST-0.01%-BSA 3%
pLKB1 S428	NBPI-19951	Novus Biological	1/500	TBST-0.01%-BSA 3%
pMTOR S2448	2971	Cell Signaling Technology	1/1000	TBST-0.01%-Milk 5%
pS6 S235/S236	4857	Cell Signaling Technology	1/1000	TBST-0.01%-Milk 5%
pSmad2 S465/S467	3101	Cell Signaling Technology	1/1000	TBST-0.01%-Milk 5%
RGS-His	34610	Qiagen	1/1000	TBST-0.01%-Milk 5%
S6	2317	Cell Signaling Technology	1/1000	TBST-0.01%-BSA 3%
Smad2/3	3102	Cell Signaling Technology	1/1000	TBST-0.01%-Milk 5%
STRADα	sc-55052	Santa Cruz Biotechnology	1/500	TBST-0.01%-BSA 3%
TNFR1	sc-8436	Santa Cruz Biotechnology	1/1000	TBST-0.01%-Milk 5%
V5	377500	Invitrogen	1/500	TBST-0.01%-Milk 5%
α-Tubulin	ab18251	Abcam	1/5000	TBST-0.01%-Milk 5%
β-Actin	A-5316	Sigma-Aldrich	1/10000	TBST-0.01%-Milk 5%
PP2A, Subunit A	07-250	Upstate	1/1000	TBST-0.01%-Milk 5%
Anti-mouse IgG, HRP-linked	7076	Cell Signaling Technology	1/5000	TBST-0.01%-Milk 5%
Goat anti Rabbit IgG (H+L)-HRP Conjugate	170-6515	Bio-Rad	1/5000	TBST-0.01%-Milk 5%

His₆-SUMOylated or His₆-NEDDylated proteins were purified as previously described (339,362). Briefly, cells were lysed in lysis buffer (6 M guanidinium-HCl, 0.1 M Na₂HPO₄/NaH₂PO₄, 0.01 M Tris-HCl pH 8, 10 mM β-mercaptoethanol, 10 mM imidazole and 0,1% Triton X-100, buffer pH 8), sonicated and then 100 μl of low density Ni²⁺-NTA-agarose beads (ABT, Spain) that had been previously coated with BSA and washed with lysis buffer were added. Lysates were incubated with beads for 3 hours in agitation at RT. After incubation, the mixture was washed with wash buffer 1 (6 M guanidinium-HCl, 0.1 M Na₂HPO₄/NaH₂PO₄, 0.01 M Tris-HCl pH 8, 10 mM β-mercaptoethanol, and 0,1% Triton X-100, buffer pH of 8) once, twice with wash buffer 2 (8 M urea, 0.1 M Na₂HPO₄/NaH₂PO₄, 0.01 M Tris-HCl pH 8, 10 mM β-mercaptoethanol, and 0,1% Triton X-100, buffer pH 8), and finally three times with wash buffer 3 (8 M urea, 0.1 M Na₂HPO₄/NaH₂PO₄, 0.01 M Tris-HCl pH 6.3, 10 mM β-mercaptoethanol, and 0,1% Triton X-100, buffer pH 6.3). After the last wash, the bound proteins were eluted with 500 mM imidazole in 5% SDS, 0.15 M Tris-HCl pH 6.8, 30% glycerol and 0.72 mM β-mercaptoethanol. The eluates were subjected to SDS-PAGE and the proteins transferred to a nitrocellulose membrane for Western blotting against LKB1 or Smad2.

Chromatin Immunoprecipitation (ChIP)

ChIP analysis was performed using the Magna ChIP assay kit (Millipore). Bcl3 cells expressing WT LKB1 or LacZ were seeded in p150 culture plates, crosslinked with 1% formaldehyde (v/v) at RT for 10 min. Cells were lysed and the DNA was sonicated into 200-500 bp using a Bioruptor plus sonicator (Diagenode, Belgium). An agarose gel was run using a sample of the sheared DNA to ensure that the majority of the DNA fragments were between 200 and 500 bp. The remaining protocol was completed following the manufacturer's instructions. IgG1 (BD Pharmingen) was used as the negative control, H3K9Me3 (Merck Millipore) as a positive control and LKB1 (Cell Signaling) as assay antibody. The primers used in the assay for the detection of the RasGRP3 promoter were: Pp1 5'-TGG GCA ATG GAG GTG ATG ACA GC-3' and Pp2 5'-AGC AAG TTT CTC TTC AAC GTG CCT-3'.

ELISA Assays

Enzyme-Linked Immunosorbent Assays (ELISA) for mouse Tumor Necrosis Factor alpha (TNF-α), Interleukin-6 (IL-6) and Transforming Growth Factor beta (TGF-β) were performed using the DuoSet ELISA Development Kit according to the manufacturer's instructions (R&D Systems, USA). Briefly, the capture antibody was left overnight to bind to the well surface. After, washing the wells, the sample (liver protein extract or Kupffer cell media) was added to the wells at RT for 3 hours to allow binding. The wells were washed again and the detection antibody was added for 3 hours at RT. Finally, the detection antibody was washed and a detection substrate was added. The resulting color was quantified using a Spectro M3 spectrophotometer. To measure TGF-β, liver protein samples were subjected to a previous acid activation step as described previously (363).

PP2AC Subunit Methylation Assay

Hepatocytes were pre-treated with 3-Deazaadenosine (Deaza; Sigma) (20 μM) during 6h, and then cultured in SAME and methionine supplemented medium during 12h. 20 μl of protein lysate (1 μg/μl) were treated with either 50 μl of preneutralized base solution (80 mM NaOH, 80 mM HCl, and 200 mM Tris pH 6.8) or with 20 μl of base (200 mM NaOH) during 20 minutes to completely demethylate PP2AC and then neutralized with 30 μl of neutralization buffer (133.3 mM HCl and 333.3 mM Tris pH 6.8). Samples were compared by immunoblot using unmethylated PP2A antibody (Upstate biotechnology, USA). Percentage of PP2A methylation was calculated by subtracting the densitometry value of unmethylated PP2A normalized with Actin, in the sample treated with base solution by the densitometry value in the control sample. Percentage was calculated by considering WT control samples as 100%.

Hydroxyproline Assay

Liver hydroxyproline content was analyzed using the Hydroxyproline Assay Kit (MAK008, Sigma-Aldrich) following the manufacturer's instructions. Briefly, approximately 10 mg of liver was

hydrolyzed in 12M HCl for 3h then 50 μ l of supernatant was transferred to a 96 well plate and placed in a 60°C oven to dry. The colorimetric reaction was achieved following the manufacturer's instructions. The mg of liver used in the assay was used to determine the amount of hydroxyproline/mg of each liver.

Luciferase Assay

Luciferase activity was measured using the Cignal SMAD Reporter Assay Kit (Qiagen, Germany). LX-2 cells were cultured in MEM 0% FBS overnight. The next day the cells were transfected with the reporter plasmids using jetPRIME for 4 hours. Cells were then treated with 8 ng/ml TGF- β and 3 μ M MLN4924 for 6 hours and luciferase activity was measured using the Dual-Glo Luciferase Assay System (Promega, USA) following the manufacturer's instructions.

4.4 Immunostaining Assays

4.4.1 Histology, Immunohistochemistry and Immunohistofluorescence

Histology and Immunohistochemistry

Paraffin-embedded sections (5 μ m thick) of formalin-fixed liver samples were initially deparaffinized in xylene or xylene-substitute and rehydrated through graded alcohol solutions. Once hydrated, sections were subjected to the following stainings:

Hematoxylin & eosin: After the deparaffinization and rehydration process, sections were subjected to conventional hematoxylin & eosin staining (http://www.ihcworld.com/_protocols/special_stains/h&e_ellis.htm).

Sirius Red: Rehydrated sections were stained with Sirius red solution 1 (0.01% Fast Green FCF in picric acid, Sigma Aldrich) for 15 min and then with Sirius red solution 2 (0.04% Fast Green FCF/0.1% Sirius red in picric acid, Sigma Aldrich) for another 15 min. The sections were then dehydrated directly in 100% alcohol and mounted in DPX mounting medium (Sigma Aldrich).

Sudan Red: Formalin fixed liver samples were washed in 60% isopropanol and then stained with fresh Sudan III (0.5% in isopropanol; Sigma Aldrich) solution for 30 min. Samples were then washed again in 60% isopropanol and then counterstained with hematoxylin and eosin. The sections were then washed with distilled water and mounted in DPX mounting medium.

Specific antibodies used in immunohistochemistry can be found in **Table 7**.

For the analysis, images were taken with an upright light microscope (Zeiss, Germany). The average sum of intensities and stained area percentage of each sample was calculated using FRIDA software (<http://bui3.win.ad.jhu.edu/frida/>, John Hopkins University).

Immunohistofluorescence

Rehydrated sections were unmasked in citrate buffer pH 6 then blocked with 3% H₂O₂ PBS for 10 min and then incubated with PBS 5% goat serum for a further 30 min. The primary antibody was incubated overnight at 4°C (F4/80: 1h at 37°C) and the corresponding secondary antibody was incubated for 30 min (Cy3). Nuclei were counterstained with DAPI. Images were taken using an Axioimager D1 (Zeiss). A list of the antibodies used in Immunohistofluorescence is available in **Table 8**.

Table 7. List of commercial antibodies used in immunohistochemistry.

Antibody	Id.	Supplier	Dilution	Source
Cleaved Caspase 3	9661	Cell Signaling Technology	1/50	Rabbit
Desmin	M0760	Dako	1/50	Mouse
F4/80	NCA497bb	Bio-Rad	1/50	Rat
GNMT	sc-33222	Santa Cruz Biotechnologies	1/100	Rabbit
Ki67	ab66155	Abcam	1/100	Rabbit
LKB1	05-832	Milipore	1/100	Mouse
NAE1	API3067C	Abgent	1/100	Rabbit
NEDD8	2745	Cell Signaling Technology	1/200	Rabbit
Pan-Ras	Ls-b5494	Lifespan Biosciences	1/100	Rabbit
RasGRP3	3334	Cell Signaling Technology	1/100	Rabbit
SUMO2/3	bs-7338R	Bioss	1/200	Rabbit

Immunocytofluorescence

Cells were seeded over 12 mm coverslips (27,000 cells/coverslip) and fixed in PBS 4% paraformaldehyde (Santa Cruz Biotechnology) for 10 min then washed three times with PBS. Coverslips were then blocked and permeabilized with PBS containing 0.1% BSA, 10% goat serum and 0.2% Triton X-100 for 30 min at RT. After blocking, the coverslips were washed in PBS and incubated overnight in a humid chamber with the primary antibody (FLAG 1:100, LKB1 1:100, LC3B 1:50; **Table.8**) in PBS. Coverslips were again washed in PBS and then incubated for 1 hour with secondary antibody (dilution 1:200, Cy3 conjugated anti-mouse or FITC-conjugated anti-rabbit, Jackson ImmunoResearch laboratories, USA) in blocking solution with DAPI but no Triton X-100 at RT. Coverslips were mounted in Dako fluorescence mounting medium (Dako, Denmark). Images were taken using an Axioimager D1 (Zeiss). LC3-II immunocytofluorescence images were taken using a Leica TCS-SP confocal laser microscope (Leica, Germany).

Table 8. List of antibodies used in immunofluorescence

Antibody	Id.	Supplier	Dilution
LKB1	3050	Cell Signaling Technology	1:100
FLAG	A8592	Sigma Aldrich	1:100
LC3B	2775	Cell Signaling Technology	1:50
NEDD8	2745	Cell Signaling Technology	1:300
Albumin	ab8940-1	Abcam	1:100
α SMA	180106	Invitrogen	1:50
F4/80	NCA497bb	Bio-Rad	1:50
FITC	111-095-003	Jackson ImmunoResearch	1:200
Cy3	115-165-003	Jackson ImmunoResearch	1:200

TUNEL Assay

Apoptosis was analyzed by using the In situ Cell Death detection Kit (Roche) following the manufacturer's instructions. Paraffin-embedded sections (5 µm thick) of formalin-fixed liver samples were treated with proteinase K for 15 min at RT and subjected to peroxide block (3% H₂O₂ in methanol) before incubation with TUNEL diluent buffer containing FITC-conjugated primary antibody (dilution 1/50) for 2 hours at 37°C. Sections were mounted in Dako fluorescence mounting medium (Dako).

4.5 Cell Viability

Caspase-3 Activity Assay

Caspase-3 activity was measured in cells as previously described (364). Cells were lysed in caspase buffer and the protein content was determined as before (**section 4.3.1**). 20 µl of 25x reaction buffer (PIPES pH 7.4 250 mM, EDTA 50 mM, 2.5% CHAPS, DTT 125 mM) was mixed with 2.5 µl of fluorogenic caspase-3 substrate (Enzo Life Sciences, USA) and with 10 to 50 µg of protein lysate in a total volumen of 500 µl. This reaction mixture was divided into two duplicates and performed in 96 well plates. The mixture was incubated at 37°C with gentle shaking for 2 hours. Readings were taken at 0, 1, and 2 hours using a Spectramax M3 spectrophotometer (excitation wavelength 390 nm, emission wavelength 510 nm). Caspase-3 activity was determined by calculating the change in fluorescence from 1 to 2 hours of incubation.

MTT assay

Plated cells were incubated for 1 hour at 37°C with 0.5 mg/ml MTT (Thiazolyl Blue Tetrazolium Bromide, Sigma Aldrich) in culture media. After incubation, culture media was removed and the MTT was resuspended in DMSO (Sigma Aldrich) for 15 min and absorbance was determined using a Spectramax M3 spectrophotometer.

Crystal Violet

Cells were stained and fixed with 0.1% Crystal violet in 20% methanol solution with gentle shaking at RT for 40 min. Next, the wells were washed 4 times with dH₂O to eliminate the excess crystal violet and the wells were left to dry overnight. Once the wells were completely dry, a 10% acetic acid solution was added (1 hour, RT) to resuspend the crystals. The resulting color was read using a Spectramax M3 spectrophotometer.

Anexin V analysis (apoptosis)

Apoptosis was measured by determining the amount of apoptotic LX-2 cells using flow cytometry. After treatment, the media and the cells were collected by trypsinization and then centrifuged. Cells were incubated with propidium iodide and annexin V for 15 min at RT while protected from light. After the incubation, the stained cells were monitored using a FACS Canto Cytometer (Becton Dickinson, USA). The percentage of cells in apoptosis was determined using the FlowJo software.

Wound Healing Assay

Huh7 cells, previously transfected with LKB1, LKB1 K178R and LacZ, were seeded to confluence over 12 mm coverslips. A pipette tip (200 µl) was used to scratch a straight line through all the wells. Media was changed twice to remove dead and unattached cells. The wells were then placed in hypoxia for 24 h, and then cultured again in normoxia. Pictures of the scratch were taken at timepoints t=0, t=12, t=24, and t=48 using an Eclipse TS100 microscope (Nikon, Japan).

4.6 Animal Experiments

All animal experimentation was conducted in accordance with the Spanish guide for the care and use of laboratory animals, and with the International Animal Care and Use Committee Standards. All procedures were approved by the CIC bioGUNE Ethical Review Committee. Mice were housed in a temperature-controlled animal facility (AAALAC-accredited) with 12-hour light/dark cycles, and fed a standard diet (Harlan Teklad) with water *ad libitum*.

Liver samples were rapidly split into several pieces, some were snap frozen in liquid nitrogen and stored at -80°C for subsequent protein and RNA analysis and others were formalin fixed for histology and immunohistochemistry. Animals had sub-mandibular blood extracted prior to their sacrifice. Alanine aminotransferase (ALT) and aspartate aminotransferase (AST) were determined from serum samples. The animals used for experimentation were:

- *Gnmt*-KO (72).
- *Stk11*/*Gnmt* double Knock Out (dKO).
- Wild-type (WT; C57BL/6J).

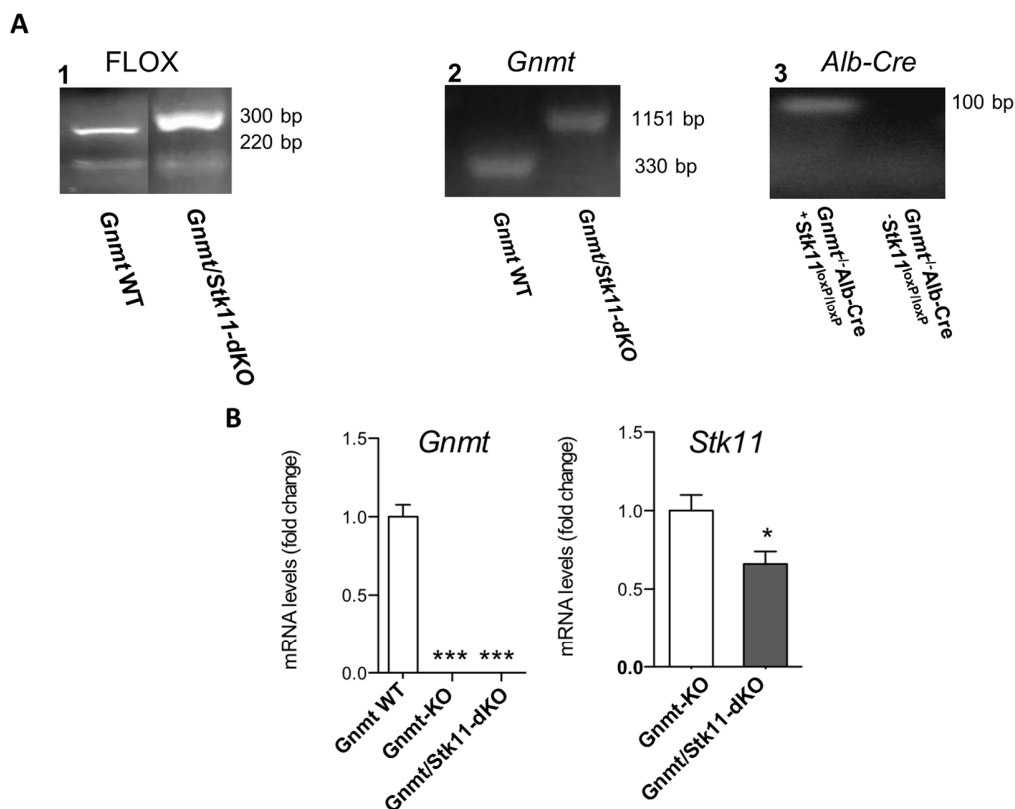


Figure 10. Generation of the *Gnmt*/*Stk11*-double Knockout. (A) Gel electrophoresis of PCR products used to genotype the *Gnmt*/*Stk11*-dKO mouse. 1, Detection of FLOX. 2, Detection of GNMT. 3, Detection of Alb-Cre. (B) mRNA levels of *Gnmt* and *Stk11* in WT, *Gnmt*-KO and *Gnmt*/*Stk11*-dKO mice.

4.6.1 Generation of the *Stk11/Gnmt*-dKO mouse

The *Gnmt*^{-/-}*Alb-Cre*+*Stk11*^{loxP/loxP} (*Stk11/Gnmt* dKO) mouse was generated by crossing the *Gnmt*^{-/-} mouse with the *Alb-Cre*+*Stk11*^{loxP/loxP} mouse (129S6-*Stk11*^{m1Rdp/Nci}-Lkb1 flox- mouse kindly provided by Arkaitz Carracedo from CIC bioGUNE, Spain). Genotyping of these mice uses the following primers using genomic DNA prepared from animal tails: **1.** PCRS5 -TCT AAC AAT GCG CTC ATC GTC ATC CTC GGC, LKB36 - GGG CTT CC ACCT GGT GCC AGC CTG T, LKB39 - GAG ATG GGT ACC AGG AGT TGG GGC T. PCRS5/LKB39 primer pair produces a 300 bp fragment for the presence of .FLOX, whereas LKB39/LKB36 primer pair gives a 220 bp product for the wild type allele. **2.** GNMT P1 -GTA CCG CAG AGT ACA AGG CG, GNMT P2 -CAA TCG CAG GAG GAA CAG CC, GNMT P3 -CTG AAT GAA CTG CAG GAC GAG. PCR amplification with P1– P2 and P3– P2 primers resulted in expected 330 and 1151 bp fragments respectively; **3.** Alb-Cre Primer 1- CCA CGA CCA AGT GAC AGC AAT, Alb-Cre Primer 2- TTC GGA TCA GCT ACA CCA (**Figure.10A,B**). *Gnmt*^{-/-} and *Stk11/Gnmt* dKO mice were no different in appearance.

4.6.2 Animal treatments

- **Bile duct ligation (BDL):** Adult male mice were subjected to BDL as described previously (193). Mice were treated with MLN4924 (Millenium Pharmaceuticals, USA) 3- (n=5) or 7- (n=5) days post BDL once a week (**60 mg/kg**, following the Millenium Corporation communication) by subcutaneous injection. 21 days (n=10) after surgery, animals were sacrificed and the livers were harvested as mentioned earlier (**Figure.11A,B**). Control mice n=5.
- **Carbon tetrachloride (CCl₄):** CCl₄ (Sigma Aldrich) was injected via intraperitoneal injection into adult male mice at a dose of 0.6 ml/kg once a week (n=8). Two weeks after the first CCl₄ dose, MLN4924-treatment by subcutaneous injection at a dose of **60 mg/kg** once a week was started (n=10). After 4 weeks of MLN4924 treatment animals were sacrificed and the livers were harvested as mentioned earlier (**Figure.11C**). Control mice n=5.
- **Methionine deficient diet (MDD):** Adult male 7 month old *Gnmt*-KO mice were analyzed for tumors by echography and their transaminase levels determined. The mice that had no tumors and had ALT levels higher than 60 were transferred to a methionine diet (S8946E020 EF AIN 76A 0.15% L-methionine, SSNIFF, Germany) for 1 month. After 1 month, mice ALT levels were determined again and mice that had normalized transaminase levels were sacrificed and their livers harvested as mentioned previously.
- **Hypoxia:** Mice were placed in an Invivo₂ 400 hypoxia Workstation to subject them to hypoxia. For acute hypoxia, mice were placed in the hypoxia chamber with an 8% O₂ concentration for 6 hours. Chronic exposure was achieved by placing the mice in the hypoxia chamber with an 8% O₂ concentration for 24 hours. Mice were sacrificed in the hypoxia chamber.

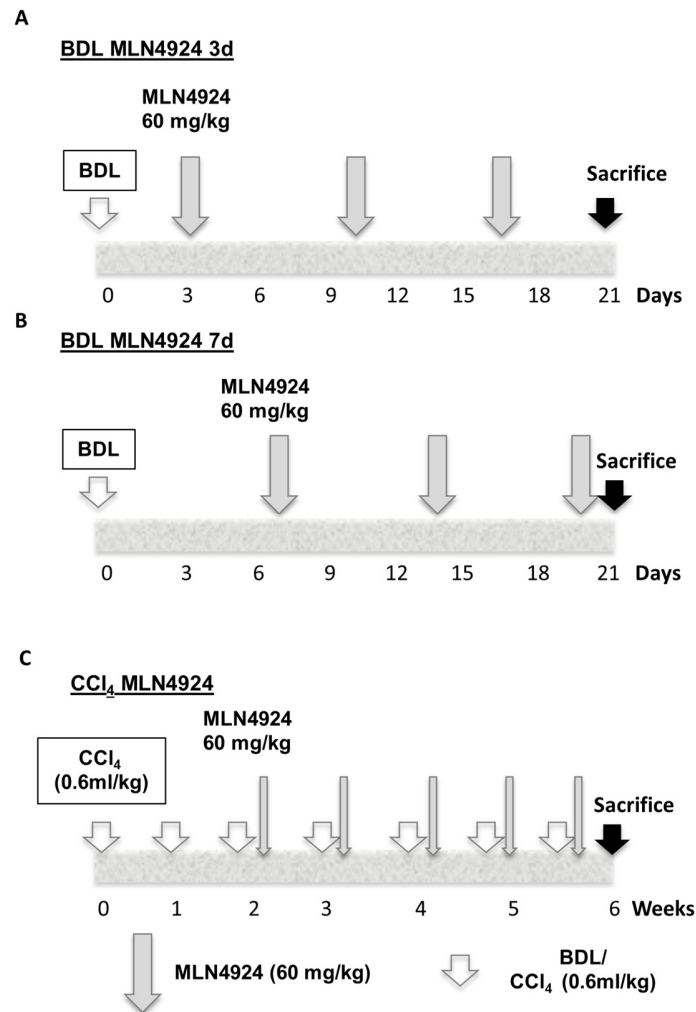


Figure 11. Experimental Procedures using MLN4924 in mice. Time frame used for bile-duct ligation (BDL) mice with MLN4924 treatment starting at (A) 3 and (B) 7 days after BDL. (C) Time frame for CCl₄ and MLN4924 treatment starting two weeks after the first CCl₄ injection.

Table 9. Characterization of liver fibrosis patients

Number of Patients	n= 15
Gender (Female/male)	9/6
Mean age (years)	44 (27-65)
Mean serum transaminases:	
AST (U/L)	38 (18-87)
ALT (U/L)	38 (14-42)
GGT (U/L)	47 (9-233)
Mean Albumin (G/DL)	4.2 (3.8-4.5)
Mean Platelet count (x10 ⁹ /L)	263 (127-410)
Metabolic syndrome (%)	47
Fibrosis:	
Stage 1- Perisinusoidal or periportal	4
Stage 2- Perisinusoidal and portal/periportal	9
Stage 3- Bridging fibrosis	2

4.7 Human Samples

Surgically resected specimens of patients from the Valdecilla Hospital, Santander, Spain, were used (n=15). Histological scoring was performed according to the NASH Clinical Research Network criteria (365). In these patients, fibrosis was staged from 0 to 4, being 0-none and 4-cirrhosis (**Table.9**). Another cohort of alcoholic and viral fibrosis samples from the Azienda Ospedaliero of Modena in Italy, were also analyzed. Healthy human liver samples were used as controls (n=13). Serum samples from non-steatotic and NAFLD patients were examined (non-steatotic= 92, NAFLD= 263). Clinical data were collected retrospectively using patient records described in a previous report (366). For the LKB1 studies (**section 5.3**) formalin-fixed paraffin-embedded liver sample sections from surgically resected specimens of healthy controls and 50 HCC patient tumors (**Table.10**) recruited from the Valdecilla Hospital were examined by immunohistochemistry. Patients gave informed consent to all clinical investigations, which were performed in accordance with the principles embodied in the 1975 Declaration of Helsinki in a priori approval by the institutional human research review committee.

Table 10. Characterization of HCC patients.

Number of patients	n= 50
Gender (female/male)	10/40
Age ¹ (years) mean ± SD	65.6 ± 7.8
Etiology (n)	
Hepatitis C virus	17
Hepatitis B virus	2
Ethanol	16
Other	15
Average time of chronic liver injury before surgery (years) mean ± SD	8.2 ± 7.5
HCC <3 cm	27
HCC >3 cm	33
BCLC stage (n)	
0	5
A	42
Unknown	3
CHILD (n)	
A	42
B	5
Unknown	3
Differentiation grade (n)	
Good	16
Bad	8
Moderate	8
Unknown	18
Recidivism (n)	
Yes	25
No	10
Exitus post-surgery	8
Unknown	7

1: At time of biopsy collection. Time between HCC detection and surgery <1 year

4.8 Liver Metabolomics analysis

Bile acids profiles were analyzed as previously described (366). Briefly, UPLC/time-of-flight mass spectrometry (TOF)-MS based platforms analyzing methanol liver extracts were combined. Data obtained with the UPLC@-MS were processed with the TargetLynx application manager for MassLynx (Waters Corp., Millford, USA) as detailed previously (366). Intra- and interbatch normalization followed the procedure described (366). Calculations were performed with R v2.13.0 (367).

4.9 Methionine and SAME measurements

Serum levels of methionine and SAME were determined by liquid chromatography/mass spectrometry (LC/MS) using a Waters Acquity ultraperformance liquid chromatography (UPLC) system equipped with a column oven, and a Waters Acquity UPLC BEH C18 column (2.1 X 100 mm, 1.7 μ m). A 3 μ L aliquot of sample was injected into the UPLC column, which was maintained at 50°C and eluted at 600 μ L/min. The mobile phase consisted of water with 0.05% formic acid (solvent A) and acetonitrile with 0.05% formic acid (solvent B). Separation was carried out starting with 1% B for 1 minute, followed by a linear gradient from 1% to 95% B for 10 minutes and staying at 95% B for 6 minutes. The UPLC system was coupled to a Waters Micromass LCT Premier Mass Spectrometer equipped with a Lockspray ionization source operating in electrospray positive ion mode (W mode, resolution 10,000 full width at half maximum). Full-scan time-of-flight MS spectra were acquired between m/z (mass-to-charge ratio) 80 and 1,000 using the dynamic range enhancement mode, with a total scan time of 0.4 seconds. Leucine enkephalin was used as a reference compound for accurate mass measurements. The reference was infused into the Lockspray reference channel, and the masses of the analyte channel were automatically mass-corrected by the software. A set of samples, prepared from all standard compounds, was acquired over the concentration range of 10 pg/ μ L to 50 ng/ μ L in order to test the linearity of the system. After analyzing all concentration levels, calibration curves were generated μ L and chromatogram traces of the protonated species of the standards were extracted with a mass window of 0.05 Da. Serum levels of methionine and SAME were automatically calculated from the calibration curves.

4.10 Lysosomal enzymatic activity

1.25 million hepatocytes were collected in PBS and dispensed in filter paper (13.5 mm). A 3 mm diameter circle from dried hepatocytes spots was used to analyze the lysosomal enzymatic activity. This method was adapted from a previously described report (368).

4.11 Energetic metabolic profile

Cellular metabolic profile was determined using a Seahorse XF24 Extracellular Flux Analyzer (Seahorse Biosciences, USA), providing real-time measurements of oxygen consumption rate (OCR) and extracellular acidification rate (ECAR). Huh7 cells previously transfected with WT LKB1, LKB1 K178R, or LacZ were seeded in collagen I coated XF24 cell culture microplates (Seahorse Bioscience), at 2.0×10^4 cells per well. Cells were placed for 24 hours in hypoxia and then growth medium was removed and replaced with 500 μ L of assay medium prewarmed to 37°C, composed of DMEM without bicarbonate containing 1 mM sodium pyruvate, 2 mM l-glutamine, and cultured at 37°C. Measurements of oxygen consumption rate (OCR) and extracellular acidification rate (ECAR) were performed after equilibration in assay medium for 1h. After an OCR and ECAR baseline measurement, sequential injections through ports in the XF Assay cartridges of pharmacologic inhibitors: Oligomycin (1mM), an inhibitor of ATP synthase, which allows a measurement of ATP-coupled oxygen consumption through oxidative phosphorylation (OXPHOS); carbonyl cyanide 4-trifluoromethoxy-phenylhydrazone (FCCP) (300 nM), an uncoupling agent that allows maximum electron transport, and therefore a measurement of maximum OXPHOS respiration capacity; and finally Rotenone (1 μ M), a mitochondrial complex 1 inhibitor were performed and changes in OCR and ECAR were analyzed.

4.12 ATP Detection Assay


ATP in Huh7 cells was detected using the ATPlite kit (PerkinElmer, USA). Huh7 cells were transfected with WT LKB1, LKB1 K178R and LacZ and then plated on 96 well plates. The plates were

then placed in hypoxia for 24 hours and ATP was detected following the manufacturer's instructions. Cells were lysed inside the hypoxia chamber.

4.13 Statistical Analysis

All experiments were performed in triplicate unless otherwise stated. Data is expressed as mean \pm SD (standard deviation). Where indicated the data is expressed as mean \pm SEM (standard error of the mean). Statistical significance was estimated using Student's t-test. A p value of < 0.05 was considered significant.

Results

The image shows two chemical structures. On the left, a lysine residue is represented as a carboxyl group (C=O) bonded to a lysine side chain (Lys-). On the right, a tripeptide is shown as Gly-Gly-Lys, where the first two glycine residues are linked together, and the third is a lysine residue. The structures are positioned around the word 'Results'.

Post-translational Modifications in Liver Disease
Imanol Zubieta Franco

5.1 Methionine and S-Adenosylmethionine levels are critical regulators of PP2A activity modulating lipophagy during steatosis.

Journal of Hepatology. 2016 Feb;64(2):409-418. doi: 10.1016/j.jhep.2015.08.037.

5.1.1 Background

The *Gnmt-KO* mouse model has high levels of SAME and methionine that leads to the development of steatohepatitis spontaneously (72,73). This mouse model has an inhibited autophagic flux that contributes to the development of steatosis. Culture of wild type hepatocytes with high levels of SAME and methionine also results in an inhibition of autophagy. Normalization of SAME and methionine levels in *Gnmt-KO* mice by feeding them with a methionine deficient diet reactivates hepatic autophagy (86), however, the mechanism by which high SAME and methionine levels inhibit autophagy in *Gnmt-KO* mice remain unknown.

5.1.2 SAME and autophagy flux

We had previously seen that either the acute treatment of wild type hepatocytes with high levels of SAME and methionine, or the chronic exposure to elevated levels of SAME and methionine of *Gnmt-KO* hepatocytes was able to inhibit autophagy flux (86). However, the mechanisms by which acute or chronic elevation of SAME and methionine levels affected autophagy flux remained unknown. We studied autophagic flux by analyzing LC3-II turnover by Western blot or LC3 puncta immunolabelling, in the presence or absence of the inhibitor of lysosome-mediated proteolysis chloroquine (Chlo). We observed that *Gnmt-KO* hepatocytes have an altered LC3-flux most likely due to an impaired lysosomal function, as shown by elevated LC3-II levels in untreated hepatocytes that do not increase after lysosomal blockage (**Figure.12A,B**). However, in WT hepatocytes cultured with SAME and methionine, the block is likely due to an inhibition of upstream autophagosome formation as shown by the reduced accumulation of LC3-II levels after lysosomal blockage (**Figure.12C**). Treatments with SAME and methionine are generally done for a maximum of 48h, whereas *Gnmt-KO* hepatocytes are exposed to high levels of SAME for months. In line with this, we observed a slight reduction in the activity of three lysosomal hydrolases (α -Galactosidase A, Arylsulphatase B and Glucoceramidase) in WT hepatocytes after 48h of SAME and methionine culture (**Figure.12D**), but we were unable to continue the experiment for longer as prolonged exposure to SAME and methionine induces cell death (**Figure.12E**).

5.1.3 *Gnmt-KO* mice have reduced MTOR activation and autophagic flux

To uncover the mechanism involved in autophagy inhibition in *Gnmt-KO* mice due to high SAME and methionine levels we studied the state of MTOR, a known inactivator of autophagy (28). Surprisingly, we found that MTOR was inactivated in *Gnmt-KO* mice (**Figure.13A**). *Gnmt-KO* mice had the same basal levels of pMTOR (S2448) and the downstream target 4E-BP1 as starved WT mice and no change was observed between fed and starved *Gnmt-KO* livers. This result was unexpected since the levels of methionine [an activator of MTOR (250)] in *Gnmt-KO* mice are elevated. To test whether SAME was responsible for MTOR inhibition, we cultured WT hepatocytes with SAME, methionine, or both (**Figure.13B**). As expected methionine by itself was able to induce pMTOR but SAME by itself or with methionine had an inhibitory effect on MTOR and 4E-BP1, as early as 9h (**Figure.13C**). The high levels of SAME were also able to inhibit MTOR activation despite treatment with insulin which is a potent activator of MTOR (**Figure.13D**). In *Gnmt-KO* hepatocytes, treatment with insulin barely increased pMTOR levels while a similar effect was seen in WT hepatocytes cultured with SAME and methionine and stimulated with insulin.

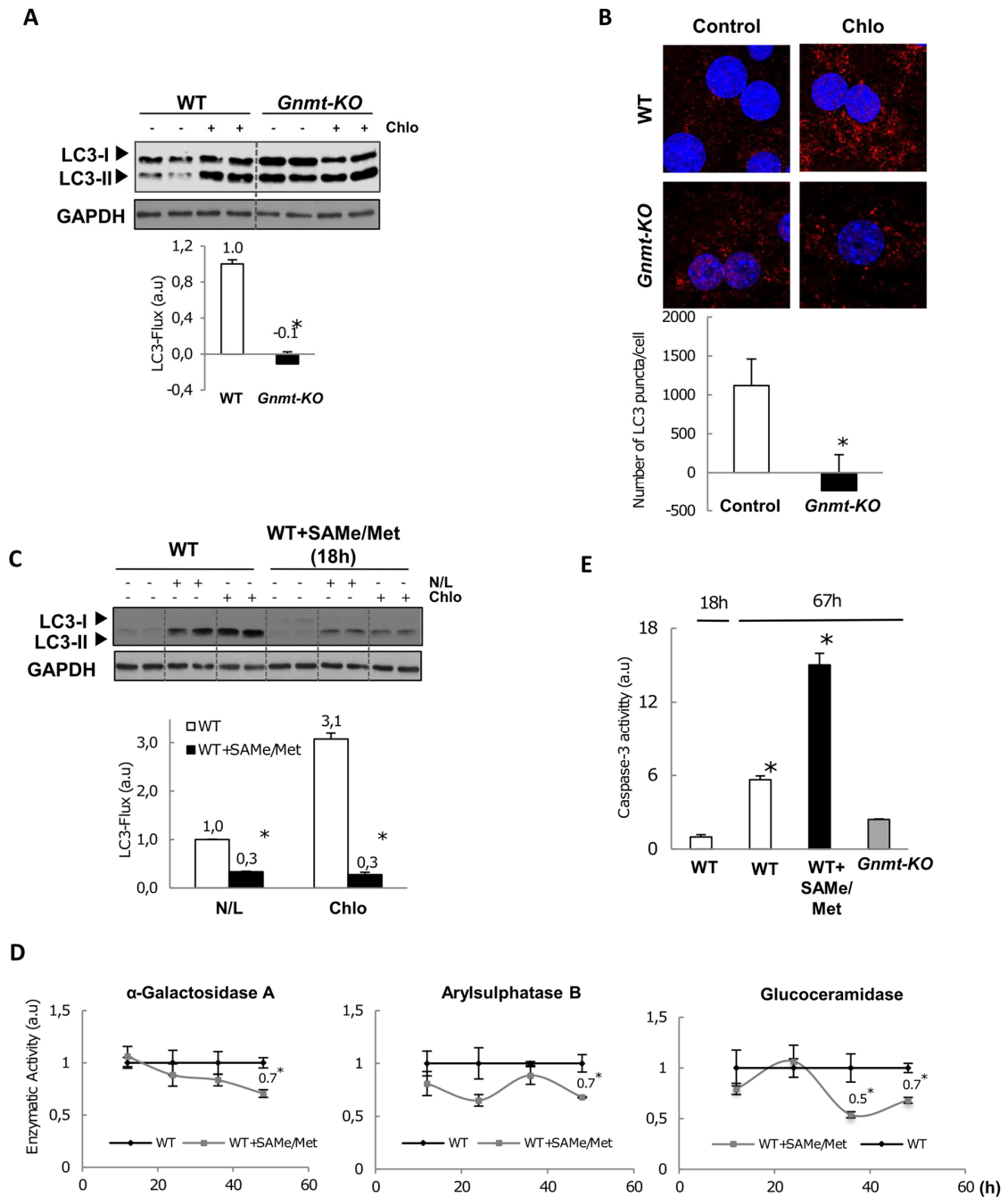


Figure 12. SAMe and methionine alter autophagic flux in hepatocytes. (A,B) WT and *Gnm1-KO* hepatocytes cultured with or without chloroquine (Chlo) during the last 4 hours. **(B)** WT hepatocytes cultured with SAMe and methionine and treated with autophagy inhibitors. **(D)** Time course of the activity of three lysosomal enzymes during SAMe and methionine culture at the indicated time points. **(E)** Caspase 3 activity in WT hepatocytes treated with SAMe and methionine for 67 hours compared to non-treated and *Gnm1-KO* hepatocytes.

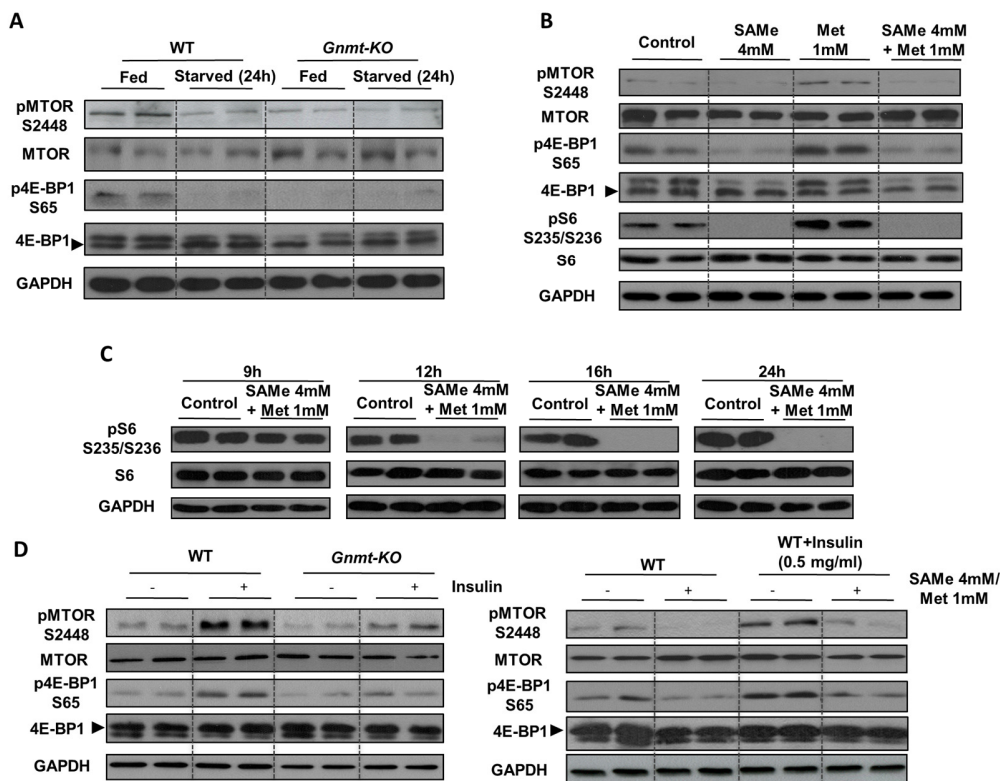


Figure 13. SAMe and methionine reduces MTOR activation. (A) Western blot of MTOR and 4E-BP1 (MTOR downstream target) in fed or starved WT and *Gnm1-Ko* mice. (B) Wb of MTOR and its downstream targets in WT hepatocytes cultured with SAMe, methionine or both. (C) Time course of the inactivation of S6 in WT hepatocytes treated with SAMe and methionine at different time points. (D) Effects of insulin (0.5 mg/ml) on MTOR and its downstream targets in WT and *Gnm1-KO* hepatocytes (left panel) Effects of SAMe and methionine culture on insulin signaling in WT hepatocytes (right panel).

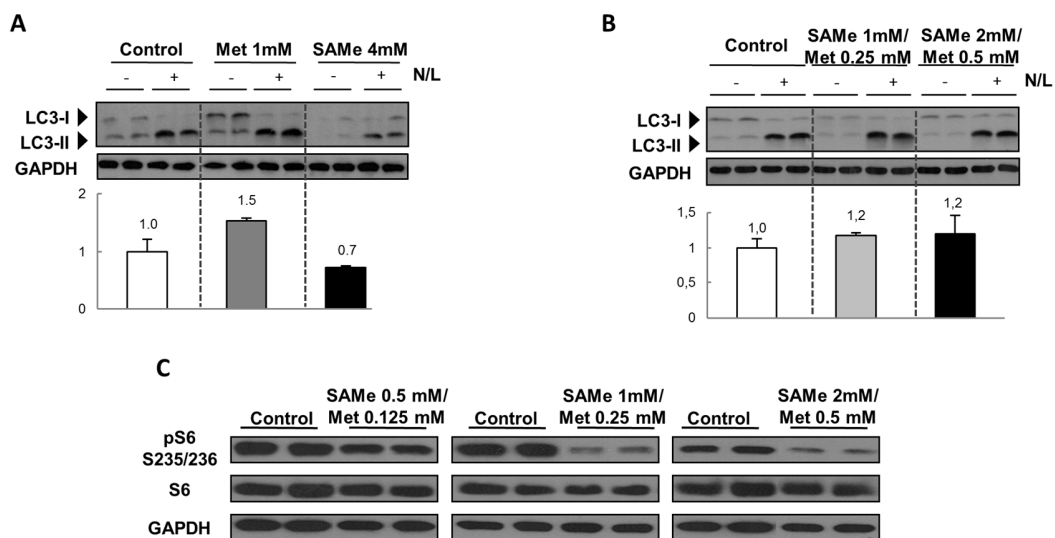


Figure 14. Both SAMe and methionine are required for autophagy inhibition. (A) Western blot of LC3 from WT hepatocytes cultured with methionine or SAMe separately and treated with N/L. (B) Wb of LC3 from WT hepatocytes cultured with reduced concentrations of both SAMe and methionine and treated with N/L. (C) Effects of reduced concentrations of SAMe and methionine on S6 dephosphorylation in WT hepatocytes. Both (A) and (B) have a densitometry analysis of the LC3 blots.

Next we looked at the effect of both molecules on autophagic flux. WT hepatocytes cultured with either SAME or methionine had a functioning autophagy (**Figure.14A**) and only when treated with both was there a reduction in LC3-flux (**Figure.12A**). Interestingly, culture at lower doses of both compounds had little effect on autophagy (**Figure.14B**) and a similar result was obtained for MTOR (**Figure.14C**).

5.1.4 SAME, methionine, MTOR and PP2A methylation

PP2A is known to inhibit MTORC1 indirectly (369). Previous studies from our laboratory have pointed out the possibility that SAME levels in liver could control protein phosphatase activity. In 2006 Martínez-Chantar *et al.* demonstrated that high SAME levels block AMPK phosphorylation through the activation of protein phosphatases (266). They also found that SAME inhibits the effects of HGF on AMPK activation through a process that involves the association of PP2A to AMPK. More recently, it has been shown that in liver regeneration after partial hepatectomy, a decrease in the hepatic levels of SAME was necessary to allow the phosphorylation of the LKB1-AMPK axis by HGF, promoting liver regeneration (69,79). To study the possible role of SAME and methionine in PP2A regulation and in MTOR phosphorylation, we treated *Gnmt-KO* hepatocytes and SAME and methionine cultured WT hepatocytes with okadaic acid, an inhibitor of protein phosphatases (**Figure.15A**), and saw an increase in MTOR phosphorylation similar to control cells. Interestingly, WT hepatocytes treated only with okadaic acid barely had an increase in pMTOR. Recent studies in yeast have demonstrated that methionine inhibits autophagy by inducing SAME-mediated methylation of PP2A (370). In line with this idea, we treated SAME and methionine cultured hepatocytes with Deaza, a potent inhibitor of methylation reactions, which led to an increase in the levels of unmethylated

PP2A (**Figure.15B**) and induced an activation of MTOR and its downstream targets (**Figure.15C**), suggesting that PP2A activation by SAME was being mediated by PP2A-methylation. The same study suggested that in yeast, methylated PP2A is able to regulate MTOR through the phosphorylation of Npr2p (370). To study the contribution of PP2A in regulating MTOR phosphorylation, we immunoprecipitated PP2A and found that MTOR co-immunoprecipitated along with PP2A and that this only happened in the presence of high levels of SAME and methionine (*Gnmt-KO* and SAME and methionine treated hepatocytes) (**Figure.15D**), suggesting that in our model, PP2A was directly interacting with and inactivating MTOR.

We next studied the role that PP2A has on autophagic flux. The PP2A inhibitor okadaic acid was able to restore autophagic flux both in *Gnmt-KO* and SAME and methionine treated hepatocytes (**Figure.16A,B**) suggesting that PP2A is able to directly control autophagy. PP2A is composed of the scaffold (PP2AA), regulatory (PP2AB) and catalytic (PP2AC) subunits. The catalytic subunit is composed of two isoforms, α and β , with the α isoform being slightly more abundant (371). The catalytic subunit is methylated by the methyltransferase Leucine carboxyl methyltransferase-1 (LCMT-1) (371). Methylation of PP2AC regulates the binding of the regulatory subunits and can determine the activity of the enzyme (372,373). We silenced the catalytic subunit (both α and β isoforms) in mouse liver progenitor MLP-29 cells treated with SAME and methionine (**Figure.16C**) and in *Gnmt-KO* hepatocytes (**Figure.16D**). Silencing PP2A was able to reactivate autophagic flux in both cell types suggesting that SAME and methionine can inhibit autophagy in hepatocytes via PP2A catalytic subunit-methylation.

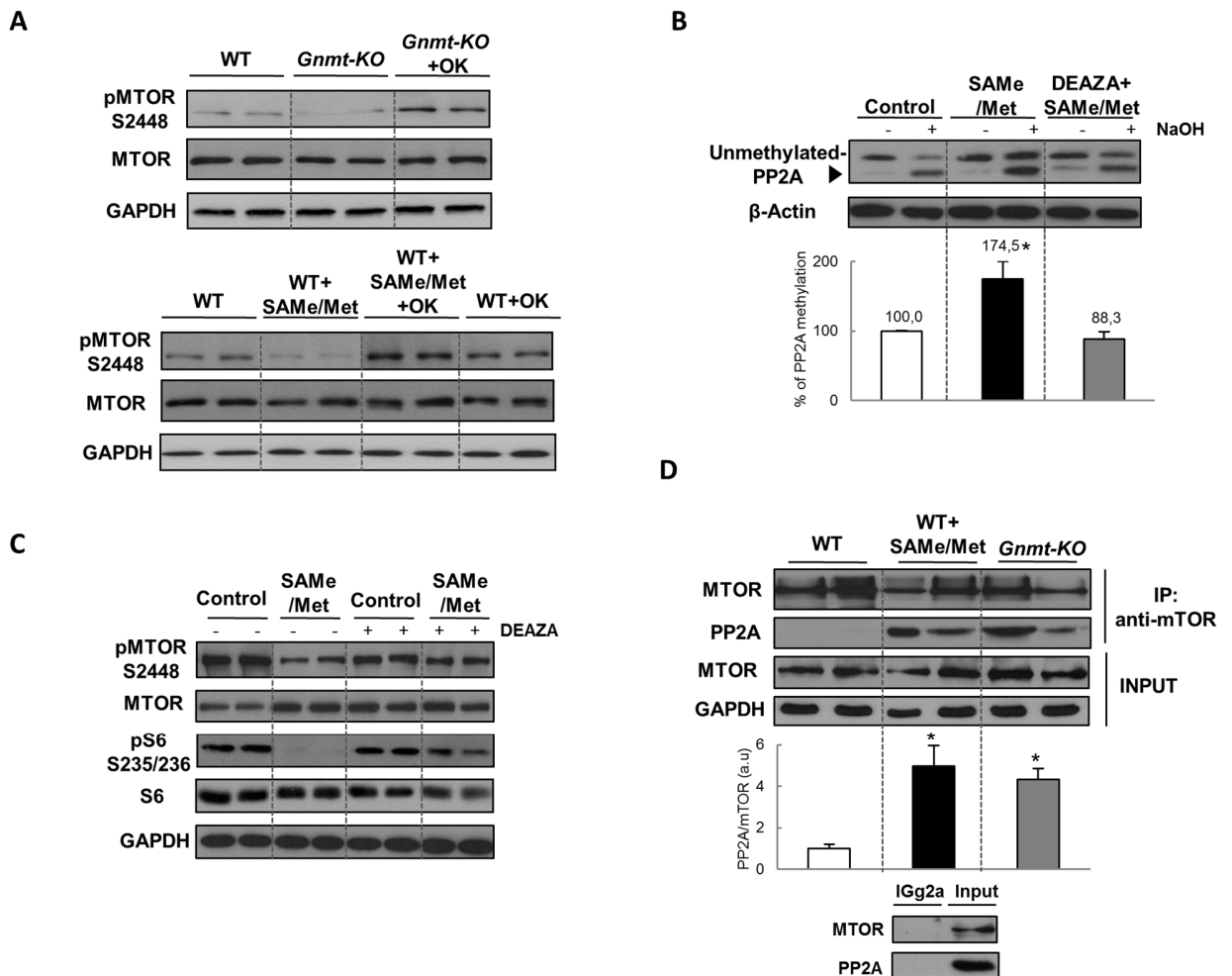


Figure 15. Methylated PP2A inhibits MTOR. (A) (upper panel) Western blot of MTOR from *Gnm1-KO* hepatocytes pretreated with okadaic acid (OK, 1 nM), (lower panel) Wb of MTOR from WT hepatocytes pretreated with okadaic acid (OK, 1 nM) and cultured with SAMe and methionine. (B) PP2A demethylation assay. Unmethylated PP2A is indicated by an arrow head. Graph shows corresponding percentage of PP2A methylation. (C) Effects on MTOR of Deaza treatment in WT hepatocytes cultured with SAMe and methionine. (D) Immunoprecipitation of MTOR from WT hepatocytes cultured with SAMe and methionine and *Gnm1-KO* hepatocyte extracts. The lower panel shows inputs.

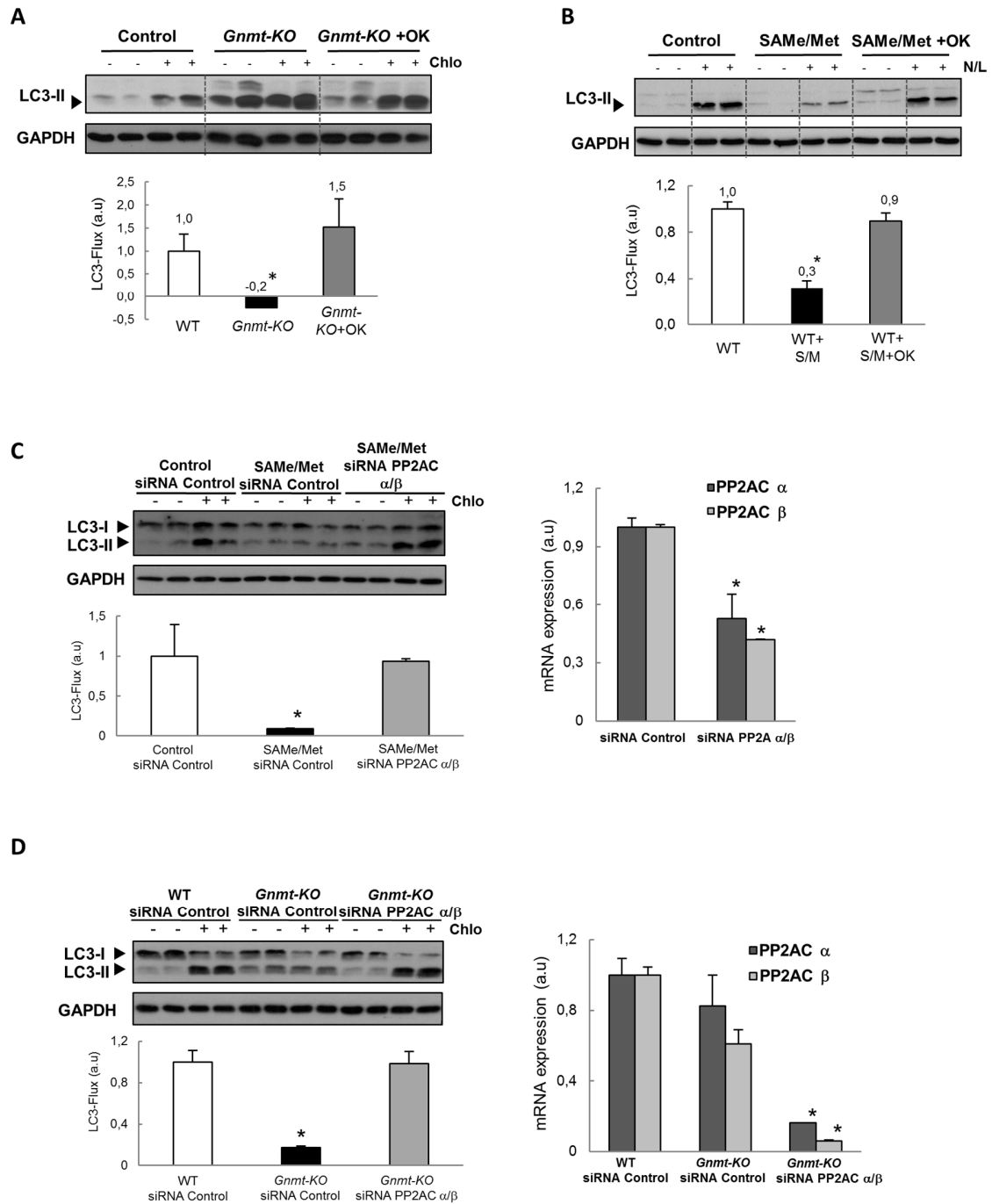


Figure 16. Methylated-PP2A inhibits autophagic flux. (A) Western blot of LC3 from *Gnmt*-KO hepatocytes treated with okadaic acid (OK) and chloroquine (Chlo). (B) Wb of LC3 from SAmE and methionine cultured WT hepatocytes treated with okadaic acid (OK) and ammonium/leupeptin (N/L). (C) Wb of LC3 in PP2A subunit c (both isoforms) silenced and SAmE and methionine treated mouse MLP29 cells. The mRNA levels of PP2AC α and PP2AC β are shown in the graph on the right panel. (D) As in (C) but in *Gnmt*-KO hepatocytes.

5.2 Deregulated NEDDylation in liver fibrosis

Hepatology. 2017;65:694-709. doi: 10.1002/hep.28933

5.2.1 Background

The ubiquitin-like protein NEDD8 is a post-translational modification that mainly targets the Cullin-RING ligases (CRL) and improves their stability. Recent work has shown that NEDD8 can also modify other proteins such as Mdm2, TGF- β Receptor II, and HuR (302). CRLs are involved in many different pathways, many of them involved in cancer, additionally; HuR and Mdm2 have also been implicated in cancer which prompted different groups to study the regulation of this PTM in cancer. Dysregulated NEDDylation has been found in different cancers such as in the liver (282) and lung (308). However, it is unclear if this dysregulation is a consequence of cancer or is present before malignant transformation.

5.2.2 Altered NEDDylation in liver fibrosis

Deregulated NEDDylation has been implicated in many pathological conditions (282,308,309,374).

Here, immunohistochemical analysis of livers from a cohort of NAFLD patients with significant fibrosis evaluated by an expert pathologist and classified either as low or moderate fibrosis, showed increased hepatic NEDDylation [measured both as levels of global protein NEDDylation and of the Nedd8 activating enzyme E1 subunit 1 (NAE1)] (**Figure.17A, Suppl. Fig. 1A, section 4.7**). These results were confirmed by Western-blot analysis of the levels of NEDDylated cullins, used as a surrogate for global protein NEDDylation (**Figure.17B**). Increased NEDDylation activity in fibrosis is not dependent on etiology, as its induction was also observed in fibrosis originating from hepatitis B infection or alcohol abuse (**Suppl. Fig 1B,C**). NEDDylation was also measured in experimental models recapitulating the key steps of fibrosis clinical progression such as Bile duct ligation (BDL), the most frequently used macrosurgical extrahepatic cholestasis experimental model (375), and in the well-established toxic model of CCl₄-induced liver fibrosis (376). Both global protein NEDDylation and NAE1 expression levels measured by IHC (**Figure.17C,D**), as well as NEDDylated cullins measured by Western blot were increased at 21 days after BDL and after 6 weeks of CCl₄ (**Figure.17E,F**). Noteworthy, NEDDylation was induced already at day 3 after BDL and 2 weeks of CCl₄ administration suggesting that increased NEDDylation is an early event in liver injury [(**Suppl. Fig 2A,B** (left panel))]. Increased NEDDylation was only observed at the post-

translational level, without significant changes at the mRNA level of either *NEDD8* or *NAE1* in the clinical and animal models of fibrosis used (**Figure.17G**).

Hepatic fibrosis is a multi-step process involving different cell types. Interestingly, double immunofluorescence staining for NEDD8 and albumin, a hepatocyte marker, were co-localized in mouse liver after BDL. Likewise, activated Kupffer cells (KC) expressing F4/80, a macrophage marker, and activated hepatic stellate cells (HSC) expressing desmin and alpha smooth muscle actin (α -SMA) co-localized with NEDD8 staining after BDL-induced injury. These findings were confirmed by Western blot after isolation of the different cell types either from control or BDL-induced fibrotic mouse livers (**Figure.18A**) and suggests that different cell types involved in liver fibrosis progression are affected by NEDDylation modifications during liver injury.

Increased NEDDylation in the BDL and CCl₄ fibrotic mouse models prompted us to investigate the impact of NEDDylation inhibition in these animals. For this purpose we used MLN4924, a first-in-class inhibitor of NAE1 that has recently entered clinical trials for cancer therapy both in solid and non-solid tumors. BDL mice were treated once a week with MLN4924 starting at 3- or 7-days after the surgery and ending at 21 days (BDL MLN4924 3d and BDL MLN4924 7d), time-points characterized either by cell death and inflammation or fibrosis onset, respectively

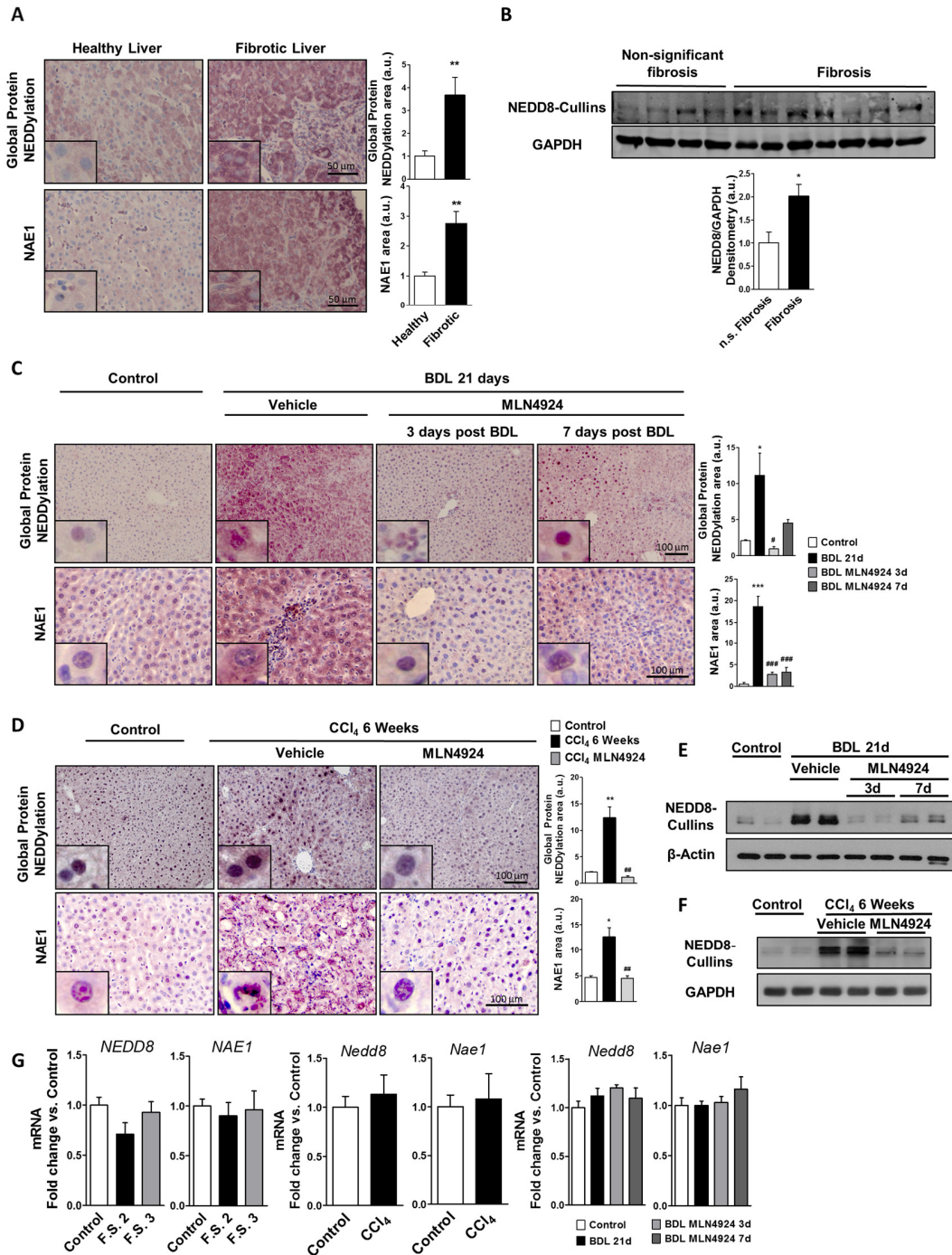


Figure 17. NEDDylation is altered in human and murine fibrosis. (A) Hepatic global protein NEDDylation and NAE1 levels in healthy (n=13) and fibrotic liver patients (n=15). (B) Western blot analysis of NEDDylated cullins from patients diagnosed with significant or non-significant fibrosis. Global liver protein NEDDylation and NAE1 levels in (C) bile duct ligation (BDL) and (D) CCl₄ treated mice and with MLN4924 (BDL 3 days post BDL and 7 days post BDL). Western blot levels of NEDDylated cullins in (E) BDL and (F) CCl₄. Messenger RNA levels of human fibrotic patients (stages 2 and 3) and BDL (including MLN4924 treated) and CCl₄ mice. (*, ** or *** = p<0.05, p<0.01 or p<0.001 respectively) vs control and (#, ## or ### = p<0.05, p<0.01 or p<0.001 respectively) MLN4924 treated vs. BDL and CCl₄. F.S= Fibrosis Stage.

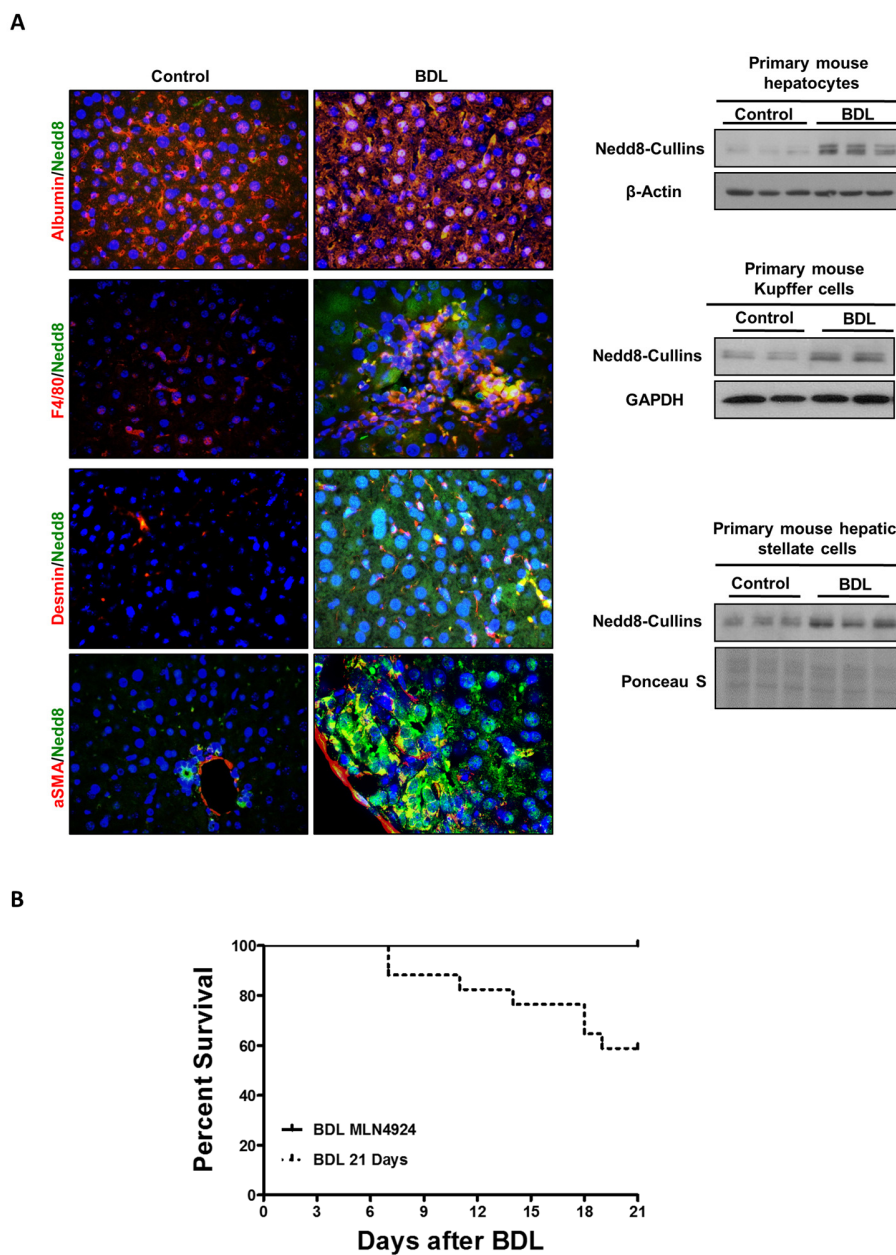


Figure 18. NEDDylation in mouse liver cells. (A) Co-immunofluorescence of albumin, an hepatocyte marker, F4/80, secreted by activated Kupffer cells, desmin and alpha smooth muscle actin (α SMA), hepatic stellate cell markers, with NEDD8 in BDL and control mice. Western blots of NEDDylated cullins from primary cells of each type with healthy controls for comparison is shown on the right. **(B)** Survival curve for mice subjected to BDL and mice subjected to BDL and treated with MLN4924.

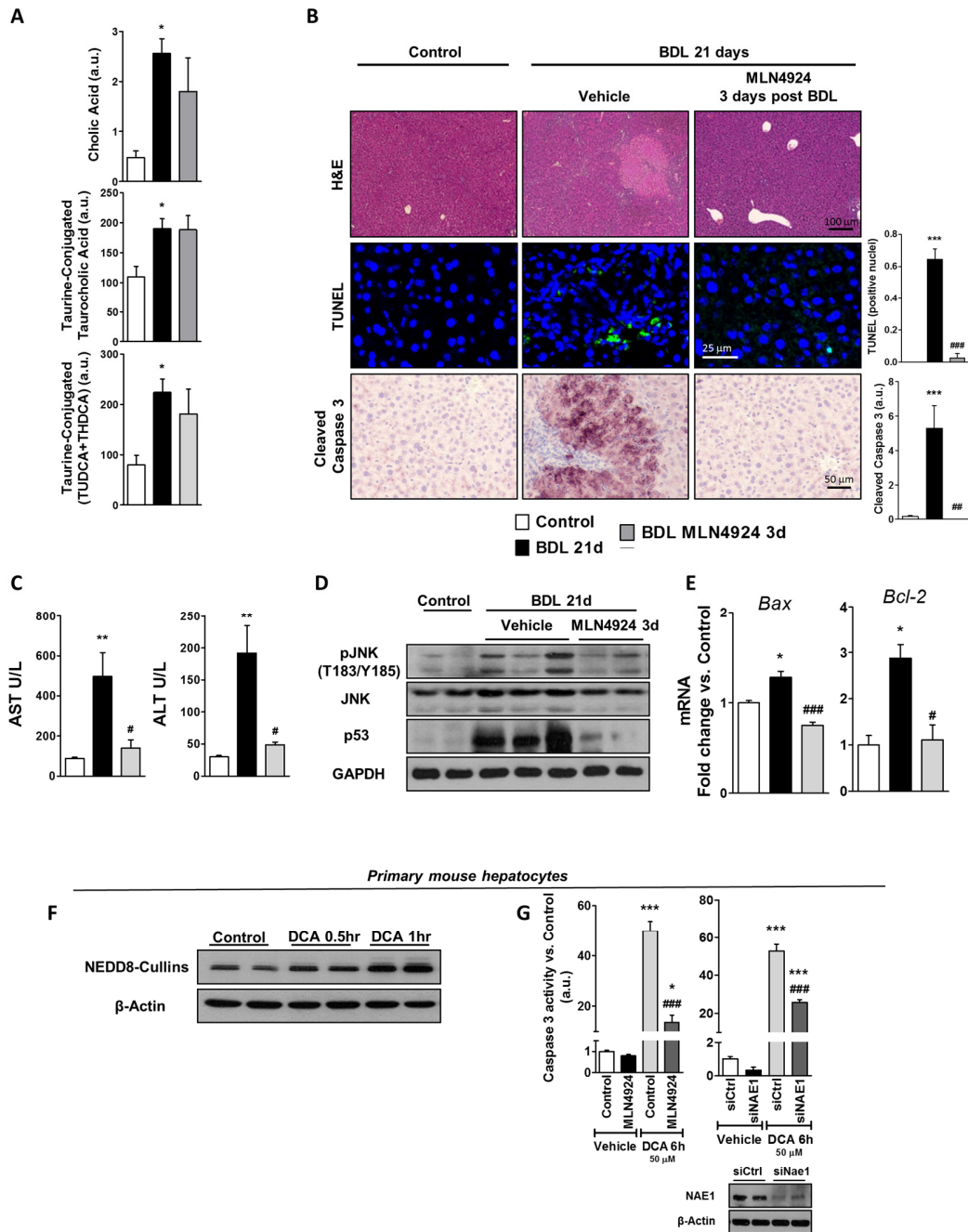


Figure 19. NEDDylation inhibition improves bile acid-induced hepatic injury. (A) Levels of three different bile acids in BDL mice and MLN4924 treated mice (3d post BDL). (B) Hematoxylin and eosin (H&E), terminal deoxynucleotidyl dUTP Nick End Labeling assay (TUNEL) and cleaved caspase 3 IHC staining of BDL mice livers. (C) Serum transaminases from BDL mice. (D) mRNA levels of Bax and Bcl-2 from BDL mice. (E) Western blot of NEDDylated cullins from primary mouse hepatocytes treated with deoxycholic acid (DCA, 50µM) for the indicated amount of time. (G) Caspase 3 activity from primary mouse hepatocytes treated with 50 µM DCA for 6 hours, with or without MLN4924 (left graph) and with NAE1 silenced (right panel). Western blot was used to confirm NAE1 silencing. (*, ** or *** = p<0.05, p<0.01 or p<0.001 respectively) vs control and (#, ## or ### = p<0.05, p<0.01 or p<0.001 respectively) MLN4924 treated vs. BDL and CCl₄.

(Suppl. Fig. 2A and Figure.11). MLN4924-treatment was also administered to CCl₄-rodents from 2 to 6 weeks of the initial CCl₄ administration, a time point where cell death, inflammation and fibrosis co-exist (Suppl. Fig. 2B, Figure.11, section 4.6.2). As expected, MLN4924-treatment decreased protein NEDDylation in both animal models studied (Figure.17C-F) without affecting mRNA levels (Figure.17G). MLN4924-treatment was also able to reduce BDL mice mortality (Figure.18B), as treated mice had a 100% survival rate whereas vehicle mice had only a 60% survival.

5.2.3 NEDDylation inhibition ameliorates bile acid- and CCl₄-induced cell death

Both intrahepatic Bile acid (BA) overload (375) and the metabolization of toxic CCl₄ (376) result in liver injury. Metabolomic analysis of mouse livers revealed that 21 days after BDL, both primary hepatic BA, such as cholic acid, and taurine-conjugated BA (tauroursodeoxycholate and taurodehydrocholic acid) were significantly increased relative to control animals whereas pharmacological treatment with MLN4924 starting 3 days after BDL had no effect in hepatic BA concentration (Figure.19A). In spite of unaltered BA hepatic content, NEDDylation inhibition *in vivo* after BDL significantly decreased the accumulation of cell death-related markers, such as parenchymal disruption, terminal deoxynucleotide transferase dUTP nick end labeling (TUNEL) and Caspase 3 cleavage (Figure.19B) with reduction of serum transaminase levels (Figure.19C). Also, MLN4924-treatment of BDL rodents reduced the activation of the pro-apoptotic and necrotic stress-activated kinase, c-Jun N-terminal kinase (JNK) and of p53 as well as of mRNA levels of genes involved in death regulation such as β -cell lymphoma 2 (*Bcl-2*) and the *Bcl-2* associated protein X (*Bax*), being the first previously described as an adaptive response to resist BA induced apoptosis (377) (Figure.19D,E). Contrary to previous studies in cancer reporting activation of p53 by MLN4924 (378), MLN4924-treatment after BDL reduced hepatic p53, an effect that we ascribe to an overall improved liver phenotype. Decreased cell death markers and serum transaminases upon MLN4924-treatment

were also observed in CCl₄-induced liver fibrosis in mouse (Figure.20A,B).

Liver fibrosis is a multi-cellular complex process where hepatocyte death mediated by BA plays an important initiation role (195,379). Therefore, to assess the role of NEDDylation inhibition in hepatocyte cell death, we isolated primary mouse hepatocytes and treated them with the toxic bile acid deoxycholic acid (DCA). Similar to our *in vivo* results, where NEDDylation was increased in hepatocytes from BDL-injured mouse livers (Figure.18, Suppl. Fig. 2A), NEDDylation was induced 30 min to 1h following DCA-stimulation in isolated healthy mouse hepatocytes (Figure.19F). Treatment with DCA significantly increased cell apoptosis, measured as caspase 3 activity (Figure.19G). This is in agreement with earlier evidence where increased death as a result of necrosis was observed in BDL whereas high toxic BA were shown to induce apoptosis in cultured hepatocytes (380). Noteworthy, NEDDylation inhibition either by MLN4924-treatment or *Nae1* silencing significantly reduced caspase 3 activity only in DCA-stimulated hepatocytes not inducing apoptosis *per se*, indicating that NEDDylation inhibition-mediated cell death is exclusively of dividing hepatoma cells or pre-tumoral hepatocytes, as previously observed (282). Overall, this data suggests that NEDDylation could mediate hepatocyte death in liver injury.

5.2.4 NEDDylation inhibition decreases liver inflammation

Upon death-induced stimulus, hepatocytes release cytokines that promote the activation of the liver resident macrophages. Thus, increased accumulation of F4/80, a cell membrane marker of macrophages, was observed in our injury models. Diminished F4/80 staining indicated that NEDDylation inhibition *in vivo* decreased KC accumulation both in BDL and CCl₄-induced liver injury (Figure.20C and Figure.21A). MLN4924-treatment to BDL rodents diminished the expression of pro-inflammatory cytokines, such as TNF α , and its receptor, the tumor necrosis factor alpha receptor (TNFR1), previously implicated in liver damage (Figure.21B) (381)

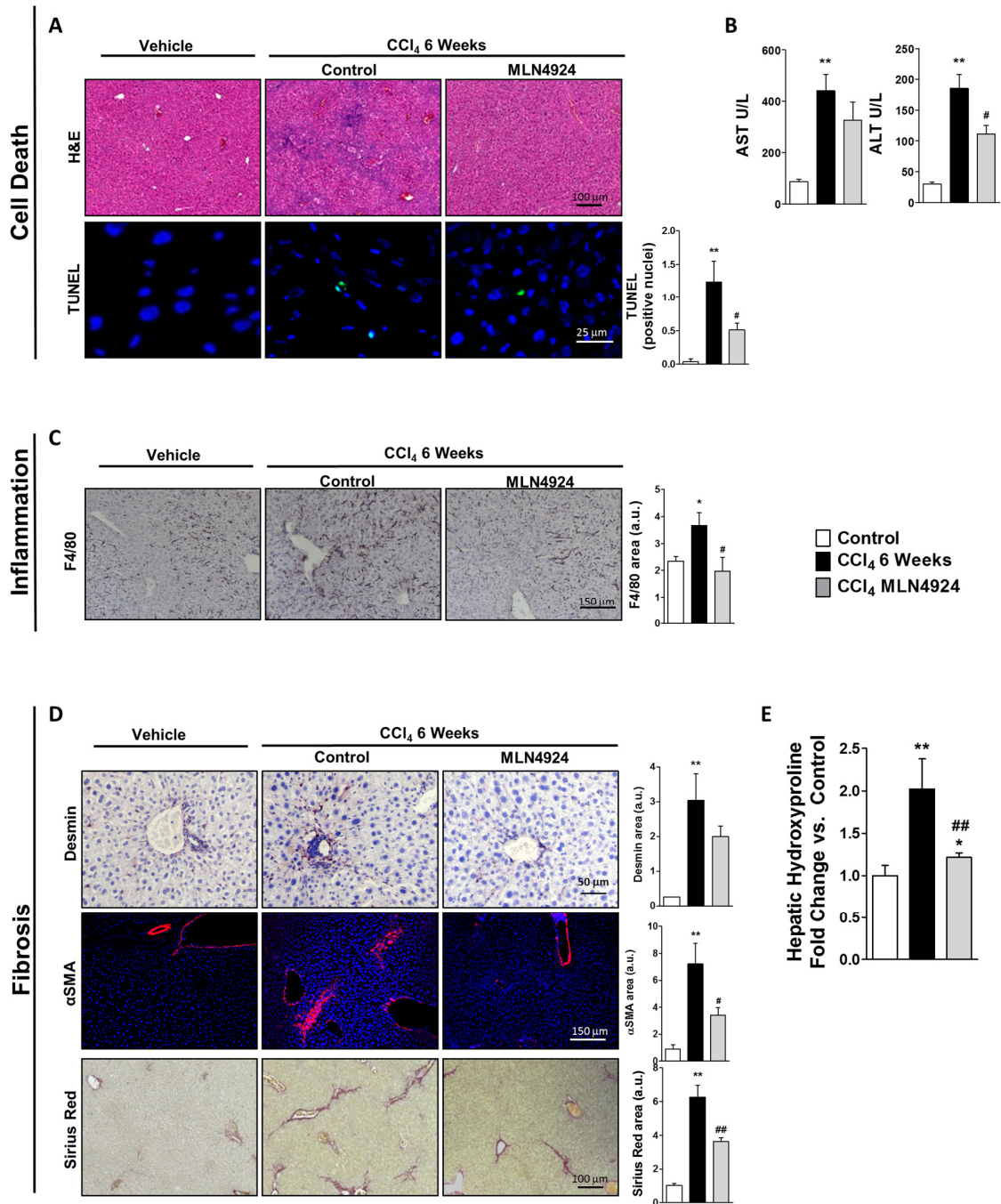


Figure 20. NEDDylation inhibition improves liver health in CCl₄ treated mice. (A) Hematoxylin and eosin (H&E) and terminal deoxynucleotidyl dUTP Nick End Labeling assay (TUNEL). (B) Serum transaminase levels from CCl₄ treated mice. (C) F4/80 staining in CCl₄ mice. (D) Desmin, αSMA, sirius red staining and (E) hepatic hydroxyproline levels from CCl₄ treated mice. (*, ** or *** = p<0.05, p<0.01 or p<0.001 respectively) vs control and (#, ## or ### = p<0.05, p<0.01 or p<0.001 respectively) MLN4924 treated vs. CCl₄.

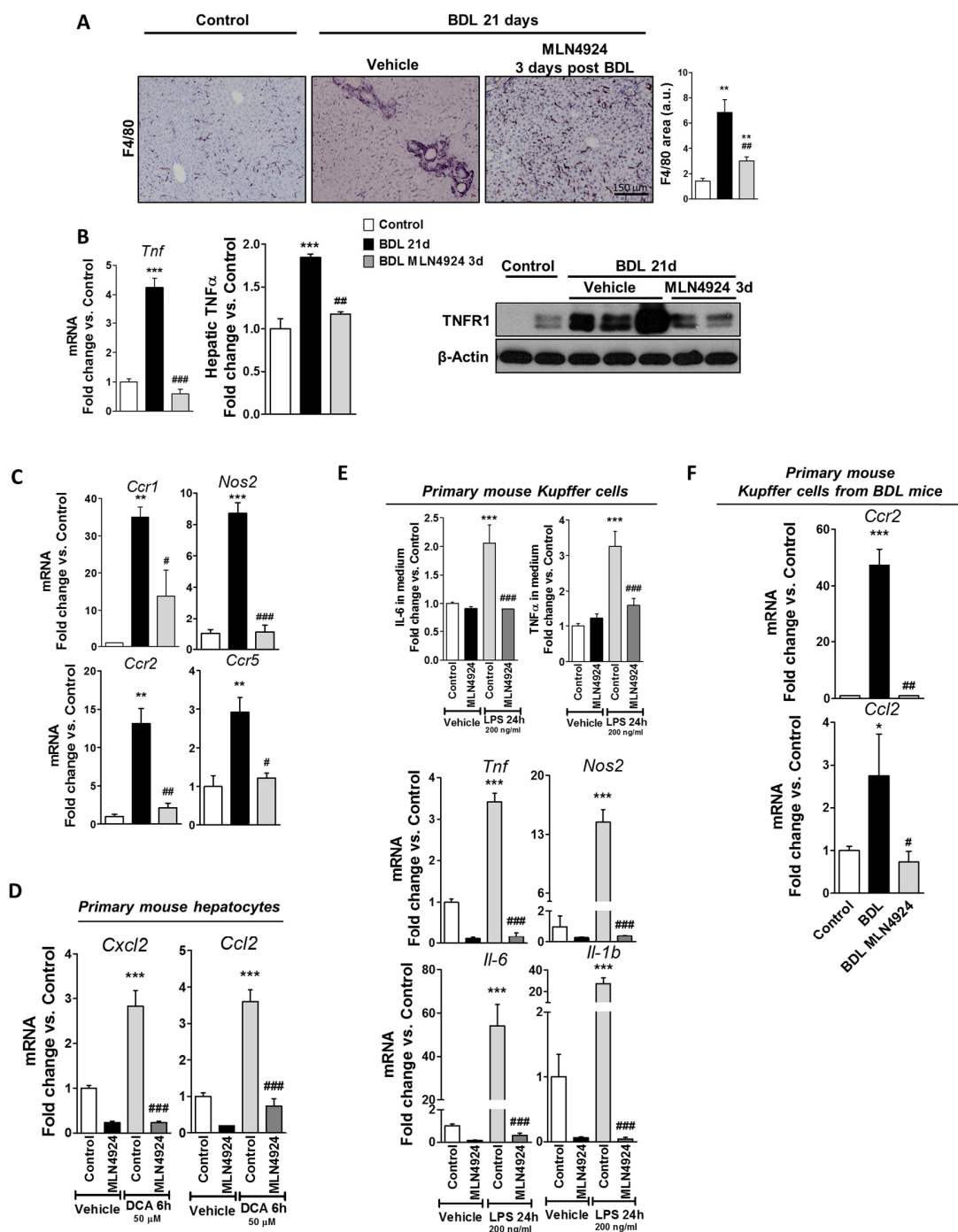


Figure 21. NEDDylation inhibition decreases liver inflammation and reduces Kupffer cell activation. (A) F4/80 staining in BDL liver. (B) Hepatic TNF α and TNF α receptor levels. (C) mRNA levels of inflammatory markers in BDL mice livers. (D) mRNA levels of *Cxcl2* and *Ccl2* in primary mouse hepatocytes exposed to 50 μ M DCA and treated with MLN4924. (E) IL-6 and TNF α levels in the extracellular medium (upper panel) and mRNA levels of inflammatory markers (lower panel) in LPS stimulated (200 ng/ml) primary mouse Kupffer cells cultured with MLN4924. (F) *Ccr2* and *Ccl2* mRNA levels in *in vivo* activated primary Kupffer cells after MLN4924 treatment. (*, ** or *** = $p < 0.05$, $p < 0.01$ or $p < 0.001$ respectively) vs control and (#, ## or ### = $p < 0.05$, $p < 0.01$ or $p < 0.001$ respectively) MLN4924 treated vs. BDL and non treated. Legend applies to: A, B and C

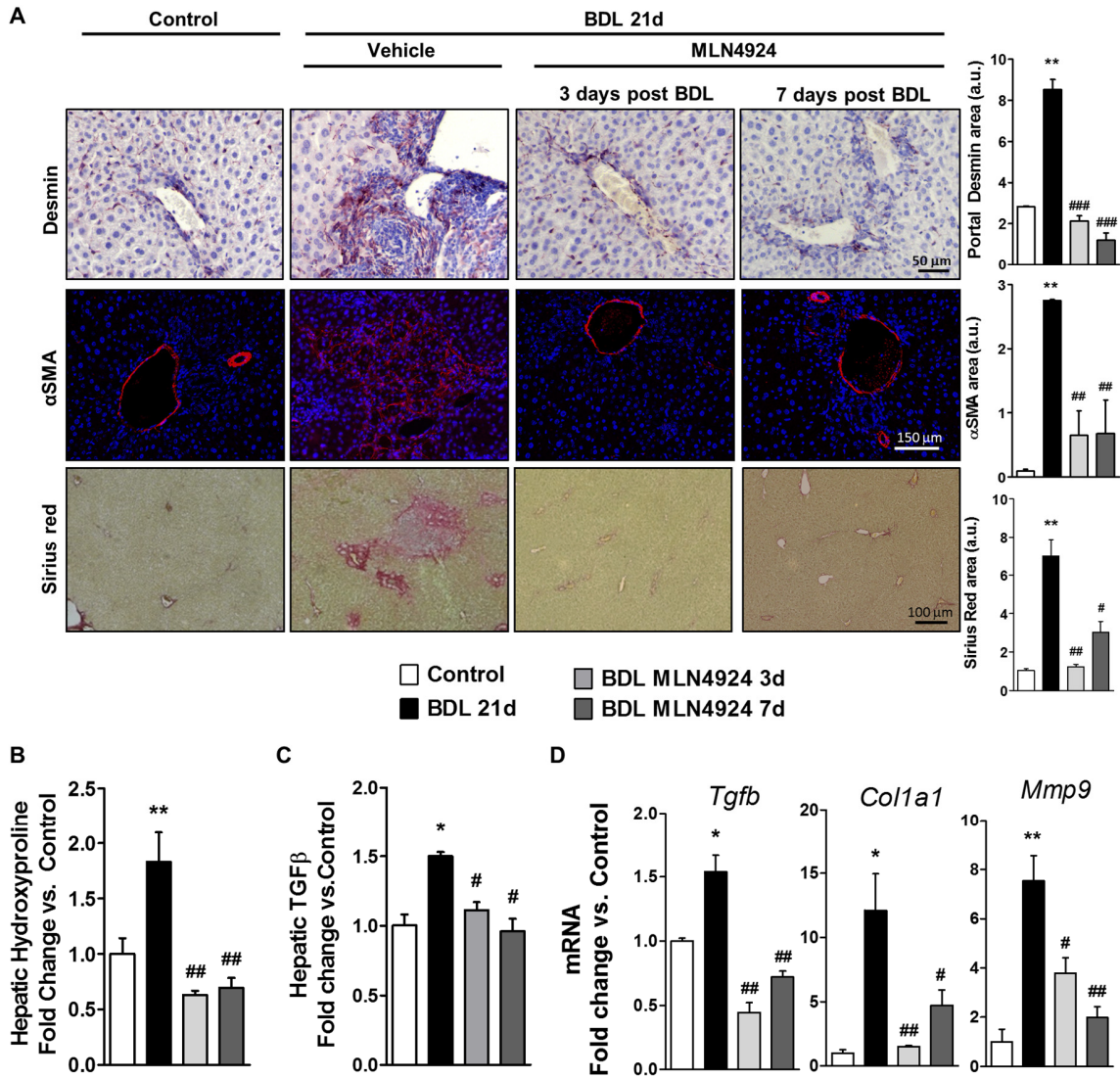


Figure 22. NEDDylation inhibition reduces fibrosis. (A) Desmin, α SMA and Sirius red staining in BDL livers. BDL mice hepatic hydroxyproline (B) and TGF- β (C) content. (D) Comparison of mRNA levels of profibrogenic markers between control, BDL and BDL MLN4924 treated mice. (*, ** or *** = $p < 0.05$, $p < 0.01$ or $p < 0.001$ respectively) vs control and (#, ## or ### = $p < 0.05$, $p < 0.01$ or $p < 0.001$ respectively) MLN4924 treated vs. BDL.

and accounted for reduced expression at the mRNA level of inducible nitric oxide synthase (*Nos2*) and the C-C chemokine receptors, *Ccr1*, *Ccr2* and *Ccr5* (**Figure.21C**).

Different liver cell types interact and play important roles on inflammation mediation. NEDDylation inhibition prevented stimulation of inflammatory markers such as the chemokine (C-X-C motif) ligand 2 (*Cxcl2*) and the chemokine (C-C motif) ligand 2 (*Ccl2*) in primary mouse hepatocytes treated with DCA (**Figure.21D**). On the other hand, previous studies have reported that lipopolysaccharide (LPS)-activated macrophages have increased NEDDylation activity (382), an outcome similar to our *in vivo* discovery of increased NEDDylation in activated KC (**Figure.18**). *In vitro* treatment with MLN4924 to isolated KC after stimulation with LPS, reduced IL-6 and TNF α cell release, as well as mRNA levels of *Il-6*, *Il1b*, *Tnfa* and *Nos2* (**Figure.21E**). Likewise, NEDDylation inhibition in isolated KC from injured livers decreased the mRNA levels of *Ccr2* and *Ccl2*, molecules involved in CC-chemokine recruitment of macrophages (**Figure.21F**) (383). All together this data suggests that NEDDylation can modulate inflammation after hepatic injury.

5.2.5 NEDDylation plays a role in hepatic stellate cell activation

As a result of maintained hepatocyte cell death and hepatic inflammation, quiescent HSC undergo a differentiation process towards an activated state, becoming the main fibrogenic cell type in the damaged liver (131,384). Thus, HSC accumulation (desmin staining) and more importantly its activation (α -SMA staining), with concomitant accumulation of collagen deposits (Sirius red staining and hydroxyproline assay) were increased after BDL and CCl₄-induced injury. MLN4924-treatment *in vivo* starting either at 3 or 7 days after BDL and after 2 weeks of CCl₄ chronic administration, showed a reduction of HSC activation and collagen deposition (**Figure.20D,E** and **Figure.22A,B**). Noteworthy, the decrease was more significant in the BDL model probably because 3 and 7 days after BDL is an initial stage of the fibrosis progression while in the CCl₄ model fibrosis is more advanced at 2-weeks after CCl₄ administration (**Suppl. Fig. 2B**). We hypothesize that, at least in the BDL mouse

model, MLN4924 treatment acts both by reducing and preventing the activation of HSC. Moreover, NEDDylation inhibition in BDL-induced liver injury, reduced the levels of the pro-fibrogenic factor, TGF- β , both at protein and mRNA level, and the expression of collagen type I alpha 1 (*Col1a1*), and the matrix metalloproteinase 9 (*Mmp9*) accounting for matrix degradation (**Figure.22C,D**).

As mentioned earlier, HSC have increased NEDDylation when activated during fibrosis (**Figure.18**). We again confirmed this increase in primary HSC cultivated on plastic. After seven days of plastic culture, primary HSC had increased NEDDylation which coincided with increased activation markers (**Figure.23A**). Treatment of these cells with MLN4924 led to a sharp decrease in the activation. Even primary HSCs that had been activated for five days on plastic had a reduction of activation markers when treated with MLN4924, the results were similar with primary HSCs extracted from BDL livers (**Figure.23B-D**). Silencing NAE1 in primary HSC led to similar results, NAE1 silenced HSCs were less activated than control cells after 7 days plastic culture (**Figure.23E**).

To continue studying the effect of NEDDylation inhibition on the activation of HSCs we used LX-2 cells, a human immortal HSC cell line (360). When treated with TGF- β , LX-2 cells increase their activation as seen by increased pSmad2 (S465/467) levels as well as increased levels of collagen, α -SMA, and PAI1 mRNA (**Figure.24A,B**). In line with our previous results, LX-2 cell activation was accompanied with increased cellular NEDDylation. When treated with MLN4924 and TGF- β , NEDDylation is reduced and collagen, α -SMA, and PAI1 mRNA levels fall back to that of control cells (**Figure.24A,B**). Interestingly, MLN4924 treatment was able to reduce total levels of Smad2, with or without TGF- β treatment, suggesting that NEDDylation plays a role in Smad2 stability. To explore the possibility that Smad2 might be directly NEDDylated we then silenced NAE1 or overexpressed NedP1, a specific NEDD8 isopeptidase, in LX-2 cells to ensure that this effect was not due to drug off target effects. In cells without NAE1 or overexpressing NedP1, Smad2 levels were again reduced when compared to controls (**Figure.24C**). To see if there was a direct

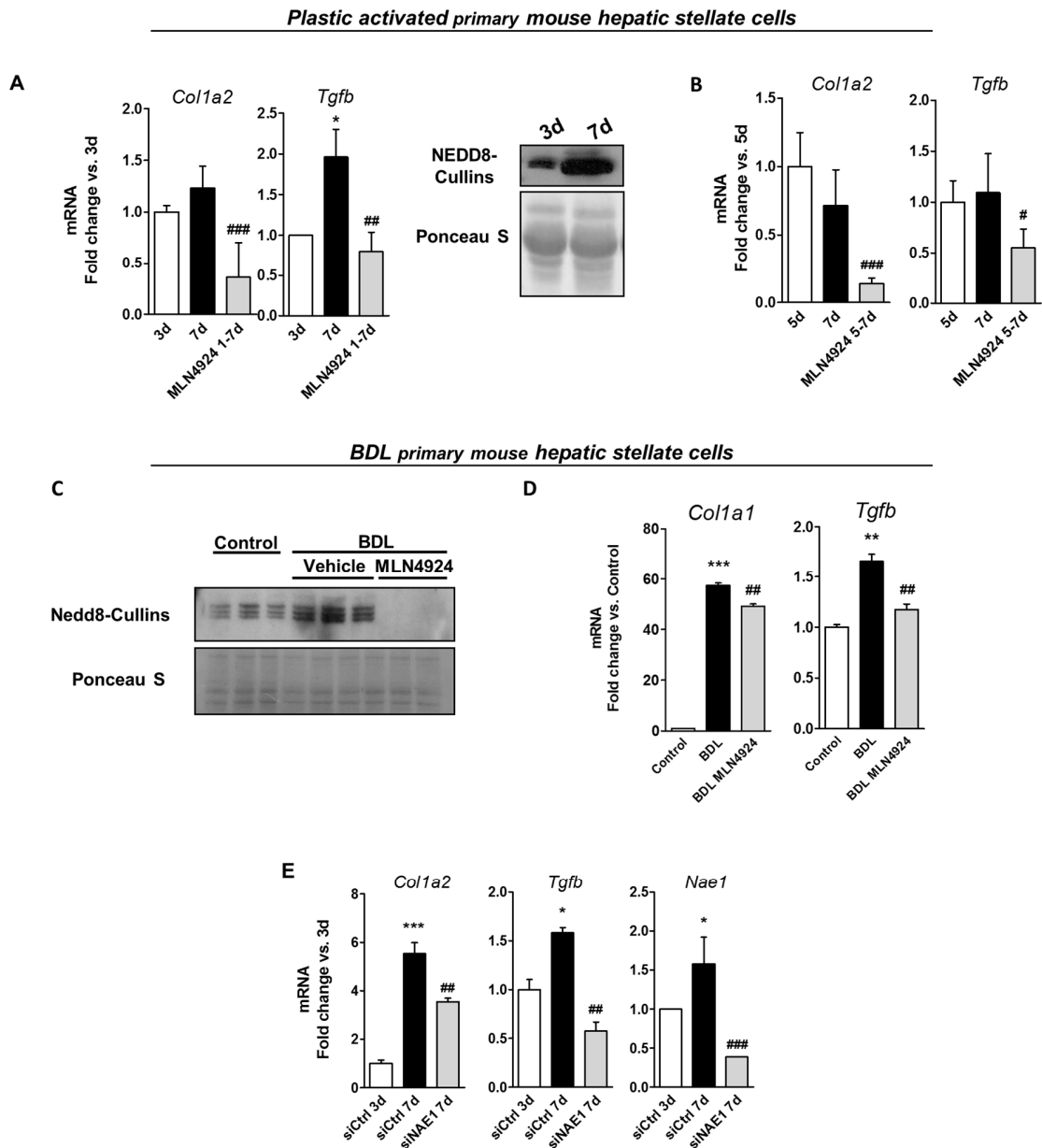


Figure 23. NEDDylation plays a role in hepatic stellate cell activation. (A) mRNA levels of profibrogenic markers in 7 day plastic activated primary mouse HSC and plastic activated primary mouse HSC cultured with MLN4924 (3 μ M) since the first day of culture. A Western blot of NEDDylated cullins from control cells is shown. **(B)** mRNA levels of profibrogenic markers in plastic activated primary mouse HSC and plastic activated primary mouse HSC cultured with MLN4924 (3 μ M) starting from the fifth day of culture. **(C)** Western blot of NEDDylated cullins from BDL *in vivo* activated primary mouse HSC and *in vivo* activated primary mouse HSC cultured with MLN4924 (3 μ M) and **(D)** mRNA levels of profibrogenic markers. **(E)** mRNA levels of profibrogenic markers in *in vivo* BDL activated HSC with NAE1 silenced and 7 days of plastic culture. The levels of *Nae1* mRNA are used to confirm NAE1 silencing. (*, ** or *** = $p < 0.05$, $p < 0.01$ or $p < 0.001$ respectively) vs control and (#, ## or ### = $p < 0.05$, $p < 0.01$ or $p < 0.001$ respectively) MLN4924 treated vs. BDL or non-treated.

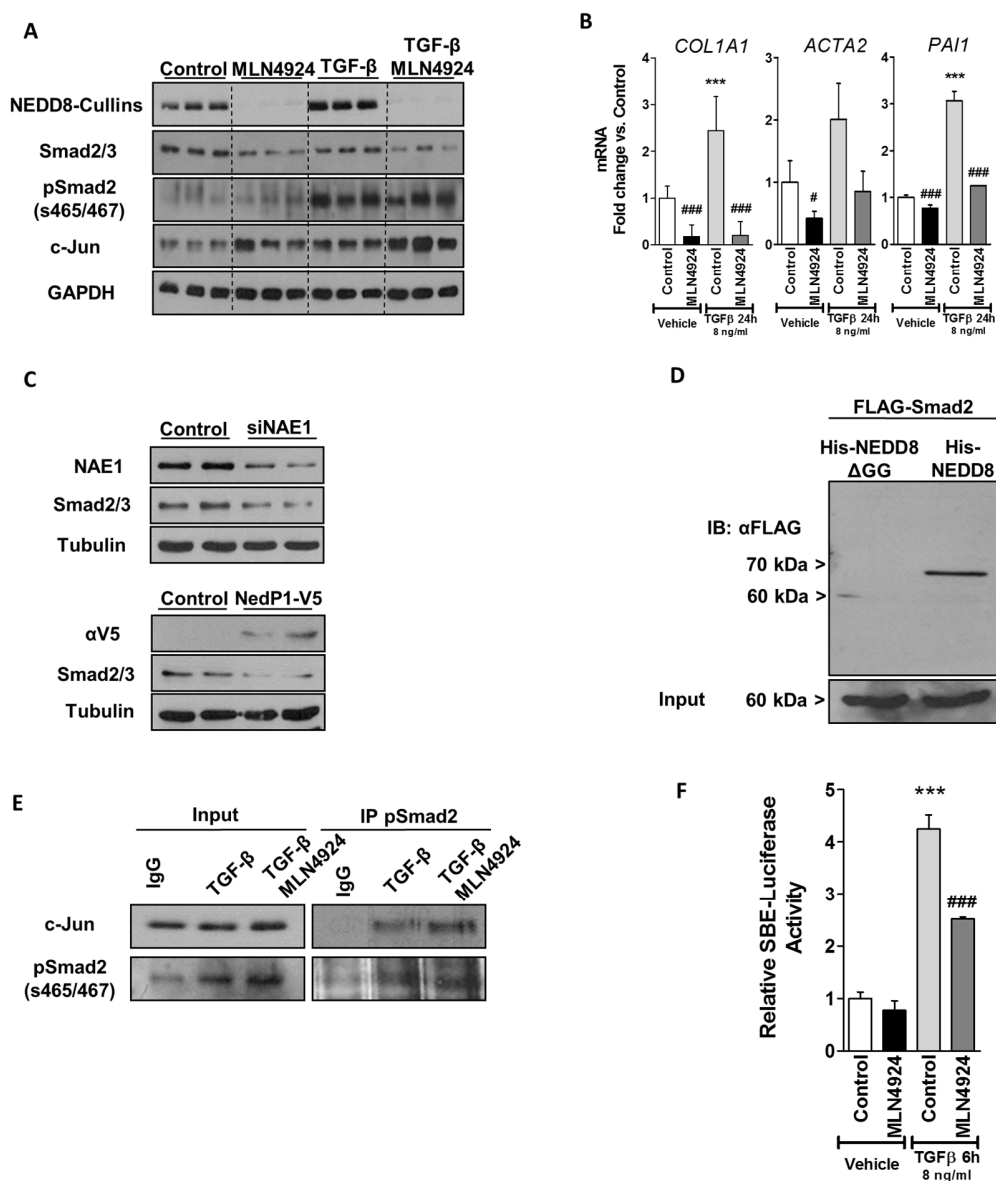


Figure 24. NEDDylation plays a role in Smad signaling. (A) Western blot of NEDDylated cullins, Smad2 and c-Jun in human LX-2 cells treated with TGF- β (8ng/ml) and MLN4924 (3 μ M). (B) mRNA levels of profibrogenic markers in human LX-2 cells treated with TGF- β (8ng/ml) and MLN4924 (3 μ M). (C) Western blot of Smad2 from human LX-2 cells with either NAE1 silenced (upper panel) or overexpressing NedP1-V5 (lower panel). (D) Ni²⁺-NTA pulldown of FLAG-Smad2 bound to His₆-NEDD8 in human LX-2 cells. (E) Immunoprecipitation (IP) of pSmad2 (S465/467) and blot against c-Jun from human LX-2 cell extracts treated with 8ng/ml TGF- β . (F) Luciferase activity of Smad binding elements (SBE) in human LX-2 cells stimulated with TGF- β (8ng/ml) and cultured with MLN4924 (3 μ M). (*, ** or *** = p<0.05, p<0.01 or p<0.001 respectively) vs control and (#, ## or ### = p<0.05, p<0.01 or p<0.001 respectively) MLN4924 treated vs. non-treated.

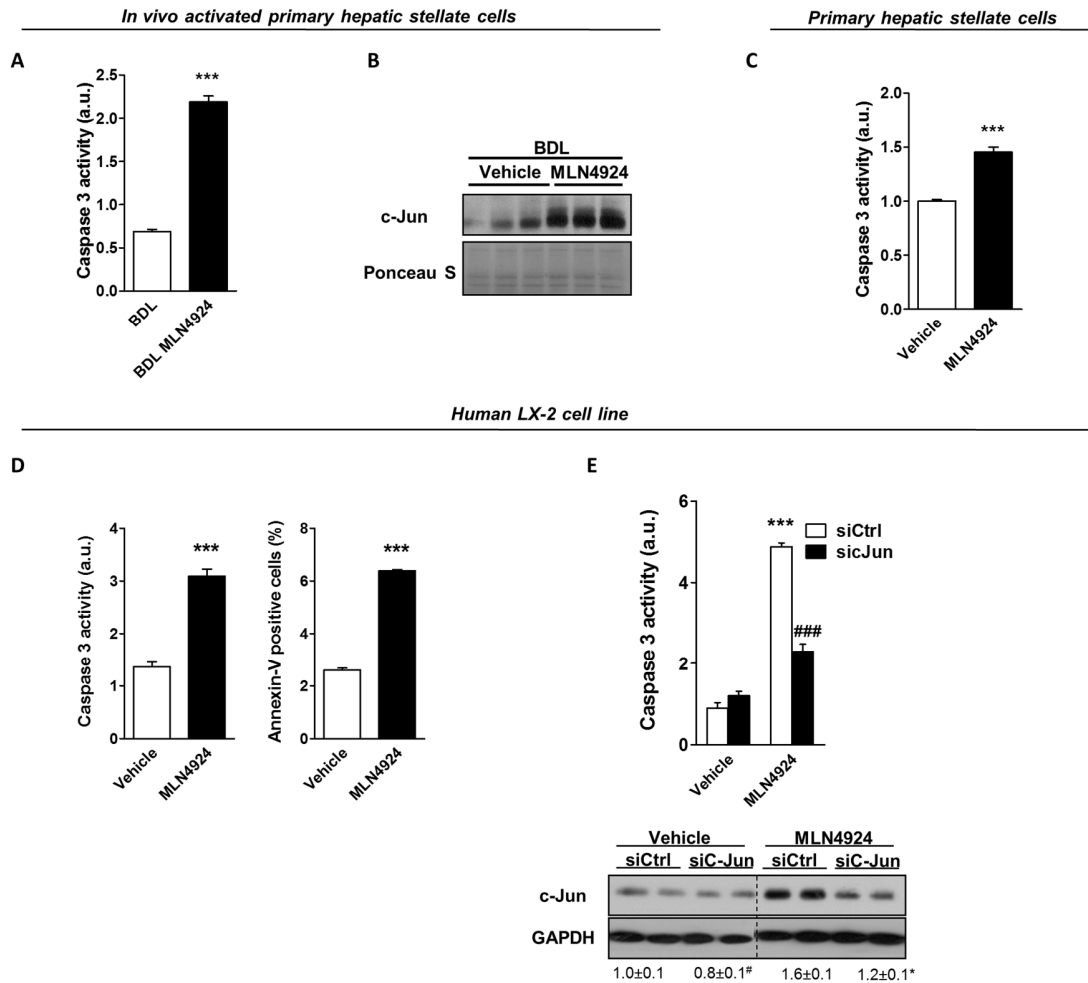


Figure 25. NEDDylation inhibition induces hepatic stellate cell apoptosis through c-Jun stability. (A and C) Caspase 3 activity of *in vivo* activated and plastic activated primary mouse HSC respectively cultured with MLN4924 (3µM). **(B)** Western blot of c-Jun levels in *in vivo* activated primary mouse HSC. **(D)** Caspase 3 activity and Anxin-V positive human LX-2 cells cultured with MLN4924 (3 µM). **(E)** Caspase 3 activity in human LX-2 cells with silenced c-Jun and cultured with MLN4924 (3 µM). Western blot was used to confirm c-Jun silencing (lower panel). (*, ** or *** = p<0.05, p<0.01 or p<0.001 respectively) vs control and (#, ## or ### = p<0.05, p<0.01 or p<0.001 respectively) MLN4924 treated vs. non-treated.

interaction between NEDD8 and Smad2 we performed a Ni²⁺-NTA agarose pull-down in LX-2 cells transfected with FLAG-Smad2 and His₆-NEDD8 or a NEDD8 mutant (His₆-ΔGG-NEDD8) which is unable to conjugate with targets. Only extracts from cells transfected with His₆-NEDD8 pulled down a band at approximately 70 kDa, indicating that Smad2 might be NEDDylated (**Figure.24D**).

Interestingly, when MLN4924 treated cells are stimulated with TGF-β, there is no decrease in pSmad2 levels even though there is a decrease in total Smad2 levels (**Figure.24A**). These results suggest that while NEDDylation may be stabilizing unmodified Smad2 it disrupts phosphorylated Smad2 levels, however, with NAE1 inhibition we see a reduced expression of Smad target genes indicating that MLN4924 is somehow disrupting the activity of activated Smad. Smad signaling can be interrupted by several mechanisms, such as Smad7, Smurf1 and 2, and c-Jun. Previous researchers have shown that c-Jun has a Smad binding element in its promoter and that it is expressed in cells stimulated with TGF-β and the increased c-Jun in the nucleus is then able to bind and intercept the Smad complex and inhibit its transcription (184,185). c-Jun is also degraded by cullins (385), and we saw an increase in c-Jun stability in LX-2 cells and primary HSCs (**Figure.24A** and **25B**). To test whether the increase in c-Jun is one of the reasons why MLN4924 treated HSCs have a reduced activation, we performed a pSmad2 immunoprecipitation in TGF-β activated LX-2 cells (**Figure.24E**). Activated cells immunoprecipitated more c-Jun than control cells. Additionally, activated LX-2 cells treated with MLN4924 have reduced activation of a

commercial Smad binding element (SBE) luciferase assay when compared to TGF-β only cells (**Figure.24F**). These results suggest that in our model c-Jun may also be blocking activation by sequestering the Smad complex and preventing activation of Smad target genes despite high levels of pSmad2.

5.2.6 NEDDylation inhibition decreases fibrosis by inducing hepatic stellate cell apoptosis

Therapies aimed at reducing fibrosis have also attempted to induce apoptosis of activated HSC to reduce their activity. To test whether NEDDylation inhibition could also be reducing fibrosis by inducing HSC apoptosis we assessed caspase-3 activity in MLN4924 treated BDL activated primary mouse HSC or TGF-β stimulated LX-2 cells (**Figure.25A,D**). The results showed that both cell types had increased apoptosis when treated with MLN4924 and apoptosis from HSC isolated from healthy animals is significantly lower than that observed in activated HSC (**Figure.25C**). Previous reports have shown that c-Jun is linked to apoptosis in several types of cells (386), including HSC (387) and inhibiting NEDDylation in both primary HSCs and LX-2 cells leads to accumulation of c-Jun (**Figure.24A** and **25B**). To confirm the role of c-Jun in HSC apoptosis we partially silenced c-Jun in LX-2 cells and this was able to reduce the apoptotic-induced actions of MLN4924 (**Figure.25E**). This evidence suggests that the accumulation of c-Jun as a result of NEDDylation inhibition may be reducing fibrosis on the one hand by reducing activation of HSC and on the other by promoting HSC apoptosis.

Post-translational Modifications in Liver Disease
Imanol Zubieta Franco

5.3 SUMO2 retains LKB1 in the nucleus and increases hepatoma cell survival

5.3.1 Background

The serine/threonine kinase LKB1 has generally been considered a tumor suppressor due to its role as the activator of AMPK and its control over cellular metabolism. Recently, a different function has been discovered for LKB1 in cell growth and cancer. In liver, we found that LKB1 was activated in liver regeneration after partial hepatectomy (69) and that patients with poor prognosis HCC have increased levels of LKB1 (267,268,282). Indeed, overexpression of LKB1 in hepatoma cells induces replication and survival through regulation of the Ras signaling pathway. Furthermore, mice livers overexpressing LKB1 show formation of preneoplastic nodules with increases expression of RasGRP3. On the other hand, hepatoma cells with silenced LKB1 have increased cell death and reduced cell growth (268). Although the effects of LKB1 on the liver are starting to be elucidated, the mechanisms by which this happens are still largely unknown.

5.3.2 LKB1 expression is induced in low GNMT tumors from HCC patients

Hepatic protein and mRNA levels of LKB1 are induced in bad prognosis HCC patients (268,282). In this context, hyperactivation of LKB1 (S428) is negatively correlated with low levels of GNMT in human HCC (268). Indeed, the absence of GNMT in the *Gnmt-KO* mouse model induces the spontaneous development of NAFLD and its progression to fibrosis and HCC highlighting the role of GNMT in liver disease (73). Importantly, 6 month old pretumoral *Gnmt-KO* mice have increased hepatic LKB1 levels (Figure.26A).

In order to evaluate if LKB1 is implicated in malignant transformation during the initial stages of liver cancer, LKB1 levels

were analyzed by immunohistochemistry in very-early or early HCC patients (BCLC stage 0 or A) with different pathological etiologies (section 4.7) and characterized by low GNMT levels (Figure.26B). In agreement with our previous work, we show that LKB1 protein levels are induced in human early stage HCC specimens compared to healthy controls and correlated with the levels of GNMT (Figure.26A,B).

To further study the role of LKB1 (gene *STK11*) in GNMT deficient hepatic tumors we created a *Stk11/Gnmt* double knockout mouse. Therefore, *Gnmt-KO* mice were crossed with the *Alb-Cre⁺Stk11^{loxP/loxP}* generating a novel animal model, the *Stk11/Gnmt dKO* with low hepatic LKB1 in the context of GNMT deficiency (Figure.10 and 27A, section 4.6.1). In these animals, LKB1 levels are reduced in hepatocytes due to the

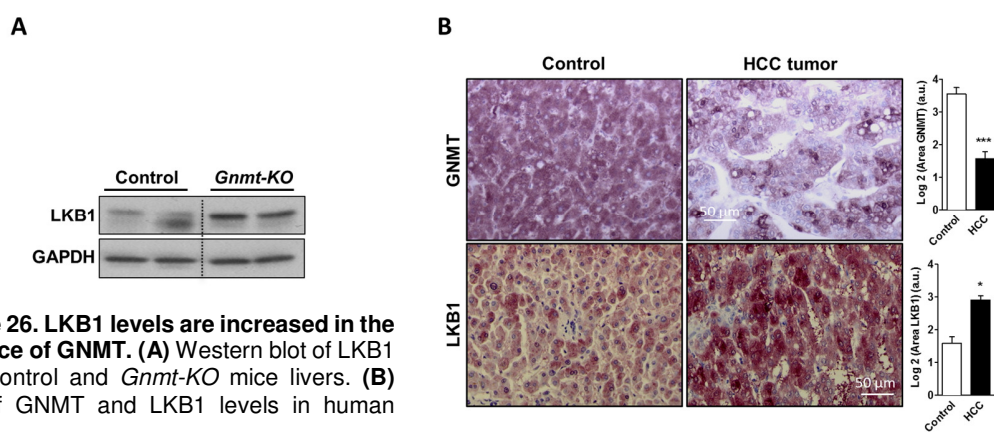


Figure 26. LKB1 levels are increased in the absence of GNMT. (A) Western blot of LKB1 from control and *Gnmt-KO* mice livers. **(B)** IHC of GNMT and LKB1 levels in human HCC.

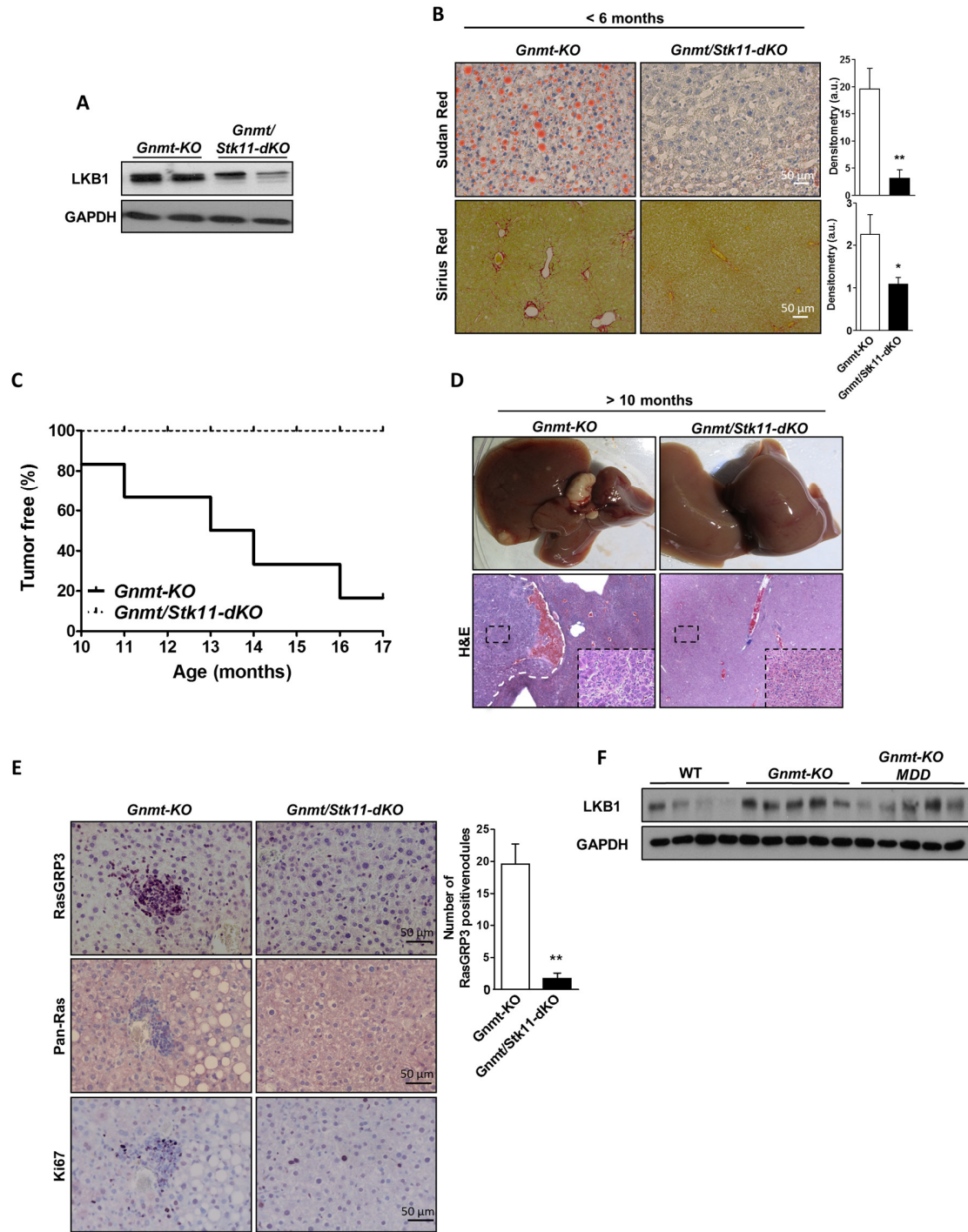


Figure 27. Loss of LKB1 in the *Gnm1*-KO mouse improves liver health. (A) Western blot of LKB1 levels in the *Gnm1*-KO and *Gnm1/Stk11*-dKO mouse models. (B) Sudan red and Sirius red staining of *Gnm1*-KO and *Gnm1/Stk11*-dKO livers less than 6 months old. (C) A Kaplan-Meier plot showing the percent of tumor free mice (*Gnm1*-KO and *Gnm1/Stk11*-dKO). (D) H&E staining and representative photographs of more than 10 month old *Gnm1*-KO and *Gnm1/Stk11*-dKO mice livers. (E) RasGRP3, Pan-RAS and Ki67 staining of *Gnm1*-KO and *Gnm1/Stk11*-dKO mice livers. (F) Wb of LKB1 from control, *Gnm1*-KO, and *Gnm1*-KO on a methionine deficient diet (MDD, 1 month).

Cre recombinase driven by the Albumin (*Alb*) gene promoter commonly used to generate adult mice with reliable hepatocyte-specific recombination of *loxP*-flanked alleles. Comparison of the *Gnmt-KO* versus *Stk11/Gnmt-dKO* mice indicated that hepatic *Stk11* silencing reduced liver NASH and fibrosis in animals younger than 6 months old (**Figure.27B**). Moreover, hepatic *Stk11* knockout completely blocked liver tumor appearance associated with GNMT deficiency in animals older than 10-months-old, as observed by ultrasound surveillance (**Figure.27C**) and later confirmed by visual inspection upon sacrifice. Hematoxylin and eosin (H&E) staining was further used to confirm the presence of liver tumors in the *Gnmt-KO* mice (**Figure.27D**). These results agree with previous evidence from our group where *Stk11* ablation in flank xenograft tumors of hepatoma cells from the *Gnmt-KO* mouse resulted in reduced tumor growth (268). Importantly, these results at this level were independent of SAME levels (**SAME levels= 3,334±623 mol/mg in *Gnmt-KO* vs. 3,413 ± 209 mol/mg in the *Stk11/Gnmt-dKO***). Interestingly, *Gnmt-KO* mice had increased

RasGRP3 and Pan-RAS levels in protumoral nodules in a similar fashion as to what we had previously seen in mice overexpressing LKB1 in the liver as well as increased inflammatory cell infiltration as seen by Ki67 staining (**Figure.27E**). Loss of LKB1 reduced the appearance of nodules and the associated hepatic inflammation along with the levels of RasGRP3 and Pan-Ras. The improved liver phenotype seen when LKB1 is deleted resembles the effects seen when *Gnmt-KO* mice are fed a methionine deficient diet (86). Normalization of SAME levels, with a methionine deficient diet in *Gnmt-KO* mice, led to a reduction of total LKB1 (**Figure.27F**), suggesting that SAME levels may play a role in determining LKB1 levels.

5.3.3 LKB1 localizes to the nucleus

The data gathered here and in previous work from our lab points to LKB1 directly influencing the activity of the Ras proliferation pathway, especially the expression of RasGRP3. Hepatoma cells derived from *Gnmt-KO* and human (Bcl3 cell line) tumors had increased mRNA and protein RasGRP3 levels when overexpressing LKB1

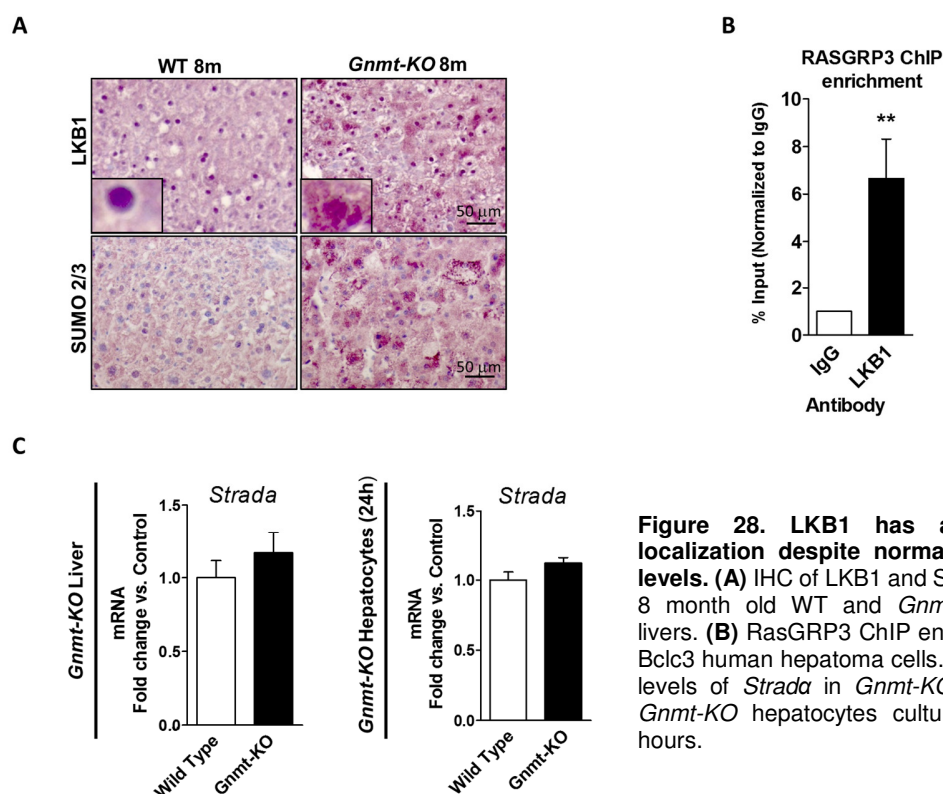


Figure 28. LKB1 has a nuclear localization despite normal STRAD α levels. (A) IHC of LKB1 and SUMO2/3 in 8 month old WT and *Gnmt-KO* mice livers. **(B)** RasGRP3 ChIP enrichment in Bcl3 human hepatoma cells. **(C)** mRNA levels of *Strada* in *Gnmt-KO* liver and *Gnmt-KO* hepatocytes cultured for 24 hours.

(268) suggesting that LKB1 overexpression may play a role in regulating cellular transcriptional activity. In 8 month old *Gnmt-KO* mice and Bcl3 hepatoma cells, LKB1 is mainly localized in the nucleus (**Figure.28A**). In order to test whether LKB1 may directly be inducing the expression of RasGRP3 we performed a ChIP assay in Bcl3 human hepatoma cells (**Figure.28B**). Interestingly, we found that the promoter of RasGRP3 co-immunoprecipitated with LKB1 suggesting that the up regulation of the mRNA levels of this Ras activator is controlled by LKB1. This data is similar to that of Scott *et al.* that saw an increased binding of nuclear LKB1 to the promoter region of Cyclin D1 (388).

Subcellular localization of LKB1 is normally controlled by the pseudokinase STRAD α . We checked the levels of STRAD α in *Gnmt-KO* mice tumors, *Gnmt-KO* hepatocytes and in the ONCOMINE database and found that STRAD α levels were not reduced (**Figure.28C** and **Table 11**). This data points to a different mechanism retaining LKB1 in the nucleus and regulating its activity.

Table 11. Oncomine database search for the STRAD α gene

HCC vs. Normal Gene: <i>STRADA</i>			
Study or subgroup	Fold change	p	n
Chen Liver	1.333	3.33E-6	197
Roessler Liver	1.203	0.002	43
Wurmbach Liver	1.186	0.004	75
TCGA Liver	1.101	3.77E-8	212
Mas Liver	1.084	0.049	115
Roessler Liver 2	1.059	0.002	445
Guichard Liver	1.040	3.77E-7	185
Guichard Liver 2	1.035	0.003	52
Mas Liver	-1.108	0.005	115

5.3.4 LKB1 is modified by SUMO2 controlling its subcellular localization

LKB1 is known to be modified by various post-translational modifications. Among them the most studied are NEDD8 and ubiquitin. NEDD8 can increase the stability of LKB1 in HCC (282) and K63 ubiquitination can increase LKB1 activity by stabilizing the formation of the LKB1-STRAD α -MO25 complex (280). One PTM that is connected to protein localization is SUMO (small ubiquitin-like modifier) and it is the only PTM with a known consensus site on its target proteins (294). While working on this project Ritho *et al.* found that LKB1 was SUMOylated by SUMO1 during starvation and that this modification increased the interaction of LKB1 with AMPK but had no effect on localization (281). We found that, like LKB1, SUMO levels are increased in 8 month old *Gnmt-KO* mice when compared to WT controls (**Figure.28A**), so to explore LKB1 SUMOylation we first used SUMO site prediction software to find any possible SUMO consensus sites in its amino acid sequence. The results showed 3 high scoring sites within LKB1 (**Figure.29A**). Since LKB1 had putative SUMO binding sites we next performed a Ni²⁺-NTA agarose bead pulldown from Huh7 cells transfected with His₆-SUMO1, 2, or 3 and LKB1. We observed that LKB1 was only modified with SUMO2 and that this result was specific because co-transfection with Ubc9 increased the SUMO2 smear (**Figure.29B, lane 5**). This modification did not require LKB1 activity as a kinase dead mutant was also modified (**Figure.29C**). Additionally, we observed an increase in SUMOylation with PIAS1 and 4 (**Figure.29D, lanes 3 and 6**) and that SENP2 was the most active LKB1 deSUMOylase (**Figure.29E, lane 4**). Interestingly, SENP7 did not modify LKB1-SUMO this may be due to its role as a SUMO chain modifier (320). To find the acceptor lysine in LKB1 we created arginine mutants of the four highest scoring consensus sites (K96, K97, K178, and K235) and performed the same pulldown as before (**Figure.29F, lane 5**). The mutant K178R had the least amount of SUMO2 smear of all the mutants tested suggesting that K178 is the primary SUMO2 acceptor.

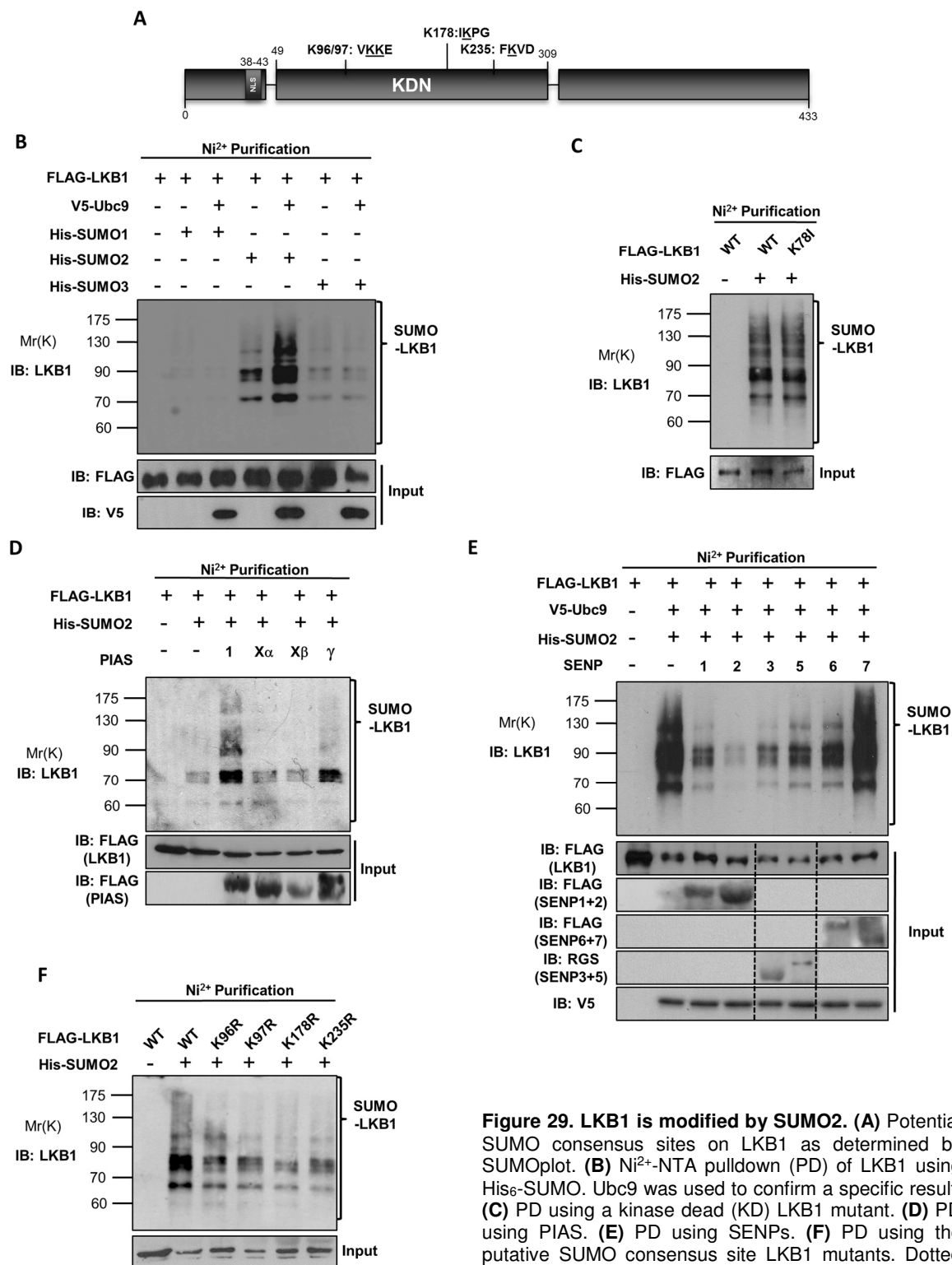


Figure 29. LKB1 is modified by SUMO2. (A) Potential SUMO consensus sites on LKB1 as determined by SUMOplot. (B) Ni²⁺-NTA pulldown (PD) of LKB1 using His₆-SUMO. Ubc9 was used to confirm a specific result. (C) PD using a kinase dead (KD) LKB1 mutant. (D) PD using PIAS. (E) PD using SENPs. (F) PD using the putative SUMO consensus site LKB1 mutants. Dotted lines represent cropped blots.

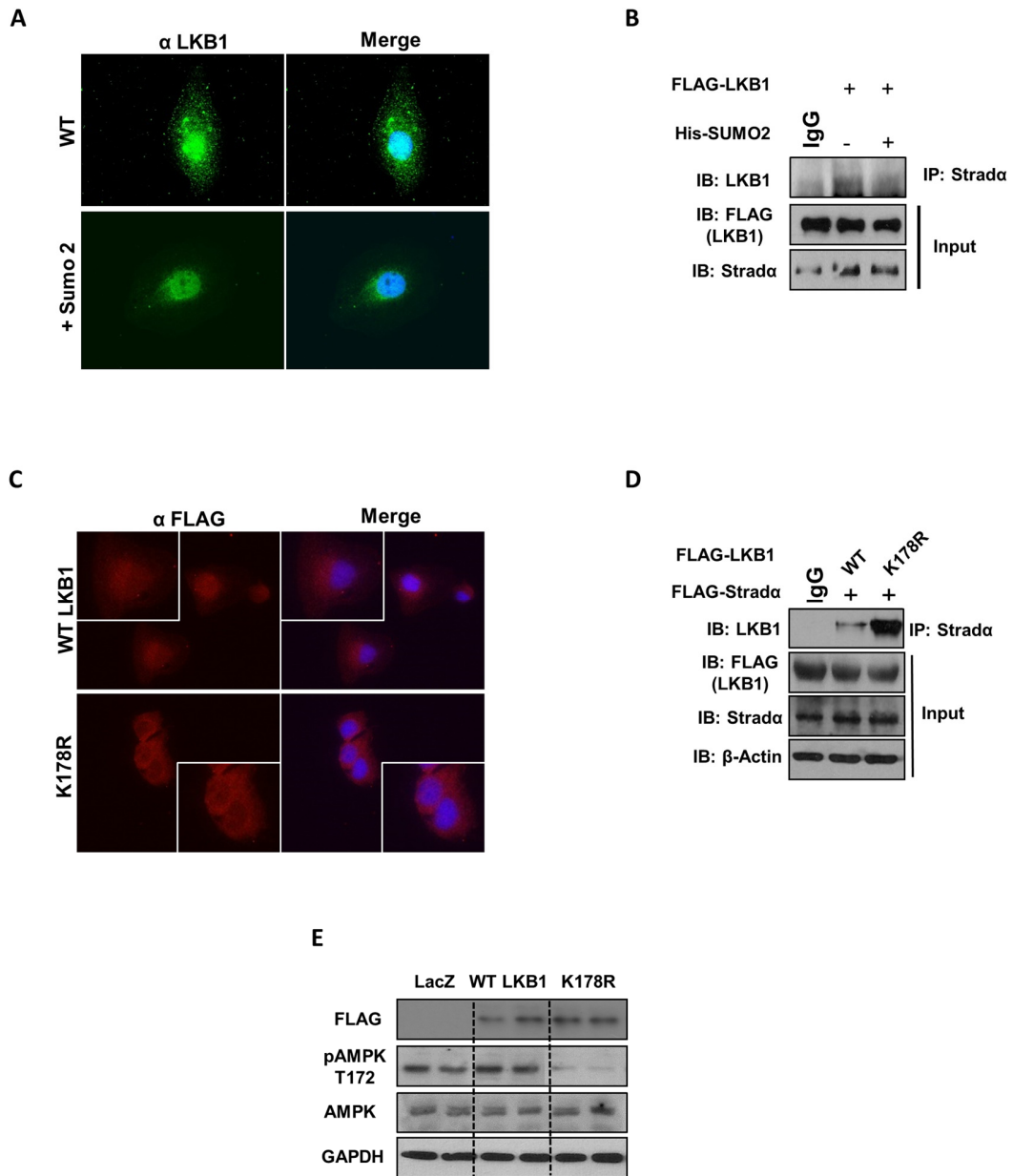


Figure 30. SUMO2 increases LKB1 nuclear localization by disrupting its union with STRAD α . (A) Immunofluorescence (IF) of LKB1 in Huh7 cells with or without SUMO2. (B) Immunoprecipitation of Strada in Huh7 cells with or without SUMO2 and blot against LKB1. (C) FLAG IF of Huh7 cells expressing WT LKB1 or LKB1 K178R mutant. Inserts are magnified 1.5 times. (D) IP of STRAD α from Huh7 cell expressing either WT LKB1 or LKB1 K178R mutant. (E) Western blot of FLAG and AMPK from Huh7 cells expressing WT LKB1 or LKB1 K178R mutant. Dotted lines represent cropped blots.

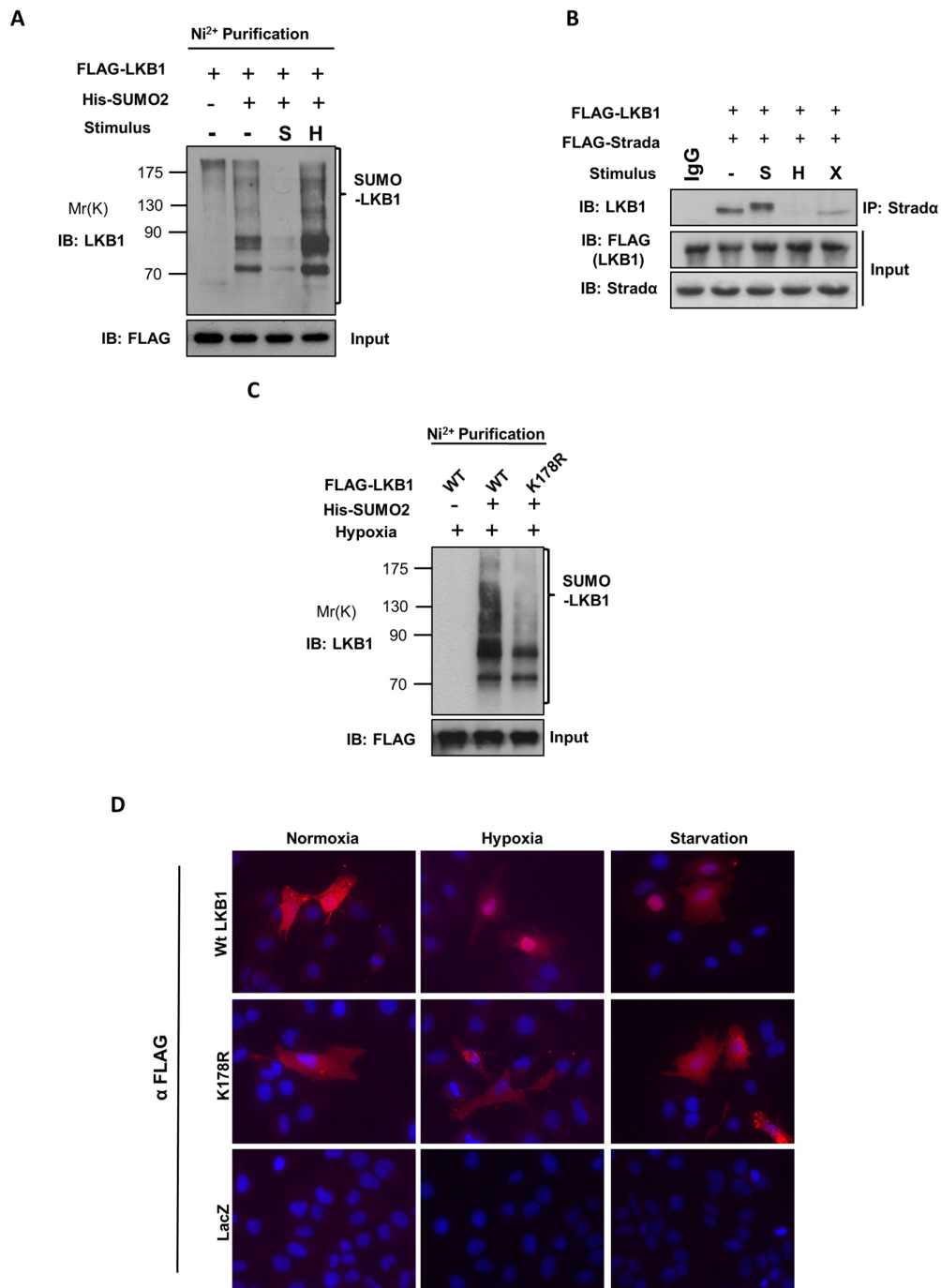


Figure 31. LKB1 SUMOylation increases during hypoxia. (A) Pulldown (PD) of LKB1 under different metabolic conditions in Huh7 cells. (B) Immunoprecipitation of Strada in Huh7 cells under different metabolic conditions and blot against LKB1. (C) PD of WT LKB1 and LKB1 K178R mutant in Huh7 cells in hypoxia. (D) FLAG immunofluorescence during hypoxia or starvation of Huh7 cells expressing WT LKB1 or LKB1 K178R mutant and LacZ expressing control cells. S= starvation, H= hypoxia, X= Ex-527 treatment (30 μ M, 24h).

To test whether SUMOylation could affect LKB1 localization we performed immunofluorescence staining of LKB1 in Huh7 cells expressing SUMO2 (**Figure.30A**). Cells that expressed more SUMO2 had increased nuclear localization of LKB1. Cells expressing both SUMO2 and STRAD α had less LKB1 co-immunoprecipitate after an IP (**Figure.30B**) suggesting that SUMO2 can control LKB1 localization by preventing the formation of the LKB1-STRAD α -complex. We next repeated the same experiments with the SUMO2 deficient mutant. Immunofluorescence of LKB1 in K178R mutant expressing cells showed an increased cytoplasmic localization (**Figure.30C**) and when immunoprecipitated, K178R had increased binding to STRAD α (**Figure.30D**).

The K178R mutant had the same stability as WT LKB1 (**Figure.30E**) suggesting that SUMO2 is not required for protein stability. The K178R mutant had reduced AMPK activation (T172) when compared to WT LKB1 despite being primarily in the cytoplasm. These results are similar to what Ritho *et al.* discovered as they observed a reduced interaction of LKB1 K178R with AMPK (281). Taken together these results suggest that SUMOylation can control LKB1 activity by retaining it in the nucleus and reducing the formation of the LKB1-STRAD α complex.

5.3.5 LKB1 is SUMOylated during hypoxia

SUMOylation is a dynamic process and usually occurs in response to cellular stress (294). Since LKB1 is mainly involved in the regulation of metabolism we next studied the SUMOylation of LKB1 during metabolic stress such as starvation and hypoxia. Under these conditions LKB1 SUMOylation is altered, during starvation LKB1 SUMOylation was barely detectable whereas in hypoxic conditions LKB1 SUMOylation was increased when compared to normoxia (**Figure.31A**). An IP of STRAD α under the same conditions resulted in more co-immunoprecipitation of LKB1 during starvation (LKB1 is located in the cytoplasm during starvation) and less during hypoxia (**Figure.31B**). As expected, the K178R mutant had no change in SUMOylation during hypoxia (**Figure.31C**). When we studied the subcellular localization of WT LKB1 during metabolic stress we saw a cytoplasmic staining during starvation and a

stronger nuclear signal during hypoxia (**Figure.31D**), however, the SUMO mutant LKB1 was localized mainly in the cytoplasm regardless of the metabolic state (**Figure.31D**). This data suggests that SUMOylation is activated during hypoxia, inactivated during starvation and that it retains LKB1 in the nucleus.

5.3.6 Acetylation is a prerequisite for SUMOylation

Previous groups have demonstrated that the acetylation status of LKB1 is able to control its cellular localization (279) in a similar fashion to what we observed. Protein acetylation can also compete with SUMO for the same lysine residue resulting in a SUMO/acetylation switch (389,390). To study the role of acetylation on the SUMOylation status of LKB1 we co-transfected LKB1 and SIRT1, a NAD dependent sirtuin that deacetylates LKB1 (279), and performed a pulldown. Huh7 cells transfected with SIRT1 had a reduced SUMO2 smear when compared to LKB1 only cells (**Figure.32A**). Interestingly, SIRT1 activity appears to be inactivated during hypoxia in our model (**Figure.32B**). To further test the effects of acetylation, we performed a pulldown with LKB1 K48R (an acetylation mutant, **Figure.32C**) (279). When compared to control, K48R had reduced SUMOylation whereas WT-LKB1 treated with the SIRT-1 inhibitor Ex-527 had an increased SUMO2 smear. The K48R mutant was not SUMOylated under hypoxia or with Ex-527 treatment (**Figure.32D**) and neither was the K178R mutant (**Figure.32E**). Ex-527 was also able to reduce the co-immunoprecipitation of LKB1 with Strad α (**Figure.31B**).

GCN5 (KAT2A) is an acetyltransferase that has been implicated in controlling cellular metabolism along with SIRT1 (391–393). When cells were treated with butyrolactone 3, a specific GCN5 inhibitor, the resulting pulldown had a reduced SUMO2 smear (**Figure.32F**) similar to SIRT1 overexpression. Taken together, these results suggest that LKB1 requires a previous acetylation step to be modified by SUMO2 during hypoxia.

5.3.7 LKB1 in hypoxic liver

To test the biological validity of LKB1 SUMOylation, we looked at the localization of

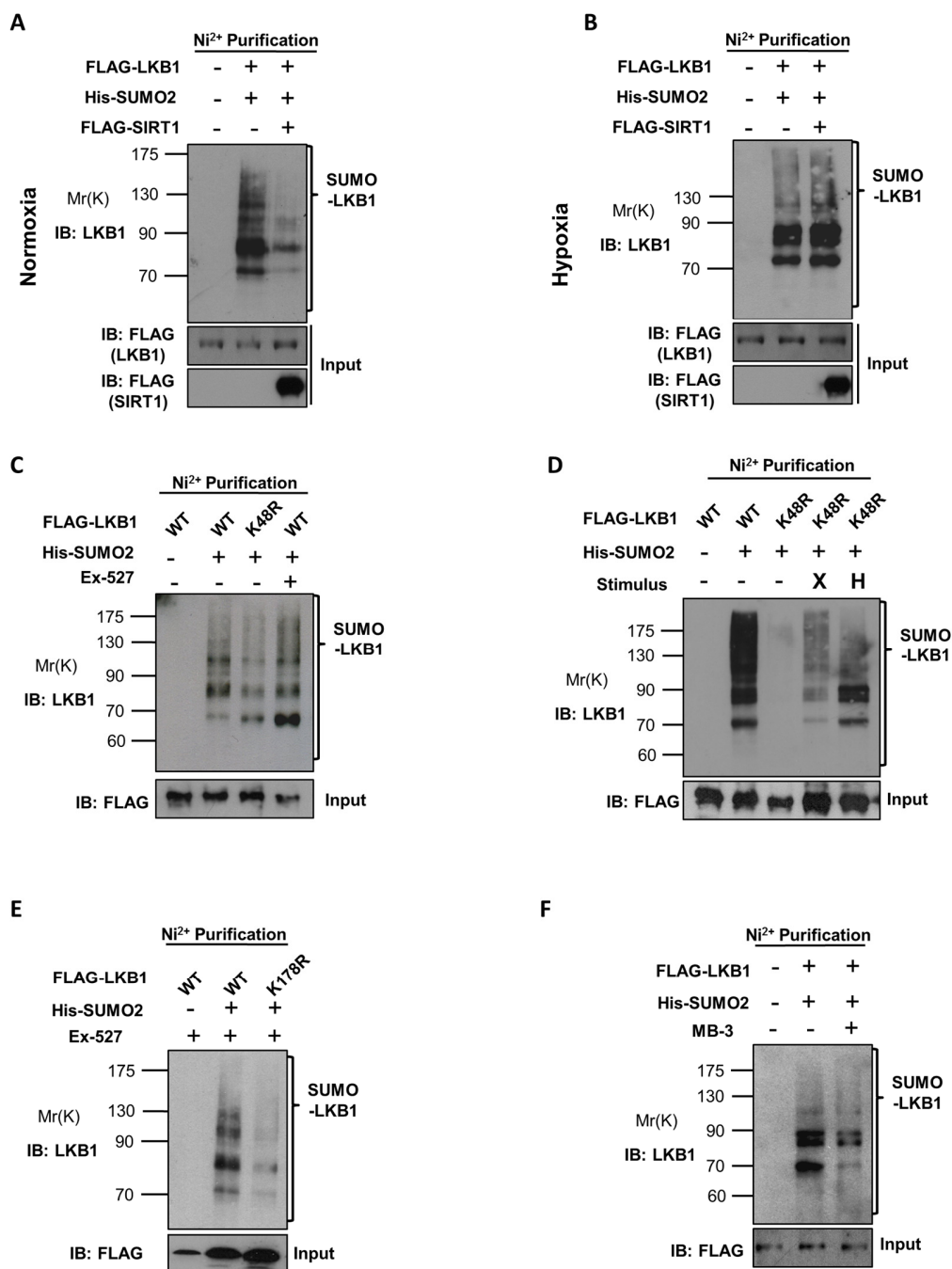


Figure 32. Acetylation is a prerequisite for LKB1 SUMOylation. (A) Pull-down (PD) of LKB1 in Huh7 cells expressing SIRT1 in normoxia and in (B) hypoxia. (C) PD of WT LKB1 and LKB1 K48R mutant in Huh7 cells and Ex-527 culture. (D) PD of the LKB1 K48R mutant in different metabolic conditions. (E) PD of LKB1 K178R mutant with Ex-527 culture. (F) PD of WT LKB1 with Butyrolactone (MB-3, 100 μ M, 24h) culture. H= hypoxia, X= Ex-527 treatment (30 μ M, 24h).

Post-translational Modifications in Liver Disease
Imanol Zubiete Franco

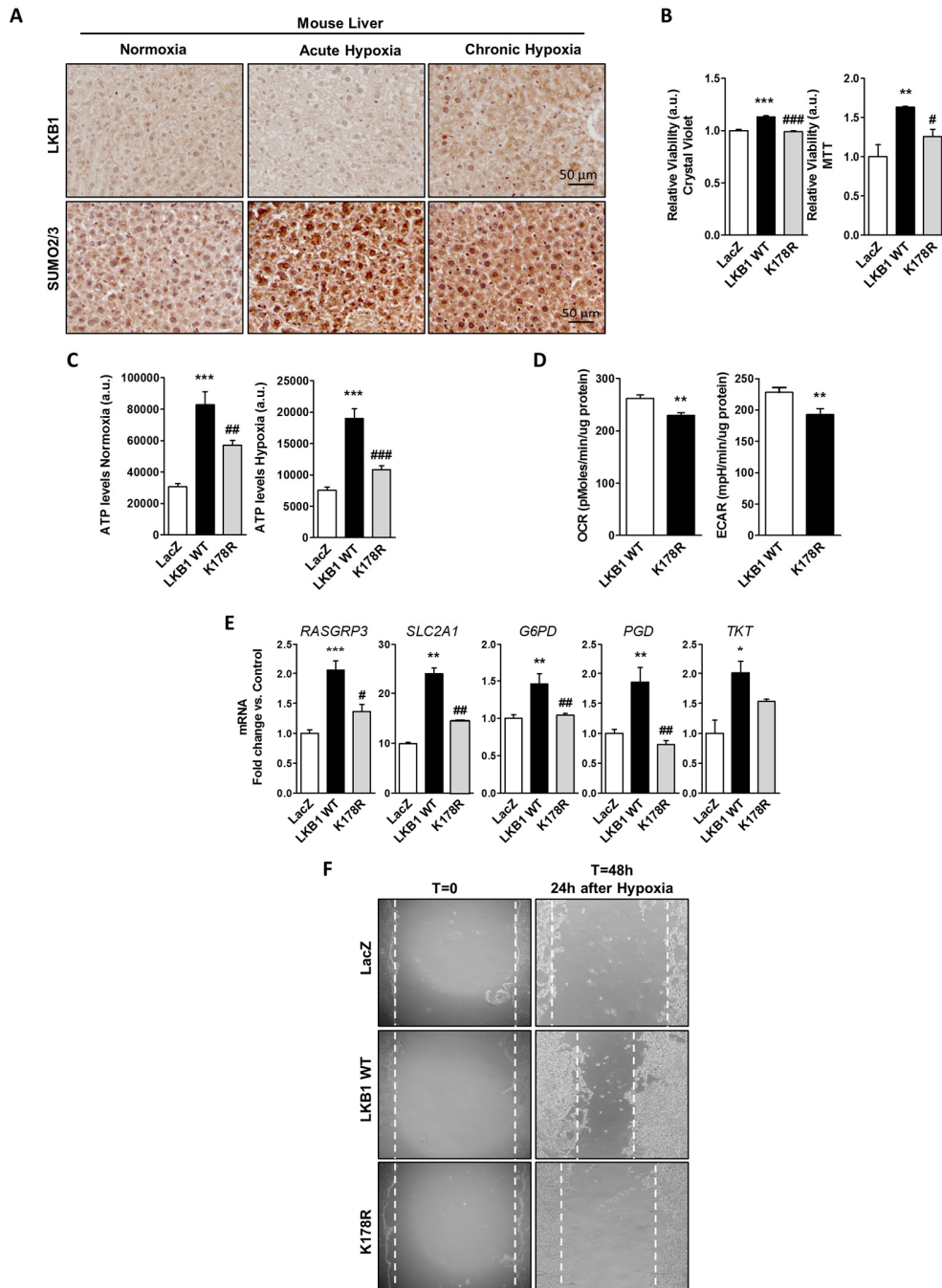


Figure 33. Nuclear LKB1 increases hepatoma cell survival. (A) Immunohistochemistry of hepatic LKB1 and SUMO2/3 from mice under acute and chronic hypoxia. **(B)** Crystal violet and MTT assays in Huh7 cells expressing WT LKB1 or LKB1 K178R mutant in normoxia. Control cells express LacZ. **(C)** ATP levels in Huh7 cells expressing WT LKB1 and LKB1 K178R mutant in normoxia and hypoxia. Control cells express LacZ. **(D)** Oxygen consumption rate (OCR, left panel) and extracellular acidification rate (ECAR, right panel) in Huh7 cells expressing WT LKB1 and LKB1 K178R mutant and subjected to 24h of hypoxia. **(E)** mRNA levels of RasGRP3, GLUT1 (SLC2A1) and parts of the pentose phosphate pathway in Huh7 cells expressing WT LKB1, LKB1 K178R mutant or LacZ control after 24h of hypoxia. **(F)** Wound healing assay of Huh7 cells expressing WT LKB1, LKB1 K178R mutant or LacZ at T=0 (left panel) and T=48h (24h of hypoxia, right panel).

LKB1 in mice exposed to hypoxia. Nuclear LKB1 increases with the duration of hypoxia as seen by immunohistochemistry and nuclear accumulation of SUMO 2/3 is also increased during hypoxia (**Figure.33A**).

5.3.8 LKB1 SUMOylation increases cell survival

We then used Huh7 hepatoma cells to study the effect of LKB1 SUMOylation on cell survival. Huh7 cells expressing WT LKB1 had increased survival and higher colony formation (**Figure.33B**). Additionally, WT LKB1 cells had more ATP under basal conditions (**Figure.33C**) and these differences were maintained during hypoxia as WT cells had more ATP levels than K178R mutants (**Figure.33C**). These differences were also seen after the cells underwent a 24h period of hypoxia and were then cultured again in normoxia. WT LKB1 expressing cells had a higher oxygen consumption rate and an increased extracellular acidification rate when compared to K178R mutants (**Figure.33D**), as measured by a Seahorse analyzer, indicating that LKB1 increases energy levels and glycolysis and reflects a more tumoral metabolism. An increased nuclear localization

of WT LKB1 also resulted in an increased expression of RasGRP3 when compared to the more cytoplasmic K178R mutant (**Figure.33E**). This was also accompanied by an increase in the mRNA levels of GLUT1 a glucose transporter that facilitates glucose transport across the membrane (**Figure.33E**). Additionally, nuclear LKB1 increased the mRNA levels of Glucose-6-phosphate dehydrogenase, Phosphogluconate dehydrogenase, and transketolase all enzymes involved in the pentose phosphate pathway (**Figure.33E**) a pathway that generates NADPH, is required for nucleotide synthesis and ROS removal and is found upregulated in many cancers (394). These results suggest that LKB1 helps the cell maintain a functional metabolism during metabolic stress. Along similar lines, WT LKB1 Huh7 expressing cells were able to close the gap in a wound healing assay at a much faster rate than the mutant LKB1 cells after 24h of hypoxia (**Figure.33F**). Taken together, our results suggest that nuclear SUMOylated LKB1 is able to protect the cell during metabolic stress and improve proliferation and malignancy once normal conditions are obtained.

Post-translational Modifications in Liver Disease
Imanol Zubieta Franco

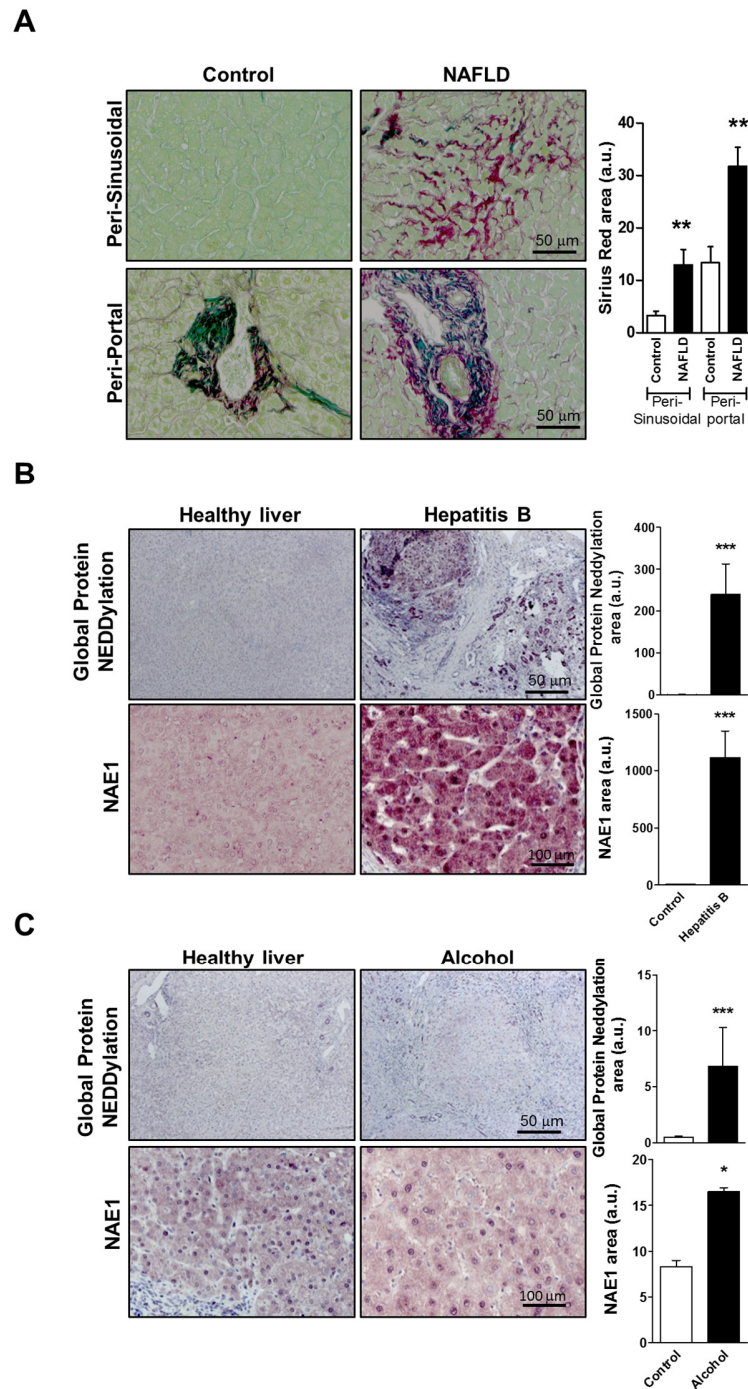
Supplemental



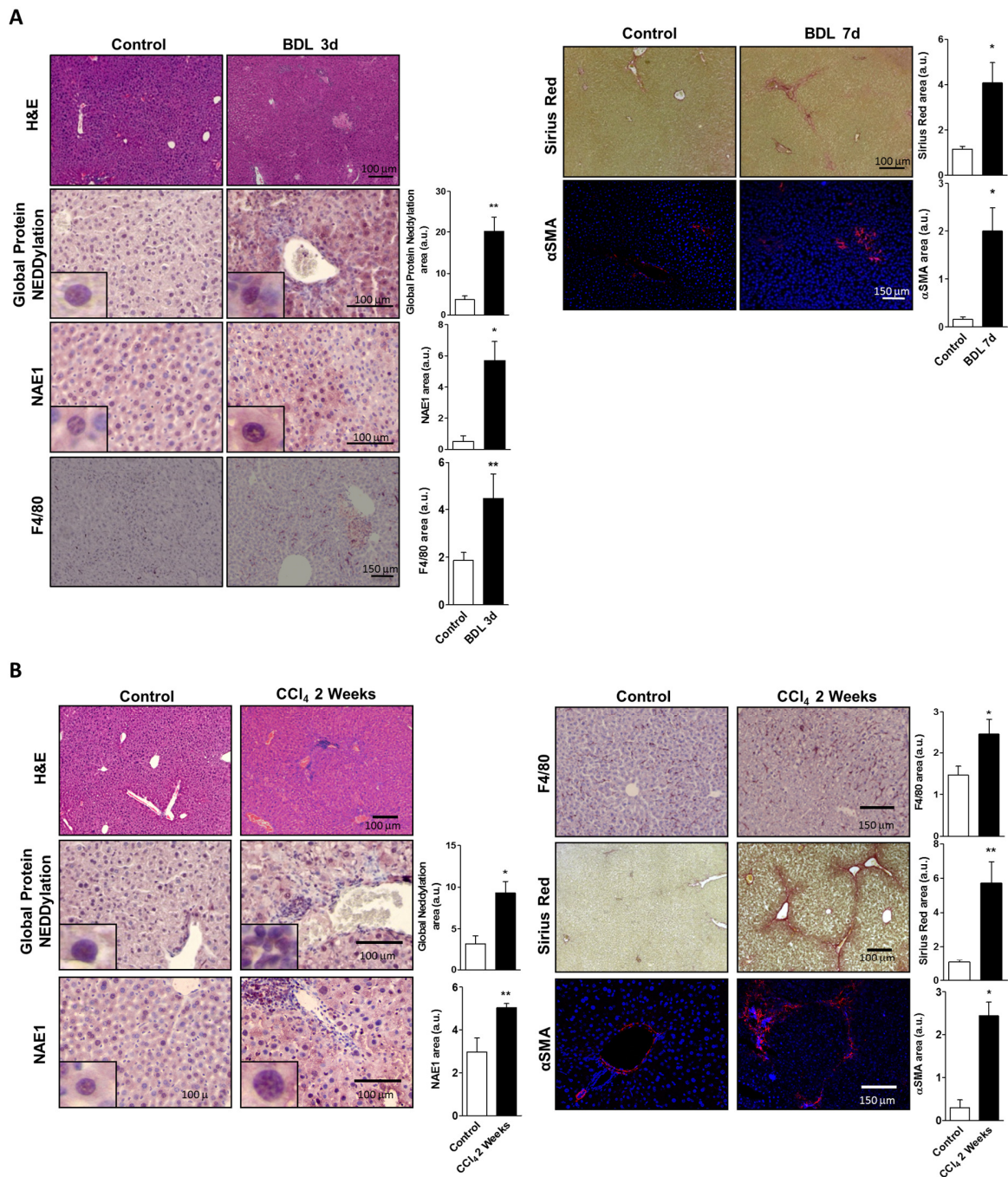
The image displays three chemical structures: two Lysine (Lys) residues, a methoxy group (CH₃O), and a Glycyl-Lysine (Gly-Lys) dipeptide. The Lysine structures are shown as Lys-C(=O)-, and the methoxy group is shown as CH₃O-C(=O)-. The Gly-Lys structure is shown as Gly-C(=O)-Lys-C(=O)-. The word 'Supplemental' is written in a large, bold, sans-serif font, with the chemical structures integrated into the letters.

Post-translational Modifications in Liver Disease
Imanol Zubieta Franco

6. Supplemental



Supplemental Figure 1. Fibrosis from different etiologies increases hepatic NEDDylation. (A) Sirius red staining of livers from healthy and NAFLD patients (Table 9) used in Figure 17. Both peri-sinusoidal and peri-portal regions are shown. **(B)** Global protein NEDDylation and NAE1 levels in fibrotic human livers caused by Hepatitis B infection **(B)** and alcohol abuse **(C)** compared to healthy controls.



Supplemental Figure 2. Inflammation and fibrosis is present at the start of MLN4924 treatment. H&E, Global protein NEDDylation, NAE1, F4/80, Sirius red and α SMA staining in BDL mice 3 days (left panel) and 7 days (right panel) after surgery (A) and in mice treated for 2 weeks with CCl₄ (B) at the time when MLN4924 treatment begins.

Discussion



Post-translational Modifications in Liver Disease
Imanol Zubieta Franco

7. Discussion

Steatosis is the accumulation of lipids in the liver due to dyslipidemia attributed to different factors. Excess lipid droplets in hepatocytes can be digested and mobilized by different means such as lipase activity or lipophagy (11). Lipophagy or autophagy has recently been shown to mobilize and hydrolyze large amounts of triglycerides in hepatocytes (10), this process allows for a fast mobilization of stored lipids by engulfing and sequestering large parts of the lipid droplet and then quickly digesting the contents using lysosomal enzymes. Defects in this process may lead to the development of fatty liver (10). Other studies have shown that reduced autophagy may be a consequence of steatosis itself by altering the membrane lipid composition and reducing autophagosome/lysosome fusion (35).

Gnmt-KO mice have elevated serum levels of methionine and SAME, which can lead to an inhibition of autophagy and contributing to the development of liver steatosis. We aimed to uncover the molecular mechanism that SAME and methionine use to inhibit autophagy in situations of GNMT deficiency (72,86). We observed that the reasons that alter autophagy in situations of acute or chronic exposition to elevated levels of SAME and methionine appear to be different in both cases. WT hepatocytes have a reduced upstream formation of the autophagosome after acute SAME and methionine treatment as seen by the reduced accumulation of LC3-II after lysosomal blockage. On the other hand, *Gnmt-KO* hepatocytes, exposed to high levels of SAME and methionine from birth, have an impaired lysosomal function resulting in autophagosome accumulation as seen by high basal LC3-II levels in untreated hepatocytes that do not increase after lysosomal blockage. There was already a hint of lysosomal dysfunction in WT hepatocytes after 40h of culture with SAME and methionine, although culture for longer periods of time led to hepatocyte death while *Gnmt-KO* hepatocytes are not affected for the time period studied. These results suggest that high levels of SAME and methionine may lead to an initial autophagy block by reducing autophagosome formation which would increase hepatocyte lipid content. This increase in lipids would lead

to an alteration of lysosomal membranes (35) which would reduce lysosomal function. *Gnmt-KO* mice also have other mechanisms that lead to lipid accumulation, as these mice have increased triglyceride synthesis due to increased PEMT activity producing more phosphatidylcholine and an increased VLDL clearance suggesting that these mechanisms can contribute along with autophagy in increasing hepatic lipid levels (76).

Hypermethionemia leads to high levels of SAME and an increase in aberrant methylation reactions. These reactions can cause aberrant methylation of different substrates such as DNA (73), lipids (77) and proteins. Here, we identified an increase in methyl-PP2A in *Gnmt-KO* hepatocytes and that this increase in activated PP2A was inhibiting autophagy. Whereas Sutter *et al.* highlight the possibility that methionine could modulate growth and MTORC1 signaling through the regulation of the methylation status of PP2A in yeast (370), we saw a direct interaction of PP2A with MTOR, and also observed that the use of demethylating agents was able to restore MTOR activity. This result explains why MTOR is surprisingly inactivated despite high levels of methionine, as amino acids are known activators of MTOR (250). MTOR is generally regarded as an inactivator of autophagy, as it phosphorylates and inhibits ULK1 (21). Here we saw an inhibition of both autophagy and MTOR pointing to possible MTOR independent pathways; although MTOR has been implicated in lysosome reformation (395) and this may be a contributing factor to inhibiting autophagy. Interestingly, PP2A is also known to inhibit the AMPK/LKB1 axis in liver regeneration if the levels of SAME are increased (69). Since PP2A is able to inactivate AMPK this also points to AMPK not being the reason for the reduced MTOR activity. Both AMPK and MTOR phosphorylate ULK1 activating or deactivating it respectively (11). It is unclear whether PP2A regulates ULK1 directly and further studies detailing the state of ULK1 in *Gnmt-KO* mice are required. Previous studies have also suggested that impaired digestion of lysosomal products may be responsible for the lack of MTOR reactivation as fibroblasts lacking lysosomal α -galactosidase activity have impaired MTOR reactivation (395). This

scenario seems unlikely in our case as we can see a reduction of MTOR activity beginning as early as 9h after treatment with SAME whereas the activity of the lysosomal enzymes began to drop after approximately 20h of treatment. Additionally, treatment with demethylating agents was also able to restore MTOR activity in *Gnmt-KO* hepatocytes.

In this study, silencing PP2A was able to restore autophagy in *Gnmt-KO* hepatocytes and SAME and methionine treated MLP29 cells, however, we were unable to identify the direct mechanism by which PP2A is able to inhibit autophagy and further work is being done in this area.

Removing the hypermethioninemia in *Gnmt-KO* mice with a methionine deficient diet can improve hepatic steatosis and reactivate autophagy (76,86). Importantly, NAFLD patients have increased serum levels of methionine (71,86) suggesting that treatments that can lower SAME levels may be a therapeutic possibility. Our data suggests that removal of methionine groups can not only reduce SAME levels but also reactivate autophagy increasing lipid digestion and as seen in previous work reducing triglyceride synthesis (76) and DNA hypermethylation (268).

In our study published in 2016, we looked at the role of autophagy in removing excess lipids in the liver (86). However, autophagy is also used by cells to recycle other components of the cytoplasm. Among the other components from the cytoplasm that are recycled are old and damaged organelles (mitophagy and peroxiphagy) and proteins (11). These different forms of autophagy share the same basic principles and based on our results it is likely that these other forms are also inhibited possibly contributing to the accumulation of damaged mitochondria and protein aggregates which in the long run may lead to the overall damaged phenotype observed in *Gnmt-KO* mice livers. Further research is required in this area.

Gnmt-KO mice spontaneously develop fibrosis (72), one of the main cell types involved in the fibrotic response is the hepatic stellate cell. Two different groups have found that autophagy plays an important role in activating HSCs (134,135). They found that lipophagy in HSCs was able to quickly digest

the vitamin A droplets making them available for use as energy and activators. It is unclear whether *Gnmt-KO* HSCs have an impaired autophagy but if they do this mouse model shows that HSCs have a diverse and varied set of pathways for their activation. We discovered that *Gnmt-KO* natural killer cells (NK) are activated during fibrosis and their inhibition can improve liver phenotype (193). This presents an alternative mechanism by which HSCs can activate if autophagy is inhibited. Additionally, the increased levels of apoptosis could be activating Kupffer cells which might be initiating the fibrotic response. Further research is required in this area.

Fibrosis is the result of chronic liver disease (102,118) and currently has no effective therapy that can halt its progression to cirrhosis (195). Traditionally fibrosis has received little pharmaceutical attention because it can generally be cured by removing the cause of chronic liver disease [alcohol, diet, etc. (195)], however, reversion of fibrosis does not always take place and in the case of NAFLD many patients are unable to achieve their dietary and exercise goals (92). Additionally, fibrosis can lead to cirrhosis and HCC which are both high causes of mortality. An effective treatment of fibrosis would be able to reverse fibrosis and thus avoid future complications such as cirrhosis and HCC. The fibrotic response is a complex cellular reaction that involves different cell types and understanding the underlying mechanisms that are activated is key for the development of effective anti-fibrotic treatments.

Here we show that the NEDD8 pathway is dysregulated in liver fibrosis in both human and mouse fibrosis from different etiologies. NEDD8 is a covalently attached post-translational modification from the ubiquitin-like family whose main substrates are the cullin-RING ligases (301,396) which are E3 ubiquitin ligases that ubiquitinate a variety of substrates involved in a multitude of cellular processes such as cell cycle control, cell growth, DNA replication, and signal transduction. Research into the regulation of the NEDD8 cycle has been done mainly in cancer such as lung and liver cancer but also with other diseases such as Alzheimer's (308,374). In the case of liver cancer, our lab has shown that NEDDylation is deregulated and that this correlates with malignancy (282).

Here we show that NEDDylation is deregulated before cirrhosis and HCC. Fibrosis is a disease characterized by inflammation and the secretion of pro-inflammatory and pro-fibrotic cytokines. Some of these cytokines, like PDGF, lead to the proliferation of HSC and others attract and induce proliferation of Kupffer and other inflammatory cells. Additionally, hepatocytes suffer high levels of apoptosis and regeneration especially during cirrhosis where regenerative nodules are a common characteristic. This behavior may explain why the NEDD8 pathway is increased in this disease, as CRLs are involved in the cell cycle and DNA replication. An increase in the NEDD8 pathway may facilitate this increased activity in the liver to promote hepatic healing. However, since fibrosis is generally a chronic disease, the elevated NEDD8 cycle may be favoring in the long run the appearance of regenerative nodules and HCC. Additionally, NEDD8 also stabilizes oncogenic proteins such as Akt and LKB1 that can also lead to malignant transformation (282). In our models, NEDD8 and NAE1 mRNA are not elevated, however, other studies in cancer (282,308) have shown that they are elevated. These results show the differences in the regulation of NEDDylation between the different diseases. A direct comparison between fibrosis, cirrhosis, and HCC would be required to see the regulation of NEDD8 in liver disease.

NEDD8 is only able to exert its activity when conjugated to its target proteins. In this project we saw an increase in total NEDD8 levels during fibrosis both at the organ and cellular level which are both total and conjugated forms of NEDD8. When we inhibited NEDDylation (only the activity of NAE1 is affected) in both liver and cells we saw a decrease in NEDD8 levels suggesting that the increase seen previously was conjugated NEDD8. This was also seen by Western blot and when we silenced NAE1 in the different cell types where the levels of NEDD8 conjugated cullins decreased but NEDD8 mRNA did not change. There may still be a change in protein stability. NAE1 has increased protein levels despite having no changes in mRNA levels. NAE1 is ubiquitinated by TRIP12 (397), an E3-ubiquitin ligase that leads to NAE1 degradation. TRIP12 appears to recognize only the regulatory

subunit (APPBP1) when it is not bound to the catalytic subunit (UBE1C) and its activity might be reduced when NAE1 has an increased activity. Other post-translational modifications can't be ruled out and further research is required in this area.

One of the most interesting results are the different effects of the NAE1 inhibitor MLN4924 on the three main cell types involved in hepatic fibrosis. Hepatocytes are protected from apoptosis induced by bile acids and toxins, Kupffer cells are inhibited, and HSC are inactivated or enter apoptosis. This ability to have such a potent effect on such different cell types might be explained by the ubiquitous nature of NEDD8 and the vital role that the CRLs play on different activities in the cell. Nuclear factor kappa-light-chain-enhancer of activated B cells (NF- κ B) is a transcription factor involved in the transcription of pro-inflammatory genes and is known to play a role in hepatocyte apoptosis (398) and Kupffer cell activation (399). The CRL SCF^{BT₁CP}, targets the NF- κ B inhibitor I κ B α for degradation promoting the nuclear accumulation of NF- κ B and activation of its target genes. NEDDylation inhibition has already been implicated in a reduced macrophage response (382,400) through NF- κ B inactivation. The drug MLN4924 may be protecting the liver from fibrosis by two different means. Its biggest role might be in the active inhibition of hepatocyte death, Kupffer cell activation, and HSC cell death and apoptosis. On the other hand, by directly protecting hepatocytes from cell death, MLN4924 might be blocking the initiation of fibrosis. Hepatocytes are generally regarded as the main targets of hepatotropic toxins and viruses and the ones that initiate the damage response. If hepatocytes can be kept alive, then the rest of the damage response (Kupffer and hepatic stellate cells) can't be activated. To discard any possible off target drug effects, we silenced NAE1 in the different cell lines and still achieved similar results suggesting that, as expected, there were no side effects. This will be further investigated with the hepatic NAE1^{+/-} mouse that our lab is currently developing. Repeating these same experiments with these mice will allow us to see if the results obtained are specific for NAE1 inhibition and not due to drug side effects. MLN4924 is currently being tested as an anti-tumoral drug for its ability to kill tumoral cells (309); however, healthy hepatocytes

treated with MLN4924 appear to be protected and further work is required to investigate the mechanisms by which hepatocytes are protected from cell death.

TGF- β is one of the most potent fibrogenic cytokines in the liver and its expression is upregulated during hepatic injury. In HSCs, TGF- β induces the expression of ECM proteins such as collagen and here we provide evidence that NEDDylation inhibition interferes with TGF- β signaling. Both an immortal HSC cell line and BDL activated primary HSC with inhibited NEDDylation have reduced mRNA levels of profibrogenic factors such as TGF- β and Col1a1. Additionally, BDL and CCl₄ mice treated with MLN4924 have similar levels of fibrotic markers as control mice even when treatment was started after the appearance of fibrosis. This suggests a dependence of TGF- β signaling on NEDD8 for its correct transmission. Further evidence for

this idea is also found in other studies. Zuo *et al.* reported that c-Cbl, an E3 ubiquitin ligase, has E3 NEDD8 activity towards T β RII and that when NEDDylated, T β RII is targeted to clathrin coated vesicles that favor receptor stability and bring it in contact with Smads to increase signal transmission. If T β RII is not NEDDylated it is instead ubiquitinated which internalizes the receptor in caveolin-1 positive lipid raft vesicles that leads to the receptors degradation and signal termination (182). Oddly enough, our results show an increased amount of activated Smad2 when treated with MLN4924 indicating the possibility of increased TGF- β signaling. This increase in pSmad2 may be due to Smurf-2, a HECT domain, E3 ubiquitin ligase that specifically targets pSmad2 for degradation (401) and, like the closely related Smurf-1, may require NEDDylation to increase its E3 ubiquitin ligase activity (402,403). An inhibited Smurf-2 may explain why there is an accumulation of

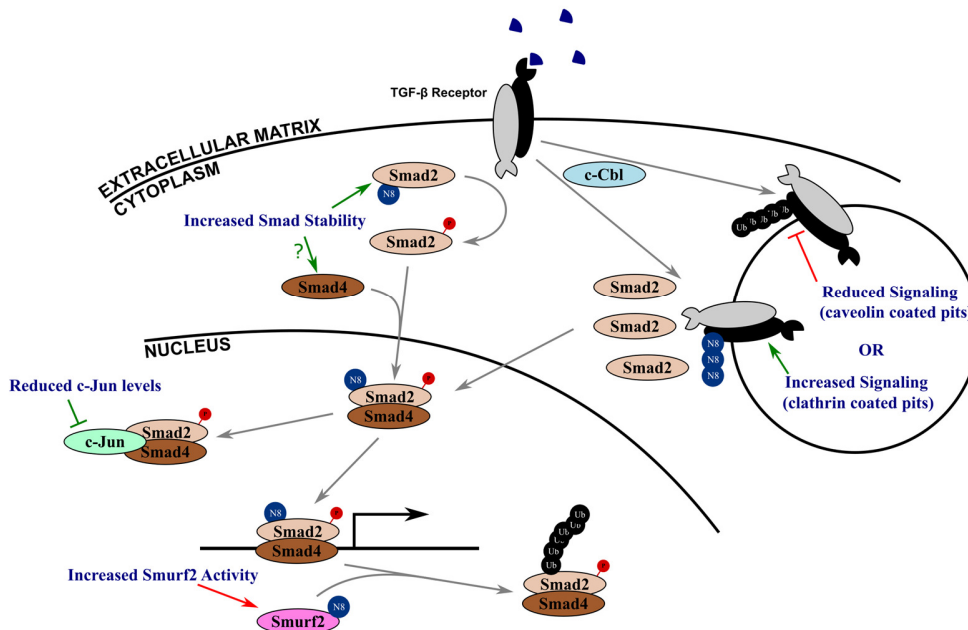


Figure 34. NEDD8 influences the TGF- β pathway at different points. Simplified diagram showing the points in the TGF- β pathway affected by NEDD8 based on the results shown here and other studies. Green arrows indicate points that favor signaling and red arrows indicate points where signaling is disrupted. N8= NEDD8 peptide, Ub= Ubiquitin peptide, P= phosphorylation

pSmad2 even though TGF- β signaling through T β RII is reduced. In here we also found that total Smad2 levels were inversely affected by NEDD8 inhibition and the evidence points to Smad2 being a possible direct NEDD8 substrate (Pulldown and NedP1 overexpression) and when NEDDylated, Smad2 appears to be more stable. More work is required to fully establish if Smad2 is really a NEDD8 substrate. Taken together with work from other groups NEDD8 appears to affect multiple parts of TGF- β signaling (**Figure.34**). Increased NEDDylation activity increases T β RII signaling by increasing its stability, NEDD8 also maintains Smad2 stability further increasing signal transmission and finally increased NEDDylation leads to increased Smurf2 activity that degrades pSmad2 and T β RII, ending signal transmission and avoiding aberrant activation. Interestingly, researchers have found that activated tyrosine kinases (EGFR, PDGFR, etc.) are degraded after being NEDDylated suggesting that NEDD8 may affect tyrosine kinase receptors in a completely different way to serine/threonine kinase receptors (404,405).

Activated myofibroblast-like HSC are extremely resistant to apoptosis and are a potential target for fibrosis therapies. Here we show that MLN4924 can lead to apoptosis of activated HSC and that this is part of the mechanism by which fibrosis is reduced. One possible mechanism by which HSC undergo increased apoptosis when treated with MLN4924 might be through c-Jun, a transcription factor that has been associated with HSC death via apoptosis (387). c-Jun is normally degraded by CRLs and an increase in its levels is seen in HSC when treated with MLN4924. Importantly, LX-2 cells have reduced caspase 3 activity when treated with MLN4924 and c-Jun is silenced. The increase in the levels of c-Jun might also be the reason that HSC have reduced mRNA levels of the profibrogenic markers TGF- β and Col1a1. c-Jun has been known to bind and inhibit the transcriptional activity of activated Smads (184,185,406). Binding of c-Jun to activated Smads leads to the recruitment of transcriptional inhibitors, additionally, c-Jun is itself a product of TGF- β signaling and its increase allows for an efficient termination of TGF- β signaling through other means such as ubiquitin mediated degradation of transcription complexes.

In summary, NEDDylation is increased in both human and mouse (both CCl₄ and BDL) fibrosis. This dysregulation leads to hepatocyte death, increases Kupffer cell activation and activates the TGF- β pathway in hepatic stellate cells. Inhibition of the NEDDylation pathway, either through MLN4924 treatment or NAE1 silencing, leads to a reduction in hepatic fibrosis by blocking the signaling cascade that leads to excessive ECM production and deposition. These results could help design new therapies that can effectively treat fibrosis and disrupt its progression to cirrhosis and HCC.

Increased NEDDylation has already been reported in different types of cancers such as lung and liver. In HCC, NEDDylation increases the stability of LKB1, a kinase increased in poor prognosis patients and linked with cell malignancy.

LKB1 is a master kinase that phosphorylates and regulates the ARKS or AMPK related kinases, the most important being AMPK (240). The role that LKB1 plays in activating AMPK and the inhibitory role this has on cell growth and replication has led to LKB1 being described as a tumor suppressor. Loss of LKB1 has been associated with different types of cancer, specifically of the lung and prostate. However, recent work has uncovered new roles for this kinase especially in the liver. Our lab has shown that LKB1 is involved in liver regeneration after partial hepatectomy (69,79). Additionally, LKB1 may have a pro-oncogenic role in some cancers such as HCC, as our lab has repeatedly shown that increased levels of LKB1, both at the protein and mRNA level, in HCC correlates with poor prognosis (268,282). Here we show further evidence for a different role for LKB1 in the liver. We have shown a negative correlation between GNMT levels and LKB1 in human HCC. Furthermore in *Gnmt-KO* mice that spontaneously develop steatosis, fibrosis, and HCC, we found an increase in LKB1 levels. For this reason we created a *Gnmt/Stk11* double knockout mouse. Liver specific deletion of LKB1 in this mouse model reduces the appearance of steatosis, fibrosis and HCC and feeding *Gnmt-KO* mice a methionine deficient diet reduces SAME and LKB1 levels suggesting that SAME plays a role in LKB1 stability. These results also point to an important role for LKB1 in liver disease other

than HCC as removal of LKB1 in *Gnmt-KO* mice improves its phenotype without altering SAME levels. Further research is required into the relationship between LKB1 and SAME. Interestingly, *Gnmt-KO* mice had nodules that contained high levels of RasGRP3 mRNA and protein and increased Ras activity, a result that was similar to what we had previously seen when overexpressing LKB1 in FVB mice and in hepatoma cells derived from *Gnmt-KO* tumors (268). Although similar, only *Gnmt-KO* mice develop HCC spontaneously whereas FVB mice overexpressing LKB1 only develop pre-neoplastic nodules that did not form cancer for the time period studied. These results suggest that LKB1 may require time to induce malignant transformation, something that is seen in Peutz-Jeghers syndrome patients. PJS patients have increased cancer incidence during their lifetime when compared to average but are not guaranteed to develop a malignancy. These results suggest that LKB1 may slowly predispose the cell and affected tissue to malignant transformation. It is interesting to note that different organs can have a different outcome with the presence or absence of LKB1. In tissues where LKB1 is considered a tumor suppressor, lack of AMPK activation leads to increased MTORC1 activity and uncontrolled cell growth and tissues, however, where LKB1 has protumoral activity, AMPK is also inactivated. Most of the LKB1 mutations lead to a truncated LKB1 (240) that is incapable of binding to STRAD α and stays in the nucleus. In our work we see increased levels of LKB1 that remain in the nucleus despite having normal levels of STRAD α . LKB1 in the nucleus (both mutant and WT) is generally regarded as an inactive form of the kinase. This is mainly seen in PJS, where mutations in LKB1 keep it in the nucleus resulting in increased MTORC1 signaling due to an inactive AMPK (228). However, recent work has shown that mutant LKB1 that remains in the nucleus can bind and activate the cyclin D1 promoter (388) suggesting that it may have more functions than previously thought. Here we show that LKB1 can also increase the expression of RasGRP3 in Huh7 cells confirming the results we had previously seen in Bcl3 cells where LKB1 was seen bound to the promoter in a CHIP assay. LKB1 overexpression in cells leads to its accumulation in the nucleus and this accumulation is lost when LKB1 is expressed in equal amounts to STRAD α . In our models

LKB1 also accumulates in the nucleus while overexpressed and under normal conditions suggesting that LKB1 does not require STRAD α to favor nuclear transcription. Interestingly, patients that suffer PMSE (Polyhydramnios, Megalencephaly, Symptomatic Epilepsy syndrome) suffer abnormal brain development, cognitive disability, and intractable epilepsy (407) due to overactive MTORC1 signaling in neurons induced by a truncated STRAD α that retains LKB1 in the nucleus. PMSE patients have a similar etiology to PJS patients (hyperactive MTORC1 due to inactive AMPK) yet suffer a completely different disease (it is unclear whether PMSE patients have intestinal polyps) (407). One difference is that PMSE patients have an intact LKB1 that due to a deficient STRAD α always stays in the nucleus possibly leading to an aberrant gene transcription that complements the activated MTORC1 in neuronal cells. In PJS patients, with a mutated LKB1, the extra gene transcription might not be so pronounced due to the different mutations disrupting LKB1 activity. A similar event may occur with the K178R mutant. The K178R mutant is not modified by SUMO2, and this modification may be necessary for complete activity of LKB1 in the nucleus. SUMO2/3 can form chains that are recognized by other proteins that contain a SUMO identification motif (SIM) (294). These SUMO2 chains on LKB1 may allow the formation of other complexes involving transcription factors that could be the ones responsible for the increased transcription seen when cells overexpress WT LKB1. In a situation where the K178R mutant could stay in the nucleus, e.g. lack of STRAD α , it should not be able to induce the formation of the transcription complexes and should still have reduced gene expression. Further research is required in this area.

LKB1 is described as a cytoplasmic kinase that requires the formation of a heterotrimeric complex with STRAD α and MO25 to exit the nucleus leading to the activation of LKB1. The formation of the heterotrimeric complex blocks the nuclear localization sequence (NLS) located on the N-terminal domain of LKB1 (242), allowing the complex to leave the nucleus and stay in the cytoplasm. A lot of research has been done into the mechanisms that take LKB1 out of the nucleus but little into the mechanisms that

keep LKB1 in the nucleus. Lan *et al.* discovered that LKB1 acetylation was able to maintain LKB1 in the nucleus (279); here we show that acetylation is a prerequisite for LKB1 SUMOylation by SUMO2 and that this keeps the protein in the nucleus by inhibiting its union with STRAD α . While we were working on the LKB1 SUMOylation project, Ritho *et al.* published that LKB1 is SUMOylated by SUMO1 and that this modification increases the binding of LKB1 to AMPK due to a SIM found on AMPK, although they found no connection with LKB1 localization (281). The increased binding also led to increased activation of AMPK. Ritho *et al.* also saw that the K178R mutant has kinase activity. Their results may also explain why we see a reduced AMPK phosphorylation (T172) even though K178R has an increased cytosolic localization and despite having kinase activity. Unfortunately, we were unable to detect SUMO1 modification of LKB1 using our system. The SUMO1 results and our SUMO2 data reflect an increased complexity in the control of LKB1 localization and activity. During starvation (when LKB1 is most needed in the cytoplasm), SIRT1 deacetylates LKB1 (279), inhibiting SUMOylation by SUMO2 and promoting SUMO1 modification further increasing cytoplasmic localization and activation of AMPK. During hypoxia, SIRT1 is inhibited, leading to increased LKB1 acetylation and further SUMO2 modification resulting in reduced AMPK activation. This would make acetylation a sort of molecular switch controlling the localization and activity of LKB1 connecting the metabolic state of the cell and the environment (starvation and hypoxia) by determining the SUMOylation status of LKB1 (**Figure.35**). Different researchers have already discovered different SUMO/acetyl switches in different proteins especially transcription factors that can regulate their activity (389,390,408). In most cases, the switches work on the same lysine that is either acetylated or SUMOylated while here we found that the acetylation of a distant lysine is able to control the SUMOylation of a different lysine. Acetylation of K48 may induce conformational changes and make the area

around lysine 178 more favorable for its modification by SUMO2, or on the other hand may make it harder for a PIAS to modify it with SUMO1. Further control can be achieved with the activity or localization of the E3 ligases and deSUMOylases, which can control the level and time a target protein is SUMOylated suggesting another possible area of LKB1 control. This may be one reason why when we over express LKB1 in hepatoma cells, we see increased nuclear LKB1 and AMPK phosphorylation (T172) is not increased when compared to control cells. The levels of the corresponding PIAS that modifies LKB1 with SUMO1 might be reduced or the corresponding SENP might be increased in hepatic hepatoma cells. Additionally, the stability of both PIAS and SENP enzymes may be altered by their own post-translational modifications (409). Both these mechanisms may contribute to further reduce AMPK activation and favor a decoupling of the LKB1-AMPK axis. The decoupling of the LKB1/AMPK axis allows the tumor cells to maintain a proliferative phenotype as activation of AMPK in hepatoma cells increases cellular apoptosis. This decoupling of the LKB1/AMPK axis is something that we and other labs have previously seen (268,273).

LKB1 can also control and regulate the AMPK related kinases resulting in an increased variety of functions. Some of the ARKs have been implicated in anti-cancer activity such as MARK which regulates cell polarity (410), a trait shared by many different tumors cells. Recent work has uncovered possible pro-oncogenic roles for some of the ARKs such as NUA1 and 2 (411). NUA1 has been related to tumor cell viability when Myc is hyper activated and c-Myc is one of the most activated signals in HCC (205,206). We did not look at the regulation of these ARKs in our project but part of the pro-oncogenic role LKB1 exerts in the liver may be due to the over activation of these kinases. It would be interesting to look at these proteins in future work and discover their contribution, if any, to hepatic carcinogenesis.

In conclusion, we discovered that the dysregulation of post-translational modifications are found in all stages of chronic liver disease. The dysregulation of the post-translational modifications opens up new possible targets for therapy and highlights the importance of these modifications in

cellular health and growth. In NAFLD derived from low GNMT activity, high methylation of PP2A inhibits autophagy and promotes liver steatosis. In fibrosis we saw an increase in NEDDylation which stimulates hepatocyte death, Kupffer cell cytokine release and HSC activation. Importantly, this increase preceded the increase in NEDDylation that we had previously seen in HCC (282) and is also a potential therapeutic target not only for reducing fibrosis but also for preventing HCC in fibrotic patients. Finally, post-translational modifications of specific proteins can also increase disease progression such as SUMOylation of LKB1, a protein related to HCC. Retention of LKB1 in the nucleus helps the cell survive metabolic stress and promotes cell growth.

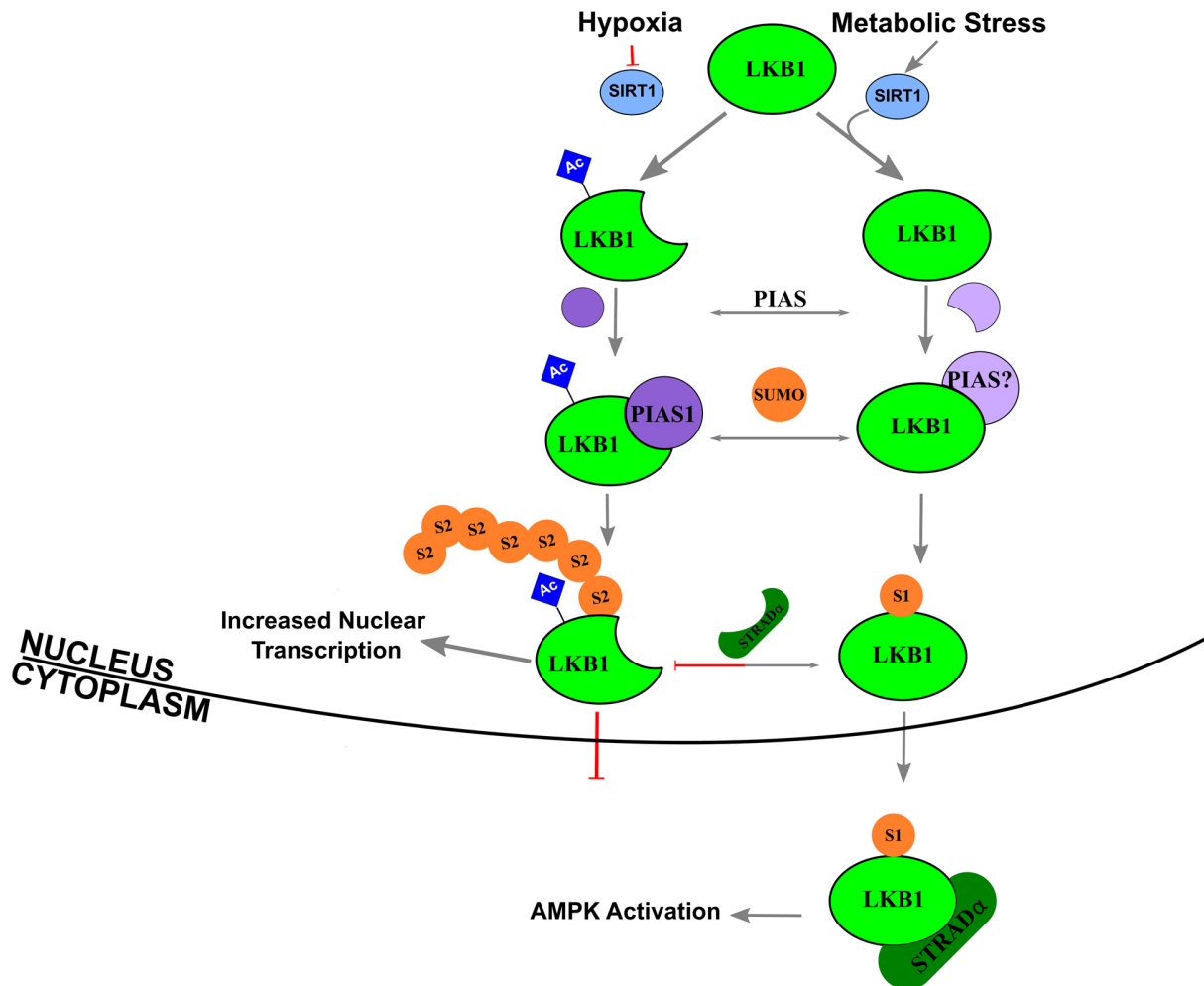


Figure 35. A SUMO/acetyl switch might control LKB1 localization. Deacetylation by SIRT1 may decide which SUMO modifies LKB1 and the resulting localization of LKB1. LKB1 acetylation may facilitate the binding of PIAS1 over another PIAS resulting in modification with SUMO2 and the inhibition of the heterotrimeric LKB1/STRADα/MO25 complex retaining LKB1 in the nucleus. Increased nuclear LKB1 may be able to increase transcription of certain genes like RasGRP3. Ac= Acetylation, S1= SUMO1, S2= SUMO2.

Conclusions



Post-translational Modifications in Liver Disease
Imanol Zubieta Franco

8. Conclusions

8.1 Methionine and S-Adenosylmethionine levels are critical regulators of PP2A activity modulating lipophagy during steatosis

- Acute treatment of hepatocytes with high levels of S-Adenosylmethionine and methionine inhibits autophagy by reducing autophagosome formation.
- Chronic high levels of S-Adenosylmethionine and methionine inhibit autophagic flux by decreased lysosomal enzyme activity.
- S-Adenosylmethionine and methionine can inhibit autophagy by increased methylation of PP2A.
- Methylated PP2A can interact directly with MTOR dephosphorylating and inactivating it.
- S-Adenosylmethionine and methionine inhibit autophagy through MTOR independent pathways.

8.2 Deregulated NEDDylation in liver fibrosis

- The NEDDylation pathway is altered in fibrotic human and mice livers regardless of etiology.
- NEDDylation is increased in the three principle cell types involved in the fibrotic response: hepatocytes, Kupffer cells, and hepatic stellate cells.
- NEDDylation inhibition reduces fibrosis by:
 - Protecting hepatocytes from apoptosis.
 - Reducing Kupffer cell activation.
 - Reducing hepatic stellate cell activation and inducing apoptosis of already activated hepatic stellate cells.
- NEDDylation inhibition reduces TGF- β signaling in hepatic stellate cells by decreasing Smad2 stability and increasing the levels of c-Jun.
- c-Jun accumulation induces activated hepatic stellate cell death via apoptosis.

8.3 SUMO2 retains LKB1 in the nucleus and increases hepatoma cell survival

- LKB1 loss can improve liver phenotype and reduce the appearance of fibrosis and tumors in *Gnmt-KO* mice.
- LKB1 in hepatoma cells and liver tumors is located mainly in the nucleus despite normal STRAD α levels.
- LKB1 contains a SUMO consensus motif and is modified by SUMO2 at lysine 178 and requires previous acetylation of lysine 48.
- SUMOylation is increased in liver tumors in hypoxic conditions and reduced during starvation.
- SUMOylation retains LKB1 in the nucleus by preventing its association with STRAD α .
- WT LKB1 protects hepatoma cells during hypoxia and increases cell proliferation and energy usage when conditions are favorable again.

Post-translational Modifications in Liver Disease
Imanol Zubieta Franco

Bibliography

Post-translational Modifications in Liver Disease
Imanol Zubieta Franco

9. Bibliography

1. Mishra A, Younossi ZM. Epidemiology and Natural History of Non-alcoholic Fatty Liver Disease. *J. Clin. Exp. Hepatol.* 2012;2:135–144.
2. Vernon G, Baranova A, Younossi ZM. Systematic review: the epidemiology and natural history of non-alcoholic fatty liver disease and non-alcoholic steatohepatitis in adults. *Aliment. Pharmacol. Ther.* 2011;34:274–285.
3. Calzadilla Bertot L, Adams LA. The Natural Course of Non-Alcoholic Fatty Liver Disease. *Int. J. Mol. Sci.* 2016;17.
4. Poordad FF. Nonalcoholic fatty liver disease: a review. *Expert Opin. Emerg. Drugs.* 2005;10:661–670.
5. Sanyal AJ. Mechanisms of Disease: pathogenesis of nonalcoholic fatty liver disease. *Nat. Clin. Pract. Gastroenterol. Hepatol.* 2005;2:46–53.
6. Adams LA, Angulo P, Lindor KD. Nonalcoholic fatty liver disease. *CMAJ Can. Med. Assoc. J. J. Assoc. Medicales Can.* 2005;172:899–905.
7. Varela-Rey M, Embade N, Ariz U, Lu SC, Mato JM, Martínez-Chantar ML. Non-alcoholic steatohepatitis and animal models: understanding the human disease. *Int. J. Biochem. Cell Biol.* 2009;41:969–976.
8. Martin S, Parton RG. Lipid droplets: a unified view of a dynamic organelle. *Nat. Rev. Mol. Cell Biol.* 2006;7:373–378.
9. Zechner R, Madeo F. Cell biology: Another way to get rid of fat. *Nature.* 2009;458:1118–1119.
10. Singh R, Kaushik S, Wang Y, Xiang Y, Novak I, Komatsu M, et al. Autophagy regulates lipid metabolism. *Nature.* 2009;458:1131–1135.
11. Martinez-Lopez N, Singh R. Autophagy and Lipid Droplets in the Liver. *Annu. Rev. Nutr.* 2015;35:215–237.
12. Lavallard VJ, Gual P. Autophagy and non-alcoholic fatty liver disease. *BioMed Res. Int.* 2014;2014:120179.
13. Lin L, Baehrecke EH. Autophagy, cell death, and cancer. *Mol. Cell. Oncol.* 2015;2:e985913.
14. Sahu R, Kaushik S, Clement CC, Cannizzo ES, Scharf B, Follenzi A, et al. Microautophagy of cytosolic proteins by late endosomes. *Dev. Cell.* 2011;20:131–139.
15. Cuervo AM, Wong E. Chaperone-mediated autophagy: roles in disease and aging. *Cell Res.* 2014;24:92–104.
16. He C, Klionsky DJ. Regulation mechanisms and signaling pathways of autophagy. *Annu. Rev. Genet.* 2009;43:67–93.
17. Kwanten WJ, Martinet W, Michielsen PP, Francque SM. Role of autophagy in the pathophysiology of nonalcoholic fatty liver disease: a controversial issue. *World J. Gastroenterol.* 2014;20:7325–7338.
18. Gomez-Sanchez JA, Carty L, Iruarrizaga-Lejarreta M, Palomo-Irigoyen M, Varela-Rey M, Griffith M, et al. Schwann cell autophagy, myelinophagy, initiates myelin clearance from injured nerves. *J. Cell Biol.* 2015;210:153–168.
19. Nakatogawa H, Suzuki K, Kamada Y, Ohsumi Y. Dynamics and diversity in autophagy mechanisms: lessons from yeast. *Nat. Rev. Mol. Cell Biol.* 2009;10:458–467.

Post-translational Modifications in Liver Disease

Imanol Zubiete Franco

20. Chan EYW, Longatti A, McKnight NC, Tooze SA. Kinase-inactivated ULK proteins inhibit autophagy via their conserved C-terminal domains using an Atg13-independent mechanism. *Mol. Cell. Biol.* 2009;29:157–171.
21. Liang XH, Jackson S, Seaman M, Brown K, Kempkes B, Hibshoosh H, et al. Induction of autophagy and inhibition of tumorigenesis by beclin 1. *Nature.* 1999;402:672–676.
22. Proikas-Cezanne T, Takacs Z, Dönnies P, Kohlbacher O. WIPI proteins: essential PtdIns3P effectors at the nascent autophagosome. *J. Cell Sci.* 2015;128:207–217.
23. Webber JL, Young ARJ, Tooze SA. Atg9 trafficking in Mammalian cells. *Autophagy.* 2007;3:54–56.
24. Mari M, Tooze SA, Reggiori F. The puzzling origin of the autophagosomal membrane. *F1000 Biol. Rep.* 2011;3:25.
25. Hanada T, Noda NN, Satomi Y, Ichimura Y, Fujioka Y, Takao T, et al. The Atg12-Atg5 conjugate has a novel E3-like activity for protein lipidation in autophagy. *J. Biol. Chem.* 2007;282:37298–37302.
26. Mizushima N, Yoshimori T. How to interpret LC3 immunoblotting. *Autophagy.* 2007;3:542–545.
27. Klionsky DJ, Abdelmohsen K, Abe A, Abedin MJ, Abeliovich H, Acevedo Arozena A, et al. Guidelines for the use and interpretation of assays for monitoring autophagy (3rd edition). *Autophagy.* 2016;12:1–222.
28. Kim J, Kundu M, Viollet B, Guan K-L. AMPK and mTOR regulate autophagy through direct phosphorylation of Ulk1. *Nat. Cell Biol.* 2011;13:132–141.
29. Settembre C, Di Malta C, Polito VA, Garcia Arencibia M, Vetrini F, Erdin S, et al. TFEB links autophagy to lysosomal biogenesis. *Science.* 2011;332:1429–1433.
30. Alexaki A, Gupta SD, Majumder S, Kono M, Tuymetova G, Harmon JM, et al. Autophagy regulates sphingolipid levels in the liver. *J. Lipid Res.* 2014;55:2521–2531.
31. Wang Y, Singh R, Xiang Y, Czaja MJ. Macroautophagy and chaperone-mediated autophagy are required for hepatocyte resistance to oxidant stress. *Hepatology.* 2010;52:266–277.
32. Amir M, Zhao E, Fontana L, Rosenberg H, Tanaka K, Gao G, et al. Inhibition of hepatocyte autophagy increases tumor necrosis factor-dependent liver injury by promoting caspase-8 activation. *Cell Death Differ.* 2013;20:878–887.
33. Stankov MV, Panayotova-Dimitrova D, Leverkus M, Vondran FWR, Bauerfeind R, Binz A, et al. Autophagy inhibition due to thymidine analogues as novel mechanism leading to hepatocyte dysfunction and lipid accumulation. *AIDS Lond. Engl.* 2012;26:1995–2006.
34. Lin C-W, Zhang H, Li M, Xiong X, Chen X, Chen X, et al. Pharmacological promotion of autophagy alleviates steatosis and injury in alcoholic and non-alcoholic fatty liver conditions in mice. *J. Hepatol.* 2013;58:993–999.
35. Koga H, Kaushik S, Cuervo AM. Altered lipid content inhibits autophagic vesicular fusion. *FASEB J. Off. Publ. Fed. Am. Soc. Exp. Biol.* 2010;24:3052–3065.
36. Kashima J, Shintani-Ishida K, Nakajima M, Maeda H, Unuma K, Uchiyama Y, et al. Immunohistochemical study of the autophagy marker microtubule-associated protein 1 light chain 3 in normal and steatotic human livers. *Hepatology. Res. Off. J. Jpn. Soc. Hepatol.* 2014;44:779–787.
37. Kinsell LW, Harper HA, Barton HC, Michaels GD, Weiss HA. Rate of Disappearance From Plasma of Intravenously Administered Methionine in Patients With Liver Damage. *Science.* 1947;106:589–590.
38. McClain CJ, Hill DB, Song Z, Chawla R, Watson WH, Chen T, et al. S-Adenosylmethionine, cytokines, and alcoholic liver disease. *Alcohol Fayettev. N.* 2002;27:185–192.

39. Best CH, Hershey JM, Huntsman ME. The effect of lecithine on fat deposition in the liver of the normal rat. *J. Physiol.* 1932;75:56–66.
40. Mato JM, Corrales FJ, Lu SC, Avila MA. S-Adenosylmethionine: a control switch that regulates liver function. *FASEB J. Off. Publ. Fed. Am. Soc. Exp. Biol.* 2002;16:15–26.
41. Finkelstein JD. Methionine metabolism in mammals. *J. Nutr. Biochem.* 1990;1:228–237.
42. Lin S, Shi Q, Nix FB, Styblo M, Beck MA, Herbin-Davis KM, et al. A novel S-adenosyl-L-methionine:arsenic(III) methyltransferase from rat liver cytosol. *J. Biol. Chem.* 2002;277:10795–10803.
43. Lu SC. S-Adenosylmethionine. *Int. J. Biochem. Cell Biol.* 2000;32:391–395.
44. Mato JM, Alvarez L, Ortiz P, Pajares MA. S-adenosylmethionine synthesis: molecular mechanisms and clinical implications. *Pharmacol. Ther.* 1997;73:265–280.
45. Finkelstein JD. Metabolic regulatory properties of S-adenosylmethionine and S-adenosylhomocysteine. *Clin. Chem. Lab. Med.* 2007;45:1694–1699.
46. Petrossian TC, Clarke SG. Uncovering the human methyltransferasome. *Mol. Cell. Proteomics MCP.* 2011;10:M110.000976.
47. Lu SC. Regulation of glutathione synthesis. *Mol. Aspects Med.* 2009;30:42–59.
48. Pegg AE, Williams-Ashman HG. Phosphate-stimulated breakdown of 5'-methylthioadenosine by rat ventral prostate. *Biochem. J.* 1969;115:241–247.
49. Dante R, Arnaud M, Niveleau A. Effects of 5'-deoxy-5'-methylthioadenosine on the metabolism of S-adenosyl methionine. *Biochem. Biophys. Res. Commun.* 1983;114:214–221.
50. Kujubu DA, Stimmel JB, Law RE, Herschman HR, Clarke S. Early responses of PC-12 cells to NGF and EGF: effect of K252a and 5'-methylthioadenosine on gene expression and membrane protein methylation. *J. Neurosci. Res.* 1993;36:58–65.
51. Della Ragione F, Pegg AE. Effect of analogues of 5'-methylthioadenosine on cellular metabolism. Inactivation of S-adenosylhomocysteine hydrolase by 5'-isobutylthioadenosine. *Biochem. J.* 1983;210:429–435.
52. Prudova A, Bauman Z, Braun A, Vitvitsky V, Lu SC, Banerjee R. S-adenosylmethionine stabilizes cystathionine beta-synthase and modulates redox capacity. *Proc. Natl. Acad. Sci. U. S. A.* 2006;103:6489–6494.
53. Mudd SH, Brosnan JT, Brosnan ME, Jacobs RL, Stabler SP, Allen RH, et al. Methyl balance and transmethylation fluxes in humans. *Am. J. Clin. Nutr.* 2007;85:19–25.
54. Graham DE, Bock CL, Schalk-Hihi C, Lu ZJ, Markham GD. Identification of a highly diverged class of S-adenosylmethionine synthetases in the archaea. *J. Biol. Chem.* 2000;275:4055–4059.
55. Glass JI, Assad-Garcia N, Alperovich N, Yooseph S, Lewis MR, Maruf M, et al. Essential genes of a minimal bacterium. *Proc. Natl. Acad. Sci. U. S. A.* 2006;103:425–430.
56. Kotb M, Mudd SH, Mato JM, Geller AM, Kredich NM, Chou JY, et al. Consensus nomenclature for the mammalian methionine adenosyltransferase genes and gene products. *Trends Genet. TIG.* 1997;13:51–52.
57. Halim AB, LeGros L, Geller A, Kotb M. Expression and functional interaction of the catalytic and regulatory subunits of human methionine adenosyltransferase in mammalian cells. *J. Biol. Chem.* 1999;274:29720–29725.

Post-translational Modifications in Liver Disease

Imanol Zubiete Franco

58. Horikawa S, Ozasa H, Ota K, Tsukada K. Immunohistochemical analysis of rat S-adenosylmethionine synthetase isozymes in developmental liver. *FEBS Lett.* 1993;330:307–311.
59. Lu SC, Mato JM. S-Adenosylmethionine in cell growth, apoptosis and liver cancer. *J. Gastroenterol. Hepatol.* 2008;23 Suppl 1:S73-77.
60. Sullivan DM, Hoffman JL. Fractionation and kinetic properties of rat liver and kidney methionine adenosyltransferase isozymes. *Biochemistry (Mosc.)*. 1983;22:1636–1641.
61. Martinov MV, Vitvitsky VM, Banerjee R, Ataullakhanov FI. The logic of the hepatic methionine metabolic cycle. *Biochim. Biophys. Acta.* 2010;1804:89–96.
62. Luka Z, Mudd SH, Wagner C. Glycine N-methyltransferase and regulation of S-adenosylmethionine levels. *J. Biol. Chem.* 2009;284:22507–22511.
63. Varela-Rey M, Iruarrizaga-Lejarreta M, Lozano JJ, Aransay AM, Fernandez AF, Lavin JL, et al. S-adenosylmethionine levels regulate the schwann cell DNA methylome. *Neuron.* 2014;81:1024–1039.
64. Mudd SH. Hypermethioninemias of genetic and non-genetic origin: A review. *Am. J. Med. Genet. C Semin. Med. Genet.* 2011;157C:3–32.
65. Lu SC, Alvarez L, Huang ZZ, Chen L, An W, Corrales FJ, et al. Methionine adenosyltransferase 1A knockout mice are predisposed to liver injury and exhibit increased expression of genes involved in proliferation. *Proc. Natl. Acad. Sci. U. S. A.* 2001;98:5560–5565.
66. Cano A, Buqué X, Martínez-Uña M, Aurekoetxea I, Menor A, García-Rodríguez JL, et al. Methionine adenosyltransferase 1A gene deletion disrupts hepatic very low-density lipoprotein assembly in mice. *Hepatology. Baltim. Md.* 2011;54:1975–1986.
67. Martínez-Chantar ML, Corrales FJ, Martínez-Cruz LA, García-Trevijano ER, Huang Z-Z, Chen L, et al. Spontaneous oxidative stress and liver tumors in mice lacking methionine adenosyltransferase 1A. *FASEB J. Off. Publ. Fed. Am. Soc. Exp. Biol.* 2002;16:1292–1294.
68. Chen L, Zeng Y, Yang H, Lee TD, French SW, Corrales FJ, et al. Impaired liver regeneration in mice lacking methionine adenosyltransferase 1A. *FASEB J. Off. Publ. Fed. Am. Soc. Exp. Biol.* 2004;18:914–916.
69. Vázquez-Chantada M, Ariz U, Varela-Rey M, Embade N, Martínez-Lopez N, Fernández-Ramos D, et al. Evidence for LKB1/AMP-activated protein kinase/ endothelial nitric oxide synthase cascade regulated by hepatocyte growth factor, S-adenosylmethionine, and nitric oxide in hepatocyte proliferation. *Hepatology. Baltim. Md.* 2009;49:608–617.
70. Kalhan SC, Edmison J, Marczewski S, Dasarathy S, Gruca LL, Bennett C, et al. Methionine and protein metabolism in non-alcoholic steatohepatitis: evidence for lower rate of transmethylation of methionine. *Clin. Sci. Lond. Engl.* 1979. 2011;121:179–189.
71. Murphy SK, Yang H, Moylan CA, Pang H, Dellinger A, Abdelmalek MF, et al. Relationship between methylome and transcriptome in patients with nonalcoholic fatty liver disease. *Gastroenterology.* 2013;145:1076–1087.
72. Luka Z, Capdevila A, Mato JM, Wagner C. A glycine N-methyltransferase knockout mouse model for humans with deficiency of this enzyme. *Transgenic Res.* 2006;15:393–397.
73. Martínez-Chantar ML, Vázquez-Chantada M, Ariz U, Martínez N, Varela M, Luka Z, et al. Loss of the glycine N-methyltransferase gene leads to steatosis and hepatocellular carcinoma in mice. *Hepatology. Baltim. Md.* 2008;47:1191–1199.
74. Liu S-P, Li Y-S, Chen Y-J, Chiang E-P, Li AF-Y, Lee Y-H, et al. Glycine N-methyltransferase^{-/-} mice develop chronic hepatitis and glycogen storage disease in the liver. *Hepatology. Baltim. Md.* 2007;46:1413–1425.

75. Lu SC, Mato JM. S-adenosylmethionine in liver health, injury, and cancer. *Physiol. Rev.* 2012;92:1515–1542.
76. Martínez-Uña M, Varela-Rey M, Cano A, Fernández-Ares L, Beraza N, Aurrekoetxea I, et al. Excess S-adenosylmethionine reroutes phosphatidylethanolamine towards phosphatidylcholine and triglyceride synthesis. *Hepatology*. 2013;58:1296–1305.
77. Martínez-Uña M, Varela-Rey M, Mestre D, Fernández-Ares L, Fresnedo O, Fernandez-Ramos D, et al. S-Adenosylmethionine increases circulating very-low density lipoprotein clearance in non-alcoholic fatty liver disease. *J. Hepatol.* 2015;62:673–681.
78. Calvisi DF, Ladu S, Gorden A, Farina M, Conner EA, Lee J-S, et al. Ubiquitous activation of Ras and Jak/Stat pathways in human HCC. *Gastroenterology*. 2006;130:1117–1128.
79. Varela-Rey M, Fernández-Ramos D, Martínez-López N, Embade N, Gómez-Santos L, Beraza N, et al. Impaired liver regeneration in mice lacking glycine N-methyltransferase. *Hepatology*. 2009;50:443–452.
80. Chen YM, Shiu JY, Tzeng SJ, Shih LS, Chen YJ, Lui WY, et al. Characterization of glycine-N-methyltransferase-gene expression in human hepatocellular carcinoma. *Int. J. Cancer*. 1998;75:787–793.
81. Tseng T-L, Shih Y-P, Huang Y-C, Wang C-K, Chen P-H, Chang J-G, et al. Genotypic and phenotypic characterization of a putative tumor susceptibility gene, GNMT, in liver cancer. *Cancer Res.* 2003;63:647–654.
82. Avila MA, Berasain C, Torres L, Martín-Duce A, Corrales FJ, Yang H, et al. Reduced mRNA abundance of the main enzymes involved in methionine metabolism in human liver cirrhosis and hepatocellular carcinoma. *J. Hepatol.* 2000;33:907–914.
83. Mudd SH, Cerone R, Schiaffino MC, Fantasia AR, Minniti G, Caruso U, et al. Glycine N-methyltransferase deficiency: a novel inborn error causing persistent isolated hypermethioninaemia. *J. Inher. Metab. Dis.* 2001;24:448–464.
84. Augoustides-Savvopoulou P, Luka Z, Karyda S, Stabler SP, Allen RH, Patsiaoura K, et al. Glycine N-methyltransferase deficiency: a new patient with a novel mutation. *J. Inher. Metab. Dis.* 2003;26:745–759.
85. Varela-Rey M, Martínez-López N, Fernández-Ramos D, Embade N, Calvisi DF, Woodhoo A, et al. Fatty liver and fibrosis in glycine N-methyltransferase knockout mice is prevented by nicotinamide. *Hepatology*. 2010;52:105–114.
86. Zubiete-Franco I, García-Rodríguez JL, Martínez-Uña M, Martínez-Lopez N, Woodhoo A, Gutiérrez-De Juan V, et al. Methionine and S-Adenosylmethionine levels are critical regulators of PP2A activity modulating lipophagy during steatosis. *J. Hepatol.* 2015;
87. Knowler WC, Barrett-Connor E, Fowler SE, Hamman RF, Lachin JM, Walker EA, et al. Reduction in the incidence of type 2 diabetes with lifestyle intervention or metformin. *N. Engl. J. Med.* 2002;346:393–403.
88. Palmer M, Schaffner F. Effect of weight reduction on hepatic abnormalities in overweight patients. *Gastroenterology*. 1990;99:1408–1413.
89. Powell EE, Cooksley WG, Hanson R, Searle J, Halliday JW, Powell LW. The natural history of nonalcoholic steatohepatitis: a follow-up study of forty-two patients for up to 21 years. *Hepatology*. 1990;11:74–80.
90. Ueno T, Sugawara H, Sujaku K, Hashimoto O, Tsuji R, Tamaki S, et al. Therapeutic effects of restricted diet and exercise in obese patients with fatty liver. *J. Hepatol.* 1997;27:103–107.

Post-translational Modifications in Liver Disease

Imanol Zubiete Franco

91. Huang MA, Greenson JK, Chao C, Anderson L, Peterman D, Jacobson J, et al. One-year intense nutritional counseling results in histological improvement in patients with non-alcoholic steatohepatitis: a pilot study. *Am. J. Gastroenterol.* 2005;100:1072–1081.
92. Bellentani S, Dalle Grave R, Suppini A, Marchesini G, Fatty Liver Italian Network. Behavior therapy for nonalcoholic fatty liver disease: The need for a multidisciplinary approach. *Hepatol. Baltim. Md.* 2008;47:746–754.
93. Ratziu V, Goodman Z, Sanyal A. Current efforts and trends in the treatment of NASH. *J. Hepatol.* 2015;62:S65-75.
94. Sanyal AJ, Chalasani N, Kowdley KV, McCullough A, Diehl AM, Bass NM, et al. Pioglitazone, vitamin E, or placebo for nonalcoholic steatohepatitis. *N. Engl. J. Med.* 2010;362:1675–1685.
95. Lutchman G, Modi A, Kleiner DE, Promrat K, Heller T, Ghany M, et al. The effects of discontinuing pioglitazone in patients with nonalcoholic steatohepatitis. *Hepatol. Baltim. Md.* 2007;46:424–429.
96. Kirpichnikov D, McFarlane SI, Sowers JR. Metformin: an update. *Ann. Intern. Med.* 2002;137:25–33.
97. Nouredin M, Mato JM, Lu SC. Nonalcoholic fatty liver disease: update on pathogenesis, diagnosis, treatment and the role of S-adenosylmethionine. *Exp. Biol. Med.* Maywood NJ. 2015;240:809–820.
98. Bugianesi E, Gentilecore E, Manini R, Natale S, Vanni E, Villanova N, et al. A randomized controlled trial of metformin versus vitamin E or prescriptive diet in nonalcoholic fatty liver disease. *Am. J. Gastroenterol.* 2005;100:1082–1090.
99. Hoofnagle JH, Van Natta ML, Kleiner DE, Clark JM, Kowdley KV, Loomba R, et al. Vitamin E and changes in serum alanine aminotransferase levels in patients with non-alcoholic steatohepatitis. *Aliment. Pharmacol. Ther.* 2013;38:134–143.
100. Ekstedt M, Franzén LE, Mathiesen UL, Thorelius L, Holmqvist M, Bodemar G, et al. Long-term follow-up of patients with NAFLD and elevated liver enzymes. *Hepatol. Baltim. Md.* 2006;44:865–873.
101. Farrell GC, Larter CZ. Nonalcoholic fatty liver disease: from steatosis to cirrhosis. *Hepatol. Baltim. Md.* 2006;43:S99–S112.
102. Friedman SL. Liver fibrosis -- from bench to bedside. *J. Hepatol.* 2003;38 Suppl 1:S38-53.
103. Albanis E, Friedman SL. Hepatic fibrosis. Pathogenesis and principles of therapy. *Clin. Liver Dis.* 2001;5:315–334, v–vi.
104. Friedman SL. Mechanisms of hepatic fibrogenesis. *Gastroenterology.* 2008;134:1655–1669.
105. Schuppan D, Afdhal NH. Liver cirrhosis. *Lancet.* 2008;371:838–851.
106. Fernández M, Semela D, Bruix J, Colle I, Pinzani M, Bosch J. Angiogenesis in liver disease. *J. Hepatol.* 2009;50:604–620.
107. Kandiah PA, Kumar G. Hepatic Encephalopathy-the Old and the New. *Crit. Care Clin.* 2016;32:311–329.
108. Ginés P, Quintero E, Arroyo V, Terés J, Bruguera M, Rimola A, et al. Compensated cirrhosis: natural history and prognostic factors. *Hepatol. Baltim. Md.* 1987;7:122–128.
109. D’Amico G, Garcia-Tsao G, Pagliaro L. Natural history and prognostic indicators of survival in cirrhosis: a systematic review of 118 studies. *J. Hepatol.* 2006;44:217–231.
110. Afdhal NH, Nunes D. Evaluation of liver fibrosis: a concise review. *Am. J. Gastroenterol.* 2004;99:1160–1174.

111. Thampanitchawong P, Piratvisuth T. Liver biopsy: complications and risk factors. *World J. Gastroenterol.* 1999;5:301–304.
112. Regev A, Berho M, Jeffers LJ, Milikowski C, Molina EG, Pyrsopoulos NT, et al. Sampling error and intraobserver variation in liver biopsy in patients with chronic HCV infection. *Am. J. Gastroenterol.* 2002;97:2614–2618.
113. Hirata M, Akbar SM, Horiike N, Onji M. Noninvasive diagnosis of the degree of hepatic fibrosis using ultrasonography in patients with chronic liver disease due to hepatitis C virus. *Eur. J. Clin. Invest.* 2001;31:528–535.
114. Ziol M, Handra-Luca A, Kettaneh A, Christidis C, Mal F, Kazemi F, et al. Noninvasive assessment of liver fibrosis by measurement of stiffness in patients with chronic hepatitis C. *Hepatol. Baltim. Md.* 2005;41:48–54.
115. Castéra L, Vergniol J, Foucher J, Le Bail B, Chanteloup E, Haaser M, et al. Prospective comparison of transient elastography, Fibrotest, APRI, and liver biopsy for the assessment of fibrosis in chronic hepatitis C. *Gastroenterology.* 2005;128:343–350.
116. Canbay A, Friedman S, Gores GJ. Apoptosis: the nexus of liver injury and fibrosis. *Hepatol. Baltim. Md.* 2004;39:273–278.
117. Higuchi H, Gores GJ. Mechanisms of liver injury: an overview. *Curr. Mol. Med.* 2003;3:483–490.
118. Bataller R, Brenner DA. Liver fibrosis. *J. Clin. Invest.* 2005;115:209–218.
119. Blomhoff R, Green MH, Berg T, Norum KR. Transport and storage of vitamin A. *Science.* 1990;250:399–404.
120. Friedman SL, Roll FJ, Boyles J, Bissell DM. Hepatic lipocytes: the principal collagen-producing cells of normal rat liver. *Proc. Natl. Acad. Sci. U. S. A.* 1985;82:8681–8685.
121. Geerts A. History, heterogeneity, developmental biology, and functions of quiescent hepatic stellate cells. *Semin. Liver Dis.* 2001;21:311–335.
122. Wake K. Structure of the sinusoidal wall in the liver. In: *Cells of the Hepatic Sinusoid. The Kupffer Cell Foundation*; 1995. p. 241–246.
123. Bachem MG, Melchior R, Gressner AM. The role of thrombocytes in liver fibrogenesis: effects of platelet lysate and thrombocyte-derived growth factors on the mitogenic activity and glycosaminoglycan synthesis of cultured rat liver fat storing cells. *J. Clin. Chem. Clin. Biochem. Z. Klin. Chem. Klin. Biochem.* 1989;27:555–565.
124. Fadok VA, de Cathelineau A, Daleke DL, Henson PM, Bratton DL. Loss of phospholipid asymmetry and surface exposure of phosphatidylserine is required for phagocytosis of apoptotic cells by macrophages and fibroblasts. *J. Biol. Chem.* 2001;276:1071–1077.
125. Canbay A, Taimr P, Torok N, Higuchi H, Friedman S, Gores GJ. Apoptotic body engulfment by a human stellate cell line is profibrogenic. *Lab. Investig. J. Tech. Methods Pathol.* 2003;83:655–663.
126. Viglianti GA, Lau CM, Hanley TM, Miko BA, Shlomchik MJ, Marshak-Rothstein A. Activation of autoreactive B cells by CpG dsDNA. *Immunity.* 2003;19:837–847.
127. Friedman SL, Wei S, Blaner WS. Retinol release by activated rat hepatic lipocytes: regulation by Kupffer cell-conditioned medium and PDGF. *Am. J. Physiol.* 1993;264:G947-952.
128. Davis BH, Kramer RT, Davidson NO. Retinoic acid modulates rat Ito cell proliferation, collagen, and transforming growth factor beta production. *J. Clin. Invest.* 1990;86:2062–2070.

Post-translational Modifications in Liver Disease

Imanol Zubiete Franco

129. Okuno M, Sato T, Kitamoto T, Imai S, Kawada N, Suzuki Y, et al. Increased 9,13-di-cis-retinoic acid in rat hepatic fibrosis: implication for a potential link between retinoid loss and TGF-beta mediated fibrogenesis in vivo. *J. Hepatol.* 1999;30:1073–1080.
130. Vogel S, Piantedosi R, Frank J, Lalazar A, Rockey DC, Friedman SL, et al. An immortalized rat liver stellate cell line (HSC-T6): a new cell model for the study of retinoid metabolism in vitro. *J. Lipid Res.* 2000;41:882–893.
131. Friedman SL. Hepatic stellate cells: protean, multifunctional, and enigmatic cells of the liver. *Physiol. Rev.* 2008;88:125–172.
132. Miyahara T, Schrum L, Rippe R, Xiong S, Yee HF, Motomura K, et al. Peroxisome proliferator-activated receptors and hepatic stellate cell activation. *J. Biol. Chem.* 2000;275:35715–35722.
133. Kawaguchi K, Sakaida I, Tsuchiya M, Omori K, Takami T, Okita K. Pioglitazone prevents hepatic steatosis, fibrosis, and enzyme-altered lesions in rat liver cirrhosis induced by a choline-deficient L-amino acid-defined diet. *Biochem. Biophys. Res. Commun.* 2004;315:187–195.
134. Thoen LFR, Guimarães ELM, Dollé L, Mannaerts I, Najimi M, Sokal E, et al. A role for autophagy during hepatic stellate cell activation. *J. Hepatol.* 2011;55:1353–1360.
135. Hernández-Gea V, Ghiassi-Nejad Z, Rozenfeld R, Gordon R, Fiel MI, Yue Z, et al. Autophagy releases lipid that promotes fibrogenesis by activated hepatic stellate cells in mice and in human tissues. *Gastroenterology.* 2012;142:938–946.
136. Iredale JP. Hepatic stellate cell behavior during resolution of liver injury. *Semin. Liver Dis.* 2001;21:427–436.
137. Han Y-P. Matrix metalloproteinases, the pros and cons, in liver fibrosis. *J. Gastroenterol. Hepatol.* 2006;21 Suppl 3:S88-91.
138. Milani S, Herbst H, Schuppan D, Grappone C, Pellegrini G, Pinzani M, et al. Differential expression of matrix-metalloproteinase-1 and -2 genes in normal and fibrotic human liver. *Am. J. Pathol.* 1994;144:528–537.
139. Han Y-P, Yan C, Zhou L, Qin L, Tsukamoto H. A matrix metalloproteinase-9 activation cascade by hepatic stellate cells in trans-differentiation in the three-dimensional extracellular matrix. *J. Biol. Chem.* 2007;282:12928–12939.
140. Murphy FR, Issa R, Zhou X, Ratnarajah S, Nagase H, Arthur MJP, et al. Inhibition of apoptosis of activated hepatic stellate cells by tissue inhibitor of metalloproteinase-1 is mediated via effects on matrix metalloproteinase inhibition: implications for reversibility of liver fibrosis. *J. Biol. Chem.* 2002;277:11069–11076.
141. Yoshiji H, Kuriyama S, Yoshii J, Ikenaka Y, Noguchi R, Nakatani T, et al. Tissue inhibitor of metalloproteinases-1 attenuates spontaneous liver fibrosis resolution in the transgenic mouse. *Hepatol. Baltim. Md.* 2002;36:850–860.
142. Pinzani M. PDGF and signal transduction in hepatic stellate cells. *Front. Biosci. J. Virtual Libr.* 2002;7:d1720-1726.
143. Wong L, Yamasaki G, Johnson RJ, Friedman SL. Induction of beta-platelet-derived growth factor receptor in rat hepatic lipocytes during cellular activation in vivo and in culture. *J. Clin. Invest.* 1994;94:1563–1569.
144. Yoshiji H, Kuriyama S, Yoshii J, Ikenaka Y, Noguchi R, Hicklin DJ, et al. Vascular endothelial growth factor and receptor interaction is a prerequisite for murine hepatic fibrogenesis. *Gut.* 2003;52:1347–1354.
145. Yu C, Wang F, Jin C, Huang X, Miller DL, Basilico C, et al. Role of fibroblast growth factor type 1 and 2 in carbon tetrachloride-induced hepatic injury and fibrogenesis. *Am. J. Pathol.* 2003;163:1653–1662.

146. Steiling H, Mühlbauer M, Bataille F, Schölmerich J, Werner S, Hellerbrand C. Activated hepatic stellate cells express keratinocyte growth factor in chronic liver disease. *Am. J. Pathol.* 2004;165:1233–1241.
147. Ikeda K, Wakahara T, Wang YQ, Kadoya H, Kawada N, Kaneda K. In vitro migratory potential of rat quiescent hepatic stellate cells and its augmentation by cell activation. *Hepatology*. 1999;29:1760–1767.
148. Kinnman N, Hultcrantz R, Barbu V, Rey C, Wendum D, Poupon R, et al. PDGF-mediated chemoattraction of hepatic stellate cells by bile duct segments in cholestatic liver injury. *Lab. Investig. J. Tech. Methods Pathol.* 2000;80:697–707.
149. Marra F, Romanelli RG, Giannini C, Failli P, Pastacaldi S, Arrighi MC, et al. Monocyte chemoattractant protein-1 as a chemoattractant for human hepatic stellate cells. *Hepatology*. 1999;29:140–148.
150. Melton AC, Yee HF. Hepatic stellate cell protrusions couple platelet-derived growth factor-BB to chemotaxis. *Hepatology*. 2007;45:1446–1453.
151. Hashmi AZ, Hakim W, Kruglov EA, Watanabe A, Watkins W, Dranoff JA, et al. Adenosine inhibits cytosolic calcium signals and chemotaxis in hepatic stellate cells. *Am. J. Physiol. Gastrointest. Liver Physiol.* 2007;292:G395-401.
152. Inagaki Y, Okazaki I. Emerging insights into Transforming growth factor beta Smad signal in hepatic fibrogenesis. *Gut*. 2007;56:284–292.
153. Davis BH. Transforming growth factor beta responsiveness is modulated by the extracellular collagen matrix during hepatic ito cell culture. *J. Cell. Physiol.* 1988;136:547–553.
154. Jarnagin WR, Rockey DC, Koteliensky VE, Wang SS, Bissell DM. Expression of variant fibronectins in wound healing: cellular source and biological activity of the E111A segment in rat hepatic fibrogenesis. *J. Cell Biol.* 1994;127:2037–2048.
155. Takemura S, Kawada N, Hirohashi K, Kinoshita H, Inoue M. Nucleotide receptors in hepatic stellate cells of the rat. *FEBS Lett.* 1994;354:53–56.
156. Rockey DC, Boyles JK, Gabbiani G, Friedman SL. Rat hepatic lipocytes express smooth muscle actin upon activation in vivo and in culture. *J. Submicrosc. Cytol. Pathol.* 1992;24:193–203.
157. Saab S, Tam SP, Tran B inh N, Melton AC, Tangkijvanich P, Wong H, et al. Myosin mediates contractile force generation by hepatic stellate cells in response to endothelin-1. *J. Biomed. Sci.* 2002;9:607–612.
158. Gaça MDA, Zhou X, Issa R, Kiriella K, Iredale JP, Benyon RC. Basement membrane-like matrix inhibits proliferation and collagen synthesis by activated rat hepatic stellate cells: evidence for matrix-dependent deactivation of stellate cells. *Matrix Biol. J. Int. Soc. Matrix Biol.* 2003;22:229–239.
159. Kisseleva T, Cong M, Paik Y, Scholten D, Jiang C, Benner C, et al. Myofibroblasts revert to an inactive phenotype during regression of liver fibrosis. *Proc. Natl. Acad. Sci. U. S. A.* 2012;109:9448–9453.
160. Radaeva S, Sun R, Jaruga B, Nguyen VT, Tian Z, Gao B. Natural killer cells ameliorate liver fibrosis by killing activated stellate cells in NKG2D-dependent and tumor necrosis factor-related apoptosis-inducing ligand-dependent manners. *Gastroenterology*. 2006;130:435–452.
161. Melhem A, Muhanna N, Bishara A, Alvarez CE, Ilan Y, Bishara T, et al. Anti-fibrotic activity of NK cells in experimental liver injury through killing of activated HSC. *J. Hepatology*. 2006;45:60–71.
162. Hudnall SD. Cyclosporin A renders target cells resistant to immune cytolysis. *Eur. J. Immunol.* 1991;21:221–226.
163. Poynard T, Mathurin P, Lai C-L, Guyader D, Poupon R, Tainturier M-H, et al. A comparison of fibrosis progression in chronic liver diseases. *J. Hepatology*. 2003;38:257–265.

Post-translational Modifications in Liver Disease

Imanol Zubiete Franco

164. Beaussier M, Wendum D, Schiffer E, Dumont S, Rey C, Lienhart A, et al. Prominent contribution of portal mesenchymal cells to liver fibrosis in ischemic and obstructive cholestatic injuries. *Lab. Investig. J. Tech. Methods Pathol.* 2007;87:292–303.
165. Forbes SJ, Russo FP, Rey V, Burra P, Rugge M, Wright NA, et al. A significant proportion of myofibroblasts are of bone marrow origin in human liver fibrosis. *Gastroenterology.* 2004;126:955–963.
166. Zeisberg M, Yang C, Martino M, Duncan MB, Rieder F, Tanjore H, et al. Fibroblasts derive from hepatocytes in liver fibrosis via epithelial to mesenchymal transition. *J. Biol. Chem.* 2007;282:23337–23347.
167. Baba S, Fujii H, Hirose T, Yasuchika K, Azuma H, Hoppo T, et al. Commitment of bone marrow cells to hepatic stellate cells in mouse. *J. Hepatol.* 2004;40:255–260.
168. Borkham-Kamphorst E, Weiskirchen R. The PDGF system and its antagonists in liver fibrosis. *Cytokine Growth Factor Rev.* 2016;28:53–61.
169. Alvarez RH, Kantarjian HM, Cortes JE. Biology of platelet-derived growth factor and its involvement in disease. *Mayo Clin. Proc.* 2006;81:1241–1257.
170. LaRochelle WJ, Jeffers M, McDonald WF, Chillakuru RA, Giese NA, Lokker NA, et al. PDGF-D, a new protease-activated growth factor. *Nat. Cell Biol.* 2001;3:517–521.
171. Shibamiya A, Muhl L, Tannert-Otto S, Preissner KT, Kanse SM. Nucleic acids potentiate Factor VII-activating protease (FSAP)-mediated cleavage of platelet-derived growth factor-BB and inhibition of vascular smooth muscle cell proliferation. *Biochem. J.* 2007;404:45–50.
172. Blazejewski S, Le Bail B, Boussarie L, Blanc JF, Malaval L, Okubo K, et al. Osteonectin (SPARC) expression in human liver and in cultured human liver myofibroblasts. *Am. J. Pathol.* 1997;151:651–657.
173. Fantl WJ, Escobedo JA, Martin GA, Turck CW, del Rosario M, McCormick F, et al. Distinct phosphotyrosines on a growth factor receptor bind to specific molecules that mediate different signaling pathways. *Cell.* 1992;69:413–423.
174. Shi Y, Massagué J. Mechanisms of TGF-beta signaling from cell membrane to the nucleus. *Cell.* 2003;113:685–700.
175. Weiss A, Attisano L. The TGFbeta superfamily signaling pathway. *Wiley Interdiscip. Rev. Dev. Biol.* 2013;2:47–63.
176. Kang Y, Chen C-R, Massagué J. A self-enabling TGFbeta response coupled to stress signaling: Smad engages stress response factor ATF3 for Id1 repression in epithelial cells. *Mol. Cell.* 2003;11:915–926.
177. Massagué J, Wotton D. Transcriptional control by the TGF-beta/Smad signaling system. *EMBO J.* 2000;19:1745–1754.
178. Bruce DL, Sapkota GP. Phosphatases in SMAD regulation. *FEBS Lett.* 2012;586:1897–1905.
179. Zhang Y, Chang C, Gehling DJ, Hemmati-Brivanlou A, Derynck R. Regulation of Smad degradation and activity by Smurf2, an E3 ubiquitin ligase. *Proc. Natl. Acad. Sci. U. S. A.* 2001;98:974–979.
180. Huse M, Chen YG, Massagué J, Kuriyan J. Crystal structure of the cytoplasmic domain of the type I TGF beta receptor in complex with FKBP12. *Cell.* 1999;96:425–436.
181. Di Guglielmo GM, Le Roy C, Goodfellow AF, Wrana JL. Distinct endocytic pathways regulate TGF-beta receptor signalling and turnover. *Nat. Cell Biol.* 2003;5:410–421.
182. Zuo W, Huang F, Chiang YJ, Li M, Du J, Ding Y, et al. c-Cbl-mediated neddylation antagonizes ubiquitination and degradation of the TGF-β type II receptor. *Mol. Cell.* 2013;49:499–510.

183. Clarke DC, Brown ML, Erickson RA, Shi Y, Liu X. Transforming growth factor beta depletion is the primary determinant of Smad signaling kinetics. *Mol. Cell. Biol.* 2009;29:2443–2455.
184. Verrecchia F, Tacheau C, Schorpp-Kistner M, Angel P, Mauviel A. Induction of the AP-1 members c-Jun and JunB by TGF-beta/Smad suppresses early Smad-driven gene activation. *Oncogene.* 2001;20:2205–2211.
185. Pessah M, Marais J, Prunier C, Ferrand N, Lallemand F, Mauviel A, et al. c-Jun associates with the oncoprotein Ski and suppresses Smad2 transcriptional activity. *J. Biol. Chem.* 2002;277:29094–29100.
186. Starkel P, Leclercq IA. Animal models for the study of hepatic fibrosis. *Best Pract. Res. Clin. Gastroenterol.* 2011;25:319–333.
187. Newell P, Villanueva A, Friedman SL, Koike K, Llovet JM. Experimental models of hepatocellular carcinoma. *J. Hepatol.* 2008;48:858–879.
188. Tag CG, Sauer-Lehnen S, Weiskirchen S, Borkham-Kamphorst E, Tolba RH, Tacke F, et al. Bile duct ligation in mice: induction of inflammatory liver injury and fibrosis by obstructive cholestasis. *J. Vis. Exp. JoVE.* 2015;
189. Wortham M, He L, Gyamfi M, Copple BL, Wan Y-JY. The transition from fatty liver to NASH associates with SAME depletion in db/db mice fed a methionine choline-deficient diet. *Dig. Dis. Sci.* 2008;53:2761–2774.
190. Smit JJ, Schinkel AH, Oude Elferink RP, Groen AK, Wagenaar E, van Deemter L, et al. Homozygous disruption of the murine *mdr2* P-glycoprotein gene leads to a complete absence of phospholipid from bile and to liver disease. *Cell.* 1993;75:451–462.
191. Mauad TH, van Nieuwkerk CM, Dingemans KP, Smit JJ, Schinkel AH, Notenboom RG, et al. Mice with homozygous disruption of the *mdr2* P-glycoprotein gene. A novel animal model for studies of nonsuppurative inflammatory cholangitis and hepatocarcinogenesis. *Am. J. Pathol.* 1994;145:1237–1245.
192. Gomez-Santos L, Luka Z, Wagner C, Fernandez-Alvarez S, Lu SC, Mato JM, et al. Inhibition of natural killer cells protects the liver against acute injury in the absence of glycine N-methyltransferase. *Hepatol. Baltim. Md.* 2012;56:747–759.
193. Fernández-Álvarez S, Gutiérrez-de Juan V, Zubiete-Franco I, Barbier-Torres L, Lahoz A, Parés A, et al. TRAIL-producing NK cells contribute to liver injury and related fibrogenesis in the context of GNMT deficiency. *Lab. Investig. J. Tech. Methods Pathol.* 2015;95:223–236.
194. Marcellin P, Gane E, Buti M, Afdhal N, Sievert W, Jacobson IM, et al. Regression of cirrhosis during treatment with tenofovir disoproxil fumarate for chronic hepatitis B: a 5-year open-label follow-up study. *Lancet Lond. Engl.* 2013;381:468–475.
195. Trautwein C, Friedman SL, Schuppan D, Pinzani M. Hepatic fibrosis: Concept to treatment. *J. Hepatol.* 2015;62:S15–S24.
196. Fattovich G, Stroffolini T, Zagni I, Donato F. Hepatocellular carcinoma in cirrhosis: incidence and risk factors. *Gastroenterology.* 2004;127:S35-50.
197. Kassebaum NJ, Bertozzi-Villa A, Coggeshall MS, Shackelford KA, Steiner C, Heuton KR, et al. Global, regional, and national levels and causes of maternal mortality during 1990-2013: a systematic analysis for the Global Burden of Disease Study 2013. *Lancet Lond. Engl.* 2014;384:980–1004.
198. Govaere O, Roskams T. Pathogenesis and prognosis of hepatocellular carcinoma at the cellular and molecular levels. *Clin. Liver Dis.* 2015;19:261–276.
199. Michelotti GA, Machado MV, Diehl AM. NAFLD, NASH and liver cancer. *Nat. Rev. Gastroenterol. Hepatol.* 2013;10:656–665.

Post-translational Modifications in Liver Disease

Imanol Zubiete Franco

200. Dhanasekaran R, Bandoh S, Roberts LR. Molecular pathogenesis of hepatocellular carcinoma and impact of therapeutic advances. *F1000Research*. 2016;5.
201. Ascha MS, Hanouneh IA, Lopez R, Tamimi TA-R, Feldstein AF, Zein NN. The incidence and risk factors of hepatocellular carcinoma in patients with nonalcoholic steatohepatitis. *Hepatology*. 2010;51:1972–1978.
202. Guzman G, Brunt EM, Petrovic LM, Chejfec G, Layden TJ, Cotler SJ. Does nonalcoholic fatty liver disease predispose patients to hepatocellular carcinoma in the absence of cirrhosis? *Arch. Pathol. Lab. Med.* 2008;132:1761–1766.
203. Ertle J, Dechêne A, Sowa J-P, Penndorf V, Herzer K, Kaiser G, et al. Non-alcoholic fatty liver disease progresses to hepatocellular carcinoma in the absence of apparent cirrhosis. *Int. J. Cancer*. 2011;128:2436–2443.
204. Tokushige K, Hashimoto E, Horie Y, Taniai M, Higuchi S. Hepatocellular carcinoma in Japanese patients with nonalcoholic fatty liver disease, alcoholic liver disease, and chronic liver disease of unknown etiology: report of the nationwide survey. *J. Gastroenterol.* 2011;46:1230–1237.
205. Forner A, Llovet JM, Bruix J. Hepatocellular carcinoma. *Lancet*. 2012;379:1245–1255.
206. Bruix J, Han K-H, Gores G, Llovet JM, Mazzaferro V. Liver cancer: Approaching a personalized care. *J. Hepatology*. 2015;62:S144–156.
207. Roskams T, Kojiro M. Pathology of early hepatocellular carcinoma: conventional and molecular diagnosis. *Semin. Liver Dis.* 2010;30:17–25.
208. Imamura H, Matsuyama Y, Tanaka E, Ohkubo T, Hasegawa K, Miyagawa S, et al. Risk factors contributing to early and late phase intrahepatic recurrence of hepatocellular carcinoma after hepatectomy. *J. Hepatology*. 2003;38:200–207.
209. Berzigotti A, Reig M, Abraldes JG, Bosch J, Bruix J. Portal hypertension and the outcome of surgery for hepatocellular carcinoma in compensated cirrhosis: a systematic review and meta-analysis. *Hepatology*. 2015;61:526–536.
210. Llovet JM, Fuster J, Bruix J. Intention-to-treat analysis of surgical treatment for early hepatocellular carcinoma: resection versus transplantation. *Hepatology*. 1999;30:1434–1440.
211. Tateishi R, Shiina S, Teratani T, Obi S, Sato S, Koike Y, et al. Percutaneous radiofrequency ablation for hepatocellular carcinoma. An analysis of 1000 cases. *Cancer*. 2005;103:1201–1209.
212. Llovet JM, Real MI, Montaña X, Planas R, Coll S, Aponte J, et al. Arterial embolisation or chemoembolisation versus symptomatic treatment in patients with unresectable hepatocellular carcinoma: a randomised controlled trial. *Lancet Lond. Engl.* 2002;359:1734–1739.
213. Lencioni R, Llovet JM, Han G, Tak WY, Yang J, Guglielmi A, et al. Sorafenib or placebo plus TACE with doxorubicin-eluting beads for intermediate stage HCC: The SPACE trial. *J. Hepatology*. 2016;64:1090–1098.
214. Lewis AL, Gonzalez MV, Lloyd AW, Hall B, Tang Y, Willis SL, et al. DC bead: in vitro characterization of a drug-delivery device for transarterial chemoembolization. *J. Vasc. Interv. Radiol. JVIR*. 2006;17:335–342.
215. Brown DB, Gould JE, Gervais DA, Goldberg SN, Murthy R, Millward SF, et al. Transcatheter therapy for hepatic malignancy: standardization of terminology and reporting criteria. *J. Vasc. Interv. Radiol. JVIR*. 2009;20:S425–434.
216. Salem R, Mazzaferro V, Sangro B. Yttrium 90 radioembolization for the treatment of hepatocellular carcinoma: biological lessons, current challenges, and clinical perspectives. *Hepatology*. 2013;58:2188–2197.

217. Lencioni R. Loco-regional treatment of hepatocellular carcinoma. *Hepatology*. 2010;52:762–773.
218. Nault JC, Mallet M, Pilati C, Calderaro J, Bioulac-Sage P, Laurent C, et al. High frequency of telomerase reverse-transcriptase promoter somatic mutations in hepatocellular carcinoma and preneoplastic lesions. *Nat. Commun.* 2013;4:2218.
219. Hollstein M, Sidransky D, Vogelstein B, Harris CC. p53 mutations in human cancers. *Science*. 1991;253:49–53.
220. Hussain SP, Schwank J, Staib F, Wang XW, Harris CC. TP53 mutations and hepatocellular carcinoma: insights into the etiology and pathogenesis of liver cancer. *Oncogene*. 2007;26:2166–2176.
221. Villanueva A, Chiang DY, Newell P, Peix J, Thung S, Alsinet C, et al. Pivotal role of mTOR signaling in hepatocellular carcinoma. *Gastroenterology*. 2008;135:1972–1983, 1983–11.
222. Luo D, Wang Z, Wu J, Jiang C, Wu J. The role of hypoxia inducible factor-1 in hepatocellular carcinoma. *BioMed Res. Int.* 2014;2014:409272.
223. Roberts AB, Wakefield LM. The two faces of transforming growth factor beta in carcinogenesis. *Proc. Natl. Acad. Sci. U. S. A.* 2003;100:8621–8623.
224. Giannelli G, Bergamini C, Fransvea E, Sgarra C, Antonaci S. Laminin-5 with transforming growth factor-beta1 induces epithelial to mesenchymal transition in hepatocellular carcinoma. *Gastroenterology*. 2005;129:1375–1383.
225. Zucman-Rossi J, Benhamouche S, Godard C, Boyault S, Grimber G, Balabaud C, et al. Differential effects of inactivated Axin1 and activated beta-catenin mutations in human hepatocellular carcinomas. *Oncogene*. 2007;26:774–780.
226. Guichard C, Amaddeo G, Imbeaud S, Ladeiro Y, Pelletier L, Maad IB, et al. Integrated analysis of somatic mutations and focal copy-number changes identifies key genes and pathways in hepatocellular carcinoma. *Nat. Genet.* 2012;44:694–698.
227. Lachenmayer A, Alsinet C, Savic R, Cabellos L, Toffanin S, Hoshida Y, et al. Wnt-pathway activation in two molecular classes of hepatocellular carcinoma and experimental modulation by sorafenib. *Clin. Cancer Res. Off. J. Am. Assoc. Cancer Res.* 2012;18:4997–5007.
228. Hemminki A, Markie D, Tomlinson I, Avizienyte E, Roth S, Loukola A, et al. A serine/threonine kinase gene defective in Peutz-Jeghers syndrome. *Nature*. 1998;391:184–187.
229. McGarrity TJ, Amos C. Peutz-Jeghers syndrome: clinicopathology and molecular alterations. *Cell. Mol. Life Sci. CMLS.* 2006;63:2135–2144.
230. Jansen M, Langeveld D, De Leng WWJ, Milne ANA, Giardiello FM, Offerhaus GJA. LKB1 as the ghostwriter of crypt history. *Fam. Cancer*. 2011;10:437–446.
231. Giardiello FM, Brensinger JD, Tersmette AC, Goodman SN, Petersen GM, Booker SV, et al. Very high risk of cancer in familial Peutz-Jeghers syndrome. *Gastroenterology*. 2000;119:1447–1453.
232. Sanchez-Cespedes M, Parrella P, Esteller M, Nomoto S, Trink B, Engles JM, et al. Inactivation of LKB1/STK11 is a common event in adenocarcinomas of the lung. *Cancer Res.* 2002;62:3659–3662.
233. Wingo SN, Gallardo TD, Akbay EA, Liang M-C, Contreras CM, Boren T, et al. Somatic LKB1 mutations promote cervical cancer progression. *PLoS One*. 2009;4:e5137.
234. Jishage K, Nezu J, Kawase Y, Iwata T, Watanabe M, Miyoshi A, et al. Role of Lkb1, the causative gene of Peutz-Jegher's syndrome, in embryogenesis and polyposis. *Proc. Natl. Acad. Sci. U. S. A.* 2002;99:8903–8908.

Post-translational Modifications in Liver Disease

Imanol Zubiete Franco

235. Miyoshi H, Nakau M, Ishikawa T, Seldin MF, Oshima M, Taketo MM. Gastrointestinal hamartomatous polyposis in Lkb1 heterozygous knockout mice. *Cancer Res.* 2002;62:2261–2266.
236. Bardeesy N, Sinha M, Hezel AF, Signoretti S, Hathaway NA, Sharpless NE, et al. Loss of the Lkb1 tumour suppressor provokes intestinal polyposis but resistance to transformation. *Nature.* 2002;419:162–167.
237. Ji H, Ramsey MR, Hayes DN, Fan C, McNamara K, Kozlowski P, et al. LKB1 modulates lung cancer differentiation and metastasis. *Nature.* 2007;448:807–810.
238. Pearson HB, McCarthy A, Collins CMP, Ashworth A, Clarke AR. Lkb1 deficiency causes prostate neoplasia in the mouse. *Cancer Res.* 2008;68:2223–2232.
239. Shorning BY, Zabkiewicz J, McCarthy A, Pearson HB, Winton DJ, Sansom OJ, et al. Lkb1 deficiency alters goblet and paneth cell differentiation in the small intestine. *PLoS One.* 2009;4:e4264.
240. Alessi DR, Sakamoto K, Bayascas JR. LKB1-dependent signaling pathways. *Annu. Rev. Biochem.* 2006;75:137–163.
241. Boudeau J, Baas AF, Deak M, Morrice NA, Kieloch A, Schutkowski M, et al. MO25alpha/beta interact with STRADalpha/beta enhancing their ability to bind, activate and localize LKB1 in the cytoplasm. *EMBO J.* 2003;22:5102–5114.
242. Dorfman J, Macara IG. STRADalpha regulates LKB1 localization by blocking access to importin-alpha, and by association with Crm1 and exportin-7. *Mol. Biol. Cell.* 2008;19:1614–1626.
243. Hardie DG. AMPK--sensing energy while talking to other signaling pathways. *Cell Metab.* 2014;20:939–952.
244. Hawley SA, Pan DA, Mustard KJ, Ross L, Bain J, Edelman AM, et al. Calmodulin-dependent protein kinase kinase-beta is an alternative upstream kinase for AMP-activated protein kinase. *Cell Metab.* 2005;2:9–19.
245. Carling D, Zammit VA, Hardie DG. A common bicyclic protein kinase cascade inactivates the regulatory enzymes of fatty acid and cholesterol biosynthesis. *FEBS Lett.* 1987;223:217–222.
246. Porstmann T, Santos CR, Griffiths B, Cully M, Wu M, Leever S, et al. SREBP activity is regulated by mTORC1 and contributes to Akt-dependent cell growth. *Cell Metab.* 2008;8:224–236.
247. Hardie DG, Ross FA, Hawley SA. AMPK: a nutrient and energy sensor that maintains energy homeostasis. *Nat. Rev. Mol. Cell Biol.* 2012;13:251–262.
248. Koo S-H, Flechner L, Qi L, Zhang X, Sreaton RA, Jeffries S, et al. The CREB coactivator TORC2 is a key regulator of fasting glucose metabolism. *Nature.* 2005;437:1109–1111.
249. Corradetti MN, Inoki K, Bardeesy N, DePinho RA, Guan K-L. Regulation of the TSC pathway by LKB1: evidence of a molecular link between tuberous sclerosis complex and Peutz-Jeghers syndrome. *Genes Dev.* 2004;18:1533–1538.
250. Kimball SR, Jefferson LS. Signaling pathways and molecular mechanisms through which branched-chain amino acids mediate translational control of protein synthesis. *J. Nutr.* 2006;136:227S–31S.
251. Wullschlegel S, Loewith R, Hall MN. TOR signaling in growth and metabolism. *Cell.* 2006;124:471–484.
252. Shackelford DB, Shaw RJ. The LKB1-AMPK pathway: metabolism and growth control in tumour suppression. *Nat. Rev. Cancer.* 2009;9:563–575.
253. Guertin DA, Sabatini DM. Defining the role of mTOR in cancer. *Cancer Cell.* 2007;12:9–22.

254. Shaw RJ, Bardeesy N, Manning BD, Lopez L, Kosmatka M, DePinho RA, et al. The LKB1 tumor suppressor negatively regulates mTOR signaling. *Cancer Cell*. 2004;6:91–99.
255. Al-Hakim AK, Göransson O, Deak M, Toth R, Campbell DG, Morrice NA, et al. 14-3-3 cooperates with LKB1 to regulate the activity and localization of QSK and SIK. *J. Cell Sci*. 2005;118:5661–5673.
256. Lefebvre DL, Rosen CF. Regulation of SNARK activity in response to cellular stresses. *Biochim. Biophys. Acta*. 2005;1724:71–85.
257. Zagórska A, Deak M, Campbell DG, Banerjee S, Hirano M, Aizawa S, et al. New roles for the LKB1-NUAK pathway in controlling myosin phosphatase complexes and cell adhesion. *Sci. Signal*. 2010;3:ra25.
258. Tomancak P, Piano F, Riechmann V, Gunsalus KC, Kempfues KJ, Ephrussi A. A *Drosophila melanogaster* homologue of *Caenorhabditis elegans* par-1 acts at an early step in embryonic-axis formation. *Nat. Cell Biol*. 2000;2:458–460.
259. Shulman JM, Benton R, St Johnston D. The *Drosophila* homolog of *C. elegans* PAR-1 organizes the oocyte cytoskeleton and directs oskar mRNA localization to the posterior pole. *Cell*. 2000;101:377–388.
260. Baas AF, Kuipers J, van der Wel NN, Batlle E, Koerten HK, Peters PJ, et al. Complete polarization of single intestinal epithelial cells upon activation of LKB1 by STRAD. *Cell*. 2004;116:457–466.
261. Huh C-G, Factor VM, Sánchez A, Uchida K, Conner EA, Thorgeirsson SS. Hepatocyte growth factor/c-met signaling pathway is required for efficient liver regeneration and repair. *Proc. Natl. Acad. Sci. U. S. A*. 2004;101:4477–4482.
262. Chen ZP, Mitchelhill KI, Michell BJ, Stapleton D, Rodriguez-Crespo I, Witters LA, et al. AMP-activated protein kinase phosphorylation of endothelial NO synthase. *FEBS Lett*. 1999;443:285–289.
263. Morrow VA, Foufelle F, Connell JMC, Petrie JR, Gould GW, Salt IP. Direct activation of AMP-activated protein kinase stimulates nitric-oxide synthesis in human aortic endothelial cells. *J. Biol. Chem*. 2003;278:31629–31639.
264. Pérez-Mato I, Castro C, Ruiz FA, Corrales FJ, Mato JM. Methionine adenosyltransferase S-nitrosylation is regulated by the basic and acidic amino acids surrounding the target thiol. *J. Biol. Chem*. 1999;274:17075–17079.
265. García-Trevijano ER, Martínez-Chantar ML, Latasa MU, Mato JM, Avila MA. NO sensitizes rat hepatocytes to proliferation by modifying S-adenosylmethionine levels. *Gastroenterology*. 2002;122:1355–1363.
266. Martínez-Chantar ML, Vázquez-Chantada M, Garnacho M, Latasa MU, Varela-Rey M, Dotor J, et al. S-adenosylmethionine regulates cytoplasmic HuR via AMP-activated kinase. *Gastroenterology*. 2006;131:223–232.
267. Martínez-López N, Varela-Rey M, Fernández-Ramos D, Woodhoo A, Vázquez-Chantada M, Embade N, et al. Activation of LKB1-Akt pathway independent of phosphoinositide 3-kinase plays a critical role in the proliferation of hepatocellular carcinoma from nonalcoholic steatohepatitis. *Hepatology*. 2010;52:1621–1631.
268. Martínez-López N, García-Rodríguez JL, Varela-Rey M, Gutiérrez V, Fernández-Ramos D, Beraza N, et al. Hepatoma cells from mice deficient in glycine N-methyltransferase have increased RAS signaling and activation of liver kinase B1. *Gastroenterology*. 2012;143:787–798–13.
269. Sapkota GP, Kieloch A, Lizcano JM, Lain S, Arthur JS, Williams MR, et al. Phosphorylation of the protein kinase mutated in Peutz-Jeghers cancer syndrome, LKB1/STK11, at Ser431 by p90(RSK) and cAMP-dependent protein kinase, but not its farnesylation at Cys(433), is essential for LKB1 to suppress cell growth. *J. Biol. Chem*. 2001;276:19469–19482.

Post-translational Modifications in Liver Disease

Imanol Zubiete Franco

270. Xie Z, Dong Y, Scholz R, Neumann D, Zou M-H. Phosphorylation of LKB1 at serine 428 by protein kinase C-zeta is required for metformin-enhanced activation of the AMP-activated protein kinase in endothelial cells. *Circulation*. 2008;117:952–962.
271. Xie Z, Dong Y, Zhang J, Scholz R, Neumann D, Zou M-H. Identification of the serine 307 of LKB1 as a novel phosphorylation site essential for its nucleocytoplasmic transport and endothelial cell angiogenesis. *Mol. Cell. Biol.* 2009;29:3582–3596.
272. Sapkota GP, Deak M, Kieloch A, Morrice N, Goodarzi AA, Smythe C, et al. Ionizing radiation induces ataxia telangiectasia mutated kinase (ATM)-mediated phosphorylation of LKB1/STK11 at Thr-366. *Biochem. J.* 2002;368:507–516.
273. Zheng B, Jeong JH, Asara JM, Yuan Y-Y, Granter SR, Chin L, et al. Oncogenic B-RAF negatively regulates the tumor suppressor LKB1 to promote melanoma cell proliferation. *Mol. Cell.* 2009;33:237–247.
274. Esteve-Puig R, Canals F, Colomé N, Merlino G, Recio JA. Uncoupling of the LKB1-AMPKalpha energy sensor pathway by growth factors and oncogenic BRAF. *PLoS One*. 2009;4:e4771.
275. Fogarty S, Hardie DG. C-terminal phosphorylation of LKB1 is not required for regulation of AMP-activated protein kinase, BRSK1, BRSK2, or cell cycle arrest. *J. Biol. Chem.* 2009;284:77–84.
276. Sapkota GP, Boudeau J, Deak M, Kieloch A, Morrice N, Alessi DR. Identification and characterization of four novel phosphorylation sites (Ser31, Ser325, Thr336 and Thr366) on LKB1/STK11, the protein kinase mutated in Peutz-Jeghers cancer syndrome. *Biochem. J.* 2002;362:481–490.
277. Collins SP, Reoma JL, Gamm DM, Uhler MD. LKB1, a novel serine/threonine protein kinase and potential tumour suppressor, is phosphorylated by cAMP-dependent protein kinase (PKA) and prenylated in vivo. *Biochem. J.* 2000;345 Pt 3:673–680.
278. Towler MC, Fogarty S, Hawley SA, Pan DA, Martin DMA, Morrice NA, et al. A novel short splice variant of the tumour suppressor LKB1 is required for spermiogenesis. *Biochem. J.* 2008;416:1–14.
279. Lan F, Cacicedo JM, Ruderman N, Ido Y. SIRT1 modulation of the acetylation status, cytosolic localization, and activity of LKB1. Possible role in AMP-activated protein kinase activation. *J. Biol. Chem.* 2008;283:27628–27635.
280. Lee S-W, Li C-F, Jin G, Cai Z, Han F, Chan C-H, et al. Skp2-dependent ubiquitination and activation of LKB1 is essential for cancer cell survival under energy stress. *Mol. Cell.* 2015;57:1022–1033.
281. Ritho J, Arold ST, Yeh ETH. A Critical SUMO1 Modification of LKB1 Regulates AMPK Activity during Energy Stress. *Cell Rep.* 2015;12:734–742.
282. Barbier-Torres L, Delgado TC, García-Rodríguez JL, Zubiete-Franco I, Fernández-Ramos D, Buqué X, et al. Stabilization of LKB1 and Akt by neddylation regulates energy metabolism in liver cancer. *Oncotarget*. 2015;6:2509–2523.
283. International Human Genome Sequencing Consortium. Finishing the euchromatic sequence of the human genome. *Nature*. 2004;431:931–945.
284. Jensen ON. Modification-specific proteomics: characterization of post-translational modifications by mass spectrometry. *Curr. Opin. Chem. Biol.* 2004;8:33–41.
285. Ayoubi TA, Van De Ven WJ. Regulation of gene expression by alternative promoters. *FASEB J. Off. Publ. Fed. Am. Soc. Exp. Biol.* 1996;10:453–460.
286. Walsh C. *Posttranslational Modification of Proteins: Expanding Nature's Inventory*. Roberts and Company Publishers; 2006.
287. Strahl BD, Allis CD. The language of covalent histone modifications. *Nature*. 2000;403:41–45.

288. Choudhary C, Kumar C, Gnad F, Nielsen ML, Rehman M, Walther TC, et al. Lysine acetylation targets protein complexes and co-regulates major cellular functions. *Science*. 2009;325:834–840.
289. Chalkiadaki A, Guarente L. The multifaceted functions of sirtuins in cancer. *Nat. Rev. Cancer*. 2015;15:608–624.
290. Goldstein G, Scheid M, Hammerling U, Schlesinger DH, Niall HD, Boyse EA. Isolation of a polypeptide that has lymphocyte-differentiating properties and is probably represented universally in living cells. *Proc. Natl. Acad. Sci. U. S. A.* 1975;72:11–15.
291. Glickman MH, Ciechanover A. The ubiquitin-proteasome proteolytic pathway: destruction for the sake of construction. *Physiol. Rev.* 2002;82:373–428.
292. Pickart CM. Ubiquitin in chains. *Trends Biochem. Sci.* 2000;25:544–548.
293. van der Veen AG, Ploegh HL. Ubiquitin-like proteins. *Annu. Rev. Biochem.* 2012;81:323–357.
294. Geiss-Friedlander R, Melchior F. Concepts in sumoylation: a decade on. *Nat. Rev. Mol. Cell Biol.* 2007;8:947–956.
295. Whitby FG, Xia G, Pickart CM, Hill CP. Crystal structure of the human ubiquitin-like protein NEDD8 and interactions with ubiquitin pathway enzymes. *J. Biol. Chem.* 1998;273:34983–34991.
296. Hori T, Osaka F, Chiba T, Miyamoto C, Okabayashi K, Shimbara N, et al. Covalent modification of all members of human cullin family proteins by NEDD8. *Oncogene*. 1999;18:6829–6834.
297. Deshaies RJ, Joazeiro CAP. RING domain E3 ubiquitin ligases. *Annu. Rev. Biochem.* 2009;78:399–434.
298. Cope GA, Suh GSB, Aravind L, Schwarz SE, Zipursky SL, Koonin EV, et al. Role of predicted metalloprotease motif of Jab1/Csn5 in cleavage of Nedd8 from Cul1. *Science*. 2002;298:608–611.
299. Gan-Erdene T, Nagamalleswari K, Yin L, Wu K, Pan Z-Q, Wilkinson KD. Identification and characterization of DEN1, a deneddylase of the ULP family. *J. Biol. Chem.* 2003;278:28892–28900.
300. Xirodimas DP. Novel substrates and functions for the ubiquitin-like molecule NEDD8. *Biochem. Soc. Trans.* 2008;36:802–806.
301. Petroski MD, Deshaies RJ. Function and regulation of cullin-RING ubiquitin ligases. *Nat. Rev. Mol. Cell Biol.* 2005;6:9–20.
302. Embade N, Fernández-Ramos D, Varela-Rey M, Beraza N, Sini M, Gutiérrez de Juan V, et al. Murine double minute 2 regulates Hu antigen R stability in human liver and colon cancer through NEDDylation. *Hepatology*. 2012;55:1237–1248.
303. Abidi N, Xirodimas DP. Regulation of cancer-related pathways by protein NEDDylation and strategies for the use of NEDD8 inhibitors in the clinic. *Endocr. Relat. Cancer*. 2015;22:T55-70.
304. Xirodimas DP, Saville MK, Bourdon J-C, Hay RT, Lane DP. Mdm2-mediated NEDD8 conjugation of p53 inhibits its transcriptional activity. *Cell*. 2004;118:83–97.
305. Chairatvit K, Ngamkitidechakul C. Control of cell proliferation via elevated NEDD8 conjugation in oral squamous cell carcinoma. *Mol. Cell. Biochem.* 2007;306:163–169.
306. Welcker M, Clurman BE. FBW7 ubiquitin ligase: a tumour suppressor at the crossroads of cell division, growth and differentiation. *Nat. Rev. Cancer*. 2008;8:83–93.
307. Haagenson KK, Tait L, Wang J, Shekhar MP, Polin L, Chen W, et al. Cullin-3 protein expression levels correlate with breast cancer progression. *Cancer Biol. Ther.* 2012;13:1042–1046.

Post-translational Modifications in Liver Disease

Imanol Zubiete Franco

308. Li L, Wang M, Yu G, Chen P, Li H, Wei D, et al. Overactivated neddylation pathway as a therapeutic target in lung cancer. *J. Natl. Cancer Inst.* 2014;106:dju083.
309. Soucy TA, Smith PG, Milhollen MA, Berger AJ, Gavin JM, Adhikari S, et al. An inhibitor of NEDD8-activating enzyme as a new approach to treat cancer. *Nature.* 2009;458:732–736.
310. Lin JJ, Milhollen MA, Smith PG, Narayanan U, Dutta A. NEDD8-targeting drug MLN4924 elicits DNA rereplication by stabilizing Cdt1 in S phase, triggering checkpoint activation, apoptosis, and senescence in cancer cells. *Cancer Res.* 2010;70:10310–10320.
311. Milhollen MA, Narayanan U, Soucy TA, Veiby PO, Smith PG, Amidon B. Inhibition of NEDD8-activating enzyme induces rereplication and apoptosis in human tumor cells consistent with deregulating CDT1 turnover. *Cancer Res.* 2011;71:3042–3051.
312. Melchior F. SUMO--nonclassical ubiquitin. *Annu. Rev. Cell Dev. Biol.* 2000;16:591–626.
313. Guo D, Li M, Zhang Y, Yang P, Eckenrode S, Hopkins D, et al. A functional variant of SUMO4, a new I kappa B alpha modifier, is associated with type 1 diabetes. *Nat. Genet.* 2004;36:837–841.
314. Saitoh H, Hincey J. Functional heterogeneity of small ubiquitin-related protein modifiers SUMO-1 versus SUMO-2/3. *J. Biol. Chem.* 2000;275:6252–6258.
315. Tatham MH, Jaffray E, Vaughan OA, Desterro JM, Botting CH, Naismith JH, et al. Polymeric chains of SUMO-2 and SUMO-3 are conjugated to protein substrates by SAE1/SAE2 and Ubc9. *J. Biol. Chem.* 2001;276:35368–35374.
316. Flotho A, Melchior F. Sumoylation: a regulatory protein modification in health and disease. *Annu. Rev. Biochem.* 2013;82:357–385.
317. Schmidt D, Müller S. Members of the PIAS family act as SUMO ligases for c-Jun and p53 and repress p53 activity. *Proc. Natl. Acad. Sci. U. S. A.* 2002;99:2872–2877.
318. Pichler A, Gast A, Seeler JS, Dejean A, Melchior F. The nucleoporin RanBP2 has SUMO1 E3 ligase activity. *Cell.* 2002;108:109–120.
319. Johnson ES. Protein modification by SUMO. *Annu. Rev. Biochem.* 2004;73:355–382.
320. Alegre KO, Reverter D. Swapping small ubiquitin-like modifier (SUMO) isoform specificity of SUMO proteases SENP6 and SENP7. *J. Biol. Chem.* 2011;286:36142–36151.
321. Kim KI, Baek SH, Jeon YJ, Nishimori S, Suzuki T, Uchida S, et al. A new SUMO-1-specific protease, SUSP1, that is highly expressed in reproductive organs. *J. Biol. Chem.* 2000;275:14102–14106.
322. Bailey D, O'Hare P. Characterization of the localization and proteolytic activity of the SUMO-specific protease, SENP1. *J. Biol. Chem.* 2004;279:692–703.
323. Mukhopadhyay D, Ayaydin F, Kolli N, Tan S-H, Anan T, Kametaka A, et al. SUSP1 antagonizes formation of highly SUMO2/3-conjugated species. *J. Cell Biol.* 2006;174:939–949.
324. Hang J, Dasso M. Association of the human SUMO-1 protease SENP2 with the nuclear pore. *J. Biol. Chem.* 2002;277:19961–19966.
325. Nishida T, Tanaka H, Yasuda H. A novel mammalian Smt3-specific isopeptidase 1 (SMT3IP1) localized in the nucleolus at interphase. *Eur. J. Biochem.* 2000;267:6423–6427.
326. Owerbach D, McKay EM, Yeh ETH, Gabbay KH, Bohren KM. A proline-90 residue unique to SUMO-4 prevents maturation and sumoylation. *Biochem. Biophys. Res. Commun.* 2005;337:517–520.

327. Bernier-Villamor V, Sampson DA, Matunis MJ, Lima CD. Structural basis for E2-mediated SUMO conjugation revealed by a complex between ubiquitin-conjugating enzyme Ubc9 and RanGAP1. *Cell*. 2002;108:345–356.
328. Yang S-H, Galanis A, Witty J, Sharrocks AD. An extended consensus motif enhances the specificity of substrate modification by SUMO. *EMBO J*. 2006;25:5083–5093.
329. Matic I, Schimmel J, Hendriks IA, van Santen MA, van de Rijke F, van Dam H, et al. Site-specific identification of SUMO-2 targets in cells reveals an inverted SUMOylation motif and a hydrophobic cluster SUMOylation motif. *Mol. Cell*. 2010;39:641–652.
330. Zhu J, Zhu S, Guzzo CM, Ellis NA, Sung KS, Choi CY, et al. Small ubiquitin-related modifier (SUMO) binding determines substrate recognition and paralog-selective SUMO modification. *J. Biol. Chem*. 2008;283:29405–29415.
331. Hoegge C, Pfander B, Moldovan G-L, Pyrowolakis G, Jentsch S. RAD6-dependent DNA repair is linked to modification of PCNA by ubiquitin and SUMO. *Nature*. 2002;419:135–141.
332. Hardeband U, Steinacher R, Jiricny J, Schär P. Modification of the human thymine-DNA glycosylase by ubiquitin-like proteins facilitates enzymatic turnover. *EMBO J*. 2002;21:1456–1464.
333. Pfander B, Moldovan G-L, Sacher M, Hoegge C, Jentsch S. SUMO-modified PCNA recruits Srs2 to prevent recombination during S phase. *Nature*. 2005;436:428–433.
334. Ihara M, Koyama H, Uchimura Y, Saitoh H, Kikuchi A. Noncovalent binding of small ubiquitin-related modifier (SUMO) protease to SUMO is necessary for enzymatic activities and cell growth. *J. Biol. Chem*. 2007;282:16465–16475.
335. Matunis MJ, Coutavas E, Blobel G. A novel ubiquitin-like modification modulates the partitioning of the Ran-GTPase-activating protein RanGAP1 between the cytosol and the nuclear pore complex. *J. Cell Biol*. 1996;135:1457–1470.
336. Mahajan R, Delphin C, Guan T, Gerace L, Melchior F. A small ubiquitin-related polypeptide involved in targeting RanGAP1 to nuclear pore complex protein RanBP2. *Cell*. 1997;88:97–107.
337. Galanty Y, Belotserkovskaya R, Coates J, Polo S, Miller KM, Jackson SP. Mammalian SUMO E3-ligases PIAS1 and PIAS4 promote responses to DNA double-strand breaks. *Nature*. 2009;462:935–939.
338. Morris JR, Boutell C, Keppler M, Densham R, Weekes D, Alamshah A, et al. The SUMO modification pathway is involved in the BRCA1 response to genotoxic stress. *Nature*. 2009;462:886–890.
339. Li R, Wei J, Jiang C, Liu D, Deng L, Zhang K, et al. Akt SUMOylation regulates cell proliferation and tumorigenesis. *Cancer Res*. 2013;73:5742–5753.
340. de la Cruz-Herrera CF, Campagna M, Lang V, del Carmen González-Santamaría J, Marcos-Villar L, Rodríguez MS, et al. SUMOylation regulates AKT1 activity. *Oncogene*. 2015;34:1442–1450.
341. Sahin U, Lapaquette P, Andrieux A, Faure G, Dejean A. Sumoylation of human argonaute 2 at lysine-402 regulates its stability. *PloS One*. 2014;9:e102957.
342. Josa-Prado F, Henley JM, Wilkinson KA. SUMOylation of Argonaute-2 regulates RNA interference activity. *Biochem. Biophys. Res. Commun*. 2015;464:1066–1071.
343. Tomasi ML, Ryoo M, Ramani K, Tomasi I, Giordano P, Mato JM, et al. Methionine adenosyltransferase $\alpha 2$ sumoylation positively regulate Bcl-2 expression in human colon and liver cancer cells. *Oncotarget*. 2015;6:37706–37723.
344. de la Cruz-Herrera CF, Baz-Martínez M, Lang V, El Motiam A, Barbazán J, Couceiro R, et al. Conjugation of SUMO to p85 leads to a novel mechanism of PI3K regulation. *Oncogene*. 2016;35:2873–2880.

Post-translational Modifications in Liver Disease

Imanol Zubiete Franco

345. Van Nguyen T, Angkasekwinai P, Dou H, Lin F-M, Lu L-S, Cheng J, et al. SUMO-specific protease 1 is critical for early lymphoid development through regulation of STAT5 activation. *Mol. Cell.* 2012;45:210–221.
346. Mo Y-Y, Moschos SJ. Targeting Ubc9 for cancer therapy. *Expert Opin. Ther. Targets.* 2005;9:1203–1216.
347. McDoniels-Silvers AL, Nimri CF, Stoner GD, Lubet RA, You M. Differential gene expression in human lung adenocarcinomas and squamous cell carcinomas. *Clin. Cancer Res. Off. J. Am. Assoc. Cancer Res.* 2002;8:1127–1138.
348. Cheng J, Bawa T, Lee P, Gong L, Yeh ETH. Role of desumoylation in the development of prostate cancer. *Neoplasia N. Y. N.* 2006;8:667–676.
349. Jacques C, Baris O, Prunier-Mirebeau D, Savagner F, Rodien P, Rohmer V, et al. Two-step differential expression analysis reveals a new set of genes involved in thyroid oncocyctic tumors. *J. Clin. Endocrinol. Metab.* 2005;90:2314–2320.
350. Mo Y-Y, Yu Y, Theodosiou E, Ee PLR, Beck WT. A role for Ubc9 in tumorigenesis. *Oncogene.* 2005;24:2677–2683.
351. Moschos SJ, Jukic DM, Athanassiou C, Bhargava R, Dacic S, Wang X, et al. Expression analysis of Ubc9, the single small ubiquitin-like modifier (SUMO) E2 conjugating enzyme, in normal and malignant tissues. *Hum. Pathol.* 2010;41:1286–1298.
352. Driscoll JJ, Pelluru D, Lefkimmatis K, Fulciniti M, Prabhala RH, Greipp PR, et al. The sumoylation pathway is dysregulated in multiple myeloma and is associated with adverse patient outcome. *Blood.* 2010;115:2827–2834.
353. Dünnebieer T, Bermejo JL, Haas S, Fischer H-P, Pierl CB, Justenhoven C, et al. Common variants in the UBC9 gene encoding the SUMO-conjugating enzyme are associated with breast tumor grade. *Int. J. Cancer.* 2009;125:596–602.
354. Synowiec E, Krupa R, Morawiec Z, Wasylecka M, Dziki L, Morawiec J, et al. Efficacy of DNA double-strand breaks repair in breast cancer is decreased in carriers of the variant allele of the UBC9 gene c.73G>A polymorphism. *Mutat. Res.* 2010;694:31–38.
355. Lee MH, Lee SW, Lee EJ, Choi SJ, Chung SS, Lee JI, et al. SUMO-specific protease SUSP4 positively regulates p53 by promoting Mdm2 self-ubiquitination. *Nat. Cell Biol.* 2006;8:1424–1431.
356. Tomasi ML, Tomasi I, Ramani K, Pascale RM, Xu J, Giordano P, et al. S-adenosyl methionine regulates ubiquitin-conjugating enzyme 9 protein expression and sumoylation in murine liver and human cancers. *Hepatology. Baltim. Md.* 2012;56:982–993.
357. Guo W-H, Yuan L-H, Xiao Z-H, Liu D, Zhang J-X. Overexpression of SUMO-1 in hepatocellular carcinoma: a latent target for diagnosis and therapy of hepatoma. *J. Cancer Res. Clin. Oncol.* 2011;137:533–541.
358. Qin Y, Bao H, Pan Y, Yin M, Liu Y, Wu S, et al. SUMOylation alterations are associated with multidrug resistance in hepatocellular carcinoma. *Mol. Med. Rep.* 2014;9:877–881.
359. Leffert HL, Koch KS, Moran T, Williams M. Liver cells. *Methods Enzymol.* 1979;58:536–544.
360. Xu L, Hui AY, Albanis E, Arthur MJ, O'Byrne SM, Blaner WS, et al. Human hepatic stellate cell lines, LX-1 and LX-2: new tools for analysis of hepatic fibrosis. *Gut.* 2005;54:142–151.
361. Ye J, Coulouris G, Zaretskaya I, Cutcutache I, Rozen S, Madden TL. Primer-BLAST: a tool to design target-specific primers for polymerase chain reaction. *BMC Bioinformatics.* 2012;13:134.
362. Rodriguez MS, Desterro JM, Lain S, Midgley CA, Lane DP, Hay RT. SUMO-1 modification activates the transcriptional response of p53. *EMBO J.* 1999;18:6455–6461.

363. Khan SA, Joyce J, Tsuda T. Quantification of active and total transforming growth factor- β levels in serum and solid organ tissues by bioassay. *BMC Res. Notes*. 2012;5:636.
364. Beraza N, Lüdde T, Assmus U, Roskams T, Vander Borgh S, Trautwein C. Hepatocyte-specific IKK gamma/NEMO expression determines the degree of liver injury. *Gastroenterology*. 2007;132:2504–2517.
365. Kleiner DE, Brunt EM, Van Natta M, Behling C, Contos MJ, Cummings OW, et al. Design and validation of a histological scoring system for nonalcoholic fatty liver disease. *Hepatology*. 2005;41:1313–1321.
366. Barr J, Caballería J, Martínez-Arranz I, Domínguez-Díez A, Alonso C, Muntané J, et al. Obesity-dependent metabolic signatures associated with nonalcoholic fatty liver disease progression. *J. Proteome Res*. 2012;11:2521–2532.
367. R Core Team. R: A Language and Environment for Statistical Computing. Vienna, Austria: R Foundation for Statistical Computing; 2014.
368. Gasparotto N, Tomanin R, Frigo AC, Niizawa G, Pasquini E, Blanco M, et al. Rapid diagnostic testing procedures for lysosomal storage disorders: alpha-glucosidase and beta-galactosidase assays on dried blood spots. *Clin. Chim. Acta Int. J. Clin. Chem*. 2009;402:38–41.
369. Yan L, Mieulet V, Burgess D, Findlay GM, Sully K, Procter J, et al. PP2A T61 epsilon is an inhibitor of MAP4K3 in nutrient signaling to mTOR. *Mol. Cell*. 2010;37:633–642.
370. Sutter BM, Wu X, Laxman S, Tu BP. Methionine inhibits autophagy and promotes growth by inducing the SAM-responsive methylation of PP2A. *Cell*. 2013;154:403–415.
371. Seshacharyulu P, Pandey P, Datta K, Batra SK. Phosphatase: PP2A structural importance, regulation and its aberrant expression in cancer. *Cancer Lett*. 2013;335:9–18.
372. Favre B, Zolnierowicz S, Turowski P, Hemmings BA. The catalytic subunit of protein phosphatase 2A is carboxyl-methylated in vivo. *J. Biol. Chem*. 1994;269:16311–16317.
373. Tolstykh T, Lee J, Vafai S, Stock JB. Carboxyl methylation regulates phosphoprotein phosphatase 2A by controlling the association of regulatory B subunits. *EMBO J*. 2000;19:5682–5691.
374. Chen Y, Neve RL, Liu H. Neddylation dysfunction in Alzheimer's disease. *J. Cell. Mol. Med*. 2012;16:2583–2591.
375. Zhang Y, Hong J-Y, Rockwell CE, Copple BL, Jaeschke H, Klaassen CD. Effect of bile duct ligation on bile acid composition in mouse serum and liver. *Liver Int. Off. J. Int. Assoc. Study Liver*. 2012;32:58–69.
376. Scholten D, Trebicka J, Liedtke C, Weiskirchen R. The carbon tetrachloride model in mice. *Lab. Anim*. 2015;49:4–11.
377. Kurosawa H, Que FG, Roberts LR, Fesmier PJ, Gores GJ. Hepatocytes in the bile duct-ligated rat express Bcl-2. *Am. J. Physiol*. 1997;272:G1587-1593.
378. Bailly A, Perrin A, Bou Malhab LJ, Pion E, Larance M, Nagala M, et al. The NEDD8 inhibitor MLN4924 increases the size of the nucleolus and activates p53 through the ribosomal-Mdm2 pathway. *Oncogene*. 2015;
379. Allen K, Jaeschke H, Copple BL. Bile acids induce inflammatory genes in hepatocytes: a novel mechanism of inflammation during obstructive cholestasis. *Am. J. Pathol*. 2011;178:175–186.
380. Woolbright BL, Jaeschke H. Novel insight into mechanisms of cholestatic liver injury. *World J. Gastroenterol. WJG*. 2012;18:4985–4993.

Post-translational Modifications in Liver Disease

Imanol Zubiete Franco

381. Leist M, Gantner F, Bohlinger I, Tiegs G, Germann PG, Wendel A. Tumor necrosis factor-induced hepatocyte apoptosis precedes liver failure in experimental murine shock models. *Am. J. Pathol.* 1995;146:1220–1234.
382. Chang F-M, Reyna SM, Granados JC, Wei S-J, Innis-Whitehouse W, Maffi SK, et al. Inhibition of neddylation represses lipopolysaccharide-induced proinflammatory cytokine production in macrophage cells. *J. Biol. Chem.* 2012;287:35756–35767.
383. Saiman Y, Friedman SL. The role of chemokines in acute liver injury. *Gastrointest. Sci.* 2012;3:213.
384. Mederacke I, Hsu CC, Troeger JS, Huebener P, Mu X, Dapito DH, et al. Fate tracing reveals hepatic stellate cells as dominant contributors to liver fibrosis independent of its aetiology. *Nat. Commun.* 2013;4:2823.
385. Wertz IE, O'Rourke KM, Zhang Z, Dornan D, Arnott D, Deshaies RJ, et al. Human De-etiolated-1 regulates c-Jun by assembling a CUL4A ubiquitin ligase. *Science.* 2004;303:1371–1374.
386. Bossy-Wetzel E, Bakiri L, Yaniv M. Induction of apoptosis by the transcription factor c-Jun. *EMBO J.* 1997;16:1695–1709.
387. Sasaki R, Kanda T, Nakamura M, Nakamoto S, Haga Y, Wu S, et al. Possible Involvement of Hepatitis B Virus Infection of Hepatocytes in the Attenuation of Apoptosis in Hepatic Stellate Cells. *PLoS One.* 2016;11:e0146314.
388. Scott KD, Nath-Sain S, Agnew MD, Marignani PA. LKB1 catalytically deficient mutants enhance cyclin D1 expression. *Cancer Res.* 2007;67:5622–5627.
389. Kim D-H, Xiao Z, Kwon S, Sun X, Ryerson D, Tkac D, et al. A dysregulated acetyl/SUMO switch of FXR promotes hepatic inflammation in obesity. *EMBO J.* 2015;34:184–199.
390. Cui W, Sun M, Zhang S, Shen X, Galeva N, Williams TD, et al. A SUMO-acetyl switch in PXR biology. *Biochim. Biophys. Acta.* 2016;1859:1170–1182.
391. Lerin C, Rodgers JT, Kalume DE, Kim S, Pandey A, Puigserver P. GCN5 acetyltransferase complex controls glucose metabolism through transcriptional repression of PGC-1alpha. *Cell Metab.* 2006;3:429–438.
392. Caton PW, Nayuni NK, Kieswich J, Khan NQ, Yaqoob MM, Corder R. Metformin suppresses hepatic gluconeogenesis through induction of SIRT1 and GCN5. *J. Endocrinol.* 2010;205:97–106.
393. Dominy JE, Lee Y, Jedrychowski MP, Chim H, Jurczak MJ, Camporez JP, et al. The deacetylase Sirt6 activates the acetyltransferase GCN5 and suppresses hepatic gluconeogenesis. *Mol. Cell.* 2012;48:900–913.
394. Patra KC, Hay N. The pentose phosphate pathway and cancer. *Trends Biochem. Sci.* 2014;39:347–354.
395. Yu L, McPhee CK, Zheng L, Mardones GA, Rong Y, Peng J, et al. Termination of autophagy and reformation of lysosomes regulated by mTOR. *Nature.* 2010;465:942–946.
396. Rabut G, Peter M. Function and regulation of protein neddylation. "Protein modifications: beyond the usual suspects" review series. *EMBO Rep.* 2008;9:969–976.
397. Park Y, Yoon SK, Yoon J-B. TRIP12 functions as an E3 ubiquitin ligase of APP-BP1. *Biochem. Biophys. Res. Commun.* 2008;374:294–298.
398. Schoemaker MH, Ros JE, Homan M, Trautwein C, Liston P, Poelstra K, et al. Cytokine regulation of pro- and anti-apoptotic genes in rat hepatocytes: NF-kappaB-regulated inhibitor of apoptosis protein 2 (cIAP2) prevents apoptosis. *J. Hepatol.* 2002;36:742–750.

399. Bellezzo JM, Britton RS, Bacon BR, Fox ES. LPS-mediated NF-kappa beta activation in rat Kupffer cells can be induced independently of CD14. *Am. J. Physiol.* 1996;270:G956-961.
400. Li L, Liu B, Dong T, Lee HW, Yu J, Zheng Y, et al. Neddylated pathway regulates the proliferation and survival of macrophages. *Biochem. Biophys. Res. Commun.* 2013;432:494-498.
401. Lin X, Liang M, Feng XH. Smurf2 is a ubiquitin E3 ligase mediating proteasome-dependent degradation of Smad2 in transforming growth factor-beta signaling. *J. Biol. Chem.* 2000;275:36818-36822.
402. Xie P, Zhang M, He S, Lu K, Chen Y, Xing G, et al. The covalent modifier Nedd8 is critical for the activation of Smurf1 ubiquitin ligase in tumorigenesis. *Nat. Commun.* 2014;5:3733.
403. Shu J, Liu C, Wei R, Xie P, He S, Zhang L. Nedd8 targets ubiquitin ligase Smurf2 for neddylation and promote its degradation. *Biochem. Biophys. Res. Commun.* 2016;474:51-56.
404. Oved S, Mosesson Y, Zwang Y, Santonico E, Shtiegman K, Marmor MD, et al. Conjugation to Nedd8 instigates ubiquitylation and down-regulation of activated receptor tyrosine kinases. *J. Biol. Chem.* 2006;281:21640-21651.
405. Friend SF, Peterson LK, Treacy E, Stefanski AL, Sosinowski T, Pennock ND, et al. The discovery of a reciprocal relationship between tyrosine-kinase signaling and cullin neddylation. *PLoS One.* 2013;8:e75200.
406. Dennler S, Prunier C, Ferrand N, Gauthier JM, Atfi A. c-Jun inhibits transforming growth factor beta-mediated transcription by repressing Smad3 transcriptional activity. *J. Biol. Chem.* 2000;275:28858-28865.
407. Puffenberger EG, Strauss KA, Ramsey KE, Craig DW, Stephan DA, Robinson DL, et al. Polyhydramnios, megalencephaly and symptomatic epilepsy caused by a homozygous 7-kilobase deletion in LYK5. *Brain J. Neurol.* 2007;130:1929-1941.
408. Stankovic-Valentin N, Deltour S, Seeler J, Pinte S, Vergoten G, Guérardel C, et al. An acetylation/deacetylation-SUMOylation switch through a phylogenetically conserved psiKXEP motif in the tumor suppressor HIC1 regulates transcriptional repression activity. *Mol. Cell. Biol.* 2007;27:2661-2675.
409. Hickey CM, Wilson NR, Hochstrasser M. Function and regulation of SUMO proteases. *Nat. Rev. Mol. Cell Biol.* 2012;13:755-766.
410. Hardie DG, Alessi DR. LKB1 and AMPK and the cancer-metabolism link - ten years after. *BMC Biol.* 2013;11:36.
411. Monteverde T, Muthalagu N, Port J, Murphy DJ. Evidence of cancer-promoting roles for AMPK and related kinases. *FEBS J.* 2015;282:4658-4671.

Post-translational Modifications in Liver Disease
Imanol Zubieta Franco

Support

The word "Support" is centered on the page. To its left, a lysine residue is shown as a carboxylate group (COO-) attached to the "Lys" label. To its right, a glycylglycyllysine dipeptide is shown as a Gly-Gly-Lys sequence, with the Gly-Gly part above the Lys part, and the Lys part below the Gly-Gly part. A horizontal line is drawn below the word "Support".

Post-translational Modifications in Liver Disease
Imanol Zubieta Franco

10. Support

This work was supported by a PFIS (Ayudas predoctorales de formación en investigación en salud) fellowship from the Instituto de Salud Carlos III during the period 2012 to 2016.

Additional support was granted by:

- NIH grants R01AR001576-11^a1 and CA172086 (Shelly C. Lu, José M. Mato, María L. Martínez-Chantar)
- Sanidad Gobierno Vasco (María L. Martínez-Chantar and Marta Varela-Rey)
- Asociación Española contra el Cáncer (Teresa C. Delgado, María L. Martínez-Chantar)
- FIS PI11/01588 (María L. Martínez-Chantar)
- FIS PS12/00402 (Naiara Beraza and Marta Varela-Rey)
- Educación Gobierno Vasco 2011 (María L. Martínez-Chantar)
- ETORTEK 2011 (María L. Martínez-Chantar)
- Plan nacional de I+D: SAF2014-54658-R and SAF2014-52097-R (José M. Mato and María L. Martínez-Chantar)
- CIBERehd, funded by the Instituto de Salud Carlos III

The work carried out during this thesis has led to:

Two published papers:

Zubiete-Franco I, et al. *Deregulated Neddylation in liver fibrosis*. Hepatology. 2016 Nov 7. doi: 10.1002/hep.28933.

Zubiete Franco I, et al. *Methionine and S-Adenosylmethionine levels are critical regulators of PP2A activity modulating lipophagy during steatosis*. J Hepatol. 2016 Feb;64(2):409-18. doi: 10.1016/j.jhep.2015.08.037

Contribution in three papers:

Barbier-Torres L, et al. *Histone deacetylase 4 promotes cholestatic liver injury in the absence of prohibitin-1*. Hepatology. 2015 Oct;62(4):1237-48. doi: 10.1002/hep.27959

Barbier-Torres L, et al. *Stabilization of LKB1 and Akt by neddylation regulates energy metabolism in liver cancer*. Oncotarget. 2015 Feb 10;6(4):2509-23.

Fernández-Álvarez S, et al. *TRAIL-producing NK cells contribute to liver injury and related fibrogenesis in the context of GNMT deficiency*. Lab Invest. 2015 Feb;95(2):223-36. doi: 10.1038/labinvest.2014.151.

Post-translational Modifications in Liver Disease
Imanol Zubieta Franco